

Springer Tracts in Modern Physics 233

George W. S. Hou

# Flavor Physics and the TeV Scale

*Second Edition*



Springer

# **Springer Tracts in Modern Physics**

Volume 233

## **Series editors**

Yan Chen, Department of Physics, Fudan University, Shanghai, China

Atsushi Fujimori, Department of Physics, University of Tokyo, Tokyo, Japan

Thomas Müller, Institut für Experimentelle Kernphysik, Universität Karlsruhe,  
Karlsruhe, Germany

William C. Stwalley, Department of Physics, University of Connecticut, Storrs,  
USA

Jianke Yang, Department of Mathematics and Statistics, University of Vermont,  
Burlington, VT, USA

Springer Tracts in Modern Physics provides comprehensive and critical reviews of topics of current interest in physics. The following fields are emphasized:

- Elementary Particle Physics
- Condensed Matter Physics
- Light Matter Interaction
- Atomic and Molecular Physics
- Complex Systems
- Fundamental Astrophysics

Suitable reviews of other fields can also be accepted. The Editors encourage prospective authors to correspond with them in advance of submitting a manuscript. For reviews of topics belonging to the above mentioned fields, they should address the responsible Editor as listed in “Contact the Editors”.

More information about this series at <http://www.springer.com/series/426>

George W. S. Hou

# Flavor Physics and the TeV Scale

Second Edition

 Springer

George W. S. Hou  
Department of Physics  
National Taiwan University  
Taipei, Taiwan

ISSN 0081-3869                      ISSN 1615-0430 (electronic)  
Springer Tracts in Modern Physics  
ISBN 978-3-662-58627-3              ISBN 978-3-662-58629-7 (eBook)  
<https://doi.org/10.1007/978-3-662-58629-7>

Library of Congress Control Number: 2018968113

1<sup>st</sup> edition: © Springer-Verlag Berlin Heidelberg 2009

2<sup>nd</sup> edition: © Springer-Verlag GmbH Germany, part of Springer Nature 2019

This work is subject to copyright. All rights are reserved by the Publisher, whether the whole or part of the material is concerned, specifically the rights of translation, reprinting, reuse of illustrations, recitation, broadcasting, reproduction on microfilms or in any other physical way, and transmission or information storage and retrieval, electronic adaptation, computer software, or by similar or dissimilar methodology now known or hereafter developed.

The use of general descriptive names, registered names, trademarks, service marks, etc. in this publication does not imply, even in the absence of a specific statement, that such names are exempt from the relevant protective laws and regulations and therefore free for general use.

The publisher, the authors and the editors are safe to assume that the advice and information in this book are believed to be true and accurate at the date of publication. Neither the publisher nor the authors or the editors give a warranty, express or implied, with respect to the material contained herein or for any errors or omissions that may have been made. The publisher remains neutral with regard to jurisdictional claims in published maps and institutional affiliations.

This Springer imprint is published by the registered company Springer-Verlag GmbH, DE part of Springer Nature

The registered company address is: Heidelberger Platz 3, 14197 Berlin, Germany

*To the memories of Prof. Chia-Chu Hou  
and Mr. Chiao-Shen Lu, beloved father,  
and father in-law.*

# Preface of Second Edition

It is almost exactly 10 years since the first edition. I was actually contacted by the hardworking editor already in 2013 for a revision. However, mostly driven by the magnificent LHCb experiment at the Large Hadron Collider, the “flavor anomalies” were just unfolding, so it appeared too early. By 2017, I decided it was time for an update, but the schedule was delayed by waiting ever eagerly for the “Run 2 update” on flavor anomalies by LHCb. Unfortunately, to date this has yet to happen, and with the Belle II experiment turning on, one should not delay any further.

The anomalies still stand, but alas, through Run 1 and now Run 2, we cannot say we have uncovered any New Physics at the LHC so far. The discovery of the Higgs boson at the LHC repeats what has happened with the discovery of the top quark at the Tevatron: confirming the Standard Model, but *No New Physics. Déjà-vu!* While that has been disappointing, it highlights the role of Flavor Physics to probe above the TeV scale, now that we have reached the TeV scale but found ourselves empty-handed from direct search.

We have made major updates to all chapters except the first two, with *Dark Sector* entering the title of Chap. 7, reflecting the times. Furthermore, the new Chap. 10 on “The Top and Higgs” has been added. We believe the top quark would become part of the Flavor Physics and CP violation, or *FPCP*, conference theme. Note that, echoing the absence of New Physics at the LHC, the fourth generation (4G) has not been found, and we give a “Requiem” in an appendix. In its place, however, the new Chap. 10 promotes extra Yukawa couplings arising from a second Higgs boson doublet.

Just like discovering the 4G enhancement of the Jarlskog invariant, in planning this update, we discovered that, with the extra top Yukawa coupling, together with the possibility of first-order phase transition—both facilitated by presence of the second Higgs doublet—*electroweak baryogenesis can be readily achieved*. In the same time frame, we found that the *alignment* phenomenon, that the observed 125 GeV boson does not seem to mix much with the exotic neutral Higgs boson(s), can help alleviate age-old issues with flavor-changing neutral Higgs couplings. Inspired, we eventually called this SM2—SM with 2 Higgs doublets, and just let Nature reveal herself.

We believe a new golden decade of flavor physics is unfolding, where Belle II would be both competitive with, and complementary to, LHCb.

Let the era begin.

Melbourne, Australia/Taipei, Taiwan  
December 2018

George W. S. Hou



# Preface of First Edition

The flavor sector carries the largest number of parameters in the Standard Model of particle physics. With no evident symmetry principle behind its existence, it is not as well understood as the  $SU(3) \times SU(2) \times U(1)$  gauge interactions. Yet it tends to be underrated, sometimes even ignored, by the erudite. This is especially so on the verge of the LHC era, where the exploration of the physics of electroweak symmetry breaking at the high-energy frontier would soon be the main thrust of the field.

Yet, the question of “Who ordered the muon?” by I. I. Rabi lingers.

We do not understand why there is “family” (or generation) replication. That three generations are needed to have  $CP$  violation is a partial answer. We do not understand why there are only three generations, but Nature insists on (just about) only three active neutrinos. But then the  $CP$  violation with three generations fall far short of what is needed to generate the baryon asymmetry of the Universe. We do not understand why most fermions are so light on the weak symmetry breaking scale (v.e.v.), yet the third-generation top quark is a v.e.v. scale particle. We do not understand why quarks and leptons look so different, in particular, why neutrinos are rather close to being massless, but then have (at least two) near-maximal mixing angles. We shall not, however, concern ourselves with the neutrino sector. It has a life of its own.

This monograph is on the usefulness of flavor physics as probes of the TeV scale, to provide a timely interface for the emerging LHC era. Historically, the kaon system has been a major wellspring for the emergence of the Standard Model. It gave us the Cabibbo angle hence quark mixings,  $K^0-\bar{K}^0$  oscillations,  $CP$  violation, absence of FCNC and the GIM mechanism, prediction of charm (mass), and ultimately the Kobayashi–Maskawa model and the prediction of the third generation. The torch, however, has largely passed on to the  $B$  meson system, the elucidation of which forms the bulk of this book. Following, and expanding on, the successful paths of the CLEO and ARGUS experiments, the B factories have dominated the scene for the past decade.

The B factories have produced a vast amount of knowledge. Fortunately, by concerning ourselves only with the TeV scale connection, a large part of the B factory output can be bypassed. We do not concern ourselves with rather indirect links to physics beyond the Standard Model, such as the measurement of CKM sides, or the consistency of the unitary phases with three generations. The advantage is that we do not need to go into the details of “precision measurement” studies, as they are now rather involved. Our emphasis is on loop-induced processes, which allow us to probe virtual TeV scale physics through quantum processes, in the good traditions of muon  $g - 2$  and rare kaon processes. In this sense, flavor physics is quite complementary to the LHC collider physics that would soon unfold before us. If New Physics is discovered by the LHC, flavor probes would provide extra information to help pin down parameters. If no New Physics emerges from the LHC, then flavor physics still provides multiple probes to physics above the TeV scale. Either way, the construction of so-called Super B factories, to go far beyond the successful B factories in luminosity, is called for.

A glance at the Table of Contents shows that two-thirds of the book is concerned with  $b \rightarrow s$  or  $b\bar{s} \leftrightarrow s\bar{b}$  transitions. The B factories have not uncovered strong hints for New Physics in  $b\bar{d} \leftrightarrow d\bar{b}$  or  $b \rightarrow d$  transitions. It is remarkable that all evidence supports the third-generation Kobayashi–Maskawa model in the so-called  $b \rightarrow d$  CKM triangle,  $V_{ud}V_{ub}^* + V_{cd}V_{cb}^* + V_{td}V_{tb}^* = 0$  (and the Nobel Prize has been awarded). Further probes in  $b \rightarrow d$  transitions tend to be marred by hadronic or Standard Model effects, and at best are part of the long road of third-generation Standard Model consistency tests that we have decided to sidestep. In contrast,  $b \rightarrow s$  transitions are not only the current frontier of flavor physics, it actually offers good hope that New Physics may soon be uncovered, maybe even before the first physics is repeated at the LHC. On the one hand, this is because the  $V_{us}V_{ub}^* + V_{cs}V_{cb}^* + V_{ts}V_{tb}^* = 0$  CKM triangle is so squashed and hardly a triangle in the Standard Model, so the expected  $CP$  violation in loop-dominated  $b \rightarrow s$  transitions is tiny. This means that any clear observation could indicate New Physics. On the other hand,  $b \rightarrow s$  transitions offer multiple probes into physics beyond the Standard Model that have come of age only recently. As we advocate, the measurement of  $\sin 2\Phi_{B_s}$  in  $B_s \rightarrow J/\psi\phi$ , analogous to  $\sin 2\phi_1/\beta$  measurement in  $B_d \rightarrow J/\psi K_S$  at the B factories, holds the best promise for an unequivocal discovery of New Physics, if its measured value at the Tevatron or LHC turns out to be sizable. It is exciting that we seem to be heading that way.

A common thread that links the several hints of New Physics in  $b \rightarrow s$  transitions, to our prediction of large and negative  $\sin 2\Phi_{B_s}$ , is the existence of a fourth generation. Of course, there are strong arguments against the existence of a fourth generation, by the aforementioned “neutrino counting,” and by electroweak precision tests. However, these objections arise from outside of flavor physics. While these should be taken seriously, one should not throw the fourth generation away when considering flavor physics, since the richness of flavor physics rests on the existence of three generations, and extending to four generations provide considerable enrichment, particularly in  $b \rightarrow s$  transitions. It also provides multiple links

between different flavor processes, through the unitarity of the  $4 \times 4$  CKM matrix. As emphasized in this book, a fourth generation could most easily enter box and electroweak penguin diagrams. Accounts of these are scattered throughout the book, as we touch upon different processes. These are effects due to large Yukawa couplings, which link flavor physics to the Higgs, or electroweak symmetry breaking sector.

While writing this book, we observed that *adding a fourth quark generation could enhance the so-called Jarlskog invariant for CP violation by a factor of  $10^{+13}$  or more*, and the (fourth generation) KM model could provide the source of CP violation for the baryon asymmetry of the Universe. A sketch of this insight is given in the final discussion chapter, which also serves as justification for our frequent mentioning of the fourth generation throughout the book. *Flavor physics could provide CP violation for the Heaven and the Earth.*

Two other chapters, on  $D^0$  mixing and  $K \rightarrow \pi\nu\nu$ , and on lepton number violating  $\tau$  decays, are loop-induced probes of New Physics that are analogous to the emphasis of our main text on  $B$  physics. Interestingly, there are still tree-level processes that can probe New Physics, such as the probe of charged Higgs boson  $H^+$  through  $B^+ \rightarrow \tau^+ \nu_\tau$ , or light dark matter or pseudoscalar Higgs boson search in  $\Upsilon(nS)$  decays.

We have taken an experimental perspective in writing this book. This means selecting *processes*, rather than the theories or models, as the basis to explore flavor physics as probe of the TeV scale. In the first few chapters, emphasis is on CP violation measurables in  $b \rightarrow s$  transitions. We then switch to using a particular process to illustrate the probe of a special kind of physics. We therefore also spend some time in elucidating what it takes to measure these processes. However, this is not a worker's manual for experimental analysis, but on bringing out the physics. For the same reason, we do not go into any detail on theoretical models. Our guiding principle has been: Unless it can be identified as the smoking gun, it is better to stick to the simplest (rather than elaborate) explanation of an effect that requires New Physics.

The origins of this monograph are the plenary talk I gave at the SUSY 2007 conference held in Karlsruhe, Germany. It was interesting to attend the SUSY conference for the first time, while giving an *experimental* plenary talk. I thank the Belle spokespersons, Masa Yamauchi in particular, for nominating me as "that special physicist" to give this talk. I also thank my old friend and former colleague, Hans Kühn, for encouraging and inviting me to expand the talk into a monograph for Springer Tracts of Modern Physics. It is impossible to thank the numerous colleagues in the field of flavor physics for benefits of discussion and insight. I acknowledge the help from Yeong-jyi Lei for help on figures. Last, and above all, I thank my family for the understanding and support throughout the period of writing this book.

# Contents

|          |  |    |
|----------|--|----|
| <b>1</b> | <b>Introduction</b> .....  | 1  |
| 1.1      | Outline, Strategy, and Apologies .....   | 2  |
| 1.2      | A Parable: What if? .....  | 4  |
| 1.3      | The Template: $\Delta m_{B_d}$ , Heavy $T$ op, and $V_{td}$ .....                                    | 6  |
|          | References .....   | 9  |
| <b>2</b> | <b><math>CP</math> Violation in Charmless <math>b \rightarrow s\bar{q}q</math> Transitions</b> ..... | 11 |
| 2.1      | The $\Delta S$ Pursuit .....   | 11 |
| 2.1.1    | Measurement of TCPV at the B Factories .....   | 12 |
| 2.1.2    | TCPV in Charmless $b \rightarrow s\bar{q}q$ Modes .....  | 15 |
| 2.2      | The $\Delta\mathcal{A}_{K\pi}$ Problem .....   | 18 |
| 2.2.1    | Measurement of DCPV in $B^0 \rightarrow K^+\pi^-$ Decay .....  | 18 |
| 2.2.2    | $\Delta\mathcal{A}_{K\pi}$ and New Physics? .....  | 21 |
| 2.3      | $\mathcal{A}_{CP}(B^+ \rightarrow J/\psi K^+)$ .....   | 25 |
| 2.4      | An Appraisal .....   | 28 |
|          | References .....   | 30 |
| <b>3</b> | <b><math>B_s</math> Mixing and <math>\sin 2\Phi_{B_s}</math></b> .....                               | 33 |
| 3.1      | $B_s$ Mixing Measurement .....   | 34 |
| 3.1.1    | Standard Model Expectations .....  | 34 |
| 3.1.2    | Tevatron Measurement of $\Delta m_{B_s}$ .....   | 38 |
| 3.2      | Search for TCPV in $B_s$ System .....  | 42 |
| 3.2.1    | $\Delta\Gamma_{B_s}$ Approach to $\phi_{B_s}$ : $\cos 2\Phi_{B_s}$ .....                             | 42 |
| 3.2.2    | Prospecting for $\sin 2\Phi_{B_s}$ , ca. 2008 .....  | 44 |
| 3.2.3    | Hints at Tevatron in 2008 .....  | 50 |
| 3.2.4    | Anticlimax: $\sin 2\Phi_{B_s} \simeq 0$ .....  | 54 |
|          | References .....   | 56 |

|          |  |     |
|----------|--|-----|
| <b>4</b> | <b><math>H^+</math> Probes: <math>b \rightarrow s\gamma</math>, and <math>B \rightarrow \tau\nu, D^{(*)}\tau\nu</math></b> | 59  |
| 4.1      | $b \rightarrow s\gamma$  | 59  |
| 4.1.1    | QCD Enhancement and the CLEO Observation   | 59  |
| 4.1.2    | Measurement of $b \rightarrow s\gamma$ at the B Factories  | 61  |
| 4.1.3    | Implications for $H^+$   | 64  |
| 4.2      | Measuring $B \rightarrow \tau\nu, D^{(*)}\tau\nu$  | 66  |
| 4.2.1    | Enhanced $H^+$ Effect in $b \rightarrow c\tau\nu$ and $B^+ \rightarrow \tau^+\nu_\tau$                                     | 66  |
| 4.2.2    | $B \rightarrow \tau\nu$ and $B \rightarrow D^{(*)}\tau\nu$ Rate Measurement  | 69  |
| 4.3      | $R_D, R_{D^*}$ Anomaly   | 75  |
| 4.3.1    | BaBar Bombshell  | 75  |
| 4.3.2    | Assessment: Towards Belle II + LHCb Era  | 79  |
|          | References   | 81  |
| <b>5</b> | <b>Electroweak Penguin: <math>b \rightarrow s\ell\ell</math>, Anomalies, <math>Z'</math></b>                               | 85  |
| 5.1      | $A_{\text{FB}}(B \rightarrow K^*\ell^+\ell^-)$   | 85  |
| 5.1.1    | Observation of $m_t$ -enhanced $b \rightarrow s\ell^+\ell^-$   | 85  |
| 5.1.2    | $A_{\text{FB}}(B \rightarrow K^*\ell^+\ell^-)$ Problem and Its Demise  | 89  |
| 5.2      | $P'_5$ and $R_{K^{(*)}}$ Anomalies   | 94  |
| 5.2.1    | $P'_5$ Anomaly   | 94  |
| 5.2.2    | $R_K, R_{K^*}$ Anomaly   | 96  |
| 5.3      | $B \rightarrow K^{(*)}\nu\nu$  | 99  |
| 5.3.1    | Experimental Search  | 99  |
| 5.3.2    | Constraint on Light Dark Matter  | 102 |
|          | References   | 104 |
| <b>6</b> | <b>Scalar Interactions and Right-Handed Currents</b>   | 107 |
| 6.1      | $B_s \rightarrow \mu^+\mu^-$ (and $B^0 \rightarrow \mu^+\mu^-$ )   | 107 |
| 6.1.1    | Tevatron Versus LHC  | 109 |
| 6.1.2    | Observation of $B_s \rightarrow \mu^+\mu^-$ at LHC   | 111 |
| 6.2      | TCPV in $B \rightarrow K_S^0\pi^0\gamma, X^0\gamma$  | 115 |
|          | References   | 118 |
| <b>7</b> | <b>Probes of the Dark Sector at Flavor Facilities</b>  | 121 |
| 7.1      | $\Upsilon$ Decay Probes  | 121 |
| 7.1.1    | $\Upsilon(3S) \rightarrow \pi^+\pi^-\Upsilon(1S) \rightarrow \pi^+\pi^- + \text{Nothing}$                                  | 121 |
| 7.1.2    | $\Upsilon(1S) \rightarrow \gamma a_1^0$ Search   | 125 |
| 7.2      | The Quest for Dark Photons   | 127 |
| 7.2.1    | Exotic Higgs-Strahlung: $e^+e^- \rightarrow A'h', h' \rightarrow A'A'$   | 128 |
| 7.2.2    | Dark Photon from ISR: $e^+e^- \rightarrow \gamma_{\text{ISR}}A'$   | 129 |
| 7.2.3    | Inclusive $A' \rightarrow \mu^+\mu^-$ Search at LHC  | 131 |
| 7.2.4    | Muonic Dark Force: $e^+e^- \rightarrow \mu^+\mu^-Z',$<br>$Z' \rightarrow \mu^+\mu^-$                                       | 132 |
|          | References   | 133 |

|           |  |     |
|-----------|--|-----|
| <b>8</b>  | <b><i>D</i> and <i>K</i> Systems: Box and EWP Redux</b>                          | 135 |
| 8.1       | <i>D</i> <sup>0</sup> Mixing   | 135 |
| 8.1.1     | SM Expectations and Observation at B Factories                                   | 136 |
| 8.1.2     | Interpretation, $\Delta A_{CP}$ Interlude, and Prospects                         | 141 |
| 8.2       | Rare <i>K</i> Decays: $K \rightarrow \pi\nu\bar{\nu}$ Pursuit                    | 143 |
| 8.2.1     | Path to $K \rightarrow \pi\nu\bar{\nu}$  | 144 |
| 8.2.2     | Pushing the Frontier: NA62 and KOTO  | 147 |
| 8.2.3     | Kaon Prospects   | 150 |
|           | References   | 152 |
| <b>9</b>  | <b>Lepton Number Violation and <math>\mu</math>, <math>\tau</math> Systems</b>   | 155 |
| 9.1       | $\mu \rightarrow e$ Transitions, $g - 2$ and EDM                                 | 156 |
| 9.1.1     | $\mu \rightarrow e$ Transitions  | 156 |
| 9.1.2     | Muon $g - 2$ and EDMs  | 159 |
| 9.2       | LFV $\tau \rightarrow \ell\gamma$ , $\ell\ell\ell'$ Decays                       | 161 |
| 9.2.1     | Lepton Universality and $\tau$ Lifetime  | 162 |
| 9.2.2     | $\tau \rightarrow \mu\gamma$ , $\ell\ell\ell'$                                   | 162 |
| 9.3       | $\tau \rightarrow \bar{\Lambda}\pi$ , $\bar{p}\pi^0$ and Baryon Number Violation | 165 |
|           | References   | 167 |
| <b>10</b> | <b>The Top and The Higgs</b>   | 169 |
| 10.1      | Top Changing Neutral Couplings   | 170 |
| 10.1.1    | TCNC: $t \rightarrow cZ^{(\prime)}$  | 170 |
| 10.1.2    | TCNH: $t \rightarrow ch$   | 172 |
| 10.2      | New Yukawa Couplings with Extra Higgs Bosons                                     | 174 |
| 10.2.1    | Flavor Changing Neutral Higgs: $h^0 \rightarrow \mu^\pm\tau^\mp$                 | 174 |
| 10.2.2    | 2HDM-III: Two Higgs Doublets Without $Z_2$                                       | 177 |
| 10.3      | SM2: SM, But with Two Higgs Doublets   | 178 |
| 10.3.1    | Lagrangian for Yukawa Couplings in SM2   | 179 |
| 10.3.2    | Prognosis  | 180 |
|           | References   | 182 |
| <b>11</b> | <b>Conclusion</b>  | 185 |
|           | References   | 191 |
|           | <b>Appendix A: A <i>CP</i> Violation Primer</b>                                  | 193 |
|           | <b>Appendix B: Requiem to 4th Generation</b>                                     | 201 |
|           | <b>Index</b>   | 205 |

# Chapter 1

## Introduction



As humans, we aspire to reach up to the heavens. It is our unquenchable nature. An old fable illustrates the point: Jack and the Beanstalk. It is simply impossible for Jack not to climb the Beanstalk, when it stands in front of him, extending all the way up, to beyond the clouds.

Let us illustrate Jack and the Beanstalk as an allegory in Fig. 1.1. In particle physics, we have strived to surpass the threshold and reach beyond the veiling clouds of the “v.e.v. scale” (the “v.,” “e.” and “v.,” unfortunately do not show up clearly in Fig. 1.1 in BW, which seems fitting), as we know firmly that a vacuum expectation value of order  $v \simeq 246$  GeV had developed in the early Universe, which broke the electroweak symmetry (EWSB) down to electromagnetism. This is the scale for all fundamental masses<sup>1</sup> in the Standard Model (SM). The conventional high energy approach is like Jack climbing straight up the Beanstalk. In 2012, the Large Hadron Collider (LHC) at CERN spectacularly discovered the Higgs boson with mass  $m_h \simeq 125$  GeV, i.e. in the Castle floating on a low cloud in Fig. 1.1. But going up in energy from 7 and 8 TeV in Run 1 to 13 TeV in Run 2 (which would finish by end of 2018), *the LHC uncovered No New Physics Beyond the SM (BSM) so far!* While the Higgs boson is relatively light, there seems to be vast emptiness beyond the darker clouds of the v.e.v., with no sign of treasures, nor the “*Giant*”.

In the direct ascent approach, Jack has to fear the *Giant*, which could even be the projects like ILC (International Linear Collider) or the 100 km circumference CEPC-SppC (Circular Electron-Positron Collider & Super proton-proton Collider). The cost of machines is becoming so prohibitive, Jack may not be able to survive or return, whatever the riches he may or may not uncover. However, “Jack” *may not* have to actually climb the Beanstalk: quantum physics allows him to stay on Earth, and let virtual “loops” do the work. The virtual Jack has no fear of getting eaten by the *Giant*.

---

<sup>1</sup>The mass of the proton (hence most Earthly masses) actually arises predominantly from a similar phenomena of chiral symmetry breaking, induced by QCD.

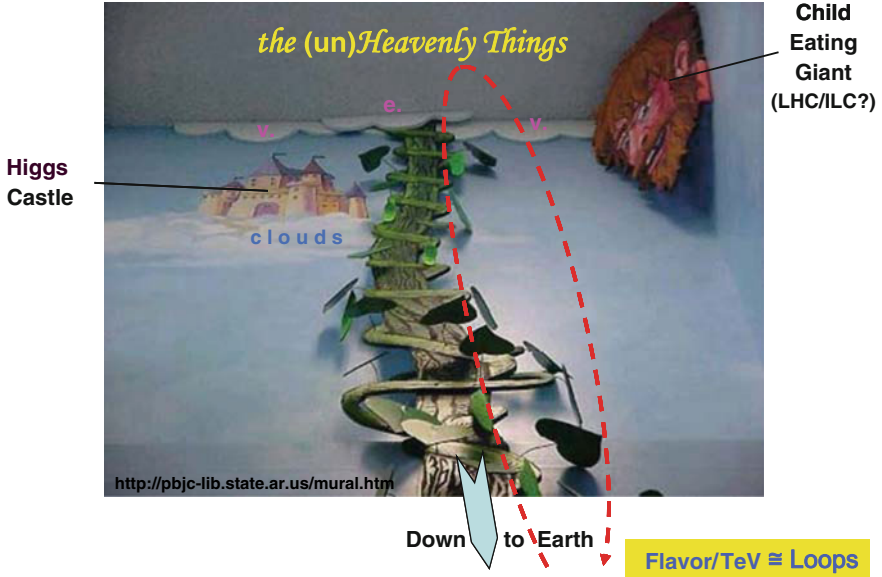


**Fig. 1.1** Parable of Jack and the Beanstalk (adapted from the mural by Henri Linton and Ariston Jacks, originally located at the Pine Bluff Public Library, Pine Bluff, Arkansas, U.S.A.; used with permission)

This parable illustrates how flavor physics offers probes of the TeV scale, at much reduced costs. The flavor connection to TeV scale physics is typically through loops. Interestingly, the current indications for “anomalies”,<sup>2</sup> or deviations from SM, all seem to arise from the flavor sector.

## 1.1 Outline, Strategy, and Apologies

The outline of this book is as follows.

We take an experimental view on the physics of flavor and the TeV scale connection. In the remainder of this chapter, we entertain a “*What if?*” question to elucidate the possible surprises from flavor physics, then use  $B^0-\bar{B}^0$  mixing as a template to illustrate loop effects. In the next chapter we cover New Physics (NP)  $CP$  violation (CPV) search in loop-induced  $b \rightarrow s$  transitions: the mixing-dependent CPV difference  $\Delta\mathcal{S}$  between  $b \rightarrow c\bar{c}s$  and  $s\bar{q}q$  processes, and the direct CPV difference  $\Delta\mathcal{A}_{K\pi}$  between  $B^+$  and  $B^0$  decay to  $K^+\pi$ . These were highlight studies of the B factory era. In Chap. 3, we continue with the New Physics CPV search in loop-induced  $b\bar{s} \leftrightarrow \bar{b}s$

<sup>2</sup>“Anomalies”, put in quotation here, are discrepancies between experimental measurement and theoretical (i.e. SM) expectation. They come and go, and mostly, *go*. The most famous “anomaly” at the LHC was the 750 GeV diphoton excess, which came with early 13 TeV data of 2015 run, but went away within a year.



transitions, namely the status and prospects for measuring the CPV phase in  $B_s$  mixing. There was some hope during 2008–2010 that *it could be large*, but ended up again SM-like, which was a disappointing triumph of the LHCb experiment in the LHC era. It remains a focus of flavor physics. In Chap. 4, we turn to the traditional probes of charged Higgs boson ( $H^+$ ) effects, namely  $b \rightarrow s\gamma$  and  $B^+ \rightarrow \tau^+\nu$ , where the latter arises from a tree diagram. The  $B \rightarrow D^{(*)}\tau\nu$  anomaly is also discussed here, together with possible New Physics. In Chap. 5, we use  $B \rightarrow K^{(*)}\ell^+\ell^-$  to show how these electroweak penguin processes provide exquisite probes of New Physics. The forward-backward asymmetry ( $A_{\text{FB}}$ ) “anomaly” rose and fell, but the  $P'_S$  and  $R_{K^{(*)}}$  anomalies unveiled by LHCb are recent highlights. The  $B \rightarrow K^{(*)}\nu\nu$  modes emerge analogously in SM, but because the experimental signature is  $B \rightarrow K^{(*)} + \text{nothing}$ , their search provide a window on light dark matter, which connects also with the kaon section. In Chap. 6, the LHC Run 1 highlight of  $B_s \rightarrow \mu^+\mu^-$  observation is discussed in the context as a probe of the extended Higgs sector, but again turned out SM-like. We then use time-dependent CPV in  $B^0 \rightarrow K_S\pi^0\gamma$  to illustrate the probes of right-handed dynamics. In Chap. 7 we detour from loop physics to discuss the bottomonium system as probe of light dark matter and exotic light Higgs bosons. This is further expanded to the broad interest of flavor facilities as probes of the Dark Sector. We then return to loop effects in  $D^0$  mixing and rare  $K \rightarrow \pi\nu\nu$  decays in Chap. 8, and lepton flavor violation in  $\mu$  and  $\tau$  decays in Chap. 9, where we also discuss briefly muon  $g - 2$  and electric dipole moments. Chapter 10 discusses the emerging field of Top-Higgs connections with flavor physics. We close with some discussions and insight, and offer our conclusions in Chap. 11. In Appendix A, we elucidate and demystify the mechanism of CPV; Appendix B is a requiem to the fourth generation.

Flavor physics is a vast subject with many rather elaborate and specialized topics. Our selection of topics is simplified by focusing on those that are *pertinent* to BSM physics, while avoiding those that are too intricate or too long to present. The emphasis is on *bringing out the physics*, rather than on the experimental or theoretical details. As the (Chinese) saying goes, one should avoid “See tree(s), not see forest”, which often happens to experts that get lost in the details.

Another criteria for selection of topics is our emphasis on the nearer-term impact. We have seen the spectacular success of the LHCb experiment, which has completely superseded the Tevatron era, while after long preparations, we are finally at the juncture where the “Super B factory” era is dawning. The unprecedented luminosities of KEKB (see Fig. 1.2) would soon take another leap upward by a factor of 40–50 to SuperKEKB, with a total of  $50 \text{ ab}^{-1}$  integrated luminosity delivered to Belle II by  $\sim 2025$ . We can finally enjoy the competition, and complementarity, between LHCb and Belle II.

We have largely picked traditional theoretical models for BSM or “New Physics”. Thanks to the B factories, flavor physics experienced a tremendous leap forward from the CLEO era of the 1990s. While the frontier has been pushed back considerably (see Fig. 1.2 again), no smoking gun BSM signal has yet emerged in an unequivocal way. With the advent of LHCb, we have seen quite a few flavor “anomalies” emerge, which is intriguing. In contrast, “*No New Physics*” at the LHC energy frontier has

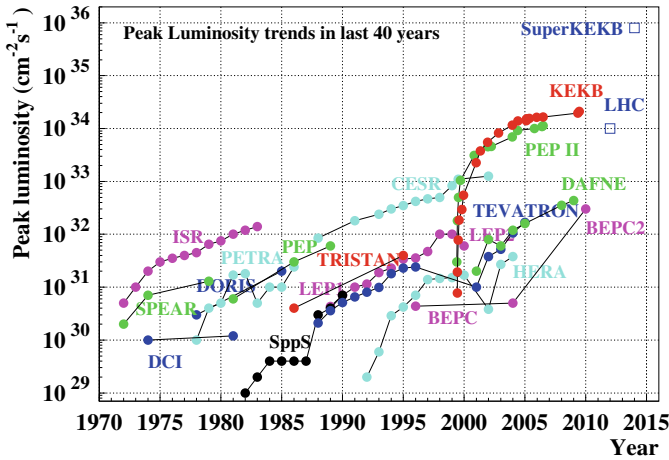


**Fig. 1.2** The luminosity frontier up to 2010. Note that the LHC has already achieved luminosities comparable to KEKB, while SuperKEKB only started in 2018. [Source <http://sabotin.p-ng.si/~sstanic/kekb/trends.html>, by Samo Stanič, used with permission]

brought on some anxiety in the theory community, not least the absence of any signal for supersymmetry (SUSY). We will not enter the “naturalness” debate, but emphasize that the current situation elevates the importance of the flavor physics and TeV scale link. EWSB physics and flavor physics are orthogonal but complementary directions. They overlap in the Yukawa coupling sector, hence our new chapter on the Top-Higgs intersection. It is gratifying that SuperKEKB would soon allow Belle II to probe, together with LHCb, the flavor frontier, hand in hand with ATLAS and CMS on the energy frontier.

Having said all this, we apologize for incomplete citations of theoretical work. We cite what we deem to be of key importance, again, to illustrate the physics. However, we are not impartial in promoting our own phenomenological work. But our previous favorite, having a fourth generation of quarks in Nature, is placed in an Appendix.

## 1.2 A Parable: What if?

Another “parable” illustrates the potential of heavy flavor physics to make impact. Let us entertain a hypothetical “*What if?*” question.

Forwarding to the recent past, on July 31, 2000, at the ICHEP conference in Osaka, the BaBar experiment announced the low value of  $\sin 2\beta \sim 0.12$  [2],

$$\sin 2\beta = 0.12 \pm 0.37 (\text{stat}) \pm 0.09 (\text{syst}). \quad (\text{BaBar, ICHEP2000}) \quad (1.1)$$

We will gradually define what  $\sin 2\beta$  means. The result of (1.1) was analyzed with a data set of  $9 \text{ fb}^{-1}$  integrated luminosity on the  $\Upsilon(4S)$  resonance, corresponding to

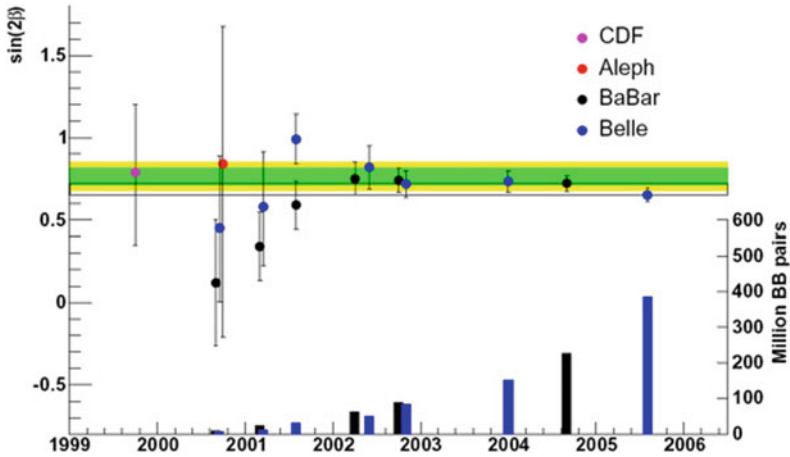


**Fig. 1.3** Measurement of  $\sin 2\beta/\phi_1$ , 2000–2005, illustrating how the combined result of Belle and BaBar settled already in 2001. [Source talk by Cahn [1] given at 2006 SLAC Summer Institute, used with permission.]

about 10M  $B\bar{B}$  meson pairs produced in the clean  $e^+e^-$  collider environment. The value for the equivalent  $\sin 2\phi_1 = 0.45^{+0.43+0.07}_{-0.44-0.09}$  [3] measurement from the Belle experiment (using  $6.2 \text{ fb}^{-1}$  data, or almost 7M  $B\bar{B}$  pairs) was slightly higher, but also consistent with zero. Note that the errors are quite large. Within the same day, however, a theory paper appeared on the arXiv [4], entertaining the implications of the low  $\sin 2\beta$  value for the strategy of exploring New Physics. It seems that<sup>3</sup> some theorists have the power to “wormhole” into the future! A year later, however, both BaBar and Belle claimed the observation [6, 7] of  $\sin 2\beta/\phi_1 \sim 1$ , which turned out to be consistent with Standard Model (SM) expectations, i.e. confirming the Kobayashi–Maskawa [8] source of CPV.

In Fig. 1.3 we illustrate how the summer 2001 measurements by Belle and BaBar “settled” the value for  $\sin 2\beta/\phi_1$ . The band is some mean value, roughly of 2002. With impressive accumulation of data, as seen in the bars at the bottom of the figure, the measured mean remains more or less the same.

*What if  $\sin 2\beta/\phi_1$  stayed close to zero?* Well, as stated already, it certainly didn’t. Otherwise, you would have heard much more about it—a definite large deviation from the SM has been found! For even in the last century, one expected from indirect data that  $\sin 2\beta/\phi_1$  had to be nonzero within SM (see Fig. 1.4). Note that within SM, with the standard phase convention of taking  $V_{cb}$  to be real, and placing the unique CPV phase in  $V_{ub}$ , one has  $\beta/\phi_1 = -\arg V_{td}$  [10]. The awkward notation of  $\beta/\phi_1$  (like the original  $J/\psi$ ) is just to respect the friendly competition across the Pacific Ocean.

<sup>3</sup>This parable was meant as a joke, but as I was preparing for my SUSY2007 talk (the starting point of this volume), the paper “Search for Future Influence from L.H.C.” appeared [5]. So it was not a joke after all. The future can wormhole back!?! It seems to have received preliminary confirmation with the magnet accident right after successful first beam at LHC in September 2008.

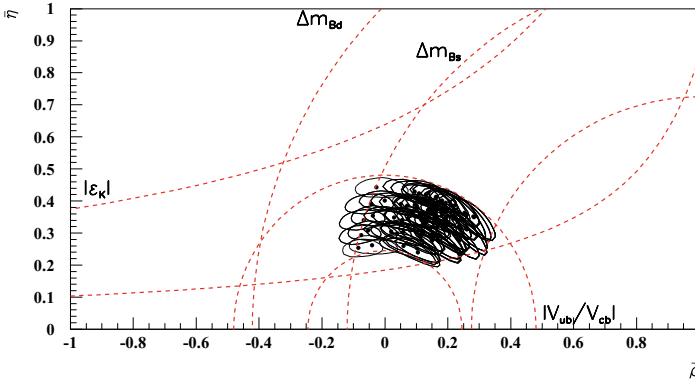


**Fig. 1.4** Expectation for  $\sin 2\beta/\phi_1$  measurement ca. 1998. [Source BaBar Physics Book, SLAC Report R-504, [9]; used with permission] This figure should be compared with Fig. 1.6; for definition of  $\bar{\rho}$  and  $\bar{\eta}$ , as well as a discussion of the CKM matrix and CPV in SM, see Appendix A

The measurement of  $\sin 2\beta/\phi_1$  is the measurement of the CPV phase in the  $B_d^0-\bar{B}_d^0$  mixing matrix element  $M_{12}^d$ . We recall that the discovery of  $B_d^0-\bar{B}_d^0$  mixing itself by the ARGUS experiment [11] more than 30 years ago was the first clear indication that the top is heavy, that it is *a v.e.v. scale quark*, a decade before the top quark was actually discovered at the Tevatron. The ARGUS discovery caused a Gestalt switch, and to this day we do not yet quite understand why the top is so heavy compared to other fermions.

Such is the impact of loop effects, and the power of the Flavor and TeV link. If an “anomaly” turns out<sup>4</sup> to be the harbinger, it becomes the page-turning *discovery* that we are looking for. With the  $B_d^0-\bar{B}_d^0$  mixing frequency  $\Delta m_{B_d}$  proportional to  $|V_{td}|^2 m_t^2$ , it is the *template* for flavor loops as probes into high energy scales. So let us learn from it.

### 1.3 The Template: $\Delta m_{B_d}$ , Heavy $\mathcal{T}$ op, and $V_{td}$

As shown in Fig. 1.5, the  $B_d^0-\bar{B}_d^0$  mixing amplitude  $M_{12}^d$  is generated by the box diagram involving two internal  $W$  bosons and top quarks in the loop.

Normally, heavy particles such as the top quark would decouple from the loop in the heavy  $m_t \rightarrow \infty$  limit. After all, our daily experience does not seem to depend on yet-unknown heavy particles. This is the case for QED and QCD. However, for chiral gauge theories, such as the electroweak theory, the longitudinal component of the  $W$  boson, which is a charged Higgs scalar that got “eaten” by the  $W$  through spontaneous symmetry breaking, couples to the top quark *mass*. This gives rise to

<sup>4</sup>Two other more recent “What if?” situations are the measurements of  $\sin 2\Phi_{B_s}$  (Chap. 3), i.e. the CPV phase in  $B_s$  mixing, and  $B_s^0 \rightarrow \mu^+\mu^-$  (Chap. 6), both ended up being consistent with SM. *What if not!?*

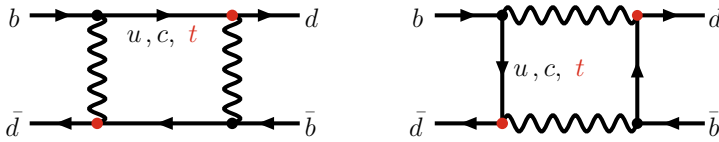


**Fig. 1.5** The box diagrams that induce  $B_d^0-\bar{B}_d^0$  mixing. The top quark dominates the loop, and brings in the CPV phase through  $(V_{td}^*V_{tb})^2$

the phenomenon of *nondecoupling* of the top quark effect from the box diagram, i.e.  $M_{12}^d \propto (V_{td}^*V_{tb})^2 m_t^2$  to first approximation. It illustrates the *Higgs affinity* of heavy SM-like (chiral) quarks, namely  $\lambda_t \sim 1$  for the top quark Yukawa coupling. It is the Yukawa coupling to the Higgs boson that links the left- and right-handed chiral quarks, which are in different representations of the  $SU(2) \times U(1)$  electroweak gauge group, that generates quark masses. The rather large Yukawa coupling of the top quark compensates for the suppression of  $V_{td}^{*2}$  ( $\sim 10^{-4}$  in strength), bringing forth the CPV phase  $\sin 2\beta/\phi_1$  that was measured by the B factories in 2001.

The formula for  $M_{12}^d$  is very well known. Since the top quark dominates, one has

$$M_{12}^d \simeq -\frac{G_F^2 m_B}{12\pi^2} \times \eta_B m_W^2 S_0(m_t^2/m_W^2) \times f_{B_d}^2 B_{B_d} \times (V_{td}^*V_{tb})^2. \quad (1.2)$$

From this formula, we can get a feeling of what a loop calculation involves. The first factor with  $G_F^2$  counts the number of  $W$  propagators. The second factor is from short distance physics and calculable, with  $\eta_B \approx 0.6$  a QCD correction factor, and

$$S_0(m_t^2/m_W^2) \approx 0.55 m_t^2/m_W^2, \quad (1.3)$$

for our purpose, which is proportional to  $m_t^2$  as stated before. For the third factor, the decay constant  $f_{B_d}$  accounts for the probability for the  $b$  and  $\bar{d}$  quarks to meet and annihilate (“wave function at the origin”), and the “bag” parameter  $B_{B_d}$  is to compensate for the so-called vacuum insertion approximation, of separating the  $[\bar{b}d][\bar{d}b]$  4-quark operator into a product of two currents, then taking the matrix element of e.g.  $[\bar{b}d]$  between the  $|B_d\rangle$  and  $|0\rangle$  states. The decay constant  $f_{B_d}$  is accessible in  $B^+$  decay, the measurement of which can help infer  $f_{B_d}$ . But in general we rely on nonperturbative calculational methods like lattice QCD for information on  $f_{B_d}^2 B_{B_d}$ . Finally,  $(V_{td}^*V_{tb})^2$  is just the product of the four CKM factors from the weak interaction vertices.

We recall that  $K^0-\bar{K}^0$  mixing, or  $\Delta m_K$ , provided the basic source of insight for the Glashow–Iliopoulos–Maiani (GIM) mechanism [12], which led to the prediction of the charm quark before it was actually discovered, even an estimation of the charm mass (using a formula similar to (1.2)). With 3 generations, as suggested by Kobayashi and Maskawa [8] (KM), the top quark in the box diagram provided the SM explanation for the origin of CPV in  $K_L \rightarrow 2\pi$  decay [13], the  $\varepsilon_K$  parameter.

None of this, however, prepared people for the  $B_d$  system. It is curious to note that the charm contribution to  $K^0-\bar{K}^0$  mixing gives the correct order of magnitude

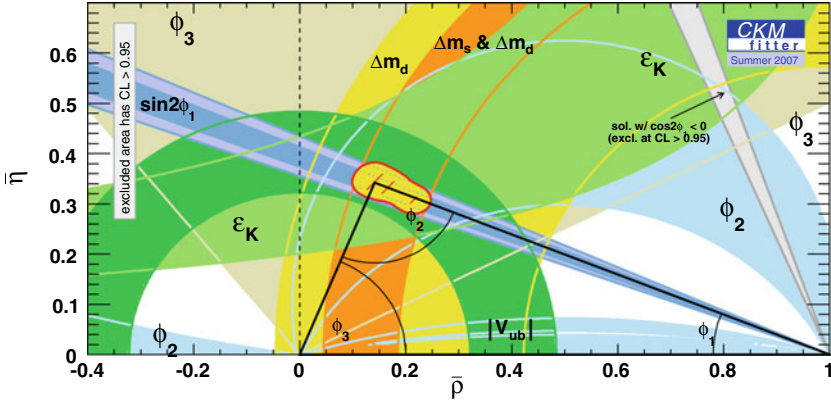


**Fig. 1.6** CKM unitarity fit to all data as of summer 2007 [from the CKMfitter group [19], used with permission]. The triangle corresponds to  $V_{ud}^* V_{ub} + V_{cd}^* V_{cb} + V_{td}^* V_{tb} = 0$

for  $\Delta m_K$ , i.e.  $x_K \equiv \Delta m_K / \Gamma_{K_S} \sim 0.5$ . This led people to expect that  $x_{B_d} \equiv \Delta m_{B_d} / \Gamma_B < 1\%$ , even when the  $B$  lifetime was found [14, 15] to be greatly prolonged (which was itself<sup>5</sup> a great *discovery*). This is because the  $B$  meson decay width is still so much larger than that of the kaon, and since people tacitly assumed that the top quark was “just around the corner”, meaning of order 20–30 GeV or less (remember the march of the  $e^+e^-$  colliders, from PEP, PETRA to Tristram, even SLC and LEP). Thus, when  $\Delta m_{B_d}$  was found to be comparable to  $\Gamma_B$ , it was quite a shock to realize that the top quark is actually a special, *v.e.v. scale* particle.

So, loop effects in  $B$  physics provided insight into the TeV scale. But that was just the beginning. It is truly remarkable that the measured  $x_{B_d} \sim 0.8$  was just right to allow the beautiful, but originally somewhat esoteric (because of the  $x_{B_d} \ll 1$  mindset), method [16, 17] for measuring mixing-dependent CPV, to suddenly appear realistic in the late 1980s. This paved the way for the construction of the  $B$  factories, but not without the key experimental insight, i.e. to boost the  $\Upsilon(4S)$ , hence the produced  $B\bar{B}$  pair. This allowed one to capitalize on vertex detector development by going to an asymmetric energy collider [18]. After intense studies, two  $B$  factories, one at SLAC in California, one at KEK in Japan, were constructed in the 1990s.

All this impact, stimulated by the observation of the nondecoupled loop effect of the heavy top quark in Fig. 1.5, at the tiny DORIS  $e^+e^-$  collider. Rather cost-effective indeed. Providing diverse probes of flavor physics, often using loop effects, the  $B$  factories themselves were quite cost-effective, as we shall see.

As we will only be interested in New Physics (NP), we note that extensive studies at the  $B$  factories (and elsewhere) indicate that  $b \rightarrow d$  transitions are consistent with the SM [20]. As illustrated in Fig. 1.6, no discrepancy is apparent with the CKM (Cabibbo–Kobayashi–Maskawa) unitarity triangle<sup>6</sup>

<sup>5</sup>The fact  $|V_{ub}|^2 \ll |V_{cb}|^2 \ll |V_{tb}|^2 \cong 1$  came only through experiment, and is not yet explained, not within SM.

<sup>6</sup>We will often refer to the Particle Data Group [10] for many useful discussions.

$$V_{ud}^* V_{ub} + V_{cd}^* V_{cb} + V_{td}^* V_{tb} = 0, \quad (1.4)$$

which is the  $db$  element of  $V^\dagger V = I$ , where  $V$  is the quark mixing matrix. An enormous amount of information and effort has gone into this figure (compare Fig. 1.4), the phase of  $V_{td}^* V_{tb}$  being only one of the prominent entries that emerged through the B factory studies. Although there are some tensions here and there, e.g. in the value of  $|V_{ub}|$ , in general, we see remarkable consistency with CKM expectations. And the CKM fit continues to improve.

What about loop-induced  $b \rightarrow s$  transitions? This frontier for heavy flavor physics offers a window into a multitude of possible TeV scale physics. It will therefore be our starting point of the next chapter.

## References

1. Cahn, R.: Talk at SLAC Summer Institute 2006, Stanford, 25 July 2006
2. Hitlin, D.: Plenary Talk at the XXXth International Conference on High Energy Physics (ICHEP2000), Osaka, Japan. 31 July 2000
3. Aihara, H.: Plenary Talk at the XXXth International Conference on High Energy Physics (ICHEP2000), Osaka, Japan. 31 July 2000
4. Kagan, A.L., Neubert, M.: Phys. Lett. B **492**, 115 (2000). [arXiv:hep-ph/0007360](https://arxiv.org/abs/hep-ph/0007360)
5. Nielsen, H.B., Ninomiya, M.: Int. J. Mod. Phys. A **23**, 919 (2008). [arXiv:0707.1919](https://arxiv.org/abs/0707.1919) [hep-ph]
6. Aubert, B., et al.: [BaBar Collaboration]: Phys. Rev. Lett. **87**, 091801 (2001)
7. Abe, K., et al.: [Belle Collaboration]: Phys. Rev. Lett. **87**, 091802 (2001)
8. Kobayashi, M., Maskawa, T.: Prog. Theor. Phys. **49**, 652 (1973)
9. BaBar Physics Book. <http://www.slac.stanford.edu/pubs/slacreports/slac-r-504.html>
10. Tanabashi, M., et al.: [Particle Data Group]: Phys. Rev. D **98**, 030001 (2018). <http://pdg.lbl.gov/>
11. Albrecht, H., et al.: [ARGUS Collaboration]: Phys. Lett. B **192**, 245 (1987)
12. Glashow, S.L., Iliopoulos, J., Maiani, L.: Phys. Rev. D **2**, 1285 (1970)
13. Christenson, J.H., Cronin, J.W., Fitch, V.L., Turlay, R.: Phys. Rev. Lett. **13**, 138 (1964)
14. Fernandez, E., et al.: [MAC Collaboration]: Phys. Rev. Lett. **51**, 1022 (1983)
15. Lockyer, N.S., et al.: [MARK II Collaboration]: Phys. Rev. Lett. **51**, 1316 (1983)
16. Carter, A.B., Sanda, A.I.: Phys. Rev. Lett. **45**, 952 (1980); Phys. Rev. D **23**, 1567 (1981)
17. Bigi, I.I.Y., Sanda, A.I.: Nucl. Phys. B **193**, 85 (1981)
18. Oddone, P.: At UCLA Workshop on Linear Collider  $B\bar{B}$  Factory Conceptual Design. Los Angeles, California (1987). January
19. CKMfitter group: <http://ckmfitter.in2p3.fr>
20. Heavy Flavor Averaging Group: (HFLAV; acronym changed from HFAG to HFLAV (2017)). <http://www.slac.stanford.edu/xorg/hflav>

# Chapter 2

## CP Violation in Charmless $b \rightarrow s\bar{q}q$ Transitions



With the study of CP violation in  $b \rightarrow d$  transitions seemingly in good agreement with Standard Model expectations, the subject of CPV studies in charmless  $b \rightarrow s$  transitions (including  $b\bar{s} \leftrightarrow s\bar{b}$ ) became the frontier of heavy flavor research. Because there is little CPV weak phase in the controlling product of CKM matrix elements for loop induced  $b \rightarrow s$  transitions,  $V_{ts}^*V_{tb}$ , any observed deviation could indicate New Physics. As transitions between 3rd to 2nd generation quarks, the subject also has  $\tau \rightarrow \mu$  transition echoes in the lepton sector, which is covered in Chap. 9. More generally, with the Sakharov conditions [1] that link CPV with the Baryon Asymmetry of the Universe (BAU), i.e. why there is no trace of antimatter in our Universe, we do expect NP sources for CPV. It is well known that the 3 generation SM falls short by *many orders of magnitude* from the CPV that is needed to generate the observed BAU, which has been the strongest motivation to search for New Physics in CP violation.

In this Chapter, we focus on three topics: the measurement of mixing- or time-dependent CPV (TCPV) in charmless  $b \rightarrow s\bar{q}q$  modes versus  $b \rightarrow c\bar{c}s$  modes,  $\Delta\mathcal{S}$ , where we elucidate also how TCPV studies are conducted; the discovery of  $\Delta\mathcal{A}_{K\pi}$  between direct CPV (DCPV) in  $B^+ \rightarrow K^+\pi^0$  and  $B^0 \rightarrow K^+\pi^-$  decays; and the DCPV asymmetry  $\mathcal{A}_{B^+ \rightarrow J/\psi K^+}$ . We close with an appraisal of New Physics search in hadronic  $b \rightarrow s$  transitions. The pursuit of  $\sin 2\Phi_B$  measurement (analogous to  $\sin 2\phi_1/\beta$  for  $B_d$  system) at the Tevatron and LHC, the frontier of the past decade, will be discussed in the next Chapter. Further charmless  $b \rightarrow s$  probes of different New Physics are covered in subsequent Chapters.

### 2.1 The $\Delta\mathcal{S}$ Pursuit

The B factories were built to measure mixing-, or time-dependent CPV (TCPV) in the  $B^0 \rightarrow J/\psi K_S$  mode [2, 3]. This is the billion dollar question that started with the ARGUS discovery of large  $B^0-\bar{B}^0$  mixing [4]. With the suggestion by Oddone [5] of boosting the  $\Upsilon(4S)$ , thereby boosting the  $B^0$  and  $\bar{B}^0$  mesons, by the late 1980s,



both SLAC and KEK initiated feasibility studies for  $e^+e^-$  colliders with asymmetric beam energies. The push towards asymmetric beam energies also contributed partly to the demise, in 1989, of the proposed PSI machine, which had a symmetric double ring design. By 1994 or so, both the PEP-II/BaBar and KEKB/Belle accelerator and detector complexes entered construction phase.

Several miraculous points that aid B factory studies are worthy of note. First,  $m_B$  is so close to  $m_{\Upsilon(4S)}/2$ , such that not only the  $\Upsilon(4S)$  decays practically 100% to  $B^0\bar{B}^0$  and  $B^+B^-$  pairs, the  $B$  mesons are produced with rather small momenta. Second,  $m_{B^+}$  and  $m_{B^0}$  are rather close in mass, such that charged and neutral  $B$  mesons are almost equally produced. Their production ratio is of course measured. One third point, which will be immediately discussed in the following, is the ‘‘EPR’’ coherence (or entanglement) of the  $B^0\bar{B}^0$  meson pair from  $\Upsilon(4S)$  decay. That is, although each meson starts to oscillate between  $B^0$  and  $\bar{B}^0$  after being produced, the pair remains in coherence, such that the determination of the  $B^0$  (or  $\bar{B}^0$ ) nature of one meson at time  $t$  in the  $\Upsilon(4S)$  frame, the other meson starts to oscillate from a  $\bar{B}^0$  (or  $B^0$ ) from time  $t$  onwards. This quantum coherence has in fact been tested at Belle [6]. Of course, Quantum Mechanics is again affirmed. The fraction of produced  $B^0$  and  $\bar{B}^0$  pairs (out of 76M) that disentangle and decay incoherently is measured to be  $0.029 \pm 0.057$ , which is consistent with zero.

### 2.1.1 Measurement of TCPV at the B Factories

At B factories, TCPV measurement utilizes the coherent production of  $B^0\bar{B}^0$  pairs from  $\Upsilon(4S)$  decay. That is, as the produced  $B^0$  (and vice versa the  $\bar{B}^0$ ) undergoes oscillations back and forth from  $B^0$  to  $\bar{B}^0$ , the pair remains coherent. As the original  $B^0$  and  $\bar{B}^0$  are produced at the same time, if one measures at time  $t$  the decay of one  $B$  meson, and find that it decays as, say,  $B^0$ , we then know from quantum coherence that the other  $B$  meson is a  $\bar{B}^0$  meson at time  $t$ . From then on, this  $\bar{B}^0$  meson again oscillates back and forth from  $\bar{B}^0$  to  $B^0$ , until time  $\Delta t$  later, where it also decays.

Having this picture visualized, we can go further and discuss what is done experimentally to measure TCPV. We repeat (A.9) of Appendix A.3 for TCPV asymmetry,

$$\begin{aligned} A_{\text{CP}}(\Delta t) &\equiv \frac{\Gamma(\bar{B}^0(\Delta t) \rightarrow f) - \Gamma(B^0(\Delta t) \rightarrow f)}{\Gamma(\bar{B}^0(\Delta t) \rightarrow f) + \Gamma(B^0(\Delta t) \rightarrow f)} \\ &= -\xi_f (\mathcal{S}_f \sin \Delta m \Delta t + \mathcal{A}_f \cos \Delta m \Delta t), \end{aligned} \quad (2.1)$$

where  $\xi_f$  is the  $CP$  eigenvalue of final state  $f$ , and  $\Delta m \equiv \Delta m_{B_d}$ . This asymmetry measures, at time  $\Delta t$ , the difference in rate between a state tagged at  $t = 0$  as  $\bar{B}^0$  versus  $B^0$ . Thus, the  $\Gamma$ 's are really shorthands for differential decay rates. With the  $\Delta t$  distribution of  $A_{\text{CP}}(\Delta t)$ , which are actually done by fitting  $\Gamma(\bar{B}^0(\Delta t) \rightarrow f)$  and  $\Gamma(B^0(\Delta t) \rightarrow f)$  distributions, the CPV parameters  $\mathcal{S}_f$  and  $\mathcal{A}_f$  are just the Fourier coefficients of the sine and cosine  $\Delta t$  oscillation terms. Of course, experimentally

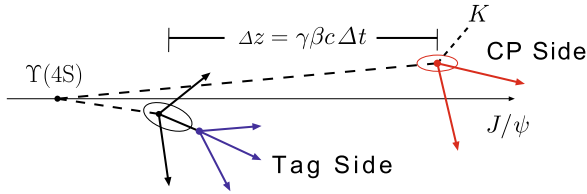
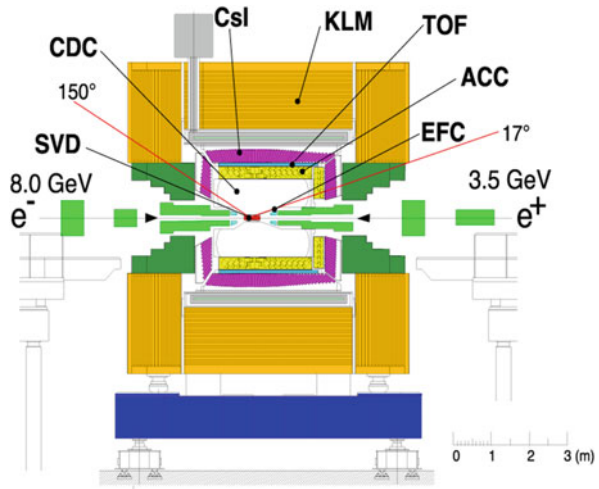


**Fig. 2.1** Figure illustrating TCPV measurement. The  $\Upsilon(4S)$ , which decays into a  $B^0-\bar{B}^0$  pair, is boosted in the  $z$  direction. After one  $B$  is tagged by its decay, quantum coherence dictates the other  $B$  would start evolving from the conjugate of the tagged state. At time  $\Delta t = \gamma\beta c\Delta z$  (can be negative), where  $\Delta z$  is the measured difference between the decay vertices, the other  $B$  decays into a  $CP$  eigenstate such as  $J/\psi K_S$ . See text for further discussion

**Fig. 2.2** Schematic side view of the Belle detector, with markings of the subdetector systems. [Source <http://belle.kek.jp/belle/transparency/detector1.html>]



one has to correct for inefficiencies and dilution factors, which we do not go into. As discussed in Chap. 1 and Appendix A,  $\mathcal{S}_{J/\psi K^0}$  is just  $\sin 2\beta/\phi_1$ , the CPV phase of  $B^0-\bar{B}^0$  mixing amplitude, while  $\mathcal{A}_{J/\psi K^0}$  is the direct CPV for this mode.

To conduct  $A_{CP}(\Delta t)$  measurement, as illustrated in Fig. 2.1, one needs to,

- (1) Tag the flavor of one  $B$  decay ( $B^0$  or  $\bar{B}^0$ ) at “ $t = 0$ ”, and
- (2) Reconstruct the other  $B$  in a  $CP$  eigenstate (cannot tell  $B^0$  versus  $\bar{B}^0$ ),
- (3) Measure decay vertices for both  $B$  decays.

For the last point, one utilizes the boost along the  $z$  or beam direction, and  $\Delta z \cong \gamma\beta c\Delta t$  is the measured difference between the two  $B$  decay vertices. The  $\gamma\beta$  factor is 0.56 and 0.43 for PEP-II and KEKB, respectively. With  $B$  lifetime of order picosecond,  $\gamma\beta c\tau_B$  is of order 200 micron or so. For the  $CP$  side, one therefore demands a  $\sigma_z$  resolution of less than 100 micron.

The BaBar and Belle detectors are rather similar to each other. A side view of the Belle detector is given in Fig. 2.2 showing subdetectors. The subdetectors of

BaBar and Belle consist of a silicon vertex detector (SVT/SVD), a central drift chamber (DCH/CDC), an electromagnetic calorimeter (EMC/ECL) based on CsI(T $\ell$ ), a particle identification detector (PID) system, superconducting solenoid magnet, and an iron flux return that is instrumented (IFR for BaBar) for  $K_L$  and muon detection (hence KLM for Belle).

The difference between the two detectors are basically only in the PID system that is crucial for flavor tagging, in particular the task of charged  $K/\pi$  separation at various energies. Note that, even for  $B \rightarrow J/\psi K$  decay,  $p_K$  is almost 1.7 GeV/c and rather relativistic, and in addition one has the boost. The Belle PID system consists of Aerogel Cherenkov Counters (ACC), a threshold device with several indices of refraction  $n$  for the silica aerogel for different angular coverage, plus a TOF counter system. BaBar uses the DIRC, basically a system of quartz bars that generate and guide the Cherenkov photons (by internal reflection) and project them into a water tank at the back end (called the Stand-off-box, or SOB) of the detector. It provides more dynamical information, but the large SOB is a little unwieldy.<sup>1</sup> One other difference between Belle and BaBar is the Interaction Region (IR), which is at the intersection between detector and accelerator. PEP-II made the conservative choice of zero angle crossing (electrostatic beam separation by permanent magnets), while KEKB used finite angle crossing. This eventually became a main limiting factor for the luminosity reach of PEP-II, although it ensured faster accelerator turn-on. In any case, it is truly impressive that both accelerators reached beyond design luminosities, especially since the asymmetric energy design was a new challenge.

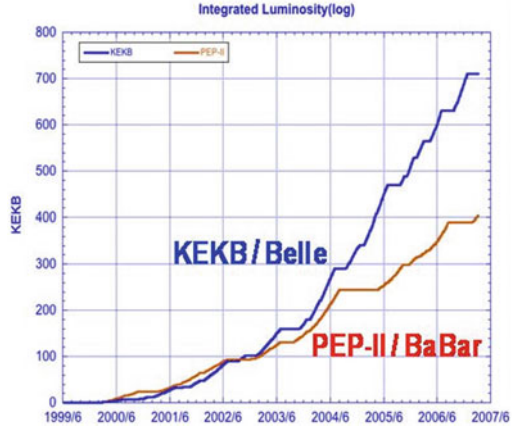
The real novelty of the B factories, of course, is the asymmetric beam energies. The  $\gamma\beta$  factor for the produced  $\Upsilon(4S)$  is 0.56 and 0.43, respectively, for PEP-II and KEKB. Boosting the  $B^0$  and  $\bar{B}^0$  mesons allowed the time difference  $\Delta t \cong \Delta z/\beta\gamma c$  used in (2.1) to be inferred from the decay vertex difference  $\Delta z$  in the boost direction, while the proximity of  $2m_{B^0}$  to  $m_{\Upsilon(4S)}$  means rather minimal lateral motion. Both the PEP-II and KEKB accelerators were commissioned in 1999 with a roaring start. By 2001, KEKB outran PEP-II in the instantaneous luminosity, and in integrated luminosity as well by the following year (see Fig. 2.3). In April 2008, PEP-II dumped its beam for the last time.

With the good performance of the accelerators, and with relatively standard detectors, by 2001, the measurement of the gold-plated mode of  $B^0 \rightarrow J/\psi K^0$  (including  $K_L^0$ ), was settled. As can be seen from Fig. 1.3, the mean value between Belle and BaBar remained largely unchanged since then. It would seem that the *raison d'être* of the B factories was accomplished just two years after commissioning!

---

<sup>1</sup>The aerogel technique was originally developed at BaBar, and adopted by Belle when there was insufficient confidence in the original design of a RICH detector system. When BaBar adopted the innovative DIRC, the extra space available, together with budget pressures, lead to a slight compromise of the EMC system.

**Fig. 2.3** Comparison of integrated luminosities achieved by KEKB/Belle and PEP-II/BaBar, up to early summer 2007



### 2.1.2 TCPV in Charmless $b \rightarrow s\bar{q}q$ Modes

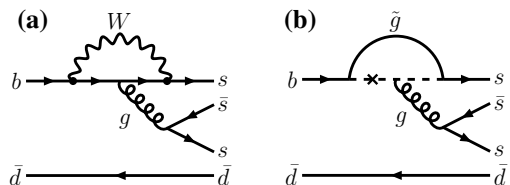
With the measurement of TCPV in  $B^0 \rightarrow J/\psi K_S$  settled in summer 2001, attention quickly turned to the  $b \rightarrow s$  penguin modes, where a virtual gluon is emitted from the virtual top quark in the vertex loop.

Let us take  $B^0 \rightarrow \phi K_S$  as example [7], where, as shown in Fig. 2.4a, the virtual gluon pops out an  $s\bar{s}$  pair. The  $b \rightarrow s$  penguin amplitude is practically real within SM, just like the tree level  $B^0 \rightarrow J/\psi K_S$ . This is because  $V_{us}^* V_{ub}$  is very suppressed, so the  $c$  and  $t$  contributions carry equal and opposite CKM coefficients  $V_{ts}^* V_{tb} \cong -V_{cs}^* V_{cb}$ , which is practically real, as can be seen from (A.3). Thus, one has the SM prediction,

$$\mathcal{S}_{\phi K_S} \cong \sin 2\phi_1/\beta, \quad (\text{SM}) \quad (2.2)$$

where  $\mathcal{S}_{\phi K_S}$  is the analogous TCPV measure in the  $B^0 \rightarrow \phi K_S$  mode, following the  $\mathcal{S}_f$  notation of (2.1). New physics induced flavor changing neutral current (FCNC) and CPV effects, such as having supersymmetric (SUSY) particles in the loop (for example,  $\tilde{b}-\tilde{s}$  squark mixing, Fig. 2.4b), could break this equality. That is, deviations from (2.2) would indicate New Physics. This prospect prompted the experiments to search vigorously.

**Fig. 2.4** **a** Strong penguin ( $P$ ) diagram for  $\bar{B}^0 \rightarrow \phi \bar{K}^0$  in SM, and **b** a possible diagram in SUSY with  $\tilde{b}-\tilde{s}$  squark mixing, which is illustrated by the cross on the squark line inside the loop



The first ever TCPV study in charmless  $b \rightarrow s\bar{q}q$  modes was performed for  $B^0 \rightarrow \eta' K_S$  [8] by Belle in 2002 with 45M  $B\bar{B}$  pairs [9]. Part of the motivation is the large enhanced rate, which is still not fully understood. But many might remember better the big splash made by Belle in summer 2003, where  $\mathcal{S}_{\phi K_S}$  was found to be opposite in sign [10] to  $\sin 2\phi_1/\beta$ , where the significance of deviation was more than  $3\sigma$ . However, the situation softened by 2004, and became far less dramatic. What happened was that the Belle value for  $\mathcal{S}_{\phi K_S}$  changed by  $2.2\sigma$ , shifting from  $\sim -1$  in 2003, to  $\sim 0$  in 2004. 123M  $B\bar{B}$  pairs were added to the analysis in 2004, but they gave the results with sign *opposite* to the earlier data of 152M  $B\bar{B}$  pairs. The new data was taken with the upgraded SVD2 silicon detector, which was installed in summer 2003. The SVD2 resolution was studied with  $B$  lifetime and mixing and was well understood, while  $\sin 2\phi_1$  measured in  $J/\psi K_S$  and  $J/\psi K_L$  modes showed good consistency between SVD2 and SVD1. Many other systematics checks were also done. By Monte Carlo study of pseudo-experiments, Belle concluded [11] that there is 4.1% probability for the  $2.2\sigma$  shift. This is a sobering and useful reminder, especially when one is conducting New Physics search, that large fluctuations do happen.

The study at Belle and BaBar expanded to include many charmless  $b \rightarrow s\bar{q}q$  modes. After several years of vigorous pursuit, some deviation persisted in an interesting but somewhat nagging kind of way. Let us not dwell on analysis details, except stress that this became one of the major, concerted efforts at the B factories. For a snapshot, compared with the 2007 average of  $\mathcal{S}_{c\bar{c}s} = 0.681 \pm 0.025$  [12] over  $b \rightarrow c\bar{c}s$  transitions,  $\mathcal{S}_f$  is smaller in practically all measured  $b \rightarrow s\bar{q}q$  modes (see Fig. 2.5), with the naive mean<sup>2</sup> of  $\mathcal{S}_{s\bar{q}q} = 0.56 \pm 0.05$  [12]. That is,

$$\mathcal{S}_{s\bar{q}q} = 0.56 \pm 0.05, \quad \text{vs} \quad \mathcal{S}_{c\bar{c}s} = 0.681 \pm 0.025. \quad (\text{HFAG 2007}) \quad (2.3)$$

The deviation  $\Delta\mathcal{S} \equiv \mathcal{S}_{s\bar{q}q} - \mathcal{S}_{c\bar{c}s} < 0$  was only  $2.2\sigma$  from zero, and the significance was slowly diminishing. However, it is worthwhile to stress that the persistence over several years, and in multiple modes, taken together made this “ $\Delta\mathcal{S}$  problem” a potential indication for New Physics from the B factories. Despite the lack in significance, it was not taken lightly, as the experiments were not able to “make it go away”. By Summer 2008 and onwards, however, HFAG updates suggest no deviation, and the “ $\Delta\mathcal{S}$  problem” now rests in the errors.

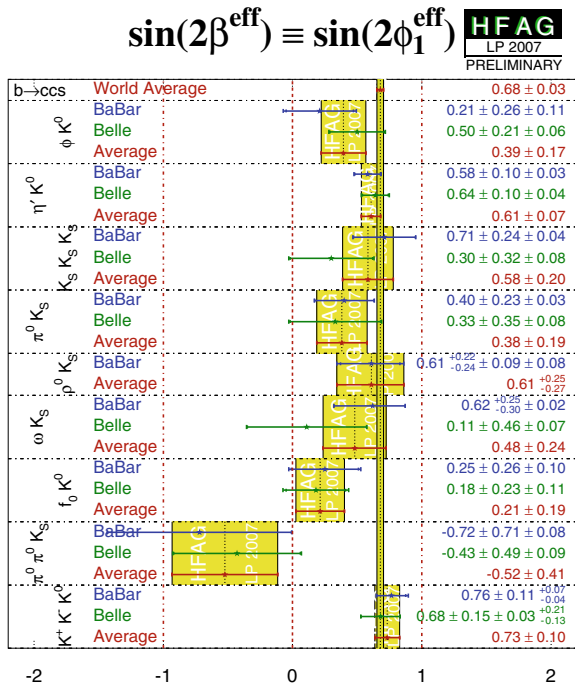
One reason that kept the interest is that theoretical studies, although troubled by hadronic effects, all gave  $\mathcal{S}_{s\bar{q}q}$  values that are *above* (see e.g. [13–16])  $\mathcal{S}_{c\bar{c}s}$ , or

$$\Delta\mathcal{S}|^{\text{TH}} > 0. \quad (2.4)$$

---

<sup>2</sup>We use the LP2007 update by HFAG that excludes the  $\mathcal{S}_{f_0(980)K_S}$  result from BaBar at that time. The Heavy Flavor Averaging Group (HFAG) itself warns “treat with extreme caution” when using this BaBar result [12]. The value is larger than  $\mathcal{S}_{c\bar{c}s}$  and is very precise, with errors 3 times smaller than the  $\phi K_S$  mode. But  $f_0(980)K_S$  actually has smaller branching ratio than  $\phi K_S$ !

**Fig. 2.5** Measurements of  $S_f$  in  $b \rightarrow s\bar{q}q$  penguin modes [12]. [Summer 2007 results from HFAG, used with permission] see footnote 2 for comment on the  $B^0 \rightarrow f_0(980)K_S$  mode



This added to the tension that was already present with the experimental situation, i.e. what lies behind the apparent  $\Delta S|^{EXP} < 0$ .

Even if New Physics hints evaporated, we remark that there are limitations for what one can interpret from deviations in penguin dominant  $b \rightarrow s$  hadronic modes. While a large, *definite* effect in a single mode, such as the relatively clean  $\phi K_S$  mode (pure  $b \rightarrow s\bar{s}s$  penguin) would clearly indicate NP, many of these modes, as well as theoretical approaches, suffer from large hadronic uncertainties, such that the NP effect would vary from mode to mode. So, whether  $\phi K_S$  or  $\eta' K_S$ , or the combined effect in  $b \rightarrow s\bar{q}q$ , one may not gain much more information by averaging over modes. We also note that the mode with the largest branching fraction, and the first mode to be studied [9], i.e.  $\eta' K_S$ , was in good agreement with  $b \rightarrow c\bar{c}s$ . This is not surprising, for it is now believed that the enhancement of  $B^0 \rightarrow \eta' K^0$  is not due so much to New Physics, but some combination of “hadronic” effects.

It is a bit frustrating for the B factory worker that, after many years of devoted work, the deviation dropped below  $2\sigma$ , and  $\Delta S$  is no longer an issue. But with the advent of the super B factory,  $\Delta S$  would surely be pursued. However, given the above experience, we need a clearer litmus test.

One possibility is a model-independent geometric approach, which suggests [17] that, once one has enough experimental precision, a deviation as little as a couple of degrees would indicate New Physics. It would be splendid if there is no loophole in this argument, for this is what is needed when we reach the precision of the Super B factory era. However, this approach needs better elucidation, before the

commissioning of Belle II, for people to grasp and appreciate the insight. Other approaches to ascertain at what level a  $\Delta\mathcal{S}_{(f)}$  deviation can be called an indication for New Physics, should also be developed.

One may think that the LHC, and the LHCb experiment in particular, should be able to make great progress on  $\Delta\mathcal{S}$  measurement. Curiously, because of lack of good vertices, or the presence of neutral ( $\pi^0, \gamma$ ) particles (a weakness for LHCb), in the leading channels of  $\eta/K_S, \phi/K_S$  and  $K_S\pi^0$ , the situation may not improve greatly with LHCb data. An improved LHCb detector (i.e. after upgrade), or some different approach, needs to be developed.

*Let us see what Belle II could unveil for us in  $\Delta\mathcal{S}$  measurements.*

## 2.2 The $\Delta\mathcal{A}_{K\pi}$ Problem

A second possible indication for physics beyond SM (BSM) arose in  $b \rightarrow s\bar{q}q$  decays. It became widely known through the Belle paper published in *Nature* [18] in March 2008. Unlike the situation with  $\Delta\mathcal{S}$ , experimentally it is very firm. But for interpretation, data now favors “hadronic effect”.

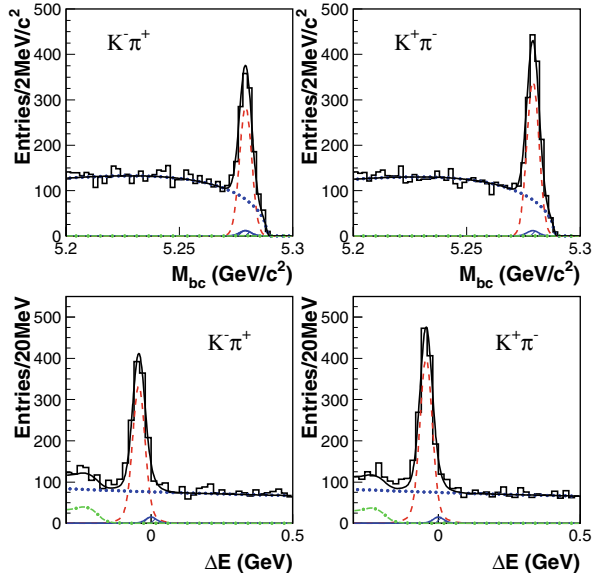
### 2.2.1 Measurement of DCPV in $B^0 \rightarrow K^+\pi^-$ Decay

Just 3 years after the observation of TCPV in  $B^0 \rightarrow J/\psi K^0$ , direct CPV (DCPV) in the B system was claimed in 2004 between BaBar and Belle [19]. This attests to the prowess of the B factories, as it took 35 years for the same evolution in the K system [19].

Unlike mixing-dependent CPV, where one needs decay time information and tagging, the measurement of DCPV is a much simpler counting experiment. In the self-tagging modes such as  $K^\mp\pi^\pm$ , one simply counts the difference between the number of events in  $K^-\pi^+$  versus  $K^+\pi^-$ . Self-tagging means that a  $K^-\pi^+$  would be decaying from a  $\bar{B}^0$ , while  $K^+\pi^-$  comes from a  $B^0$ .

Of course, there is the standard rare  $B$  reconstruction techniques, to reject continuum (from  $e^+e^- \rightarrow q\bar{q}$ , where  $q$  is a  $u, d, s$  or  $c$  quark) and other backgrounds by some multivariate “filters”. We do not go into these technical details. But it is worthwhile to mention a special technique at the B factories that utilizes the kinematics of the  $\Upsilon(4S)$  production environment. One reconstructs  $m_B$  of a potential candidate, by replacing the measured energy sum with the known center-of-mass beam energy. This trick utilizes the fact that for  $\Upsilon(4S) \rightarrow B\bar{B}$  two body production (which has  $\sim 100\%$  branching fraction), the  $B$  meson would carry exactly the C.M.S. beam energy,  $E_{\text{CM}}/2$ . One then checks the signal region around  $\Delta E \sim 0$ , where the energy difference between the measured energy sum and  $E_{\text{CM}}/2$  should vanish for a genuine  $B$  candidate, but for a background event it would not vanish.

**Fig. 2.6**  $M_{bc}$  and  $\Delta E$  projection plots for  $\bar{B}^0 \rightarrow K^-\pi^+$  versus  $B^0 \rightarrow K^+\pi^-$  from Belle [20], based on 275M  $B\bar{B}$  pairs [Copyright (2004) by The American Physical Society]. The CPV asymmetry is apparent, with more  $K^+\pi^-$  events than  $K^-\pi^+$



Thus, the two standard variables are the *beam-constrained mass*  $M_{bc}$  (called “beam-energy substituted mass” by BaBar,  $m_{ES}$ ), and the *energy difference*  $\Delta E$ ,

$$M_{bc} = \sqrt{(E_{CM}/2)^2 - \sum (\mathbf{p}_i)^2}, \quad \Delta E = \sum E_i - E_{CM}/2, \quad (2.5)$$

where  $E_i$  and  $\mathbf{p}_i$  are the measured energy and momentum for particle  $i$ , and  $E_{CM} = \sqrt{s}$  is precisely known from the accelerator. A correctly reconstructed  $B$  meson event would peak in  $M_{bc}$  and  $\Delta E$ , as can be visualized by 1D projection plots illustrated in Fig. 2.6, while background events would not. Note that the  $K^\pm$  and  $\pi^\pm$  in  $B \rightarrow K^\pm \pi^\mp$ ,  $\pi^\pm \pi^\mp$  decays are rather highly boosted, hence PID performance is very critical for the separation of  $K^\pm \pi^\mp$  versus  $\pi^+ \pi^-$  events.

With these relatively standard techniques, it was a matter of time, and providence (which specific mode), for one to eventually catch the first DCPV measurement, which happened to be the  $B^0 \rightarrow K^+ \pi^-$  mode.

Indications for a negative DCPV in this mode, defined as

$$\mathcal{A}_{K^+\pi^-} \equiv \mathcal{A}_{CP}(B^0 \rightarrow K^+\pi^-) = \frac{\Gamma(\bar{B}^0 \rightarrow K^-\pi^+) - \Gamma(B^0 \rightarrow K^+\pi^-)}{\Gamma(\bar{B}^0 \rightarrow K^-\pi^+) + \Gamma(B^0 \rightarrow K^+\pi^-)}, \quad (2.6)$$

(basically the same definition as in (A.2)) had been emerging for a couple of years. BaBar announced (using 227M  $B\bar{B}$  pairs) a value [21] with  $4.2\sigma$  significance just before ICHEP 2004, while at that conference, the Belle measurement [20] (using 275M  $B\bar{B}$  pairs) was reported with  $3.9\sigma$  significance. The  $M_{bc}$  and  $\Delta E$  results from Belle are plotted in Fig. 2.6. It is clear by inspection that the number of



$\bar{B}^0 \rightarrow K^-\pi^+$  events are fewer than  $B^0 \rightarrow K^+\pi^-$ . The combined Belle and BaBar result that year was  $\mathcal{A}_{K^+\pi^-} = -0.114 \pm 0.020$ , with  $5.7\sigma$  significance, which established DCPV in the  $B$  system. The QCD factorization (QCDF) approach had predicted the opposite sign [22], while the perturbative QCD factorization (PQCD) approach [23, 24] predicted the correct sign and magnitude. Thus, the measurement has implications for the theory of hadronic  $B$  decays.

The CDF experiment at the Tevatron also measured  $\mathcal{A}_{K^+\pi^-}$  with  $1 \text{ fb}^{-1}$  data [25] at  $3.5\sigma$  significance, and the result is consistent with the B factories. Let us give a very brief account of the CDF study, as the production environment is quite different. Two opposite-charged track events from a common displaced vertex were selected. But there is not enough invariant mass resolution to separate different contributions clearly. Nor does CDF have sufficient PID capability to separate  $K^\pm$  from  $\pi^\pm$  in  $B$  decay (which is more boosted than at B factories). Using tagged  $D^{*\pm}$  decays, charged  $K$ ,  $\pi$  separation with  $dE/dx$  from tracker response is only at  $1.4\sigma$ . But by combining kinematic and PID information into an unbinned maximum likelihood fit, CDF obtained  $\mathcal{A}_{K^+\pi^-} = -0.086 \pm 0.023 \pm 0.029$ , based on  $1 \text{ fb}^{-1}$  data. This should be compared with the subsequent values from BaBar [26],  $-0.107 \pm 0.018_{-0.004}^{+0.007}$  (383M  $B\bar{B}$ ), and Belle [18],  $-0.094 \pm 0.018 \pm 0.008$  (535M  $B\bar{B}$ ), where statistical error dominates.

Comparing the BaBar and Belle studies, one can see that the analysis philosophy is slightly different, and in any case, the  $5.5\sigma$  significance for BaBar versus  $4.8\sigma$  for Belle largely reflects a stronger central value for BaBar. Comparing CDF versus the B factory results, one can see the effect of lack of PID on the systematic error. A statistical power of  $1.6 \text{ fb}^{-1}$  at CDF could already be comparable to current B factories. However, without improvement in systematic error, CDF cannot be competitive in this study. The advent of LHCb experiment changed this situation, since it has active RICH systems for PID.

We have spent some effort describing how DCPV studies are done, at B factory versus hadronic environment, largely for sake of comparison. Incorporating even the CLEO measurement [19] done in 2000 (with just  $9.7\text{M } B\bar{B}$ ), the 2007 world average [12] was<sup>3</sup>

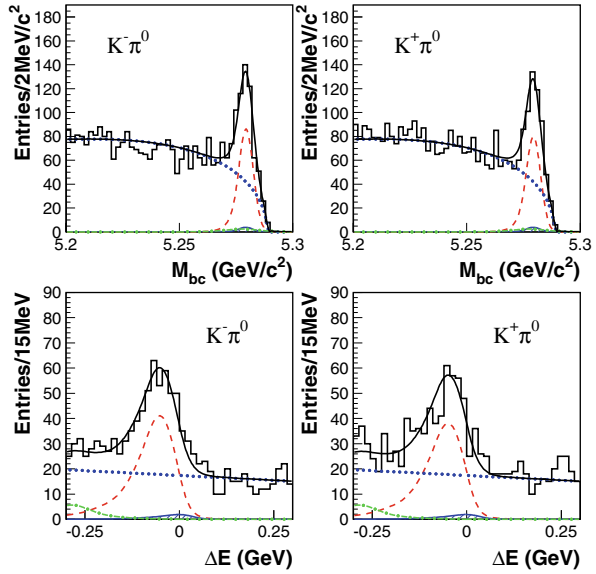
$$\mathcal{A}_{B^0 \rightarrow K^+\pi^-} = -0.097 \pm 0.012. \quad [\text{HFAG 2007}] \quad (2.7)$$

This by itself does not suggest New Physics, but rather, it indicates the presence of a finite strong phase  $\delta$  between the strong penguin ( $P$ ) and tree ( $T$ ) amplitudes, where the latter provides the weak phase via  $V_{us}^* V_{ub}$  (see Appendix A). Most QCD based factorization approaches failed to predict  $\mathcal{A}_{K^+\pi^-}$ , largely because of lack of control over how to properly generate  $\delta$ .

Even in 2004, however, there was a whiff of a puzzle [20]. With large errors,  $\mathcal{A}_{\text{CP}}(B^+ \rightarrow K^+\pi^0)$  was found to be consistent with zero for both Belle and BaBar, and the mean was  $\mathcal{A}_{K^+\pi^0} = +0.049 \pm 0.040$ . We plot the  $M_{bc}$  and  $\Delta E$  results from

<sup>3</sup>The 2017 PDG update value, dominated by LHCb, is [19]  $\mathcal{A}_{K^+\pi^-} = -0.0862 \pm 0.006$ , which is statistics limited. The final CDF result is also statistics limited.

**Fig. 2.7**  $M_{bc}$  and  $\Delta E$  projection plots for  $B^\pm \rightarrow K^\pm\pi^0$  from Belle [20], based on 275M  $B\bar{B}$  pairs [Copyright (2004) by The American Physical Society]. The CPV asymmetry is consistent with zero, with a slight hint for more  $K^-\pi^0$  events



Belle in Fig. 2.7. Comparing with the 2004 mean value of  $-0.114 \pm 0.020$  for  $\mathcal{A}_{K^+\pi^-}$  (see Fig. 2.6 for the corresponding Belle plot), there seemed to be a difference<sup>4</sup> between DCPV in  $B^+ \rightarrow K^+\pi^0$  versus  $B^0 \rightarrow K^+\pi^-$ , a point which was emphasized already in the Belle paper [20].

The difference between the charged and neutral mode has steadily strengthened since 2004, and the 2007 [12] average of

$$\mathcal{A}_{B^+ \rightarrow K^+\pi^0} = +5.0 \pm 2.5 \%, \quad [\text{HFAG 2007}] \quad (2.8)$$

showed some significance for the sign being *positive*, i.e. opposite to the sign of  $\mathcal{A}_{K^+\pi^-}$  in (2.7).

### 2.2.2 $\Delta\mathcal{A}_{K\pi}$ and New Physics?

In a paper published in *Nature*, the Belle collaboration used 535M  $B\bar{B}$  pairs to demonstrate the difference [18]

$$\Delta\mathcal{A}_{K\pi} \equiv \mathcal{A}_{K^+\pi^0} - \mathcal{A}_{K^+\pi^-} = +0.164 \pm 0.037, \quad [\text{Belle 2008}] \quad (2.9)$$

<sup>4</sup>Actually, the 2003 value by BaBar, with 88M  $B\bar{B}$  pairs, was  $\mathcal{A}_{K^+\pi^0} = -0.09 \pm 0.09 \pm 0.01$ . But with 227M  $B\bar{B}$  pairs, the 2004 value by BaBar changed sign [27], becoming  $\mathcal{A}_{K^+\pi^0} = +0.06 \pm 0.06 \pm 0.01$ . Combining with the positive value of Belle,  $\mathcal{A}_{K^+\pi^0} = +0.04 \pm 0.05 \pm 0.02$  (based on 275M  $B\bar{B}$ ), this made the difference between  $\mathcal{A}_{K^+\pi^0}$  and  $\mathcal{A}_{K^+\pi^-}$  stand out already in 2004.



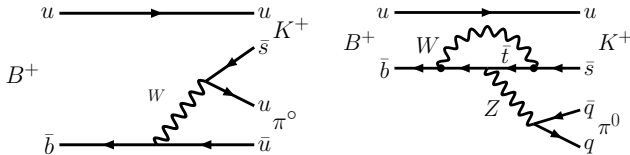


**Fig. 2.9** **a** Color-suppressed tree diagram ( $C$ ) and **b** electroweak penguin diagram ( $P_{EW}$ ) for  $B^+ \rightarrow K^+\pi^0$

where  $\phi_3 = \arg V_{ub}^*$ ,  $\delta$  is the strong phase difference between the tree amplitude  $T$  and strong penguin amplitude  $P$ , and  $r \equiv |T/P|$  is the ratio of tree versus penguin amplitude strength. It is the interference between the two kinds of phases (Appendix A) that generates DCPV, i.e.  $\mathcal{A}_{K^+\pi^-} \equiv \mathcal{A}_{CP}(K^+\pi^-)$ .

We remark that for TCPV, the equivalent to the strong phase is  $\delta = \Delta m_B \Delta t$ , where  $\Delta m_B$  is the already well measured  $B^0-\bar{B}^0$  oscillation frequency, and  $\Delta t$  is part of the time-dependent measurement. This is the beauty [2, 3] of mixing dependent CPV studies, that it is much less susceptible to hadronic effects, especially in single amplitude processes such as the tree dominant  $B^0 \rightarrow J/\psi K^0$  mode. One has *direct access* to the CPV phase of the  $B^0-\bar{B}^0$  mixing amplitude, the equivalent of  $\phi_3$  in (2.11). In comparison, DCPV relies on the presence of strong interaction phase differences. The hadronic nature of these  $CP$  invariant phases make them difficult to predict. Although DCPV is one of the simplest things to measure experimentally, the strong phase difference in a decay amplitude is usually hard to extract.

The  $B^+ \rightarrow K^+\pi^0$  decay amplitude is similar to the  $B^0 \rightarrow K^+\pi^-$  one, up to sub-leading corrections, that is

$$\sqrt{2}\mathcal{M}_{K^+\pi^0} - \mathcal{M}_{K^+\pi^-} = C + P_{EW}, \quad (2.12)$$

where  $C$  is the color-suppressed tree amplitude, while  $P_{EW}$  is the electroweak penguin (replacing the virtual gluon in  $P$  by  $Z$  or  $\gamma$ ) amplitude. These diagrams are illustrated in Fig. 2.9. In the limit that these subleading terms vanish, one expects  $\Delta\mathcal{A}_{K\pi} \sim 0$ . For a very long time before the experimental measurement, this was broadly expected to be the case. But, eventually, it turned out contrary to the experimental result of (2.10). It was therefore not predicted by any calculations.

Although the case is now basically closed (hadronic effect!), let us discuss the “*What if?*” questions, to capture the excitement of the times.

### 2.2.2.1 Large $C$ ? Need Large “Finesse”!

Could  $C$  be greatly enhanced? This is certainly possible, and it is the attitude taken by many [30]. Indeed, fitting with data, one finds  $|C/T| > 1$  is needed [31], in strong contrast to the very tiny value for  $C$  suggested 10 years prior [32]. Note that, from the usual large  $N_C$  expansion argument, which is nonperturbative, one expects

color-suppression to be stronger than  $1/N_C$ . There is further difficulty for an enhanced  $C$  amplitude. As this amplitude has the same weak phase  $\phi_3$  as  $T$ , the enhancement of  $C$  has to contrive in its strong phase structure, to cancel the effect of the strong phase difference  $\delta$  between  $T$  and  $P$  that helped induce the sizable  $\mathcal{A}_{K^+\pi^-}$  of (2.7) in the first place. The amount of “finesse” needed is therefore quite considerable.

We reiterate that the  $\Delta\mathcal{A}_{K\pi}$  difference was *not* anticipated by any calculations beforehand, and theories that do possess calculational capabilities<sup>5</sup> have only played catching up, after the experimental fact. In perturbative QCD factorization (PQCD) calculations at next to leading order (NLO) [15], taking cue from data,  $C$  does move in the right direction. But the central value is insufficient to account for experiment, and the claim to consistency with data is actually hiding behind large errors. For QCD factorization (QCDF), it has been declared [34] that  $\Delta\mathcal{A}_{K\pi}$  is difficult to explain, that it would need very large and *imaginary*  $C$  (or electroweak penguin) compared to  $T$ , which is “Not possible in SM plus factorization [approach].” In the rather sophisticated Soft Collinear Effective Theory (SCET) approach [35],  $\mathcal{A}_{K^+\pi^0}$  was actually predicted, in 2005, to be even more negative than  $\mathcal{A}_{K^+\pi^-}$ , with the latter taken as input. As the  $\Delta\mathcal{A}_{K\pi}$  problem persisted, the SCET people admitted to the problem [36]. On whether it could be New Physics, SCET needs to “see a coherent pattern of deviations”, before it can be convinced about the need for New Physics. In any case, the problem appears to be with SCET itself, or its application to  $B$  decay, rather than with experiment.

### 2.2.2.2 Large $P_{EW}$ ? Then New Physics!

The other option is to have a large CPV contribution from the electroweak penguin [29, 31, 37] amplitude,  $P_{EW}$ . The interesting point is that *this calls for a New Physics CPV phase*, as it is known that  $P_{EW}$  carries practically no weak phase within SM ( $V_{ts}^*V_{tb}$  is practically real, see (A.4)), and has almost the same strong phase as  $T$  [38].

— So, what New Physics can this be? —

Note that this would not so easily arise from SUSY, since SUSY effects tend to be of the “decoupling” kind, compared to the *nondecoupling* of the top quark effect already present, in fact dominating, in the  $Z$  penguin loop.<sup>6</sup> The latter is very analogous to what happens in box diagrams.

---

<sup>5</sup>For the non-computational approaches of fitting data with  $T$ ,  $P$ ,  $C$  and  $P_{EW}$  etc., we stress that they are just that, fitting to data. Without being able to compute these contributions, they are saying nothing more than “Data implies a large  $C$ ”, which is a tautological statement in essence, or just a translation of data. For example, in the pre-B factory era, by *assuming*  $|C| \ll |T|$ , there was the suggestion [33] to combine  $\mathcal{A}_{CP}(K^+\pi^0)$  with  $\mathcal{A}_{CP}(K^+\pi^-)$  for sake of increasing statistics. With *experimental indication* that  $|C/T|$  is finite, the same mentality flips over [30] to allow  $C/T$ , both in strength and (strong) phase, to be free parameters.

<sup>6</sup>In Fig. 2.4, we compared the gluonic penguin  $P$  for  $b \rightarrow s\bar{s}s$  in SM with a possible SUSY effect through  $\bar{b}-\bar{s}$  mixing. This is possible in SUSY. Unlike the  $Z$  penguin, the top quark mass effect in the gluonic penguin largely decouples, as it is of weaker than logarithmic dependence [39]. The

So, can there be more *nondecoupled* quarks beyond the top in the  $Z$  penguin loop? This is the so-called (sequential) fourth generation. It would naturally bring into the  $b \rightarrow s\bar{q}q$  electroweak penguin amplitude  $P_{EW}$  (but not so much in the strong penguin amplitude  $P$ ) a new CPV phase, in the new CKM product  $V_{t's}^* V_{t'b}$ . It was shown [37] that (2.9) can be accounted for in this extension of SM. We will look further into this, after we discuss NP prospects in  $B_s$  mixing.

With the two hints for New Physics in  $b \rightarrow s$  penguin modes in 2007, i.e. the  $\Delta S$  (TCPV) and  $\Delta\mathcal{A}_{K\pi}$  (DCPV) problems, one might expect possible NP in  $B_s$  mixing. Although the measurements (see next chapter) of  $\Delta m_{B_s}$  and  $\Delta\Gamma_{B_s}$  turned out SM-like, the real test clearly should be in the CPV measurables  $\sin 2\Phi_{B_s}$  and  $\cos 2\Phi_{B_s}$ , as the NP hints all involve CPV. This is the subject of the next chapter.

### 2.3 $\mathcal{A}_{CP}(B^+ \rightarrow J/\psi K^+)$

The  $\Delta\mathcal{A}_{K\pi}$  problem motivated a crosscheck study. If it is genuinely rooted in the electroweak penguin amplitude  $P_{EW}$ , a corollary is to check the  $B^+ \rightarrow J/\psi K^+$  mode: Rather than becoming a  $\pi^0$ , the  $Z^*$  from the effective  $bsZ^*$  vertex could produce a  $J/\psi$ . If there is New Physics in the  $B^+ \rightarrow K^+\pi^0$  electroweak penguin, one can then contemplate DCPV in  $B^+ \rightarrow J/\psi K^+$  as a probe of NP.

$B^+ \rightarrow J/\psi K^+$  decay is dominated, of course, by the color-suppressed  $b \rightarrow c\bar{c}s$  amplitude (Fig. 2.10a), which is proportional to the CKM element product  $V_{cs}^* V_{cb}$  that is real to very good approximation. At the loop level, the penguin amplitudes are proportional to  $V_{ts}^* V_{tb}$  in the SM. Because  $V_{us}^* V_{ub}$  is very suppressed,  $V_{ts}^* V_{tb} \cong -V_{cs}^* V_{cb}$  is not only practically real (see (3.5) in next chapter), it has the same phase as the tree amplitude, and can be absorbed into it, as far as the CKM factor is concerned. Hence, it is commonly argued that DCPV is less than  $10^{-3}$  in this mode, and  $B^+ \rightarrow J/\psi K^+$  has often been viewed as a *calibration* mode in search for DCPV. However, because of possible hadronic effects, there is no firm prediction that can stand scrutiny. A calculation [40] of  $B^0 \rightarrow J/\psi K_S$  that combines QCDF-improved factorization and the PQCD approach confirms the 3 generation SM expectation that  $\mathcal{A}_{CP}(B^+ \rightarrow J/\psi K^+)$  should be at the  $10^{-3}$  level. Thus, if % level asymmetry is observed, it would support the scenario of New Physics in  $b \rightarrow s$  transitions, and in particular stimulate theoretical efforts to compute the strong phase difference between  $C$  and  $P_{EW}$ .

Using the 4th generation to account for the  $\Delta\mathcal{A}_{K\pi}$  difference, it was argued [41] that DCPV in  $B^+ \rightarrow J/\psi K^+$  decay could be at the % level. The SM electroweak penguin amplitude is given in Fig. 2.10b. Within SM, the same remark as before holds, and little CPV is generated. But, as we have seen for  $B \rightarrow K\pi$  decay, if  $P_{EW}$  picks up a sizable New Physics CPV phase, then it can interfere with the  $C$  amplitude

---

usual image of top dominance in the strong penguin loop is somewhat misplaced. It really is just due to operator running from  $W$  scale, rather than a genuine heavy top mass effect. It does rely on  $m_t$  being heavier than  $M_W$ , but QCD running between  $m_t$  and  $M_W$  is rather mild.

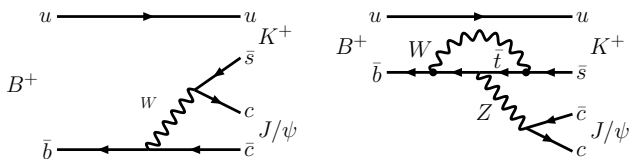


**Fig. 2.10** **a** Color-suppressed tree diagram (C) and **b** electroweak penguin diagram ( $P_{EW}$ ) for  $B^+ \rightarrow K^+ J/\psi$

and generate DCPV, if there is a strong phase difference. More generally, one can view the  $P_{EW}(b \rightarrow s\bar{c}c)$  amplitude as a four quark operator (e.g. flavor-changing  $Z'$  models). Then the CPV phase of this amplitude is not constrained by the effect in  $B \rightarrow K^+ \pi^0$ .

Experiment by 2006 was consistent with zero, but had a somewhat checkered history [19]. In particular, the opposite sign between Belle and BaBar measurements suppressed the central value, with error at 2% level. This already ruled out, for example, the suggestion [42] of enhanced  $H^+$  effect at 10% level.

One impediment to the further study of the available higher statistics at the B factories is the control of the systematic error. It seemed formidable to break the 1% barrier. Progress was made, however, by the  $D\theta$  experiment at the Tevatron. Based on  $2.8 \text{ fb}^{-1}$  data,  $D\theta$  reconstructed around 40000  $B^\pm \rightarrow J/\psi K^\pm$  events, together with  $\sim 1600 B^\pm \rightarrow J/\psi \pi^\pm$ . The  $M(J/\psi K)$  distribution is shown in Fig. 2.11.  $D\theta$  measures [43]

$$\mathcal{A}_{B^+ \rightarrow J/\psi K^+} = (0.75 \pm 0.61 \pm 0.30)\%. \quad [D\theta \text{ 2008}] \quad (2.13)$$

We should note that there is a correction twice as large as the central value in (2.13) for the  $K^\pm$  asymmetry due to detector effects, because the detector is made of *matter*. This is because the  $K^- N$  cross section is different from  $K^+ N$  cross section, especially for lower  $p_K$ , because of the  $\bar{u}$  quark, which leads to lower reconstruction efficiency for  $K^-$ . This “kaon asymmetry” from detector effect is directly measured in the same data. One enjoys a larger control sample in hadronic production, as compared with B factories.  $D\theta$  compares  $D^* \rightarrow D^0 \pi^+$  ( $D^0 \rightarrow \mu^+ \nu K^-$ ) with the charge

**Fig. 2.11**  $M(J/\psi K)$  distribution for  $B^\pm \rightarrow J/\psi K^\pm$  events by  $D\theta$  [43] with  $2.8 \text{ fb}^{-1}$  data [Copyright (2008) by The American Physical Society], where there is a rather small component for  $B^\pm \rightarrow J/\psi \pi^\pm$

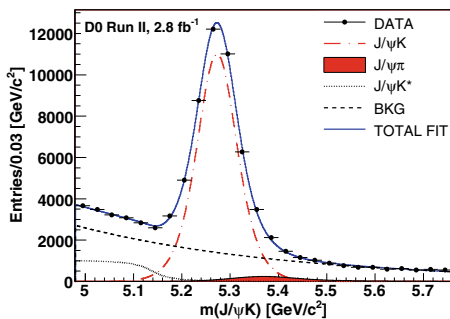
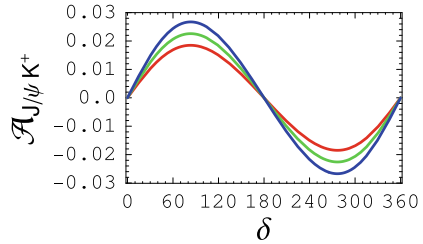


**Fig. 2.12**  $\mathcal{A}_{J/\psi K^+}$  versus strong phase difference  $\delta$  between  $C$  and  $P_{EW}$  in the 4th generation model [41]. A nominal  $\delta \sim 30^\circ$  is expected from strong phases in  $J/\psi K^*$  mode. Negative asymmetries are ruled out by the  $D\theta$  result given in (2.13)



conjugate process, and the kaon asymmetry is measured for different kaon momentum and convoluted with  $B \rightarrow J/\psi K$  decay. It was found that the detector matter induced asymmetry for  $B \rightarrow J/\psi K$  is of order  $-0.0145$ . Correcting the measured one at order  $-0.007$  gives the result in (2.13). One other crucial aspect of the  $D\theta$  analysis is the cancellation of reconstruction efficiency differences between positive and negative particles. For these purposes,  $D\theta$  periodically reverses the magnet polarity for equivalent periods.

Overall, in comparison to the challenge at the B factories, of special note is the rather small ( $\sim 0.3\%$ ) systematic error of the  $D\theta$  measurement. Thus, even scaling up to  $10 \text{ fb}^{-1}$ , one is still statistics limited, and  $2\sigma$  sensitivity for  $\%$  level asymmetries could be attainable. CDF should have similar sensitivity, and the situation can drastically improve with LHCb data, but there may be an issue of magnet polarity flip.

The  $D\theta$  measurement at the Tevatron was in fact inspired by the theoretical 4th generation study [41], which followed the lines presented in the previous sections, and with 4th generation parameters taken from the  $\Delta\mathcal{A}_{K\pi}$  study [37]. By making analogy with what is observed in  $B \rightarrow D\pi$  modes, and especially between different helicity components in  $B \rightarrow J/\psi K^*$  decay, the dominant color-suppressed amplitude  $C$  for  $B^+ \rightarrow J/\psi K^+$  would likely<sup>7</sup> possess a strong phase of order  $30^\circ$ . The  $P_{EW}$  amplitude is assumed to factorize and hence does not pick up a strong phase. Heuristically this is because the  $Z^*$  produces a small, color singlet  $c\bar{c}$  that penetrates and leaves the hadronic “muck” without much interaction, subsequently projecting into a  $J/\psi$  meson. With strong phase in  $C$  and weak phase in  $P_{EW}$ , one finds  $\mathcal{A}_{J/\psi K^+} \simeq \pm 1\%$ .

We plot  $\mathcal{A}_{J/\psi K^+}$  versus strong phase difference  $\delta$  in Fig. 2.12, with weak phase  $\phi_{sb}$  fixed to the range corresponding to (3.25), and the notation is as in Fig. 3.10 (we refrain until Chap. 3 for further motivation for, and a more detailed discussion of, the 4th generation scenario). The negative sign is ruled out by the  $D\theta$  result, (2.13). But of course, DCPV is directly proportional to the strong phase difference, which is not predicted, so  $\mathcal{A}_{J/\psi K^+} \sim +1\%$  is consistent with the  $D\theta$  result, and can be probed further. We remark that other exotic models like  $Z'$  with FCNC couplings [44] could also generate similar effects. For example, with  $\delta \sim 30^\circ$ ,  $\mathcal{A}_{J/\psi K^+}$  could be considerably larger than a percent. With the  $D\theta$  result of (2.13), however, only  $\%$

<sup>7</sup>Ironically, the theoretical paper [41] went unpublished, because the referee could not agree with the argument, by analogy, for strength of strong phase.



level asymmetries are allowed, ruling out a large (and in any case quite arbitrary) region of parameter space for possible  $Z'$  effects.

Prodded by the  $D\bar{0}$  paper, Belle published their result [45] based on 772M  $B\bar{B}$  pairs,  $\mathcal{A}_{J/\psi K^+} = (-0.76 \pm 0.50 \pm 0.22)\%$ , which also has impressive systematic errors, but with sign opposite (2.13), which is reminiscent of the situation prior to 2007.  $D\bar{0}$  continued to pursue the measurement, producing the final value [46] of  $\mathcal{A}_{J/\psi K^+} = (0.59 \pm 0.36 \pm 0.07)\%$  with  $10.4 \text{ fb}^{-1}$  data, which affirms their result in (2.13), and with very impressive systematic error. But given that the two values are *opposite in sign*, it not only resulted in a subdued mean, but with enlarged overall error for PDG 2017 average  $\mathcal{A}_{J/\psi K^+} = (0.3 \pm 0.6)\%$ . With advent of LHCb, their Run 1 result [47] of  $\mathcal{A}_{J/\psi K^+} = (0.09 \pm 0.27 \pm 0.07)\%$  leads to the current average of [19]

$$\mathcal{A}_{J/\psi K^+} = (1.8 \pm 3.0) \times 10^{-3}, \quad [\text{PDG 2018}] \quad (2.14)$$

which is approaching  $10^{-3}$  level, with no sign of CPV.

We have traced some history here to illustrate the interaction between experiment and theory and vice versa, and also because this resulted in precision measurement, demonstrating that  $B^+ \rightarrow J/\psi K^+$  decay can indeed be used as calibration mode for DCPV studies. In any case, a subpercent asymmetry in (2.14) cannot escape the curse of incomputability of strong, hadronic phases.

## 2.4 An Appraisal

In Chap. 1, we teased with the early hint that  $\sin 2\phi_1/\beta$  could be much smaller than expected. However, the SM expectation was subsequently rather quickly affirmed. It is remarkable that the studies at the B factories confirm the 3 generation CKM unitarity triangle for  $b \rightarrow d$  transitions, i.e. (1.6).

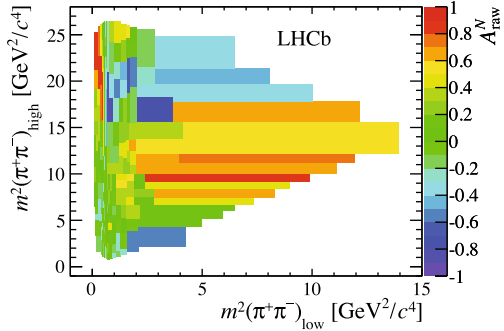
With unprecedented luminosities (see Fig. 1.2), there were high hopes for the B factories to uncover *some* Beyond the Standard Model physics, in particular in CPV in  $b \rightarrow s\bar{q}q$  decays. There were indeed ups and downs, excitements and disappointments. The 2003  $B^0 \rightarrow \phi K_S$  TCPV splash faded with more data and more modes, turning into the  $\Delta\mathcal{S}$  problem, which also gradually faded. Experimentally it was never fully established, while theoretically it is hampered by hadronic uncertainties, which further vary from mode to mode,<sup>8</sup> making the combination of modes dubious.

For the  $\mathcal{A}_{B^+ \rightarrow K^+ \pi^0}$  versus  $\mathcal{A}_{B^0 \rightarrow K^+ \pi^-}$  DCPV difference, experimentally it is genuine. But the presence of a possible  $C$  amplitude, though rather demanding on

---

<sup>8</sup>Before the start of the B factories, there were high hopes that the  $m_B$  scale would allow charmless  $B$  decay amplitudes to be computable by perturbative QCD, or “factorize”. But as data emerged, both for rates as well as DCPV asymmetries, the QCDF approach introduced process-dependent fudge factors, which is admitting defeat to some extent.

**Fig. 2.13** Measured DCPV asymmetries for  $B^+ \rightarrow \pi^+\pi^-\pi^+$  across the Dalitz plot [Courtesy LHCb experiment, [51]], which can reach above 80%



factorization calculations, has convinced the majority that this  $\Delta\mathcal{A}_{K\pi}$  problem is yet another hadronic effect:  $|C| \sim |T|$  in strength, but  $C$  and  $T$  differ in strong phase.

But around 2008, there was a rather good prospect that the  $\Delta\mathcal{A}_{K\pi}$  problem is a genuine harbinger for New Physics in CPV  $b \rightarrow s\bar{q}q$  transitions, via the electroweak penguin. We will continue to discuss this in the next Chapter on the implications for  $\sin 2\Phi_B$  measurement. However, the problem of hadronic uncertainties for hadronic  $b \rightarrow s\bar{q}q$  transitions cannot be taken lightly. Even for DCPV in  $B^+ \rightarrow J/\psi K^+$ , if it did emerge experimentally at the 1% level, as discussed in the previous section, people would still question what is the genuine value within SM, whether it cannot reach close-to-percent level, i.e. attributing it again to “hadronic effect”.

To top it off, and in comparison, we mention briefly the surprisingly large transverse polarization in several charmless  $B \rightarrow VV$  final states that emerged around 2004. When this emerged experimentally [19], e.g. the longitudinal polarization fraction  $f_L$  in  $B \rightarrow \phi K^*$  was only 50%, it was suggested [48] that this could be due to New Physics. However, in part by improved understanding of the  $B \rightarrow K^*$  form factor  $A_0$  [49], it is now widely believed to be due to hadronic physics. What convinced people that this is likely not New Physics, is through the polarization and triple product correlation measurements [50], which showed no sign of  $CP$ - nor  $T$ -odd asymmetries.

As a final note on the curse of the “hadronic menace”, with the advent of the LHCb experiment, there are now brilliant pictures [51] of DCPV asymmetries in charmless  $B^+ \rightarrow K^+\pi^-\pi^+, K^+K^-K^+, \pi^+\pi^-\pi^+$  and  $\pi^+K^-K^+$  decays across the 3-body Dalitz plot, as illustrated in Fig. 2.13. The rapid variation in DCPV asymmetries reflect rapid change in hadronic phase difference between underlying competing amplitudes, and even if there is New Physics, it would be practically impossible to extract.

Regardless of the source for  $\Delta\mathcal{A}_{K\pi}$ , there is an important CPV asymmetry sum rule [52, 53] that can test the presence of BSM physics,

$$\begin{aligned}
 & A_{K^+\pi^-} + A_{K^0\pi^+} \frac{\mathcal{B}(K^0\pi^+)}{\mathcal{B}(K^+\pi^-)} \frac{\tau_0}{\tau_+} \\
 &= A_{K^+\pi^0} \frac{2\mathcal{B}(K^+\pi^0)}{\mathcal{B}(K^+\pi^-)} \frac{\tau_0}{\tau_+} + A_{K^0\pi^0} \frac{2\mathcal{B}(K^0\pi^0)}{\mathcal{B}(K^+\pi^-)}, \quad (2.15)
 \end{aligned}$$

where  $\tau_0$  and  $\tau_+$  are  $B^0$  and  $B^+$  lifetimes. What is still missing is a precision measurement of  $A_{K^0\pi^0}$ . With  $A_{K^0\pi^+}$  expected to be very small because of its pure penguin nature, the current result [19] of  $A_{K^0\pi^0} = 0.00 \pm 0.13$  is in contrast with the sum rule projection of  $A_{K^0\pi^0} = -0.129 \pm 0.027$ , with uncertainty dominated by  $A_{K^+\pi^0}$ . As  $\pi^0$  is involved, this is a topic for Belle II, which needs 20 times Belle data to test.

## References

1. Sakharov, A.D.: Pisma Zh. Eksp. Teor. Fiz. **5**, 32 (1967); [JETP Lett. **5**, 24 (1967)]
2. Carter, A.B., Sanda, A.I.: Phys. Rev. Lett. **45**, 952 (1980); Phys. Rev. D **23**, 1567 (1981)
3. Bigi, I.I.Y., Sanda, A.I.: Nucl. Phys. B **193**, 85 (1981)
4. Albrecht, H., et al.: [ARGUS Collaboration]: Phys. Lett. B **192**, 245 (1987)
5. Oddone, P.: At UCLA Workshop on Linear Collider  $B\bar{B}$  Factory Conceptual Design. Los Angeles, California (1987)
6. Go, A., Bay, A., et al.: [Belle Collaboration]: Phys. Rev. Lett. **99**, 131802 (2007)
7. Grossman, Y., Worah, M.P.: Phys. Lett. B **395**, 241 (1997)
8. London, D., Soni, A.: Phys. Lett. B **407**, 61 (1997)
9. Chen, K.F., Hara, K., et al.: [Belle Collaboration]: Phys. Lett. B **546**, 196 (2002)
10. Abe, A., et al.: [Belle Collaboration]: Phys. Rev. Lett. **91**, 261602 (2003)
11. Chen, K.F., et al.: [Belle Collaboration]: Phys. Rev. D **72**, 012004 (2005)
12. Heavy Flavor Averaging Group (HFLAV): acronym changed from HFAG to HFLAV in March 2017). <http://www.slac.stanford.edu/xorg/hflav>
13. Beneke, M.: Phys. Lett. B **620**, 143 (2005)
14. Cheng, H.Y., Chua, C.K., Soni, A.: Phys. Rev. D **72**, 014006 (2005)
15. Li, H.n., Mishima, S., Sanda, A.I.: Phys. Rev. D **72**, 114005 (2005)
16. Williamson, A.R., Zupan, J.: Phys. Rev. D **74**, 014003 (2006)
17. Sinha, R., Misra, B., Hou, W.-S.: Phys. Rev. Lett. **97**, 131802 (2006)
18. Lin, S.W., Unno, Y., Hou, W.-S., Chang, P., et al.: [Belle Collaboration]: Nature **452**, 332 (2008)
19. Tanabashi, M., et al. [Particle Data Group]: Phys. Rev. D **98**, 030001 (2018). <http://pdg.lbl.gov/>
20. Chao, Y., Chang, P., et al.: [Belle Collaboration]: Phys. Rev. Lett. **93**, 191802 (2004)
21. Aubert, B., et al.: [BaBar Collaboration]: Phys. Rev. Lett. **93**, 131801 (2004)
22. Beneke, M., Buchalla, G., Neubert, M., Sachrajda, C.T.: Nucl. Phys. B **606**, 245 (2001)
23. Keum, Y.Y., Li, H.n., Sanda, A.I.: Phys. Rev. D **63**, 054008 (2001)
24. Keum, Y.Y., Sanda, A.I.: Phys. Rev. D **67**, 054009 (2003)
25. Morello, M. (for the CDF Collaboration): Talk at B-Physics at Hadron Machines (Beauty 2006), Oxford, England, 2006, appeared as Nucl. Phys. Proc. Suppl. **170**, 39 (2007); and CDF Public Note 8579
26. Aubert, B., et al.: [BaBar Collaboration]: Phys. Rev. Lett. **99**, 021603 (2007)
27. Aubert, B., et al.: [BaBar Collaboration]: Phys. Rev. Lett. **94**, 181802 (2005)
28. Aubert, B., et al.: [BaBar Collaboration]: Phys. Rev. D **76**, 091102 (2007)
29. Peskin, M.E.: Nature **452**, 293 (2008), Companion Paper [33]
30. Gronau, M.: Talk at Flavour Physics and CP Violation Conference (FPCP2007), Bled, Slovenia (2007)
31. Baek, S., London, D.: Phys. Lett. B **653**, 249 (2007)
32. Neubert, M., Stech, B.: In: Buras, A.J., Lindner, M. (eds.) Heavy Flavours II. World Scientific, Singapore (1998)
33. Gronau, M., Rosner, J.L.: Phys. Rev. D **59**, 113002 (1999)

34. Beneke, M.: Talk at Flavor Physics and CP Violation Conference (FPCP2008). Taipei, Taiwan (2008)
35. Bauer, C.W., Rothstein, I.Z., Stewart, I.W.: Phys. Rev. D **74**, 034010 (2006)
36. Rothstein, I.: Talk at Flavor Physics and CP Violation Conference (FPCP2008). Taipei, Taiwan (2008)
37. Hou, W.-S., Nagashima, M., Soddu, A.: Phys. Rev. Lett. **95**, 141601 (2005)
38. Neubert, M., Rosner, J.L.: Phys. Rev. Lett. **81**, 5076 (1998)
39. Hou, W.-S.: Nucl. Phys. B **308**, 561 (1988)
40. Li, H.n., Mishima, S.: JHEP **0703**, 009 (2007)
41. Hou, W.-S., Nagashima, M., Soddu, A.: hep-ph/0605080, 2018
42. Wu, G.H., Soni, A.: Phys. Rev. D **62**(056005), 2018 (2000)
43. Abazov, V.M., et al.: [DØ Collaboration]: Phys. Rev. Lett. **100**, 211802 (2008)
44. Barger, V., Chiang, C.-W., Langacker, P., Lee, H.S.: Phys. Lett. B **598**, 218 (2004)
45. Sakai, K., Kawasaki, T., et al.: (Belle Collaboration): Phys. Rev. D **82**, 091104 (2010)
46. Abazov, V.M., et al.: [DØ Collaboration]: Phys. Rev. Lett. **110**, 241801 (2013)
47. Aaij, R., et al.: [LHCb Collaboration]: Phys. Rev. D **95**, 052005 (2017)
48. Kagan, A.L.: Phys. Lett. B **601**, 151 (2004)
49. Li, H.n.: Phys. Lett. B **622**, 63 (2005)
50. Chen, K.F., et al.: (Belle Collaboration): Phys. Rev. Lett. **94**, 221804 (2005)
51. Aaij, R., et al.: (LHCb Collaboration): Phys. Rev. D **90**, 112004 (2014)
52. Gronau, M.: Phys. Lett. B **627**, 82 (2005)
53. Atwood, D., Soni, A.: Phys. Rev. D **58**, 036005 (1998)

# Chapter 3

## $B_s$ Mixing and $\sin 2\Phi_{B_s}$



There were two intriguing hints for New Physics at the B factories in the study of CP violation in  $b \rightarrow s$  transitions.  $\Delta S$ , the difference in time-dependent CPV between charmless  $b \rightarrow s\bar{q}q$  modes and  $\sin 2\phi_1/\beta$  measured in the  $b \rightarrow c\bar{c}s$  modes, despite early promise, faded in experimental significance, and we await further scrutiny by Belle II.  $\Delta A_{K\pi}$ , the difference in direct CPV asymmetries in  $B^+ \rightarrow K^+\pi^0$  versus  $B^0 \rightarrow K^+\pi^-$  decays, is experimentally established, and it could indeed arise from New Physics CPV through the electroweak penguin amplitude. However, despite the challenge it poses to theoretical calculations, it appears that the color-suppressed amplitude is enhanced in a major and specific way so as to generate  $\Delta A_{K\pi}$  in (2.10).

In this chapter we turn to another focus on New Physics search, in the  $B_s^0-\bar{B}_s^0$  mixing amplitude, i.e.  $b \leftrightarrow s$  transitions. The oscillation between  $B_s^0$  and  $\bar{B}_s^0$  mesons is too rapid for the B factories to resolve. This brings us to the hadron colliders, which enjoy a large boost for the produced B mesons. But one then has to face the much higher background levels in a hadronic environment.  $B_s^0$  mixing was finally measured in 2006 by the CDF experiment [1] at the Tevatron. However, the real interest is in the CPV phase  $\sin 2\Phi_{B_s}$  of the  $B_s^0-\bar{B}_s^0$  mixing amplitude, analogous to  $\sin 2\phi_1/\beta$  for  $B_d^0-\bar{B}_d^0$  mixing case (which could have been called  $\sin 2\Phi_{B_d}$ ). After all, the  $\Delta S$  and  $\Delta A_{K\pi}$  problems are all CPV measures. The SM expectation for  $\sin 2\Phi_{B_s}$  is almost zero, hence offers a great window for BSM effects. As we will discuss, any evidence for finite  $\sin 2\Phi_{B_s}$  before the arrival of LHC data would amount to an indication for New Physics. Indications at the Tevatron were indeed in this direction, attracting growing interest in the 2008–2010 period, and great anticipation towards LHC. Alas, with the advent of the LHCb experiment, a *forward* detector tailored for B physics at the LHC, by 2011, once again  $\sin 2\Phi_{B_s}$  emerged [2] as being consistent with SM expectations. Hope for BSM physics is not yet lost, but it has become a precision measurement.

The measurement of  $\sin 2\Phi_{B_s}$  still allows deviation from SM at current precision of LHC experiments, which the Super B factory cannot make direct impact. But it is in fact the consistency of  $\sin 2\Phi_{B_s}$  with SM, rather than showing a large deviation,

which suggest that the large  $\Delta A_{K\pi}$  is likely due to “unsuppressed color-suppressed amplitude”  $C$ . Unlike DCPV in  $B \rightarrow K\pi$ ,  $\sin 2\Phi_{B_s}$  is not marred by hadronic effects.

### 3.1 $B_s$ Mixing Measurement

The measurement of  $B_s$  mixing has been pursued since the LEP (and SLC) era, as well as at the Tevatron Run I. By 2005, the world limit had been hovering around  $\Delta m_{B_s} > 14.5 \text{ ps}^{-1}$  [3] for several years, in wait for Tevatron Run II. In fact, LEP data showed a  $2\sigma$  indication for  $\Delta m_{B_s}$  around  $17.2 \text{ ps}^{-1}$ .

It had been advertised that  $\Delta m_{B_s}$  measurement would be easy for CDF in Tevatron Run II, that a SM value could be measured with several hundred  $\text{pb}^{-1}$ . But things did not work out as planned, and, as can be seen from Fig. 3.1, the Tevatron Run II had a rather slow start. Only by 2004 did the accelerator performance finally start to pick up. By summer 2005 or so, each experiment had collected  $1 \text{ fb}^{-1}$  data, and interesting results started to come out. The CDF and DØ experiments finally collected  $\sim 10 \text{ fb}^{-1}$  integrated luminosity per experiment for Tevatron Run II. With the LHC performance picking up in 2010, the Tevatron was shutdown in 2011.

#### 3.1.1 Standard Model Expectations

As shown in Fig. 3.2a, analogous to the case for  $B_d$  oscillations, the amplitude for  $B_s$  mixing in SM behaves as  $M_{12}^s \propto (V_{tb}V_{ts}^*)^2 m_t^2$  to first approximation, i.e.

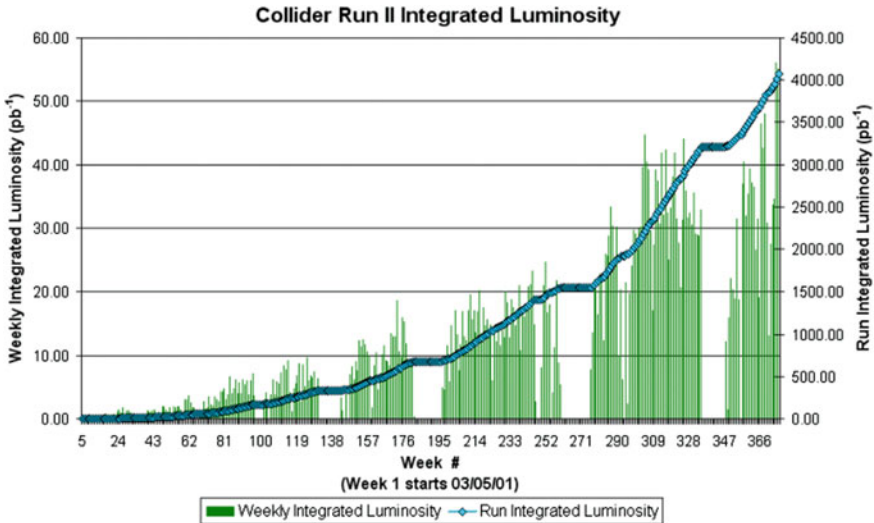


**Fig. 3.1** Integrated luminosity for Tevatron Run II, up to early May 2008. [Source <http://www.fnal.gov/pub/now/tevlum.html>, by the Fermilab Accelerator Division, used with permission]

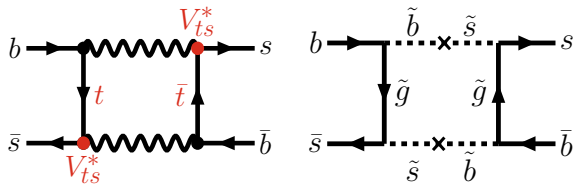


**Fig. 3.2** For  $B_s^0-\bar{B}_s^0$  mixing, **a** one of the box diagrams in SM, where the CPV phase is brought in through  $(V_{ts}^*V_{tb})^2$  from top quark dominance; **b** a possible SUSY contribution through  $\tilde{s}-\tilde{b}$  squark mixing. The  $c\bar{c}$  contribution in the SM box diagram, though negligible for  $M_{12}^s$ , generates  $\Gamma_{12}^s$ , since  $b \rightarrow c\bar{c}s$  is a major component of  $b$  decay

$$M_{12}^s \simeq -\frac{G_F^2 m_W^2 S_0(m_t^2/m_W^2) \eta_{B_s}}{12\pi^2} m_{B_s} f_{B_s}^2 B_{B_s} (V_{ts}^* V_{tb})^2. \quad (\text{SM}) \quad (3.1)$$

This is of the same form as (1.2), with simple replacement of  $d \rightarrow s$ . With top quark dominance, to very good approximation, one therefore has

$$\frac{\Delta m_{B_s}}{\Delta m_{B_d}} = \frac{f_{B_s}^2 B_{B_s} m_{B_s}}{f_{B_d}^2 B_{B_d} m_{B_d}} \frac{|V_{ts}|^2}{|V_{td}|^2} \equiv \xi^2 \frac{m_{B_s}}{m_{B_d}} \frac{|V_{ts}|^2}{|V_{td}|^2}, \quad (\text{SM}) \quad (3.2)$$

where  $\Delta m \equiv 2|M_{12}|$  is the oscillation frequency. With  $\xi > 1$ , one immediately sees that  $\Delta m_{B_s}$  is much larger than  $\Delta m_{B_d} \simeq 0.5 \text{ ps}^{-1}$  in the SM. We note that  $f_{B_s}^2 B_{B_s}$  in (3.1) needs to be computed in lattice QCD, which still carry sizable errors. But with (3.2), like in experimental errors, many lattice errors cancel in the ratio  $\xi^2 = f_{B_s}^2 B_{B_s} m_{B_s} / f_{B_d}^2 B_{B_d} m_{B_d}$ . This is why in Fig. 1.6, the constraint from “ $\Delta m_s$  &  $\Delta m_d$ ” is considerably better than from the experimentally well measured  $\Delta m_d \equiv \Delta m_{B_d}$  alone. Thus, from the SM perspective, the measurement of  $\Delta m_{B_s}$ , together with  $\Delta m_{B_d}$ , provide a constraint on  $|V_{ts}|^2/|V_{td}|^2$ , modulo the lattice errors on  $\xi$ , or<sup>1</sup>

$$\frac{1}{\lambda} \frac{|V_{td}|}{|V_{ts}|} = \frac{\xi}{\lambda} \sqrt{\frac{\Delta m_{B_d} m_{B_s}}{\Delta m_{B_s} m_{B_d}}} \simeq \sqrt{(1-\rho)^2 + \eta^2}, \quad (\text{SM}) \quad (3.3)$$

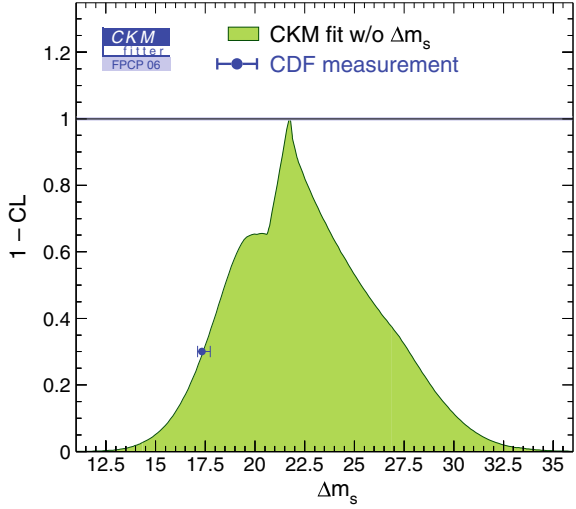
where  $\lambda \equiv V_{us}$ .

### Implications of 3 Generation Unitarity

Assuming 3 generation CKM unitarity, gathering all information, including that on  $\xi$ , the CKM unitarity fitter groups gave the predictions of  $\Delta m_{B_s} = 20.9_{-4.2}^{+4.5} \text{ ps}^{-1}$  (CKMfitter [5, 6]) and  $21.2 \pm 3.2 \text{ ps}^{-1}$  (UTfit [7]), respectively, before the CDF announcement [4] of evidence for  $\Delta m_{B_s}$  at the FPCP 2006 conference in Vancouver, Canada. We show in Fig. 3.3 the results of CKM fitter group using all data other than

<sup>1</sup>For our purpose of New Physics search, we will not distinguish between  $\rho, \eta$  and  $\bar{\rho}, \bar{\eta}$ . See [3] and the Appendix.

**Fig. 3.3** SM expectation for  $\Delta m_{B_s}$  at FPCP 2006 conference, combining all information other than  $B_s$  mixing itself, just before CDF announcement [4] of evidence for  $\Delta m_{B_s}$ , which is also shown in the figure. [From CKMfitter group [5], used with permission]



$\Delta m_{B_s}$ , plotted together with the CDF result. This illustrates the power and impact of the  $\Delta m_{B_s}$  measurement. It also indicates how the CDF result is slightly on the low side. But, of course, the errors from the unitarity fits were very forgiving to make this point somewhat mute. The experimental measurement is discussed in the following subsection.

CPV in  $B_s$  mixing is controlled by the phase of  $V_{ts}$  in SM. Since  $|V_{us}^* V_{ub}|$  is rather small, unlike the analogous case for  $b \rightarrow d$  transitions, (1.4), the triangle relation

$$V_{us}^* V_{ub} + V_{cs}^* V_{cb} + V_{ts}^* V_{tb} = 0 \quad (3.4)$$

$$\implies V_{ts}^* V_{tb} \simeq -V_{cb}, \quad (3.5)$$

i.e. collapses to approximately a line, and  $V_{ts}^* V_{tb}$  is practically real (in the standard phase convention [3] that  $V_{cb}$  is real; see Appendix A.1). In practice, defining

$$\Phi_{B_s} \equiv \frac{1}{2} \arg M_{12} \quad (3.6)$$

$$\simeq \arg V_{ts}^* V_{tb} \simeq -\lambda^2 \eta \sim -0.02 \text{ rad} \quad (\text{SM}), \quad (3.7)$$

which is tiny<sup>2</sup> compared to the well measured  $\Phi_{B_d}|^{\text{SM}} \simeq \arg V_{td}^* V_{tb} = \beta/\phi_1 \sim 0.37 \text{ rad}$ .

At this point it is instructive to give a geometric picture of the discussion above. The “ $b \rightarrow d$  triangle” corresponding to the  $db$  element of  $V^\dagger V = I$ , i.e.  $V_{ud}^* V_{ub} + V_{cd}^* V_{cb} + V_{td}^* V_{tb} = 0$ , or (1.4), is the normal looking triangle in Fig. 3.4. This is

<sup>2</sup>See (A.6) of Appendix A.1 for a discussion on phase of  $V_{ts}$  in the Wolfenstein parametrization of  $V_{\text{CKM}}$  to order  $\lambda^5$ .



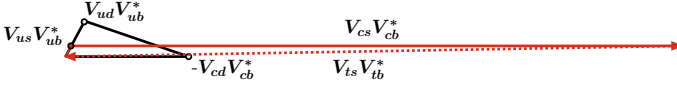


**Fig. 3.4** Geometric representations of the three generation unitarity relations (1.4) and (3.4), the latter being the long, squashed triangle. This picture is identical to Fig. A.2 in the Appendix

the same triangle that is now suitably well measured, as shown in Fig. 1.6. For the “ $b \rightarrow s$  triangle” corresponding to the  $sb$  element of  $V^\dagger V = I$ , i.e.  $V_{us}^* V_{ub} + V_{cs}^* V_{cb} + V_{ts}^* V_{tb} = 0$ , or (3.4), one has a rather squashed triangle in Fig. 3.4. This can be easily seen:  $|V_{us}^* V_{ub}| \sim \lambda |V_{ud}^* V_{ub}|$ , so this side is 1/4 the length of  $b \rightarrow d$  case; on the other hand,  $|V_{cs}^* V_{cb}| \sim \lambda^{-1} |V_{cd}^* V_{cb}|$ , so this side is about 4 times as long. This results in the squashedness, or elongation, of the  $b \rightarrow s$  triangle. One thus sees that the angle on the far right,  $\Phi_{B_s}$ , becomes rather diminished with respect to  $\Phi_{B_d}$  of the  $b \rightarrow d$  case. Note also that the orientation of the  $b \rightarrow s$  triangle is opposite to the  $b \rightarrow d$  triangle, hence the sign difference between the phase angles  $\Phi_{B_s}$  versus  $\Phi_{B_d}$ .

Thus, not only  $B_s^0 - \bar{B}_s^0$  oscillation is much faster than  $B_d$  case because of  $\sim \lambda^{-2}$  enhancement (plus hadronic factors), the associated CPV phase is so small in SM, it is very challenging to measure. If  $\Phi_{B_s}$  is at the SM expectation of a few percent level, then only the LHCb experiment, which is designed for  $B$  physics studies at the LHC, would have enough sensitivity to probe it. It also means that  $\sin 2\Phi_{B_s}$  is an excellent window on BSM [8]: Any observation that deviates from

$$\sin 2\Phi_{B_s}|^{\text{SM}} \cong -0.04, \quad (3.8)$$

would be indication for New Physics. In SUSY, this could arise from squark-gluino loops with  $\tilde{s} - \tilde{b}$  mixing, which is illustrated in Fig. 3.2b.

### Mass Versus Width Mixing

Unlike the  $B_d^0 - \bar{B}_d^0$  situation, the  $B_s^0 - \bar{B}_s^0$  system is in fact richer than just oscillations. Recall the  $K^0 - \bar{K}^0$  system. Besides the mass difference  $\Delta m_K$ , or oscillations, it was well known beforehand that the two states  $K_S^0$  and  $K_L^0$  differ very much in lifetime, since by  $CP$  symmetry the former decays via  $2\pi$  while the latter by  $3\pi$  ( $CP$  violation was discovered through the observation of  $K_L^0 \rightarrow \pi^+ \pi^-$  [9]). For the present case of the box diagram of Fig. 3.2a, if one replace the  $t$  quark by the  $c$  quark, and cut on both the  $c$  quark lines, the amplitude is that of the  $b \rightarrow c\bar{c}s$  decay amplitude interfering with the antiquark process, which is just the decay rate for this subprocess. As the  $b \rightarrow c\bar{c}s$  subprocess is a major component for  $b$  decay, i.e. there is no additional CKM suppression, this generates the absorptive  $\Gamma_{12}^s$  (a width), namely

$$H_{12}^s = M_{12}^s - i \frac{\Gamma_{12}^s}{2}, \quad (3.9)$$

for the full Hamiltonian that mediates  $B_s^0-\bar{B}_s^0$  transitions.  $\Gamma_{12}^s$  leads to a width difference<sup>3</sup>  $\Delta\Gamma_{B_s}$ , or mixing in width. Both  $M_{12}^s$  and  $\Gamma_{12}^s$  are complex in the presence of CPV. We remark that this bears only formal resemblance to the  $K^0-\bar{K}^0$  system. For  $B_s^0-\bar{B}_s^0$  system, not only  $|\Gamma_{12}^s/M_{12}^s|$  is quite different from the kaon case, we have far richer final states for  $B_s$  to decay to, allowing for interference effects in many channels.

We do not wish to get too deep into formalism. We just note that it is difficult for New Physics to affect tree level  $b \rightarrow c\bar{c}s$  transitions, where the CKM coefficient  $V_{cs}^*V_{cb}$  have been chosen to be real by convention. Also, since one already knows by experiment that  $\Delta m_{B_s} \gg \Gamma_{B_s}$ , we know that  $|M_{12}^s| \gg |\Gamma_{12}^s|$ . With these understandings, we therefore just quote the formula [8],

$$\Delta\Gamma_{B_s} = \Delta\Gamma_{B_s}^{\text{SM}} \cos 2\Phi_{B_s}. \quad (3.10)$$

A finite  $\sin 2\Phi_{B_s}$ , deviating from zero (or (3.8)) would lead to a dilution of the width difference in flavor-specific final states. In (3.10),  $\Delta\Gamma_{B_s}^{\text{SM}}$  is calculated within SM, where a typical value is [10],

$$\Delta\Gamma_{B_s}^{\text{SM}} = 0.096 \pm 0.039 \text{ ps}^{-1}, \quad (3.11)$$

and can be measured via decay to a  $CP$  eigenstate. That is, one could measure  $\Delta\Gamma_{B_s}^{\text{CP}}$  via  $B_s^0 \rightarrow D_s^+ D_s^-$ , which in principle can also be measured using  $\Upsilon(5S) \rightarrow B_s^0 \bar{B}_s^0$  at B factories. A general study of say  $B_s \rightarrow J/\psi\phi$  to explore width difference effects, one can infer  $\cos 2\Phi_{B_s}$ , offering a different route to New Physics CPV phase, *without* necessarily resolving the rapid  $B_s^0-\bar{B}_s^0$  oscillations.

### 3.1.2 Tevatron Measurement of $\Delta m_{B_s}$

With measurement of  $B_s^0-\bar{B}_s^0$  oscillations infeasible at the B factories, the task fell on the Tevatron experiments. With a traditional design augmented by a silicon vertex detector (SVX), CDF had the advantage, as  $D\bar{\theta}$  followed the UA2 path and was originally calorimeter-based. But as we have seen,  $D\bar{\theta}$  had a few tricks up its sleeves. We follow some historical development, as  $\Delta m_{B_s}$  measurement was a major triumph at the Tevatron.

#### Two-Sided Bound from $D\bar{\theta}$

Based on  $\sim 1 \text{ fb}^{-1}$  data, the  $D\bar{\theta}$  experiment studied [11]  $B_s^0-\bar{B}_s^0$  oscillations using semileptonic  $B_s^0 \rightarrow \mu^+ D_s^- X$  decays, reconstructing  $D_s^-$  in the  $\phi\pi^-$  final state, with  $\phi \rightarrow K^+ K^-$ . Assuming both the width difference and CPV are small, one measures

---

<sup>3</sup>The usual definition is  $\Delta m_{B_s} = 2|M_{12}^s| = M_H - M_L$ , and  $\Delta\Gamma_{B_s} = 2|\Gamma_{12}^s| = \Gamma_L - \Gamma_H$ , where  $H$  ( $L$ ) stand for the heavier (lighter) mass eigenstate from mixing.

the so-called no-oscillation and oscillation probability, i.e. the probability density  $P^+$  or  $P^-$  for a  $\bar{B}_s^0$  meson produced at  $t = 0$  to decay as a  $\bar{B}_s^0$  or a  $B_s^0$  at time  $t$ ,

$$P_{B_s^\pm}^\pm(t) = \frac{\Gamma_{B_s}}{2} e^{-\Gamma_{B_s} t} (1 \pm \cos \Delta m_{B_s} t), \quad (3.12)$$

where  $\Gamma_{B_s}$  is the mean width. Just like in (2.1), the notation of  $P_{B_s^\pm}^\pm(t)$  used by experiments are shorthand for differential probability densities.

Compared with the study of  $B_d^0-\bar{B}_d^0$  oscillations at the B factories, there are several additional difficulties, or loss of information. By requiring just a  $\mu^+$  to form a common  $B_s^0$  vertex with the reconstructed  $D_s^-$ , the missing neutrino and other particles from semileptonic  $B_s^0$  decay smear the proper decay time, because of insufficient knowledge of the  $B_s^0$  momentum (hence boost). One does not have the advantage of knowing the ‘‘beam profile’’ (and boost) at the B factories. The effect of smearing is studied by Monte Carlo (MC). Also, unlike the coherent  $B_d^0-\bar{B}_d^0$  production from  $\Upsilon(4S)$  decay, the  $B_q-\bar{B}_q$  pairs are produced incoherently at a hadron collider. To determine the  $B_s^0$  or  $\bar{B}_s^0$  flavor at  $t = 0$ , DØ uses opposite side tagging (OST). The purity was studied with  $B^+ \rightarrow \mu^+ \bar{D}^0 X$  and  $B_d^0 \rightarrow \mu^+ D^{*-} X$  decays, where the former does not oscillate, while the latter has some oscillations from  $B_d^0$ . The determined effectiveness of flavor tagging,  $\epsilon \mathcal{D}^2$ , is about 2.5%, where  $\epsilon$  is the tagging efficiency (fraction of signal candidates with flavor tag), and  $\mathcal{D} = 1 - 2w$  is the dilution ( $\mathcal{D} = 0$  when the probability of wrong tag  $w$  is 50%).

The amplitude scan method [12] was exploited, which includes an additional oscillation amplitude coefficient  $\mathcal{A}$  for  $\cos \Delta m_{B_s} t$  in (3.12). One fixes the oscillation frequency  $\Delta m_{B_s}$  and fit for  $\mathcal{A}$ , which should give  $\mathcal{A} \sim 1$  when this  $\Delta m_{B_s}$  value is the true value, but yield  $\mathcal{A} \sim 0$  when the chosen  $\Delta m_{B_s}$  value is far from the true oscillation frequency. With this method, DØ found  $\Delta m_{B_s} > 14.8 \text{ ps}^{-1}$  at 95% C.L., which is better than previous studies. Using an unbinned likelihood ( $\mathcal{L}$ ) fit, i.e.  $-\Delta \log \mathcal{L}$  versus  $\Delta m_{B_s}$ , DØ found the maximum likelihood at  $\sim 19 \text{ ps}^{-1}$ , with rather well-behaved confidence interval around this value. Assuming the uncertainties are Gaussian, DØ obtained the 90% C.L. interval of  $17 \text{ ps}^{-1} < \Delta m_{B_s} < 21 \text{ ps}^{-1}$ , the first two-sided experimental bound [11] for  $B_s^0-\bar{B}_s^0$  oscillations, rather rapid indeed.

### CDF Observation of $B_s^0-\bar{B}_s^0$ Oscillations

Despite the earlier announcement made by DØ in Winter 2006, the CDF experiment quickly surpassed it, first by showing evidence [4] at FPCP 2006, then by actual observation, all within a matter of months. By Summer 2006, based on  $1 \text{ fb}^{-1}$  data,  $B_s$  mixing became a precision measurement [1],

$$\Delta m_{B_s} = 17.77 \pm 0.10 \pm 0.07 \text{ ps}^{-1}, \quad (\text{CDF 2006}) \quad (3.13)$$

which is a watershed. The amplitude scan plot is given in Fig. 3.5.

But it should be remembered that CDF had advertised that measurement of  $\Delta m_{B_s}$  in the SM predicted range should be achievable with just a few hundred  $\text{pb}^{-1}$  at Run

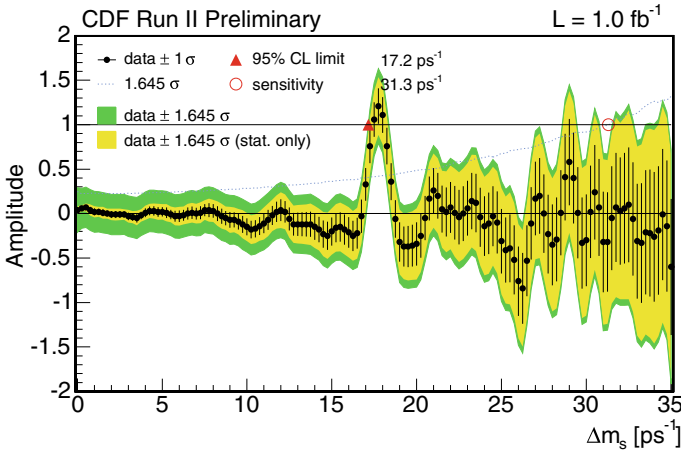


**Fig. 3.5** “Amplitude” plot (all modes combined) versus  $\Delta m_{B_s}$  from CDF analysis with  $1 \text{ fb}^{-1}$  data [1], giving an apparent peak value at  $17.77 \text{ ps}^{-1}$  with amplitude consistent with 1. [Copyright (2006) by The American Physical Society]

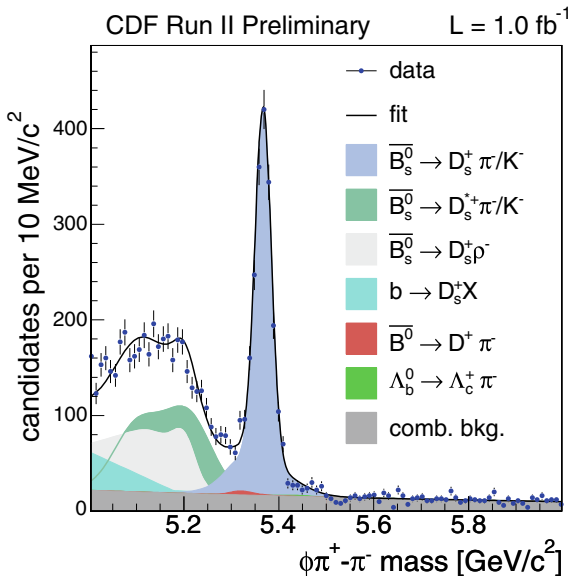
II. This was based on several improvements special to CDF: (1) Increased signal sample: Silicon Vertex Trigger (SVT) for displaced vertices; (2) Better flavor tagging: Opposite Side Tag (OST) as well as<sup>4</sup> Same Side Kaon Tag (SSKT); (3) Improved proper time resolution: the silicon “Layer 00” (L00) placed right on the beampipe, at  $\sim 1.5 \text{ cm}$  from the beam. These innovations brought high hopes, but it is understandable that it took more time to get everything to work, as well as validated. Unfortunately, the performance turned out to be not as good as expected.<sup>5</sup>

Having used silicon vertex detectors already since Tevatron Run I, CDF implemented a two-track SVT trigger, capable of finding tracks in the silicon detector in  $20 \mu\text{s}$  to determine displaced vertices. This was quite successful, but the signal yield turned out smaller than originally expected (less than  $1/5$  for fully reconstructed events). Flavor tagging also turned out much harder than expected, especially for OST, where  $\epsilon D^2 \simeq 1.8\%$  was only  $\sim 1/4$  of what was expected. Fortunately, the situation was saved by the SSKT performance, which was at expected levels, even slightly better than expected for semileptonic modes. But SSKT was difficult to understand, and took time to incorporate into the analysis. Of critical importance is the combined PID of a special TOF, together with  $dE/dx$ . Though the discrimination power is not spectacular, but since the  $K^+/K^-$  from  $b$  quark fragmentation used to

<sup>4</sup>Same side tagging [13–15] is based on flavor correlations from  $b$  quark fragmentation. Most naively, a  $\bar{B}_d^0$  ( $B_u^-$ ) would be accompanied by a  $\pi^-$  ( $\pi^+$ ), while a  $\bar{B}_s^0$  is accompanied by a  $K^-$ . For a  $\bar{B}_s^0$  meson, the initial  $\bar{b}$  picks up an  $s$  quark from a nearby  $s\bar{s}$  pair, with the  $\bar{s}$  ending up in a  $K^+$  meson in the “vicinity”.

<sup>5</sup>With brand new—and colossal—accelerator and detectors in an unprecedentedly harsh environment, despite the innovations and diligence, one should be prepared for setbacks which often get overcome eventually.

**Fig. 3.6** The “golden” modes  $\bar{B}_s^0 \rightarrow D_s^+ \pi^-$  (with  $D_s^+ \rightarrow \phi \pi^+$ ) as well as  $D_s^{*+} \pi^-$  and  $D_s^+ \rho^-$ , picked up by the two track SVT trigger of the CDF experiment [Copyright (2006) by The American Physical Society]. Since the  $B_s$  is fully reconstructed, these modes offer the best proper time resolution for  $\Delta m_{B_s}$  determination (from [1])



tag the  $B_s^0/\bar{B}_s^0$  is relatively slow, both TOF and  $dE/dx$  gave the critical  $1\sigma$  or slightly better discrimination. In the end, for hadronic and semileptonic SSKT,  $\epsilon D^2 \simeq 3.7\%$  and  $4.8\%$  respectively, turned out to be more than a factor of two better than OST. For the L00, the purpose of which is to improve timing resolution, the single-sided layer of silicon placed at  $\sim 1.5$  cm from the beam, operating in a hadronic environment is bound to be difficult. Noise problems reduced the efficiency and resolution. Using a large sample of prompt  $D^+$  candidates, the decay-time resolution for fully reconstructed hadronic events was found to be 87 fs, rather than the expected 45 fs.

Despite all these setbacks and disappointments, the investments of CDF finally paid off, even though  $1 \text{ fb}^{-1}$  rather than a few hundred  $\text{pb}^{-1}$  data was needed. The measurement of  $\Delta m_{B_s}$  in (3.13) is still a great achievement. Let us now present some highlight [1, 4] results of this analysis.

The secret of success is the fully reconstructed hadronic modes, where the *two* (displaced) *track trigger* was the major advantage that CDF had over  $D\phi$ . In Fig. 3.6 we plot the invariant mass distribution for  $\bar{B}_s^0 \rightarrow D_s^+ \pi^-$  (with  $D_s^+ \rightarrow \phi \pi^+$ ). These modes provide the best decay time resolution, since, unlike semileptonic decays where at least a neutrino is missing, full reconstruction means the  $\bar{B}_s^0$  momentum is directly measured. There are also partially reconstructed hadronic modes. The amplitude scan plot for the combined result is already shown in Fig. 3.5. The peak at  $\Delta m_{B_s} = 17.77 \text{ ps}^{-1}$  gives an observed amplitude  $\mathcal{A} = 1.21 \pm 0.20$  (stat) which is consistent with 1, and inconsistent with  $\mathcal{A} = 0$  at  $\mathcal{A}/\sigma_{\mathcal{A}} \simeq 6$ , indicating that data is consistent with oscillations at this frequency. Using an unbinned maximum likelihood fit for  $\Delta m_{B_s}$ , by fixing  $\mathcal{A} = 1$ , one finds the result in (3.13), with significance over  $5\sigma$ . Collecting the hadronic samples in five bins of proper decay time, one finds data to be consistent with  $\cos \Delta m_{B_s} t$  with an amplitude of  $\mathcal{A} = 1.28$ .

Using  $\Delta m_{B_d}$  values from PDG, and  $\xi \simeq 1.2$  from lattice, a value of  $|V_{td}/V_{ts}| \simeq 0.206$  is extracted, which goes into the “ $\Delta m_s$  &  $\Delta m_d$ ” band in Fig. 1.6. With the nominal values for  $f_{B_s}$ , e.g. from lattice studies at the time, the result of (3.13) seemed slightly on the small side, which is reflected in Fig. 3.3 from the CKMfitter group. This was supported by  $f_{D_s}$  measured via  $D_s^+ \rightarrow \ell^+ \nu$  decay rates by CLEO [16] and Belle [17], which were considerably higher than the lattice results. However, because of the large hadronic uncertainties in  $f_{B_s}^2 B_{B_s}$ , we cannot take this as a hint for New Physics, but have to turn to CPV which is less prone to hadronic physics.

Equation (3.13) agrees well with the current PDG value [3] of  $\Delta m_{B_s} = 17.757 \pm 0.021 \text{ ps}^{-1}$ .

## 3.2 Search for TCPV in $B_s$ System

As stated,  $\sin 2\Phi_{B_s}$  is expected to be very small in SM. Although SM has withstood challenge after challenge without giving much ground, we have argued that  $b \rightarrow s$  and  $b \leftrightarrow s$  transitions are the current frontier for New Physics search. TCPV in  $B_s$  system holds particularly good hope, since  $\sin 2\Phi_{B_s}$ , once measured, does not suffer from hadronic uncertainties in its interpretation. But one has to overcome the challenge of very rapid oscillations, among other things, as we now elucidate.

### 3.2.1 $\Delta\Gamma_{B_s}$ Approach to $\phi_{B_s}$ : $\cos 2\Phi_{B_s}$

Let us first briefly comment on the approach through width mixing, i.e.  $\Delta\Gamma_{B_s}$  and  $\phi_{B_s}$ , from untagged  $B_s^0 \rightarrow J/\psi\phi$  and other lifetime studies. With a large partial width for  $b \rightarrow c\bar{c}s$  decay, the large fraction of common final states in  $b\bar{s}$  versus  $\bar{b}s \rightarrow c\bar{c}s\bar{s}$  (i.e. the  $c\bar{c}$  cut in the box diagram amplitude for  $B_s^0-\bar{B}_s^0$  mixing) can generate a width difference. This enriches the possible CPV observables compared to the  $B_d$  system.

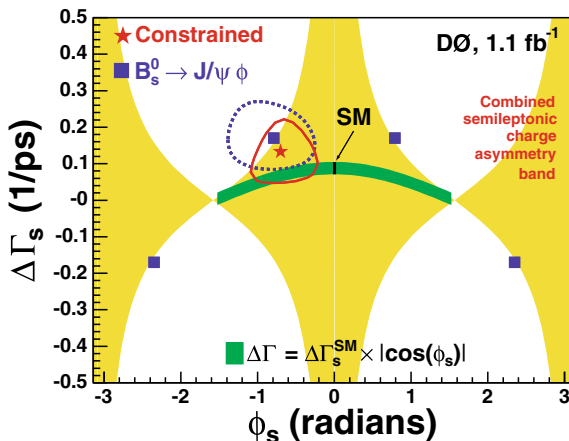
Using a data set of  $1.1 \text{ fb}^{-1}$ , the DØ experiment made a concerted effort in measuring the dimuon charge asymmetry  $A_{\text{SL}}$ , the untagged single muon charge asymmetry  $A_{\text{SL}}^s$ ,<sup>6</sup> and the lifetime difference in *untagged*  $B_s \rightarrow J/\psi\phi$  decay (hence does not involve oscillations). DØ holds the advantage in periodically flipping magnet polarity to reduce the systematic error on  $A_{\text{SL}}$ . Combining the three studies, they probe the CPV phase  $\cos 2\Phi_{B_s}$  via

$$\Delta\Gamma_{B_s} = \Delta\Gamma_{B_s}^{\text{CP}} \cos 2\Phi_{B_s}, \quad (3.14)$$

---

<sup>6</sup>The same sign dilepton charge asymmetry and the single lepton charge asymmetry are familiar from kaon physics, where they are related to  $\varepsilon_K$ . The SM predictions [10] for the analogous  $\varepsilon_{B_d^0}$  and  $\varepsilon_{B_s^0}$  are below the 0.1% level, and very hard to measure, even at the B factories [19, 20]. At hadronic machines, it is further complicated by  $B_d^0$  and  $B_s^0$  production fractions.

**Fig. 3.7** Combined analysis of  $A_{\text{SL}}$ ,  $A_{\text{SL}}^s$  and lifetime difference in untagged  $B_s \rightarrow J/\psi \phi$  by  $D\theta$  [18], based on  $1.1 \text{ fb}^{-1}$  data. [Copyright (2007) by The American Physical Society]



where  $\Delta\Gamma_{B_s}^{\text{CP}} \cong \Delta\Gamma_{B_s}^{\text{SM}}$ . The main result of interest is given in Fig. 3.7, where<sup>7</sup>  $\phi_s = 2\Phi_{B_s}$  and  $\Delta\Gamma_s = \Delta\Gamma_{B_s}^{\text{CP}}$ . The fitted width difference of  $0.13 \pm 0.09 \text{ ps}^{-1}$  was larger than the SM expectation [10] of  $|\Delta\Gamma_{B_s}|^{\text{SM}} = 0.096 \pm 0.039 \text{ ps}^{-1}$  (see (3.11)), but not inconsistent. The extracted “first” measurement of  $|\phi_s| = 0.70^{+0.39}_{-0.47}$  is somewhat off zero with large central values. The sensitivity to both  $\cos \phi_s$  and  $\sin \phi_s$  is because of interference terms between different angular amplitudes that arise through CPV. But given the large errors, the result was both consistent with SM expectation, but allows for NP.

CDF followed with an untagged, angular resolved study [21] of  $B_s \rightarrow J/\psi \phi$  using  $1.7 \text{ fb}^{-1}$  data, finding  $\Delta\Gamma_{B_s} = 0.076^{+0.059}_{-0.063} \pm 0.006 \text{ ps}^{-1}$ , assuming  $CP$  conservation (i.e. setting  $\Phi_{B_s} = 0$ ), which is consistent with the SM expectation of (3.11). Allowing for CPV, one is still consistent with  $\Phi_{B_s} = 0$ . However, sizable  $\Phi_{B_s}$  values are allowed.

Overall, the  $\cos 2\Phi_{B_s}$  approach is somewhat a “blunt instrument” for  $\Phi_{B_s}$  measurement. The reason why we bring up Fig. 3.7 from [18], is that it eventually lead to the  $A_{\text{SL}}$  “anomaly” of  $D\theta$ ,<sup>8</sup> which still stands. The “ $A_{\text{SL}}$  anomaly” is recorded in PDG as follows. With  $A_{\text{SL}}^q \cong 4 \text{Re } \varepsilon_{B_q} / (1 + |\varepsilon_{B_q}|^2)$ , the 2017 world averages (including  $3 \text{ fb}^{-1}$  results from LHCb) are  $\text{Re } \varepsilon_{B_d} / (1 + |\varepsilon_{B_d}|^2) = (-0.1 \pm 0.4) \times 10^{-3}$  and  $\text{Re } \varepsilon_{B_s} / (1 + |\varepsilon_{B_s}|^2) = (0.0 \pm 1.1) \times 10^{-3}$ , where the latter has errors scaled up because of some conflict between LHCb and  $D\theta$  measurements. However, there is a special entry

$$\text{Re } \varepsilon_b / (1 + |\varepsilon_b|^2) = (1.24 \pm 0.38 \pm 0.18) \times 10^{-3},$$

a semileptonic asymmetry for a mixture of  $B$ -hadrons, including baryons and  $B_s$ , which solely comes from  $D\theta$  [23]. This standalone result has not been independently

<sup>7</sup> $D\theta$  uses the definition  $\phi_s = 2\Phi_{B_s}$ , and because one probes  $\cos \phi_s$ , there is a 4-fold degeneracy, as can be seen from the four squares in Fig. 3.7.

<sup>8</sup>For a phenomenological digest and a glimpse of the times, see [22].

confirmed, given that the Tevatron collides protons with antiprotons, but the LHC is a  $pp$  collider. For further discussion, see [24].

Another reason for discussing the approach of (3.14), and early results such as Fig. 3.7, is because they suggested a potentially sizable  $\Delta\Gamma_s$  that deviates from SM expectation of (3.11). While New Physics is not likely to be the source, but it could arise from long distance effects. However, an exhaustive study [25] showed, from  $B_s$  decay data, that the latter cannot be the case, and the SM estimate of (3.11) should be robust. The 2017 PDG result is  $\Delta\Gamma_{B_s} = 0.084 \pm 0.007 \text{ ps}^{-1}$ .

### 3.2.2 Prospecting for $\sin 2\Phi_{B_s}$ , ca. 2008

The more direct approach to measuring  $\sin 2\Phi_{B_s}$  is via tagged TCPV study of  $B_s \rightarrow J/\psi\phi$ . The  $B_s \rightarrow J/\psi\phi$  decay is analogous to  $B_d \rightarrow J/\psi K_s$ , except it is a  $VV$  final state. Thus, besides measuring the decay vertices, one also needs to perform an angular analysis to separate the  $CP$  even and odd components. As  $J/\psi$  is reconstructed in the dimuon final state, there are in general no triggering issues. A situation arose ca. 2008 regarding whether  $\sin 2\Phi_{B_s}$  could be sizable, which led to a competition between Tevatron and LHC for the measurement of  $\sin 2\Phi_{B_s}$ , an interesting chapter in the pursuit of New Physics in the flavor sector.

We have highlighted the measurement of  $\Delta m_{B_s}$  at the Tevatron. But measuring  $\sin 2\Phi_{B_s}$  is much more challenging, and prospects looked slim, given that the SM expectation is minuscule, and that LHC was expected to collide proton beams by 2008. Since trigger is not an issue, CDF and DØ should have comparable sensitivity. Assuming  $8 \text{ fb}^{-1}$  per experiment, the Tevatron could reach an ultimate sensitivity of [26]

$$\sigma(\sin 2\Phi_{B_s}) \sim 0.2/\sqrt{2} \quad (\text{Tevatron combined}). \quad (3.15)$$

Of course, as one continues improving techniques at the Tevatron, the gain may be more than just in luminosity. Still, trying to compete with LHCb (see Fig. 3.8 for the detector schematics) seemed rather uphill.

However, after achieving first beam in September 2008, the LHC suffered a catastrophic magnet accident soon after! Keeping in mind the slow start of Tevatron Run II, how fast can LHC produce physics results became an open question. If one adopts a conservative estimate [28] for the “first year”—uncertain in actual calendar terms at the time—running of LHC:  $2.5 \text{ fb}^{-1}$  for ATLAS and CMS, and  $0.5 \text{ fb}^{-1}$  for LHCb, the projection for ATLAS (CMS) is  $\sigma(\sin 2\Phi_{B_s}) \sim 0.16$ , not much better than the Tevatron, while for LHCb one has  $\sigma(\sin 2\Phi_{B_s}) \sim 0.04$ . The situation turned volatile, and we list these sensitivities side by side in Table 3.1, the reference values for 2010–2011.

If SM again holds sway, as we have witnessed time and again *for decades*, then LHCb would clearly be the winner, since  $\sigma(\sin 2\Phi_{B_s}) \sim 0.04$  starts to probe the SM expectation of (3.8). After all, the forward detector design (see Fig. 3.8) aims for



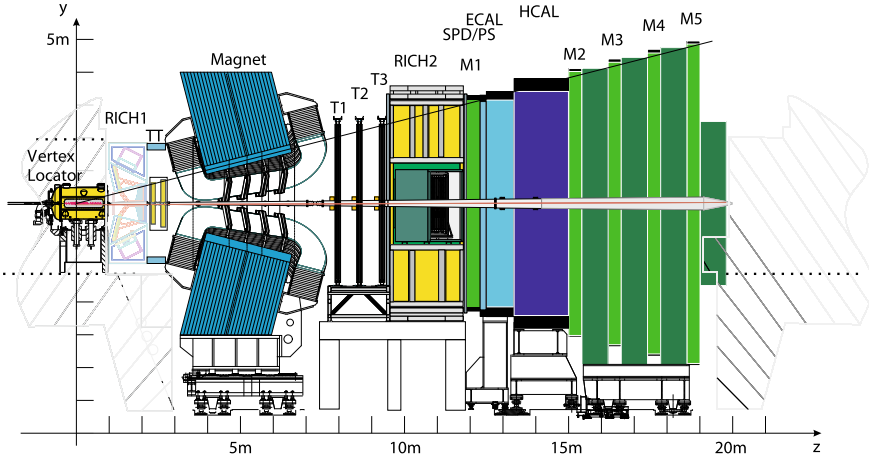


**Fig. 3.8** The LHCb detector. [Adapted from Fig. 2.1 of [27], used with permission [Copyright of Institute of Physics and IOP Publishing Limited 2008]]

**Table 3.1** Projected rough sensitivity for  $\sin 2\Phi_{B_s}$  measurement, ca. 2010

|                            | CDF/DØ                | ATLAS/CMS               | LHCb                    |
|----------------------------|-----------------------|-------------------------|-------------------------|
| $\sigma(\sin 2\Phi_{B_s})$ | 0.2/expt              | 0.16/expt               | 0.04                    |
| $\int \mathcal{L} dt$      | (8 fb <sup>-1</sup> ) | (2.5 fb <sup>-1</sup> ) | (0.5 fb <sup>-1</sup> ) |

*B* physics: It takes advantage of the large collider cross section for  $b\bar{b}$  production, while implementing a fixed-target-like detector configuration, which allows more space for, besides the Vertex Locator (VELO), devices such as RICH detectors for PID, and a better ECAL. We have seen how important a good PID system is for flavor-tagging.

We stress, however, that 2009(–2010) looked rather interesting—Tevatron might get really lucky: it could glimpse the value of  $\sin 2\Phi_{B_s}$ , but *only if its strength is large; but if  $|\sin 2\Phi_{B_s}|$  is large, it would definitely indicate New Physics.* Thus,

*The Tevatron could preempt LHCb and grab the glory of discovering physics beyond the Standard Model in  $\sin 2\Phi_{B_s}$ .*

(stressed since 2005 [29], and esp. since [30] early 2007). For this and other reasons, the Tevatron should perhaps run longer, especially if LHC dangles further. This attests to the value of flavor physics in parallel with Higgs search.

So, the question became ...

**Can  $|\sin 2\Phi_{B_s}| > 0.5$ ?**

The answer should clearly be in the positive, as it is a question to be reckoned with by experiment. However, to be true, around the time there were few believers—The

SM had been too successful! In the following, we provide some phenomenological insight on an *existence proof* during the period that link with the hints for New Physics discussed in the previous chapter. That is, it is of interest to explore whether New Physics hints in  $\Delta B = 1$  ( $b \rightarrow s$ ) processes of Chap. 2 have implications for the  $\Delta B = 2$  ( $b\bar{s} \rightarrow s\bar{b}$ ) processes. This subsection therefore has phenomenology connotations, but should be an excellent example of the synergies of theory and experiment.

One can of course resort to squark-gluino box diagrams, Fig. 3.2b. However, while possibly generating  $\Delta\mathcal{S}$ , squark-gluino loops cannot really move  $\Delta\mathcal{A}_{K\pi}$  because their effects are decoupled in  $P_{EW}$ . If one wishes to have contact with both hints for NP in  $b \rightarrow s$  transitions from the B factories, then one should pay attention to some common nature between  $b \rightarrow s$  electroweak penguin diagrams and the box diagrams for  $B_s$  mixing. If there are new *nondecoupled* quarks in the loop, then both  $\Delta\mathcal{A}_{K\pi}$  and  $\Delta\mathcal{S}$  could be touched. It also affects  $B_s$  mixing, as it is well known that the top quark effect in electroweak penguin and box diagrams are rather similar. Such new nondecoupled quarks are traditionally called the 4th generation quarks,<sup>9</sup>  $t'$  and  $b'$ .

Having the  $t'$  quark in the loop adds a term proportional to

$$V_{t's}^* V_{t'b} \equiv r_{sb} e^{i\phi_{sb}}, \quad (3.16)$$

to (3.4). It is useful to visualize this,

$$V_{us}^* V_{ub} + V_{cs}^* V_{cb} + V_{ts}^* V_{tb} + V_{t's}^* V_{t'b} = 0 \quad (3.17)$$

$$\implies V_{ts}^* V_{tb} \simeq -V_{cb}^* V_{tb} - V_{t's}^* V_{t'b}, \quad (3.18)$$

where the last step again follows from  $|V_{us}^* V_{ub}| \ll 1$ . Note that  $V_{cb}^* V_{tb}$  continues to be real by phase convention, but the  $t'$  contribution brings in the additional NP CPV phase  $\arg(V_{t's}^* V_{t'b}) \equiv \phi_{sb}$  with even larger *Higgs affinity*, i.e. Yukawa coupling  $\lambda_{t'} > \lambda_t \simeq 1$ , since  $m_{t'} > m_t$  by definition. The new weak phase enters the  $t$  quark contribution as well, through (4-generation) CKM unitarity. Dynamically speaking, these effects of  $t'$  are not different from what is already present in the 3 generation SM (or SM3; we shall refer to the 4th generation Standard Model as SM4), since both the presence of CPV, and large  $\lambda_t$ , are already verified by experiment.

---

<sup>9</sup>Before the advent of the 125 GeV Higgs boson, there were two main problems [31] with the 4th generation. One is the existence of only 3 light neutrinos, which has been known since 1989. The other problem is that the electroweak precision tests (EWPT) seem to rule out the 4th generation with high confidence. We take the 4th generation as an illustration that touches on many aspects of flavor physics and CPV (just like the top). In regards neutrino counting in  $Z$  decay, we know that there is more to the neutral lepton sector, since the observation of large neutrino mixing in 1998. The strict, minimal SM with “no right-handed neutrinos” is no more, and the neutrino sector carries a mass scale. As for EWPT, the paper by Kribs et al. [32] challenged the orthodox PDG view [31]. These authors cited that the constraints by the LEP Electroweak Working Group (LEP EWVG) at the time were more forgiving [33] for a 4th generation: The  $t'$  and  $b'$  should be heavy but slightly split in mass (difference less than  $M_W$ ), i.e. cannot be degenerate. At the time of  $\sin 2\Phi_{B_s}$  prospecting, these put limits on the parameter space, but should not be taken as strong discouragement.

It was shown [34] that the 4th generation could account for  $\Delta\mathcal{A}_{K\pi}$ , and  $\Delta\mathcal{S}$  then moves in the right direction [35]. This was done in the PQCD approach up to next-to-leading order (NLO), which was state of the art at the time. We note that PQCD is the only QCD-based factorization approach that *predicted* [36] both the strength and sign of  $\mathcal{A}_{\text{CP}}(B^0 \rightarrow K^+\pi^-)$  in (2.7). At NLO in PQCD [37] factorization, an enhancement of  $C$  does relax a bit the  $\Delta\mathcal{A}_{K\pi}$  problem discussed in Sect. 2.2.2 (see (2.9) and (2.10)). But it demonstrates that a (perturbative) calculational approach could not generate  $|C/T| > 1$ . It is nontrivial, then, that incorporating the nondecoupled 4th generation  $t'$  quark to account for  $\Delta\mathcal{A}_{K\pi}$ , it can also move  $\Delta\mathcal{S}$  in the right direction.

The really exciting implication, however, is the impact on  $\sin 2\Phi_{B_s}$  [29, 30]: the  $t'$  effect in the box diagram also enjoys nondecoupling. As the difference of  $\Delta\mathcal{A}_{K\pi}$  in (2.10) is large, both the strength and phase of  $V_{t's}^*V_{t'b}$  are sizable [34], with the phase not far from maximal. A near maximal phase from  $t'$  is precisely what allows the minimal impact on  $\Delta m_{B_s}$ , as it adds only in quadrature to the real contribution from top, but makes maximal impact on  $\sin 2\Phi_{B_s}$ . The  $t'$  effect can in fact partially cancel against too large a  $t$  contribution in the real part, and could in principle bring  $\Delta m_{B_s}$  down to a lower value.

### Some Formalism for 4th Generation

At this point, it is illuminating to get a feeling of how these *nondecoupling  $t'$  effects* emerge. Ignoring  $V_{us}^*V_{ub}$ , i.e. taking (3.18) literally, the effective Hamiltonian for loop-induced  $b \rightarrow s\bar{q}q$  transitions becomes,

$$H_{\text{eff}}^{\text{loop}} \propto \sum_{i=3}^{10} (v_c C_i^t - v_{t'} \Delta C_i) O_i, \quad (3.19)$$

where  $C_i$ s are the effective Wilson coefficients of the (four-quark) operators  $O_i$  that arise from quantum loop effects, and the CKM product

$$v_q \equiv V_{qs}^* V_{qb}. \quad (3.20)$$

The first  $v_c C_i^t$  term is the usual SM, or SM3, effect, while

$$-v_{t'} \Delta C_i \equiv -v_{t'} (C_i^{t'} - C_i^t) \quad (3.21)$$

is the effect of the 4th generation. Note that the latter vanishes not only with  $v_{t'} = V_{t's}^* V_{t'b}$ , but also as  $m_{t'} \rightarrow m_t$ , which are the twin requirements of the GIM mechanism [38]. This is a condition that quite a few calculations in the literature that involve the 4th generation do not respect. We plot in Fig. 3.9a the functions  $\Delta C_i$  for  $i = 4, 6$  (strong penguin), 7 (electromagnetic penguin) and 9 (electroweak penguin). The functions for  $i = 3, 5$  are similar to 4, 6 case, while for  $i = 8$  (10), it is similar to 7 (9).

Let us understand the  $m_{t'}$  dependence. First, note that the different  $\Delta C_i$ s converge to zero for  $m_{t'} \rightarrow m_t$ , as required by GIM. We have normalized  $-\Delta C_i$  by  $|C_4^t|$ , the

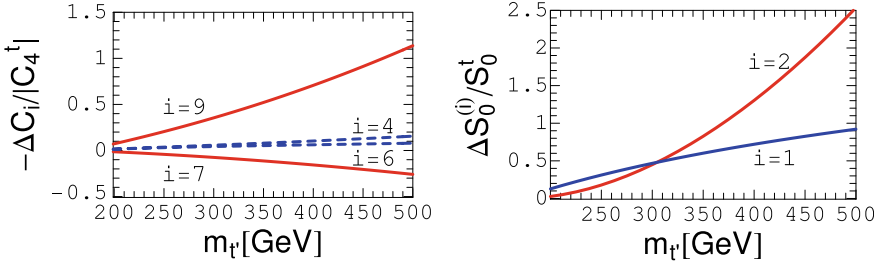


**Fig. 3.9** The  $t'$  correction **a**  $-\Delta C_i$  normalized to strength of strong penguin coefficient  $|C_4^t|$  (both at  $m_b$  scale), and **b**  $\Delta S_0^{(i)}$  normalized to  $S_0^t$  versus  $m_{t'}$ , showing nondecoupling of  $t'$  effect (from [30]). [Copyright (2007) by The American Physical Society]

top contribution to the strong penguin coefficient. We see that  $-\Delta C_{4(6)}$  has rather mild  $m_{t'}$  dependence, and is always small compared to the top contribution. This is because, as mentioned in Footnote 6 of Chap. 2, the strong penguin has less than logarithmic dependence on the heavy quark mass  $m_Q$  in the loop. Thus, when one subtracts  $C_{4(6)}^t$  from  $C_{4(6)}^{t'}$ , not much is left [39].

The situation is rather different for the electroweak penguin coefficient  $\Delta C_9$ , which has linear  $x_{t'} \equiv m_{t'}^2 / M_W^2$  dependence arising from  $Z$  and box diagrams [40], as can be seen very clearly from Fig. 3.9a. This is the nondecoupling of heavy  $t$  and  $t'$  effects through their large Higgs affinity, or Yukawa couplings,  $\lambda_t$  and  $\lambda_{t'}$ . For  $m_{t'} > 350$  GeV,  $|\Delta C_9|$  already exceeds  $\frac{1}{2}|C_4^t|$ . For the electromagnetic penguin coefficient  $\Delta C_7$ , the behavior is in between  $\Delta C_4$  and  $\Delta C_9$ . The  $m_t$  dependence of  $C_7$  is roughly logarithmic, hence there is some difference between  $t'$  and  $t$  effect when they are not too close to being degenerate, but the difference is far less prominent than for  $C_9$ . We note that the functional dependence of  $C_i$ s on heavy top mass can be traced to the so-called Inami–Lim functions [41] derived for kaons, independently rediscovered [40] for electroweak penguin induced  $B$  decays.<sup>10</sup>

Adding a  $t'$  quark to the box diagram of Fig. 3.2a, with obvious notation, one makes the following effective substitution [30] in (3.1),

$$v_t^2 S_0(t, t) \rightarrow v_c^2 S_0(t, t) - 2v_c v_{t'} \Delta S_0^{(1)} + v_{t'}^2 \Delta S_0^{(2)}, \quad (3.22)$$

where  $v_q$  is defined in (3.20), and (3.18) has been used. It is clear that the first term is just the SM3 effect, and is practically real, while

$$\Delta S_0^{(1)} \equiv S_0(t, t') - S_0(t, t), \quad (3.23)$$

$$\Delta S_0^{(2)} \equiv S_0(t', t') - 2S_0(t, t') + S_0(t, t). \quad (3.24)$$

<sup>10</sup>In paper [42], the predecessor paper to [40], the electroweak penguin contribution was simply dropped with respect to the electromagnetic contribution by  $G_F$  power counting arguments. So, nondecoupling is not intuitive.

These  $\Delta S_0^{(i)}$ 's respect GIM cancellation, and their effects vanish with  $v_{t'}$ , analogous to the  $\Delta C_i$  terms in (3.19). Normalizing them to  $S_0^t = S_0(t, t)$ , they are plotted versus  $m_{t'}$  in Fig. 3.9b. Their behavior can be compared to  $\Delta C_9$  plotted in Fig. 3.9a. The strong  $m_{t'}$  dependence illustrates the nondecoupling of SM-like heavy quarks from box and EWP diagrams [40].

With large nondecoupling effects because of the heavy  $t'$  mass, and bringing in a New Physics CPV phase into  $b \rightarrow s$  transitions, the 4th generation is of particular interest for processes involving boxes and Z penguins.

### Impact: Large and Negative $\sin 2\Phi_{B_s}$

We show in Fig. 3.10 the variation of  $\Delta m_{B_s}$  and  $\sin 2\Phi_{B_s}$  with respect to the new CPV phase  $\phi_{sb} \equiv \arg V_{t's}^* V_{t'b}$  in the 4th generation model, for the nominal  $m_{t'} = 300$  GeV and  $r_{sb} \equiv |V_{t's}^* V_{t'b}| = 0.02, 0.025, \text{ and } 0.03$ , where stronger  $r_{sb}$  gives larger variation. Using the central value of  $f_{B_s} \sqrt{B_{B_s}} = 295 \pm 32$  MeV, we get a nominal 3 generation value of  $\Delta m_{B_s}|^{\text{SM}} \sim 24 \text{ ps}^{-1}$ , which is the dashed line. The CDF measurement of (3.13) is the rather narrow solid band, attesting to the precision already reached by experiment, and that it is below the nominal SM value shown as the dashed line.

Combining the information from  $\Delta \mathcal{A}_{K\pi}$ ,  $\Delta m_{B_s}$  and  $\mathcal{B}(b \rightarrow s \ell^+ \ell^-)$ , the predicted value is [30]

$$\sin 2\Phi_{B_s} = -0.5 \text{ to } -0.7 \quad (\text{4th generation, ca. 2007}), \quad (3.25)$$

where even the sign is predicted. Compared with the SM expectation in (3.8), the strength is enormous. The motivation arose from the  $\Delta \mathcal{A}_{K\pi}$  (and  $\Delta S$ ) problem. However, the range can be demonstrated by using the (stringent)  $\Delta m_{B_s}$  versus (less stringent)  $\mathcal{B}(B \rightarrow X_s \ell^+ \ell^-)$  constraints alone, with  $\Delta \mathcal{A}_{K\pi}$  selecting the minus sign in (3.25), as can be read off from Fig. 3.10. Note that for different  $m_{t'}$ , it maps into a different  $\phi_{sb}$ - $r_{sb}$  range, with minor changes in the predicted range for  $\sin 2\Phi_{B_s}$ .

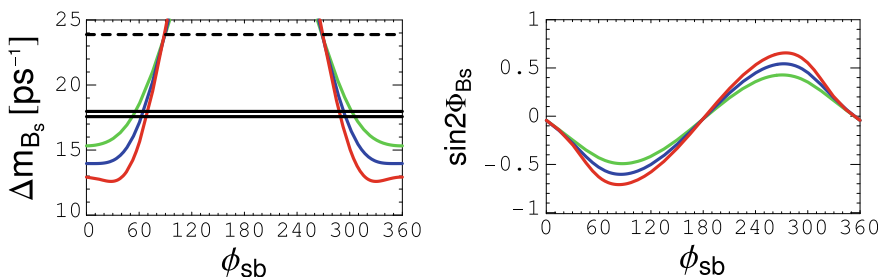


**Fig. 3.10**  $\Delta m_{B_s}$  and  $\sin 2\Phi_{B_s}$  vs  $\phi_{sb} \equiv \arg V_{t's}^* V_{t'b}$  for the 4th generation extension of SM [30], where  $|V_{t's}^* V_{t'b}| = 0.02, 0.025, 0.03$  (larger value gives stronger variation) and  $m_{t'} = 300$  GeV, which are for illustration [Copyright (2007) by The American Physical Society]. Dashed horizontal line is the nominal 3 generation SM expectation taking  $f_{B_s} \sqrt{B_{B_s}} = 295$  MeV. Solid band is the experimental measurement by CDF [1]. The narrow range implied by  $\Delta m_{B_s}$  measurement project out large values for  $\sin 2\Phi_{B_s}$ , where the right branch is excluded by the sign of  $\Delta \mathcal{A}_{K\pi}$ , (2.10)

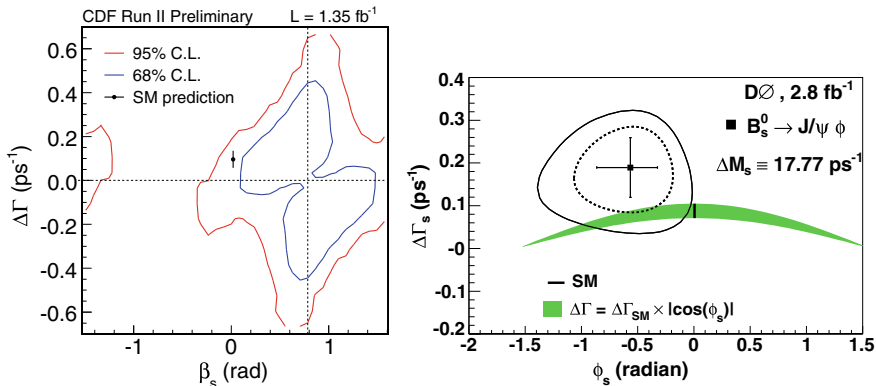


**Fig. 3.11**  $\Delta\Gamma_{B_s}$  versus  $\Phi_{B_s}$  from first tagged time-dependent studies by CDF [43] using  $1.35\text{ fb}^{-1}$  data, and DØ [44] using  $2.8\text{ fb}^{-1}$  data [Copyright (2008) by The American Physical Society]. Note that  $-\beta_s = \phi_s/2 = \Phi_{B_s}$

### 3.2.3 Hints at Tevatron in 2008

As stressed already, because of the predicted enormous strength, (3.25) can be probed even before LHCb gets first data, and should help motivate the Tevatron experiments. Inspection of Table 3.1, 2010–2011 indeed appeared rather interesting. The Tevatron could well come out the winner. From SUSY 2007, when the writing of this monograph commenced, strides were made at the Tevatron, and interestingly, things started to look optimistic from experimental side in 2008! In the spirit of “*What if?*”, let us convey the situation to capture the excitement at the time. We also utilize these first measurements to illustrate the rudiments of the analysis approach.

Using  $1.35\text{ fb}^{-1}$  data, CDF performed the first tagged and angular-resolved time-dependent CPV study of the  $B_s \rightarrow J/\psi\phi$  decay process. The result [43], in terms of  $\Delta\Gamma_{B_s}$  versus  $\beta_s = -\Phi_{B_s}$ , is shown in Fig. 3.11. Using  $2.8\text{ fb}^{-1}$  data, DØ followed shortly with a similar analysis, assuming (3.13) for  $\Delta m_{B_s}$  as input. The result [44], in terms of  $\phi_s = 2\Phi_{B_s}$ , is also shown in Fig. 3.11. Up to a two-fold ambiguity in the CDF result,<sup>11</sup> to the eye, one sees that both experiments find  $\Phi_{B_s}$  to be negative, and with central values that are more consistent with the 4th generation prediction of (3.25), than with the SM expectation given in (3.8). With this, interest in the 4th generation grew.

Let us understand how Fig. 3.11 was reached. Both the  $\cos 2\Phi_{B_s}$  approach, discussed in the previous section, and the  $\sin 2\Phi_{B_s}$  approach study the  $B_s^0$  decay to  $J/\psi\phi$  final state, but the  $\sin 2\Phi_{B_s}$  approach bears more similarities to the  $\sin 2\phi_1/\beta$  ( $\equiv \sin 2\Phi_{B_d}$ ) study at the B factories. One needs to resolve the time dependence of  $B_s^0$ – $\bar{B}_s^0$  oscillations. So, just like the measurement of  $\Delta m_{B_s}$  discussed in Sect. 3.1, one

<sup>11</sup>For the DØ result, this ambiguity is removed by assuming the strong phases in  $B_s^0 \rightarrow J/\psi\phi$  helicity amplitudes are the same as in  $B \rightarrow J/\psi K^{*0}$ .

needs to tag the  $B_s^0$  or  $\bar{B}_s^0$  flavor at time of production,  $t = 0$ , and be able to resolve the time  $t$  of  $B_s^0 \rightarrow J/\psi\phi$  decay. The study is actually closer to the  $B_d^0 \rightarrow J/\psi K^{*0}$  analysis at B factories: the  $VV$  final state is not a  $CP$  eigenstate, and one needs to perform an angular analysis to separate the  $CP$  even ( $S$ - and  $D$ -wave) and odd ( $P$ -wave) final states, to correct for the  $CP$  eigenvalue  $\xi_f$  in (A.9) for the given partial wave (note that  $J/\psi$  and  $\phi$  are both  $CP$  even). Thus, the study is rather involved.

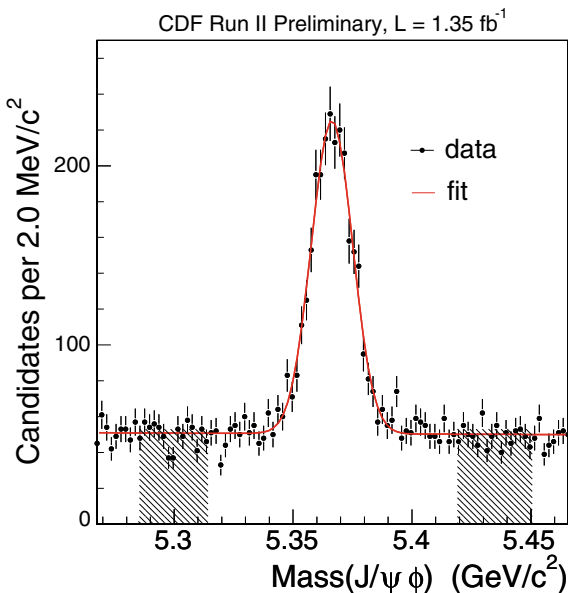
### Collection of Signal Events

Both CDF and DØ reconstruct  $J/\psi\phi$  via  $J/\psi \rightarrow \mu^+\mu^-$  and  $\phi \rightarrow K^+K^-$  that emerge from a common vertex. The dimuon implies that, unlike the situation for  $\Delta m_{B_s}$  measurement, there is no problem for DØ with triggering the events, although the muon trigger threshold of  $2.0 \text{ GeV}/c$  is higher than the  $1.5 \text{ GeV}/c$  threshold for CDF. For CDF, as in their  $\Delta m_{B_s}$  study, an artificial neural network (ANN) is employed to separate  $B_s^0 \rightarrow J/\psi\phi$  signals from background. The ANN is trained with Monte Carlo (MC) data for the signal, and the background is taken from the sideband of actual data. In this way, with  $1.35 \text{ fb}^{-1}$  data, CDF observed  $\sim 2000$  signal events with  $S/B \sim 1$ , which we plot in Fig. 3.12. Using similar method,  $\sim 7800 B_d^0 \rightarrow J/\psi K^{*0}$  events were reconstructed as control sample. DØ also reconstructed  $\sim 2000$  signal events, but with a larger  $2.8 \text{ fb}^{-1}$  dataset. Since the study is statistics limited, this illustrates the efficacy of an ANN analysis, as well as a lower muon trigger threshold.

### Flavor Tagging

Turning to flavor-tagging, for the CDF study, the mean effectiveness  $Q \equiv \epsilon \mathcal{D}^2$  is only  $\sim 1.2\%$  for opposite side tagging (OST), lower than the  $1.8\%$  achieved for  $\Delta m_{B_s}$ .

**Fig. 3.12**  $M(J/\psi\phi)$  distribution for  $B_s^0 \rightarrow J/\psi\phi$  events reconstructed in  $J/\psi \rightarrow \mu^+\mu^-$  and  $\phi \rightarrow K^+K^-$  by CDF [43] with  $1.35 \text{ fb}^{-1}$  data. [Copyright (2008) by The American Physical Society]



measurement [1], while the mean  $Q$  for same side kaon tagging (SSKT) is  $\sim 3.6\%$ , also slightly lower than  $\Delta m_{B_s}$  measurement. This slightly lower  $Q$  for  $B_s \rightarrow J/\psi\phi$  TCPV study, as compared to the  $B_s$  mixing study, is in part due to a lower average  $p_T$ . In contrast, for the  $D\emptyset$  study, by incorporating same side tagging as well as OST,  $\epsilon\mathcal{D}^2$  is improved significantly, from  $\sim 2.5\%$  for the purely OST analysis of the  $\Delta m_{B_s}$  measurement [11], to  $\sim 4.7\%$ , becoming comparable to CDF.

### Angular Resolved TCPV: Rich Interference

Although the need to perform angular analysis makes it much more involved, it provides considerably more analyzing power. The angular amplitudes are decomposed in the transversity basis [45]. There are three components  $A_0$ ,  $A_{\parallel}$  and  $A_{\perp}$ , corresponding to linear polarization states of the vector mesons  $J/\psi$  and  $\phi$  being either longitudinal (0) or transverse to their direction of motion, and parallel ( $\parallel$ ) or perpendicular ( $\perp$ ) to each other. There are 5 variables: three amplitude strengths, and two strong phase differences. The time-evolution of the  $|A_f(t)|^2$ , besides the classic  $\xi_f \sin 2\Phi_{B_s} \sin \Delta m_{B_s} t$  term (which is why we call this the  $\sin 2\Phi_{B_s}$  approach), where  $\xi_f$  is the  $CP$  eigenvalue for amplitude  $f$ , there is also a  $\xi_f \cos 2\Phi_{B_s} \sinh \Delta\Gamma_{B_s} t$  term from  $CP$  violation through width mixing. This enriches the simpler formula,<sup>12</sup> (A.9), for  $B_d^0$  studies where width difference is negligible. The time evolution of the  $\text{Re}(A_0^*(t)A_{\parallel}(t))$  interference term is likewise, except that it is modulated by  $\cos \delta_{\parallel 0}$  of the strong phase difference  $\delta_{\parallel 0} \equiv \delta_{\parallel} - \delta_0$ .

The existence of  $CP$  violation itself, as well as difference in the final state strong phases, enrich further the interference between  $CP$  even and odd amplitudes, namely  $\text{Im}(A_0^*(t)A_{\perp}(t))$  and  $\text{Im}(A_{\parallel}^*(t)A_{\perp}(t))$  terms. Take  $\text{Im}(A_0^*(t)A_{\perp}(t))$  for example, one has a CPV term  $\cos 2\Phi_{B_s} \sin \Delta\Gamma_{B_s} t$  modulo  $\cos \delta_{\perp 0}$ , but there is also a  $\sin \delta_{\perp 0}$  final state interaction effect in the  $\cos \Delta m_{B_s} t$  Fourier component that mimics CPV.

### The Emergent Hint

We can now try to understand the results in Fig. 3.11. The dotted cross lines in Fig. 3.11a show a reflection symmetry in the  $\Phi_{B_s} - \Delta\Gamma_{B_s}$  plane, which is due to the presence of both CPV and  $CP$  conserving phases. This results in a two-fold ambiguity for  $\Phi_{B_s}$  (but not for  $\sin 2\Phi_{B_s}$ ). Note, however, that flavor-tagging has reduced the four-fold ambiguity present in Fig. 3.7, to two-fold. The SM prediction of  $\Phi_{B_s} \simeq -0.04$  and  $\Delta\Gamma_{B_s} = 0.096 \text{ ps}^{-1}$  is also plotted in Fig. 3.11a, which lies between the 68% and 95% C.L. curves. The deviation from SM is  $1.5\sigma$  for CDF. For the  $D\emptyset$  plot of Fig. 3.11b, an input of  $\Delta m_{B_s} = 17.77 \pm 0.12 \text{ ps}^{-1}$  was used, and a more aggressive assumption of fixing  $\delta_{\perp 0} = 2.92 \text{ rad}$  and  $\delta_{\perp \parallel} = -0.46 \text{ rad}$ , within a Gaussian width of  $\pi/5$ , which are the favored values from  $B_d^0 \rightarrow J/\psi K^{*0}$  studies at the B factories [46]. Though questionable (a dubious ‘‘SU(3)’’ assumption), it removes the negative  $\Delta m_{B_s}$

<sup>12</sup>In this discussion, direct CPV has been ignored for the  $B_s^0 \rightarrow J/\psi\phi$  process. That is,  $|\lambda_{B_s^0 \rightarrow J/\psi\phi}| = 1$  is assumed. Allowing for DCPV would further enrich the  $B_s^0 \rightarrow J/\psi\phi$  study. However, considering our discussions in Sect. 2.3, ignoring DCPV here is a good approximation, as well as simplification, for discussing New Physics search.



solution.  $D\bar{0}$  then finds a  $1.8\sigma$  deviation from SM. We should stress that, though the two fold ambiguity involves a sign flip with  $\Delta m_{B_s}$ , it does not affect the value for  $\sin 2\Phi_{B_s}$ .

For sake of comparison, we choose to present the values for the  $1\sigma$  ranges (caution: non-Gaussian) for  $\sin 2\Phi_{B_s}$ , assuming strong phase structure in  $B_s^0 \rightarrow J/\psi\phi$  is similar to  $B_d^0 \rightarrow J/\psi K^{*0}$ , and constraining  $\Delta\Gamma_{B_s} = \Delta\Gamma_{B_s}|^{\text{SM}} \cos 2\Phi_{B_s}$ . Thus,

$$\begin{aligned} \sin 2\Phi_{B_s} &\in [-0.4, -0.9] \quad \text{CDF } 1.35 \text{ fb}^{-1}; \\ &[-0.2, -0.7] \quad D\bar{0} \text{ } 2.8 \text{ fb}^{-1}. \end{aligned} \quad (3.26)$$

We have used only one digit of significance, and the CDF result also constrains the mean  $B_s$  width to the  $B_d$  width. The result of (3.26) is certainly not yet a demonstration that  $\sin 2\Phi_{B_s}$  is nonzero and negative, and deviating from SM prediction of  $-0.04$ , but comparison with the 4th generation prediction, (3.25), is staggering. For  $D\bar{0}$ , we have used the value of  $\sin 2\Phi_{B_s} = -0.46 \pm 0.28$ , which is for  $2.8 \text{ fb}^{-1}$ . If  $D\bar{0}$  could improve signal event reconstruction efficiency, e.g. employ some ANN approach, together with at least doubling the data set, a smaller error than the estimation of 0.2 offered in Sect. 3.2.2 seems reachable. Likewise, if we take the CDF result in (3.26) and assume Gaussian error, one has  $\sin 2\Phi_{B_s} = -0.66 \pm 0.27$ . Since this is for  $1.35 \text{ fb}^{-1}$  data, even though the error is probably not Gaussian, an error less than 0.2 seems reachable.<sup>13</sup> Although there is still the strong phase ‘‘nuisance’’ in  $B_s^0 \rightarrow J/\psi\phi$  to unravel, the prospects for measuring  $\sin 2\Phi_{B_s}$  in the range of (3.25) appeared promising.

In fact, the UTfit group boldly combined the results of  $\Delta m_{B_s}$  as well as Figs. 3.7 and 3.11, and made a strong claim of *first evidence* ( $3.7\sigma$ ) for New Physics in  $b \leftrightarrow s$  transitions [47], with  $\Phi_{B_s} = -19.9^\circ \pm 5.6^\circ$ , or

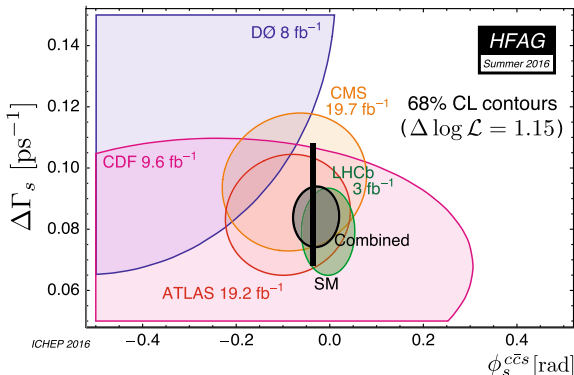
$$\sin 2\Phi_{B_s} = -0.64_{-0.14}^{+0.16} \quad (\text{UTfit, Winter 2008}). \quad (3.27)$$

We will not go into what assumptions were made to reach this value, since it seems the significance is even better than our account above (UTfit dropped to  $\sim 3\sigma$  in published version), maybe in part because it contains information beyond  $B_s \rightarrow J/\psi\phi$  TCPV analysis, e.g. those discussed in Sect. 3.2.1. But there is no escape that the value is tantalizingly consistent with (3.25), the prediction of the 4th generation model! It is useful to remember, then, that the latter combines  $\Delta m_{B_s}$  and  $\Delta\mathcal{A}_{K\pi}$  results. Thus, in 2008 there were good reasons to be optimistic that Nature may prefer linking  $\Delta\mathcal{A}_{K\pi} > 0$  ( $b \rightarrow s\bar{q}q$  transition) with large and negative  $\sin 2\Phi_{B_s}$  in  $B_s^0$  TCPV ( $b\bar{s} \leftrightarrow s\bar{b}$  transition). And the link is most natural through nondecoupled chiral quarks. We note that models like squark-gluino loops, or  $Z'$  models with specially chosen couplings, could also give large  $\sin 2\Phi_{B_s}$ , but they would be unable to link with  $\Delta\mathcal{A}_{K\pi}$ , and the two observables are not correlated in these scenarios.

---

<sup>13</sup>Extending to  $1.7 \text{ fb}^{-1}$ , the ANN signal yield [21] for  $B_s^0 \rightarrow J/\psi\phi$  increased consistently from 2000 to 2500.

**Fig. 3.13**  $\Delta\Gamma_{B_s}$  versus  $\phi_s = 2\Phi_{B_s}$  from HFAG 2016 combination [48] of world data as of summer 2016



### 3.2.4 Anticlimax: $\sin 2\Phi_{B_s} \simeq 0$

Even without taking the more aggressive stance of UTfit, (3.27), anticipation grew for measurement of  $\sin 2\Phi_{B_s}$ , that it might well unveil New Physics. If the central value stays, observation at Tevatron with data up to 2010 seems likely [49]. What remained to be seen was how fast LHCb could produce physics results with their 2010 or 2011 data. The performance of LHC after recovering from the 2008 accident lead to closure of the Tevatron by 2011, but not before CDF and DØ each collected of order  $10\text{fb}^{-1}$  data.

But now we know [3] that  $\sin 2\Phi_{B_s}$  really *is* small, and consistent with SM within error bars,

$$\sin 2\Phi_{B_s} = -0.030_{-0.034}^{+0.034} \quad (\text{PDG 2017}). \quad (3.28)$$

We give in Fig. 3.13 the HFAG combination plot for summer 2016, shown as the black ellipse, which is in good agreement with SM expectations, the thick vertical black strip. The experimental measurement for  $\Delta\Gamma_{B_s}$  is now better than theoretical prediction, while gone is the “prospect” for large values of  $|\sin 2\Phi_{B_s}|$  discussed in the previous subsection.

Some comments can be made to bring about a perspective to Fig. 3.13.

The combination is dominated by LHCb, the detector (Fig. 3.8) that is specialized for B physics at the LHC. However, there is some interesting story behind the LHCb value [50] of  $\phi_s = 2\Phi_{B_s} = -0.010 \pm 0.039$  rad, which is the combined Run 1 (full  $3\text{fb}^{-1}$ ) result between  $B_s \rightarrow J/\psi K^+ K^-$  and  $J/\psi \pi^+ \pi^-$ . The central value is small because the two modes gave comparable results of opposite sign, i.e.  $0.029 \pm 0.025 \pm 0.003$  rad [50] versus  $-0.035 \pm 0.034 \pm 0.004$  rad [51], respectively. Furthermore, as recorded in PDG, each mode went through a sign change in going from  $1\text{fb}^{-1}$  (at 7 TeV) to  $3\text{fb}^{-1}$  (7 and 8 TeV) data. Thus, not only more data matters, having two different modes with different approach, hence systematics, is also important as internal crosscheck within the same experiment. We do not trace

the details of these sophisticated analyses, but they involve signal collection, flavor tagging, angular analysis as illustrated in Sect. 3.2.3. PID is clearly crucial in separating the  $K^+K^-$  and  $\pi^+\pi^-$  modes.

The two ellipses next large in size are the measurements by CMS [52] and ATLAS [53], respectively. Though with larger errors, it is these two measurements that brought the central value in (3.28) closer to SM expectation. Without realistic  $K/\pi$  separation ability, the analyses assume, in association with a  $J/\psi$  reconstructed in  $\mu^+\mu^-$  final state, two opposite sign charged tracks to be kaons and select signal events around the  $\phi$  meson mass. Thus, there is no possibility to study the  $B_s \rightarrow J/\psi f_0(980)$  mode. Still, it is very important that the two central collider detectors provide crosscheck to LHCb.

The two large ellipses that are not fully contained within the plot are those from the Tevatron, with data amounting to analyzable full datasets. The central values are consistent with (3.26), but the measurements are also consistent with the world average. It records some memory of the original anticipation for large and negative  $\sin 2\Phi_{B_s}$ .

### Reappraisal

The saga of, or quest for,  $\sin 2\Phi_{B_s}$  measurement is not over, but the value is small, with no inkling of large New Physics effect. The value is consistent with SM, and also consistent with zero. Although not yet measured, but like  $\Delta m_{B_s}$ , it has now turned into a precision measurement, and one should not expect fast progress, but rather a waiting game of statistics and honing the tools. New Physics might still turn up here.

Was it false hope to look forward to a large deviation at turn-on of LHC, as presented in the two previous subsections? Certainly not! The original anticipation is still partially preserved in the two measurements of CDF and DØ in Fig. 3.13, so the anticipation was genuine, as much as it also reflected the yearning for New Physics. In fact, the earliest, public but unpublished [54] result of LHCb, based on  $0.036 \text{ fb}^{-1}$  data collected in 2010, also entertained large and negative  $\sin 2\Phi_{B_s}$  values that are not inconsistent with (3.26). In this sense, the biggest disappointment was probably within the LHCb experiment, when the box was opened for the result to be presented at Lepton-Photon 2011 held in Mumbai. It was this measurement, based on  $0.37 \text{ fb}^{-1}$  at 7 TeV and leading to the published [2] value of  $\phi_s = 2\Phi_{B_s} = 0.15 \pm 0.18 \pm 0.06 \text{ rad}$ , which is consistent with zero, that eliminated (3.25).

But (3.25) is the other side of the story. The measured  $\Delta\mathcal{A}_{K\pi}$  was a genuine effect, and the case was good that it could indicate New Physics through the electroweak penguin, with the 4th generation providing a rather natural explanation, which in turn suggested the large and negative  $\sin 2\Phi_{B_s}$  in (3.25). With the emergent experimental value in accord, one had good reason to be expectant. Conversely, it is the result of (3.28), which fully excludes (3.25), that drastically enhances the plausibility of “enhanced color-suppressed amplitude  $C$ ” explanation for the  $\Delta\mathcal{A}_{K\pi}$  problem. This is a great disappointment, as it renders the problem to a nonperturbative, hadronic effect.

There is one aspect that, from hindsight, the SM-like outcome for  $\sin 2\Phi_{B_s}$  may be natural. In Fig. 3.10, illustrated for  $m_{\nu} = 300 \text{ GeV}$ , the values of  $|V_{t's}^* V_{t'b}|$  were at

similar order in strength with  $|V_{ts}^* V_{tb}|$  in SM (which is rooted in the large value for  $\Delta A_{K\pi}$ ). Given that each element in the CKM product involves an extra generation jump, this would go against the observed CKM pattern of the first three generations. The  $m_{t'} = 300 \text{ GeV}$  value, of course, reflects experimental bounds ca. 2005–2007. Direct search for  $t'$  and  $b'$ , in part stimulated by the interest in  $\sin 2\Phi_{B_s}$ , advanced quickly [55, 56] with the advent of LHC data. If one takes  $t'$  and  $b'$  to be close to TeV scale, then the values of  $|V_{t's}^* V_{t'b}|$  would become more reasonable. But for such heavy sequential quarks, their Yukawa couplings would become ultrastrong, bringing in a different problem. In fact, it was the emergence of a SM-like, and rather light at 125 GeV, Higgs boson that ultimately “killed” the 4th generation, because the cross section was SM-like rather than enhanced by factor of 9, and 4th generation search evolved into heavy vector-like quark search [3] at the LHC. We give a *requiem to the 4th generation* in Appendix B, accounting for the hope that the ultrastrong Yukawa coupling of 4th generation quarks could in principle lead to dynamical generation of its own mass hence break electroweak symmetry, but conclude that the observation (by CMS [57] and ATLAS [58]) of  $t\bar{t}h^0$  production to be SM-like, is probably the final nail in the coffin.

Would  $\sin 2\Phi_{B_s}$  eventually reveal New Physics? One has to be patient.

## References

1. Abulencia, A., et al. [CDF Collaboration]: Phys. Rev. Lett. **97**, 242003 (2006)
2. Aaij, R., et al. [LHCb Collaboration]: Phys. Rev. Lett. **108**, 101803 (2012)
3. Tanabashi, M., et al. [Particle Data Group]: Phys. Rev. D **98**, 030001 (2018). <http://pdg.lbl.gov/>
4. Gómez-Ceballos, G.: Talk at Flavor Physics and CP Violation Conference (FPCP2006), Vancouver, Canada, April 2006
5. CKMfitter Group: <http://ckmfitter.in2p3.fr>
6. Charles, J., et al. [CKMfitter Group]: Eur. Phys. J. C **41**, 1 (2005)
7. Bona, M., et al. [UTfit Collaboration]: JHEP **07**, 028 (2005)
8. Duniety, I., Fleischer, R., Nierste, U.: Phys. Rev. D **63**, 114015 (2001)
9. Christenson, J.H., Cronin, J.W., Fitch, V.L., Turlay, R.: Phys. Rev. Lett. **13**, 138 (1964)
10. Lenz, A., Nierste, U.: JHEP **06**, 072 (2007)
11. Abazov, V.M., et al. [DØ Collaboration]: Phys. Rev. Lett. **97**, 021802 (2006)
12. Moser, H.G., Roussarie, A.: Nucl. Instrum. Methods A **384**, 491 (1997)
13. Ali, A., Barreiro, F.: Z. Phys. C **30**, 635 (1986)
14. Gronau, M., Nippe, A., Rosner, J.L.: Phys. Rev. D **47**, 1988 (1993)
15. Gronau, M., Rosner, J.L.: Phys. Rev. D **49**, 254 (1994)
16. Artuso, M., et al. [CLEO Collaboration]: Phys. Rev. Lett. **99**, 071802 (2007)
17. Widhalm, L., et al. [Belle Collaboration]: Phys. Rev. Lett. **100**, 241801 (2008)
18. Abazov, V.M., et al. [DØ Collaboration]: Phys. Rev. D **76**, 057101 (2007)
19. Aubert, B., et al. [BaBar Collaboration]: Phys. Rev. Lett. **96**, 251802 (2006)
20. Nakano, E., et al. [Belle Collaboration]: Phys. Rev. D **73**, 112002 (2006)
21. Aaltonen, T., et al. [CDF Collaboration]: Phys. Rev. Lett. **100**, 121803 (2008)
22. Hou, W.-S., Mahajan, N.: Phys. Rev. D **75**, 077501 (2007)
23. Abazov, V.M., et al. [DØ Collaboration]: Phys. Rev. D **89**, 012002 (2014)
24. Artuso, M., Borissov, G., Lenz, A.: Rev. Mod. Phys. **88**, 045002 (2016)

25. Chua, C.-K., Hou, W.-S., Shen, C.-H.: Phys. Rev. D **84**, 074037 (2011)
26. See, e.g. the last backup slide of talk by Bedeschi, F.: At the 4th Workshop on the CKM Unitarity Triangle (CKM2006), Nagoya, Japan, December 2006
27. Alves, A.A., et al. [LHCb Collaboration]: JINST **3**, S08005 (2008)
28. Nakada, T.: Talk at Flavour in the Era of the LHC Workshop, CERN, Geneva, Switzerland, March 2007
29. Hou, W.-S., Nagashima, M., Soddu, A.: Phys. Rev. D **72**, 115007 (2005)
30. Hou, W.-S., Nagashima, M., Soddu, A.: Phys. Rev. D **76**, 016004 (2007)
31. Amsler, C., et al.: Phys. Lett. B **667**, 1 (2008)
32. Kribs, G.D., Plehn, T., Spannowsky, M., Tait, T.M.P.: Phys. Rev. D **76**, 075016 (2007)
33. See <http://lepewwg.web.cern.ch/LEPEWWG/plots/summer2006/>
34. Hou, W.-S., Nagashima, M., Soddu, A.: Phys. Rev. Lett. **95**, 141601 (2005)
35. Hou, W.-S., Li, H.N., Mishima, S., Nagashima, M.: Phys. Rev. Lett. **98**, 131801 (2007)
36. Keum, Y.Y., Sanda, A.I.: Phys. Rev. D **67**, 054009 (2003)
37. Li, H.N., Mishima, S., Sanda, A.I.: Phys. Rev. D **72**, 114005 (2005)
38. Glashow, S.L., Iliopoulos, J., Maiani, L.: Phys. Rev. D **2**, 1285 (1970)
39. Hou, W.-S.: Nucl. Phys. B **308**, 561 (1988)
40. Hou, W.-S., Willey, R.S., Soni, A.: Phys. Rev. Lett. **58**, 1608 (1987)
41. Inami, T., Lim, C.S.: Prog. Theor. Phys. **65**, 297 (1981)
42. Eilam, G., Soni, A., Kane, G.L., Deshpande, N.G.: Phys. Rev. Lett. **57**, 1106 (1986)
43. Aaltonen, T., et al. [CDF Collaboration]: Phys. Rev. Lett. **100**, 161802 (2008)
44. Abazov, V.M., et al. [DØ Collaboration]: Phys. Rev. Lett. **101**, 241801 (2008)
45. Dighe, A.S., Dunietz, I., Fleischer, R.: Eur. Phys. J. C **6**, 647 (1999)
46. Barberio, E., et al. [Heavy Flavor Averaging Group]: [arXiv:0704.3575](https://arxiv.org/abs/0704.3575) [hep-ex]
47. Bona, M., et al. [UTfit Collaboration]: PMC Phys. A **3**, 6 (2009)
48. Heavy Flavor Averaging Group (HFLAV; acronym changed from HFAG to HFLAV in March 2017). <http://www.slac.stanford.edu/xorg/hflav>
49. See the parallel session talk by Tonelli, D.: [arXiv:0810.3229](https://arxiv.org/abs/0810.3229) [hep-ex], at the 34th International Conference on High Energy Physics (ICHEP2008), Philadelphia, USA, 29 July–5 August 2008; see also the plenary talk by Paulini, M
50. Aaij, R., et al. [LHCb Collaboration]: Phys. Rev. Lett. **114**, 041801 (2015)
51. Aaij, R., et al. [LHCb Collaboration]: Phys. Lett. B **736**, 186 (2014)
52. Khachatryan, V., et al. [CMS Collaboration]: Phys. Lett. B **757**, 97 (2016)
53. Aad, G., et al. [ATLAS Collaboration]: JHEP **1608**, 147 (2016)
54. See p. 24 of talk slides of Golutvin, A.: Presented at CERN LHC RRB, April 2011
55. Chatrchyan, S., et al. [CMS Collaboration]: Phys. Lett. B **701**, 204 (2011)
56. Chatrchyan, S., et al. [CMS Collaboration]: JHEP **1205**, 123 (2012)
57. Sirunyan, A.M., et al. [CMS Collaboration]: Phys. Rev. Lett. **120**, 231801 (2018)
58. Aaboud, M., et al. [ATLAS Collaboration]: Phys. Lett. B **784**, 173 (2018)

## Chapter 4

# $H^+$ Probes: $b \rightarrow s\gamma$ , and $B \rightarrow \tau\nu$ , $D^{(*)}\tau\nu$



When the observation of  $b \rightarrow s\gamma$  was first announced by CLEO [1] in 1994 with  $2\text{ fb}^{-1}$  data on the  $\Upsilon(4S)$ , it immediately became one of the most powerful constraints on many kinds of New Physics that enter the loop. In this Chapter, we illustrate by the stringent bound it provides on the charged Higgs boson  $H^+$  that automatically exists in minimal SUSY. A second probe of the  $H^+$  boson is, surprisingly a *tree level* effect in  $B^+ \rightarrow \tau^+\nu$ , which became relevant only when full-reconstruction tag (of the other  $B$ ) method matured at the B factories. This in turn led finally to the measurement of the  $B \rightarrow D^{(*)}\tau\nu$  modes, which are tree level processes with large decay rates, and turned surprisingly into a leading “anomaly” in the LHC era.

### 4.1 $b \rightarrow s\gamma$

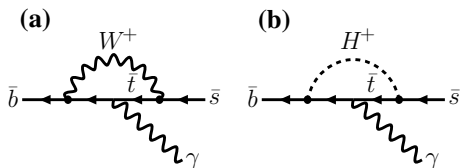
#### 4.1.1 QCD Enhancement and the CLEO Observation

The  $b \rightarrow s\gamma$  decay process is of great theoretical interest because of large QCD corrections [2, 3] that enhance the rate, and because of its sensitivity [4, 5] to charged Higgs boson effects. We give the leading order SM diagram in Fig. 4.1a. Dressing with QCD and dealing with resummation of large logarithms,<sup>1</sup> QCD enhances the  $b \rightarrow s\gamma$  rate by a factor of 2–3 for heavy top quark (enhancement greater for low top mass). To extract information on possible underlying New Physics, and also for its own sake, this marked the start of a major systematic QCD computation effort, moving from next-to-leading order (NLO), to [6] next-to-next-to-leading order (NNLO),

---

<sup>1</sup>These are of the form  $(\alpha_s \log M_W^2/m_b^2)^n$ , as was originally uncovered by the “large QCD corrections” for  $n = 1$  [2, 3]. It represents the accumulation of QCD corrections over the large difference in scale between  $M_W$  (and  $m_t$ ) and  $m_b$ . The detailed treatment involves effective theory renormalization group evolution, and is rather technical. We remark that the the “large” QCD correction is somewhat a misnomer. It is not a breakdown of perturbation theory, but results from the  $n = 0$  term being very strongly suppressed by the GIM mechanism.

**Fig. 4.1** **a** A diagram for  $\bar{b} \rightarrow \bar{s}\gamma$  with a  $W$  boson loop, and **b** with  $W^+$  replaced by  $H^+$



and further refinements [7]. At order  $\alpha_s^2$ , one has hundreds (3-loop) and thousands (4-loop) of diagrams. A rather close dialogue between theory and experiment has developed as the experimental error improved.

The leading order diagram with the charged Higgs boson replacing the  $W$  is given in Fig. 4.1b. Its effect can be readily accommodated in the QCD computation as a short distance correction. As the charged Higgs boson naturally occurs in supersymmetry, and because of intriguing sensitivity [4, 5] of  $b \rightarrow s\gamma$  rate to  $m_{H^+}$ , the process has been a focus of attention for both theory and experiment.

After making a large investment on electromagnetic calorimetry based on CsI crystals for their detector upgrade to CLEO II, the CLEO experiment observed [8] the exclusive  $B \rightarrow K^*\gamma$  decay in 1993. This is the first ever “penguin” process to be established in  $B$  physics, and ushered in the golden age for CLEO. Unlike the inclusive  $b \rightarrow s\gamma$  decay that is of higher theoretical interest, the exclusive process has large hadronic uncertainties, but it is certainly easier experimentally. To search for inclusive  $b \rightarrow s\gamma$  decay, one requires an energetic photon, with  $\pi^0$  and  $\eta$  veto. Since background control is critical, and since a dominant type of background comes from the continuum (or non- $B\bar{B}$ )  $q\bar{q}$  background, one needs to take significant amount of data off the  $\Upsilon(4S)$  resonance (typically 60 MeV) and make a subtraction. In the first CLEO observation of  $b \rightarrow s\gamma$ , the on- and off-resonance data were of order 2 and  $1 \text{ fb}^{-1}$ , respectively. In the following, we will not quote off resonance data taking any further.

There are basically two approaches that one can take for inclusive measurement. The first approach, called the fully inclusive, uses all information available, combined in some discriminant to suppress background. The second approach is the technique called “partial reconstruction”. That is, identifying the experimentally defined  $B \rightarrow X_s\gamma$  with the quark level  $b \rightarrow s\gamma$  decay (called “duality”), one reconstructs only a subset of the recoil  $X_s$  system, i.e. in  $K + n\pi$  modes [1] where  $K$  is either charged or as  $K_S \rightarrow \pi^+\pi^-$ , and  $n\pi$  stands for 1–4 pions, with at most one  $\pi^0$ . Admittedly, this may cause a bias compared to the fully inclusive  $B \rightarrow X_s\gamma$ , as duality is lost. However, in this way CLEO managed to put background under control, observing 100 or so events. The fully inclusive approach had more events, but suffered from larger background. Combining the results of both approaches (taking correlations into account), CLEO gave

$$B_{B \rightarrow X_s\gamma} = (2.32 \pm 0.57 \pm 0.35) \times 10^{-4}, \quad (\text{CLEO 95}) \quad (4.1)$$

for  $2.2 < E_\gamma < 2.7 \text{ GeV}$ . The photon energy (in  $\Upsilon(4S)$ , or  $e^+e^-$  CM frame) is an additional parameter used for background control.

The measurement of (4.1) almost instantly became one of the most important probes of NP, and is the best cited paper by CLEO. For instance, using calculations available at that time, CLEO gave the bound [1]

$$M_{H^+} > [244 + 63/(\tan \beta)^{1.3}] \text{ GeV}, \quad (\text{CLEO 95}) \quad (4.2)$$

for the charged  $H^+$  boson, where  $\tan \beta = v_2/v_1$  (not to be confused with the weak phase  $\beta \equiv \phi_1$  of previous chapters) is the ratio of v.e.v.s of the two Higgs doublets that give rise to a physical  $H^+$  boson.

Good electromagnetic calorimetry, so far based on CsI(T $\ell$ ), i.e. Thallium-doped CsI crystals, became standard for the B factories.

### 4.1.2 Measurement of $b \rightarrow s\gamma$ at the B Factories

CLEO updated with their full 10M  $B\bar{B}$  data in 2001, using the fully inclusive approach and a photon energy cut of  $E_\gamma > 2.0$  GeV. The early analysis of Belle with 6.5M  $B\bar{B}$  data used the partial reconstruction approach, but Belle then switched to the fully inclusive analysis. BaBar, however, followed the partial reconstruction path, enlarging it to 38 modes in 2005, allowing for two  $\pi^0$ 's,  $\eta$  mesons, and 3 kaons. With the photon energy cut at  $E_\gamma > 1.9$  GeV, the result is found to be [9]  $\mathcal{B}_{B \rightarrow X_s \gamma} = (3.27 \pm 0.18_{-0.40-0.09}^{+0.55+0.04}) \times 10^{-4}$ , where the last error is due to theory.

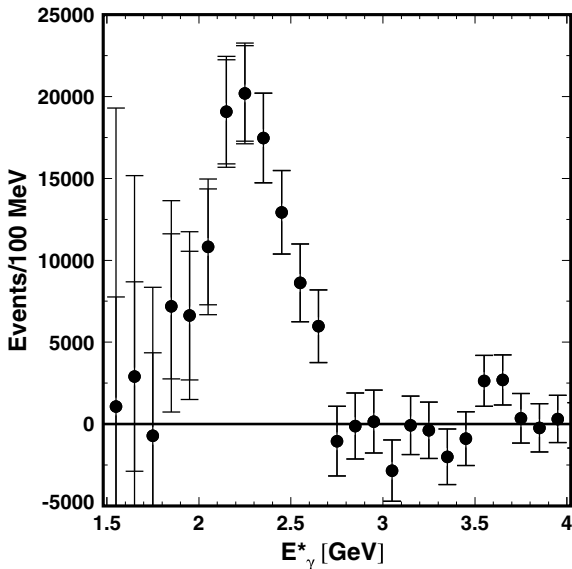
At this point we should remark on the photon energy cut. From  $E_\gamma \simeq m_b/2$  at the parton level, the photon energy spectrum is smeared by Fermi motion inside the meson, plus gluon radiation, hence the photon “line” gets Doppler broadened. This distribution, or shape function, contains information on  $m_b$  and  $\mu_\pi^2$  [10], the parameters related to  $b$  quark mass and momentum inside the  $B$  meson. These parameters are independent of New Physics, but relates to similar functions in other processes, e.g. in  $b \rightarrow c\ell\nu$  decay. We will not get into this, because it becomes rather involved technically, and because it is farther removed from our quest for New Physics. The experimental study, however, typically requires a cut on photon energy to control background. To recover the fully inclusive rate, correspondence with the theoretical spectral distribution is necessary, although this itself ought to be checked.

A photon energy cut on the full spectrum is also needed from the theory side, to avoid nonperturbative effects at lower energies that are not under good control. Theory typically sets an  $E_\gamma$  cut at 1.6 GeV, *in the B meson rest frame*, and extrapolation has to be made for proper comparison. For our purpose, suffice it to say that in the operator product expansion treatment of the  $E_\gamma$  distribution, the fraction of events with  $E_\gamma > 2.0, 1.9$  and 1.8 GeV are roughly 89, 94 and 97%, respectively, of the full  $E_\gamma > 1.6$  GeV spectrum.

With 152M  $B\bar{B}$  pairs and photon energy cut  $E_\gamma > 1.8$  GeV, Belle used [11] the fully inclusive approach. Besides  $\pi^0$  and  $\eta$  veto and on-off resonance subtractions, the remaining  $B\bar{B}$  backgrounds were subtracted using Monte Carlo distributions checked by data-controlled samples. The result is  $\mathcal{B}_{B \rightarrow X_s \gamma} = (3.55 \pm 0.32_{-0.31-0.07}^{+0.30+0.11}) \times 10^{-4}$ ,



**Fig. 4.2** The  $E_\gamma$  spectrum in  $\Upsilon(4S)$  frame from fully inclusive  $b \rightarrow s\gamma$  analysis by Belle [11], with a photon energy cut at 1.8 GeV for 152M  $B\bar{B}$  pairs. [Copyright (2004) by The American Physical Society]



where the last error is again due to theory. For illustration, we plot the observed photon energy spectrum in Fig. 4.2. Noting the  $E_\gamma > 1.8$  GeV cut, the Doppler-broadened (also from gluon radiation) lineshape is apparent. To compare the various measurements, and to compare with theory, one needs to subtract  $b \rightarrow d\gamma$ , correct for different  $E_\gamma$  range (including boosting to  $B$  rest frame), and extrapolate [12] to 1.6 GeV (and  $B$  frame). The HFAG average in 2006 gives [13]

$$\mathcal{B}_{B \rightarrow X_s \gamma} = (3.55 \pm 0.26) \times 10^{-4} \quad (E_\gamma > 1.6 \text{ GeV}; \text{ HFAG 06}), \quad (4.3)$$

where we have combined the various errors. Compared with the theoretical NLO result [14] at the start of the millennium,

$$\mathcal{B}_{B \rightarrow X_s \gamma}^{\text{NLO}} = (3.57 \pm 0.30) \times 10^{-4} \quad (E_\gamma > 1.6 \text{ GeV}), \quad (4.4)$$

the agreement is excellent, both in central value and error (experimental error smaller!). This leaves little space for New Physics, i.e. just in the error bars. This good agreement between experiment and theory lasted until 2007.

The reduction in experimental error inspired a large theory effort at NNLO, or to  $\alpha_s^2$  order, also to reduce the renormalization scale dependence. The outcome, however, resulted in a downward shift in central value [6],

$$\mathcal{B}_{B \rightarrow X_s \gamma}^{\text{NNLO}} = (3.15 \pm 0.23) \times 10^{-4} \quad (E_\gamma > 1.6 \text{ GeV}). \quad (4.5)$$

With error now slightly smaller than experiment, the central value became more than  $1\sigma$  below experimental central value in (4.3). Another approach gave a number that is even lower [15]. This progress in theory puts the ball back in the court of experiment.

With much more data to play with, Belle presented in 2008 a fully inclusive analysis with 657M  $B\bar{B}$  pairs, managing to lower the  $E_\gamma$  cut to 1.7 GeV, which is more than 97% of full  $E_\gamma > 1.6$  GeV spectrum. The observed photon energy spectrum is similar in appearance to Fig. 4.2. The final result [16] is  $\mathcal{B}_{B \rightarrow X_s \gamma} = (3.45 \pm 0.15 \pm 0.40) \times 10^{-4}$  for  $E_\gamma > 1.7$  GeV, where the errors are statistical and systematic. Agreement with theory is slightly improved, in part because of a slight drop in central value. Note that the systematic error is now larger than the earlier published [11] result with  $E_\gamma$  cut at 1.8 GeV, because lowering  $E_\gamma$  cut is at the cost of bringing in more background. With systematic error now dominant, it seems that relying on MC for subtraction off remaining  $B\bar{B}$  background may not be easy to extend to larger datasets.

The HFAG 2014 combination of all experimental data gives [13]

$$\mathcal{B}_{B \rightarrow X_s \gamma} = (3.43 \pm 0.22) \times 10^{-4} \quad (E_\gamma > 1.6 \text{ GeV}; \text{ HFAG 14}), \quad (4.6)$$

where errors are combined. Meanwhile, theory was updating with all improved calculations at  $\alpha_s^2$  order since 2006, resulting in more than 6% upward shift in central value [7],

$$\mathcal{B}_{B \rightarrow X_s \gamma}^{\text{NNLO}} = (3.36 \pm 0.23) \times 10^{-4} \quad (E_\gamma > 1.6 \text{ GeV}, 2015), \quad (4.7)$$

but the total error hardly changed. This theory paper advocated the use of  $R_\gamma = (\mathcal{B}_{s\gamma} + \mathcal{B}_{d\gamma})/\mathcal{B}_{c\ell\nu}$ , the ratio of inclusive  $b \rightarrow q\gamma$  ( $q = s, d$ ) with inclusive  $b \rightarrow c\ell\nu$  rates as a more convenient observable for the future.

While errors in (4.6) and (4.7) are now comparable, it does seem that the central values “chase” each other, to state it mildly. A fresher approach may eventually be needed. A promising crosscheck, as data increases in the Belle II era, is the *full reconstruction of the tag side B meson* (for more discussion, see next section). With this approach, the signal side is then just an isolated energetic photon, without the need to specify or reconstruct the  $X_s$  system, and signal purity is improved. One also knows the charge, flavor and momentum of the signal  $B$ , hence the photon energy spectrum is directly measured in the  $B$  frame. The systematics would be quite different from the previous approaches, be it partial reconstruction or fully inclusive. A first attempt was performed by BaBar [17] using 232M  $B\bar{B}$  pairs. Roughly 0.68M pairs are tagged by one  $B$  decaying hadronically: the advantage of full reconstruction of tag side  $B$  comes at the cost of  $3 \times 10^{-3}$  in efficiency. BaBar set an  $E_\gamma$  cut at 1.9 GeV. Scaling by a factor of 0.936, the result is  $\mathcal{B}_{B \rightarrow X_s \gamma} = (3.91 \pm 0.91 \pm 0.64) \times 10^{-4}$  for  $E_\gamma > 1.6$  GeV. It should be stressed that the systematic errors can improve with a larger dataset. Thus, this may be a path to follow in the long run, in particular at Belle II (but not yet tried at Belle).

The NNLO theory development was clearly prompted by the capabilities at the B Factories. Will we see the continuation of the supreme dialogue between theory versus experiment in  $b \rightarrow s\gamma$  in the Super B factory era? Likely, as much as it looks formidable.

### 4.1.3 Implications for $H^+$

This close dialogue allowed  $b \rightarrow s\gamma$  to provide one of the most stringent bounds on New Physics models. The process is sensitive to all types of possible NP in the loop, such as stop-charginos, where a large literature exists. However,  $b \rightarrow s\gamma$  is best known for its stringent constraint on the MSSM (minimal SUSY SM) type of  $H^+$  boson. Furthermore, the SUSY related studies all need mechanisms to cancel against the large charged Higgs effect, which turns out to be constructive [4, 5] with SM. We therefore focus on the  $H^+$  effect in the loop, which is illustrated in Fig. 4.1b.

MSSM demands at least two Higgs doublets (2HDM), where one Higgs doublet couples to right-handed down type quarks, the other to up type, each developing a v.e.v. to give mass. The physical  $H^+$  is a cousin of the  $\phi_{W^+}$  Goldstone boson in SM that gets eaten to become the longitudinal component of the  $W^+$  boson. It is the  $\phi_{W^+}$  that couples to mass, which is at the root of the nondecoupling phenomenon of the heavy top quark in the loop. In  $bs\gamma$  coupling for heavy top,<sup>2</sup> however, the top is effectively decoupled, i.e. the dependence on  $m_t$  is weak for large  $m_t$  (less than logarithmic). This arises by a subtlety of gauge invariance, or the demands of current conservation<sup>3</sup> of the  $bs\gamma$  vertex, and is the reason underlying why QCD corrections make such a large impact [2, 3] on this loop-induced decay. It is for the same reason that the process is sensitive to NP such as  $H^+$ .

Replacing the  $W^+$  by  $H^+$  in the loop, in the MSSM type of 2HDM, the  $H^+$  effect *always enhances the  $b \rightarrow s\gamma$  rate, regardless of  $\tan\beta = v_2/v_1$* , where  $\tan\beta$  is the ratio of v.e.v.s between the two doublets. This effect was pointed out 30 years ago [4, 5]. Basically, the  $H^+$  couples to  $m_t \cot\beta$  at one end of the loop, and to  $-m_b \tan\beta$  at the other end, making this contribution independent of  $\tan\beta$ , and the sign is fixed such that it is always constructive with the SM amplitude.

As stated, a main motivation for the large effort to push the QCD calculation to NNLO is to match the experimental error, to better interpret the New Physics impact of the measurement. The effective field theory approach allows NP contributions at short distance to be readily incorporated. Without further ado, in Fig. 4.3 we show the plot [6] where the NNLO result of (4.5) for  $\mathcal{B}(B \rightarrow X_s\gamma)$  versus  $m_{H^+}$  is compared with the 2006 combined data [13] of (4.3). A nominal  $\tan\beta = 2$  is taken. In Fig. 4.3, the solid lines give the  $H^+$  effect, which approaches the dashed lines for  $m_{H^+}$  much greater than  $m_t$  (decoupling of heavy  $H^+$ ), the SM expectation. For lighter  $m_{H^+}$ , however, one has enhancement. One can compare with Fig. 4.1 of [5], where ‘‘Model 1’’ in this paper is the more popularly called Two Higgs Doublet Model II (2HDM-II),

<sup>2</sup>If the top quark turned out to be light compared to the  $W$ , one has  $m_t^2/M_W^2$  power suppression [4, 5].

<sup>3</sup>Basically, current conservation allows two conserved effective  $bs\gamma$  couplings, of the form  $\bar{s}q^2\gamma_\mu Lb$  and  $\bar{s}\sigma_{\mu\nu}q_\nu m_b Rb$  (each contracted with a photon field  $A_\mu$ ), where  $q_\mu$  is the photon momentum. While the former coupling vanishes with  $q^2$ , the latter can radiate a real photon with  $q^2 = 0$ . The form of the effective couplings demands an expansion in  $q^2 (< m_b^2)$  and  $q_\nu m_b$  in the computation of the effective coefficients. In contrast, for the  $bsZ$  vertex, the current is not conserved (the conserved part is gauge related to  $bs\gamma$ ), hence there is no need to make such expansions, and what replaces the previous  $q^2$  and  $qm_b$  turns out to be  $m_t^2$ .

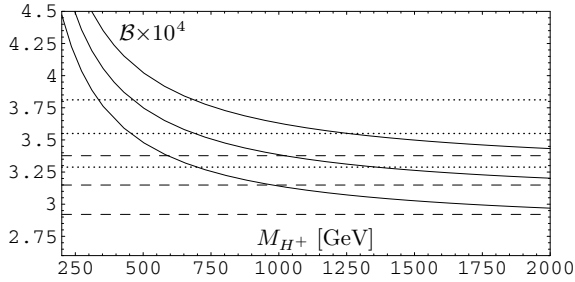


**Fig. 4.3**  $\mathcal{B}(B \rightarrow X, \gamma) (\times 10^4)$  versus  $m_{H^+}$  (in GeV) in MSSM type two Higgs doublet model, with  $\tan \beta = 2$  (taken from [6]) [Copyright (2007) by The American Physical Society]. For large  $m_{H^+}$ , one approaches SM (dashed lines), while for low  $m_{H^+}$  there is great enhancement. Dotted lines give the  $1\sigma$  experimental range, (4.3)

which automatically arises in MSSM. When  $H^+$  is not much heavier than the top, its contribution can get even larger than SM effect!

Of course, experiment and NNLO theory are in reasonable agreement, therefore one can extract a bound on the  $m_{H^+}$ - $\tan \beta$  plane. We follow [6] and continue to use  $\tan \beta = 2$  for illustration. By comparing the lower range of the NNLO result with the higher range of (4.3), shown as the dotted lines in Fig. 4.3, one has the bound

$$m_{H^+} > 295 \text{ GeV} \quad (\text{NNLO} + \text{HFAG ca. 2007}), \quad (4.8)$$

at 95% C.L. This may seem to be barely an improvement over the first CLEO observation in 1995, i.e. (4.2), where one gets the bound of  $\sim 270$  GeV using  $\tan \beta = 2$ . This is due to some tension between NNLO theory versus experiment, i.e. theory is a bit on the low side.

If one takes the central value of both results seriously, one could say [6] that an  $H^+$  boson with mass around 695 GeV (where the central values of theory and experiment meet) is needed to bring the NNLO rate up to the experimental central value of (4.3). This is because the  $H^+$  effect in the MSSM type of 2HDM is always constructive [5] with the  $\phi_{W^+}$  effect in SM, and again illustrates why the theory-experiment correspondence in  $b \rightarrow s\gamma$  must go on. We remark that, given that the NNLO result is lower than experiment, models that give a destructive effect to SM is constrained stronger. For example, in the other (non-MSSM) type of 2HDM, where both  $u$  and  $d$  quarks get mass from the same Higgs doublet (usually called 2HDM-I), the  $H^+$  effect is destructive [5]. One would then need either a larger  $H^+$  effect that overpowers the SM contribution, or one would need *additional* New Physics to bring the rate up to experiment.

The NNLO result of (4.5) is lower in central value than experiment, (4.3), with slightly better errors. Thus, both theory and experiment marched on, and we have the 2015 result of (4.7) and (4.6), respectively, which once again are in better agreement: theory went up, and experiment came slightly down, with comparable errors. The  $H^+$  bound now becomes

$$m_{H^+} > 480 \text{ GeV} \quad (\text{NNLO} + \text{HFAG ca. 2015}), \quad (4.9)$$

at 95% C.L. This bound is still in general better than direct search bounds at the LHC, even with unfolding of full Run 1 data at 7 and 8 TeV.

As reported [18] at ICHEP 2016, Belle made an update with full 772M  $B\bar{B}$  events, applied multivariate analysis tools (boosted decision trees, or BDTs), and extracted shape function parameters  $m_b$  and  $\mu_\pi^2$  directly by fitting the measured spectrum, which gave a rather good fit. They also followed the suggestion of [7] to report  $\mathcal{B}(\bar{B} \rightarrow X_{s+d}\gamma)$  directly, but also the reference result of  $\mathcal{B}_{B \rightarrow X_s\gamma} = (3.12 \pm 0.10 \pm 0.19 \pm 0.08) \times 10^{-4}$  for  $E_\gamma > 1.6$  GeV, where the last error is due to theory. Besides being the most precise measurement, most notable is the lower central value compared with (4.6), where Belle did their own analysis to give the bound of  $m_{H^+} > 580$  GeV at 95% C.L. With experiment now lower than the NNLO central value of (4.7), a phenomenological analysis [19] of all available data suggests that the Belle bound on  $m_{H^+}$  is conservative, and that the bound now depends quite sensitively on the method applied, in particular the choice of photon energy cut.

The ongoing saga should be watched, where Belle II at SuperKEKB is expected to gain 40 (50) fold in data! It would be interesting with further search at LHC for the charged Higgs boson. Whether an  $H^+$  boson would be discovered, much more information could be extracted in the future together with Belle II data, while the current bound of 500 GeV or so roughly explains why an  $H^+$  boson is yet unseen at the LHC.

But will theorists be courageous enough to go beyond NNLO?

## 4.2 Measuring $B \rightarrow \tau\nu, D^{(*)}\tau\nu$

As a cousin of the  $\phi_{W^+}$ , the  $H^+$  boson has an amazing tree level effect that has only come to fore by the prowess of the B factories, namely the measurement of  $B \rightarrow \tau\nu$  at  $10^{-4}$  level, as well as the *subsequent* measurement of  $B \rightarrow D^{(*)}\tau\nu$  at the percent level. As the initially “large”  $B \rightarrow \tau\nu$  rate came down to be consistent with SM, it was replaced by the “ $B \rightarrow D^{(*)}\tau\nu$  anomaly”, a leading anomaly that would carry us into the Super B Factory era.

Before going into these, let us first give some historic backdrop.

### 4.2.1 Enhanced $H^+$ Effect in $b \rightarrow c\tau\nu$ and $B^+ \rightarrow \tau^+\nu_\tau$

In the early CLEO and ARGUS (as well as CUSB) era of  $B$  physics studies, there was once a “semileptonic branching ratio” (or  $\mathcal{B}_{sl}$ ) problem. The measured  $\mathcal{B}_{sl}$  at 10% or so, becoming more and more precise, was lower than the spectator model expectations of 12%. Most naively one would have guessed that  $\mathcal{B}_{sl}$  is roughly of order 16%, so the spectator model already incorporated many corrections. Although this  $\mathcal{B}_{sl}$  problem

eventually dissipated and concerns us no more, a simple and potentially exciting possibility was that 10–20% of  $B$  meson decays went into New Physics enhanced processes that were difficult to observe experimentally, hence had not been probed.

### Enhanced $b \rightarrow sg$ or $b \rightarrow c\tau\nu$ ?

Two possibilities [20] could be provided by the charged Higgs boson, in the Two Higgs Doublet Model context. One possibility is the non-MSSM type of model, i.e. 2HDM-I. In this model, the  $H^+$  effect is destructive [5, 21] with SM, and  $b \rightarrow s\gamma$  and  $b \rightarrow sg$  (gluon is “on-shell”) rates could be easily enhanced (or suppressed). Since  $b \rightarrow s\gamma$  was as yet unmeasured in 1990, it was proposed [20] that a rather enhanced  $b \rightarrow sg$ , at the 10–20% level, could be the cause of the  $\mathcal{B}_{sl}$  problem. This requires low  $\tan\beta$ , and would have been interesting also for the “charm deficit” problem (another problem of that time that has since dissipated), since  $b \rightarrow sg$  has no charm in the final state, and would suppress the charm count in  $B$  decays. Another corollary would be a suppressed  $b \rightarrow s\gamma$ , as the  $\tan\beta$ - $m_{H^+}$  parameter space falls in a region of destructive [21] effect in  $b \rightarrow s\gamma$  where the  $H^+$  effect overwhelms the SM. This fascinating possibility has been subsequently ruled out by the CLEO bound [22] of  $\mathcal{B}_{b \rightarrow sg} < 6.8\%$  at the 90% C.L. Though the bound is by far not stringent,<sup>4</sup> it excludes the possibility that  $\mathcal{B}_{b \rightarrow sg}$  is above 10%.

The second possibility [20] is an enhanced  $b \rightarrow c\tau\nu_\tau$ , which could occur in 2HDM-II (i.e. SUSY-type) for large  $\tan\beta$ . The  $b \rightarrow c\tau\nu_\tau$  decay, or  $B \rightarrow \tau\nu_\tau + X$ , is a fraction of  $B \rightarrow c\ell\nu_\ell$  (for  $\ell = e, \mu$ ) in rate because of phase space suppression by having two heavy particles in the final state. Compounded by the poor signature with two missing neutrinos, the mode had been basically ignored experimentally. It had been known that this mode could be enhanced if  $\tan^2\beta m_b m_\tau / m_{H^+}^2$  is large [24]. With the  $\mathcal{B}_{sl}$  problem, this mechanism was invoked to enhance  $b \rightarrow c\tau\nu_\tau$  to the 10–20% level, which aroused interests for search at LEP, where one has highly boosted  $B$  hadrons. By 1993, using the large missing energy associated with the two neutrinos as a tag for the  $b \rightarrow \tau\bar{\nu}_\tau + X$  events, the ALEPH experiment measured [25]  $\mathcal{B}_{B \rightarrow \tau\nu_\tau + X} = (4.08 \pm 0.76 \pm 0.62)\%$ , which ruled out the possibility of large enhancement of  $b \rightarrow c\tau\nu_\tau$  rate. Subsequent measurements at LEP have settled at [26]

$$\mathcal{B}_{B \rightarrow \tau\nu_\tau + X} = (2.41 \pm 0.23)\%, \quad (4.10)$$

and dominated by ALEPH. The  $B \rightarrow \tau\nu_\tau + X$  rate is  $\sim 1/4.5$  the rate of  $B \rightarrow \ell\nu_\ell + X$  (where  $\ell = e, \mu$ ), basically as expected in SM.

<sup>4</sup>The SM expectation for  $b \rightarrow sg$  is at the 0.1% level [23], not particularly small. However, to date it remains a curiosity whether the rate is enhanced in Nature. We lack tools to isolate an “on-shell” gluon  $b \rightarrow sg$  decay in the hadronic  $B$  decay environment. Had the  $b$  quark been at 20 GeV or heavier, the gluon and the  $s$  quark “jets” could possibly be distinguished. But  $m_b$  is too low.

### $H^+$ Effect on $B^+ \rightarrow \tau^+\nu_\tau$

Soon after the first ALEPH measurement that ruled out large enhancement of the inclusive  $B \rightarrow \tau\nu_\tau + X$  rate, it was pointed out [27] that the limit of  $\mathcal{B}_{B^+ \rightarrow \mu^+\nu_\mu} < 2 \times 10^{-5}$  by CLEO [28] at that time gave a limit on  $\tan\beta$  that is slightly better than the ALEPH measurement. Both implied  $\tan\beta < 0.5$  ( $m_{H^+}/1$  GeV) or so. Second, if one could improve the limit of  $\mathcal{B}_{B^+ \rightarrow \tau^+\nu_\tau} < 1.2\%$  by a factor of two, the  $B^+ \rightarrow \tau^+\nu_\tau$  mode could surpass the previous two processes and hold the best long term prospect.

Analogous to the  $\pi^+$  and  $K^+ \rightarrow \ell^+\nu_\ell$  decay, the formula for  $B^+ \rightarrow \tau^+\nu_\tau$  decay in SM is well known,

$$\mathcal{B}_{B^+ \rightarrow \tau^+\nu_\tau}^{\text{SM}} = \frac{G_F^2 m_B m_\tau^2}{8\pi} \left[ 1 - \frac{m_\tau^2}{m_B^2} \right] \tau_B f_B^2 |V_{ub}|^2, \quad (4.11)$$

where  $f_B$  is the  $B$  meson decay constant. Adding a SUSY-type (2HDM-II) charged Higgs  $H^+$  boson, the formula is simply replaced by [27]

$$\mathcal{B}_{B^+ \rightarrow \tau^+\nu_\tau}^{H^+} = r_H \mathcal{B}_{B^+ \rightarrow \tau^+\nu_\tau}^{\text{SM}}, \quad r_H = \left[ 1 - \frac{m_{B^+}^2}{m_{H^+}^2} \tan^2 \beta \right]^2. \quad (4.12)$$

For light leptons  $\ell = e, \mu$ , one simply replaces  $\tau$  by  $\ell$  in both (4.11) and (4.12). Interestingly, the factor  $r_H$  depends only on  $\tan\beta$  and  $m_{B^+}/m_{H^+}$ , but not on  $m_\tau$ , nor does it have hadronic uncertainties. All hadronic uncertainties are contained in the decay constant  $f_B$ , just like in SM itself.

Since the effect is at tree level and easy to understand (but not obvious), we give a little detail. The two processes, mediated by  $W^+$  and  $H^+$  respectively, are illustrated in Figs. 4.4a, b. The effective four-Fermi interaction is

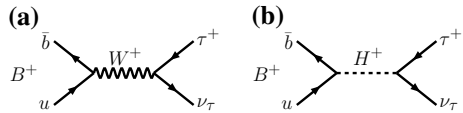
$$\frac{G_F}{\sqrt{2}} V_{ub} \left\{ [\bar{u}\gamma_\mu Lb][\bar{\tau}\gamma_\mu L\nu_\tau] - R_\tau [\bar{u}Rb][\bar{\tau}L\nu_\tau] \right\} + \text{h.c.}, \quad (4.13)$$

where h.c. stands for hermitian conjugate, and

$$R_\tau = \frac{m_b m_\tau}{m_{H^+}^2} \tan^2 \beta. \quad (4.14)$$

The  $m_b$  and  $m_\tau$  factors are due to the couplings of  $H^+$  at each end of Fig. 4.4b, where we have ignored  $m_u$ .

**Fig. 4.4**  $B^+ \rightarrow \tau^+\nu$  via **a** a  $W^+$  boson, and **b** with  $W^+$  replaced by  $H^+$



The SM axial-vector current and pseudoscalar density induce  $B^\pm \rightarrow \tau^\pm\nu$  decay via the matrix elements,

$$\langle 0|\bar{u}\gamma_\mu\gamma_5b|B^- \rangle = if_B p_{B\mu}, \quad \langle 0|\bar{u}\gamma_5b|B^- \rangle = -if_B \frac{m_B^2}{m_b}. \quad (4.15)$$

which are simply related. Within SM, the  $W^+$  gauge boson effect is helicity suppressed, hence the effect vanishes with the  $m_\tau$  mass due to the need for helicity flip. This comes about because  $p_{B\mu}$  of the axial-vector current matrix element contracts with  $\bar{\tau}\gamma_\mu L\nu_\tau$ . For the  $H^+$  charged Higgs boson effect, there is no helicity suppression, but one has the aforementioned ‘‘Higgs affinity’’ factor, i.e. mass dependent couplings. With  $m_u$  (and  $m_\nu$  certainly) negligible, the  $H^+$  couples as  $m_\tau m_b \tan^2 \beta$ , as in (4.14).

The absence of helicity suppression for the  $H^+$  effect, but still having a dynamical coupling to the tau lepton mass, results in the  $R_H$  factor. The  $m_b$  in the  $m_b m_\tau$  factor in (4.14) is cancelled by the  $1/m_b$  in the density matrix element in (4.15), while  $m_\tau$  factors out as a common factor (though of different origins) with the  $W^+$  contribution, and  $m_b m_\tau$  gets replaced by the physical  $m_B^2$ . Thus,  $r_H$  in (4.12) is independent of the quark mass  $m_b$ , but depend only on the physical  $m_B$  mass. The sign between the SM and  $H^+$  contributions, fixed by the relative sign in (4.13), is always destructive [27].

Note [27] that there are no interesting effects in 2HDM-I, as the  $-\tan^2 \beta$  factor is replaced by  $\cot \beta \tan \beta = 1$ , and  $m_{B^\pm}^2/m_{H^\pm}^2$  would always be small.

## 4.2.2 $B \rightarrow \tau\nu$ and $B \rightarrow D^{(*)}\tau\nu$ Rate Measurement

$B^+ \rightarrow \tau^+\nu$  followed by  $\tau^+$  decay results in at least two neutrinos, which makes background very hard to suppress in the  $B\bar{B}$  decay environment. Thus, for a long time, the limit on  $B^+ \rightarrow \tau^+\nu$  was rather poor and not so interesting. This had allowed for the possibility that the effect of the  $H^+$  could even dominate over SM, given that the SM expectation was only at  $10^{-4}$  level. Even at the end of the CLEO era, the experimental limit was at the  $10^{-3}$  level.

### Full Reconstruction Tag

The change came with the enormous number of B mesons accumulated by the B factories, which allowed the full reconstruction method mentioned in Sect. 4.1.2 to finally become useful for rare and difficult decays. Fully reconstructing the tag side B meson in, e.g.  $B^- \rightarrow D^0\pi^-$  decay, one has an efficiency of only 0.1–0.3%. At this cost, however, one effectively has a ‘‘B beam’’. The situation is similar to Fig. 2.1, where the tag  $B$  is fully reconstructed, hence one knows the remaining event is an opposite flavor  $B$  meson. It is useful to visualize the technique. We illustrate in Fig. 4.5 a full reconstruction event with the signal  $B$  decaying to  $f^+\nu\bar{\nu}$ , where  $f$  could be  $e$  or  $\mu$  or  $\pi$  from  $\tau$  decay, or a kaon, which will be discussed in Sect. 5.3.



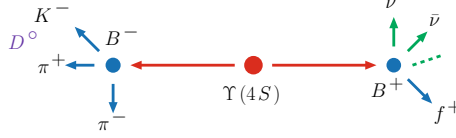
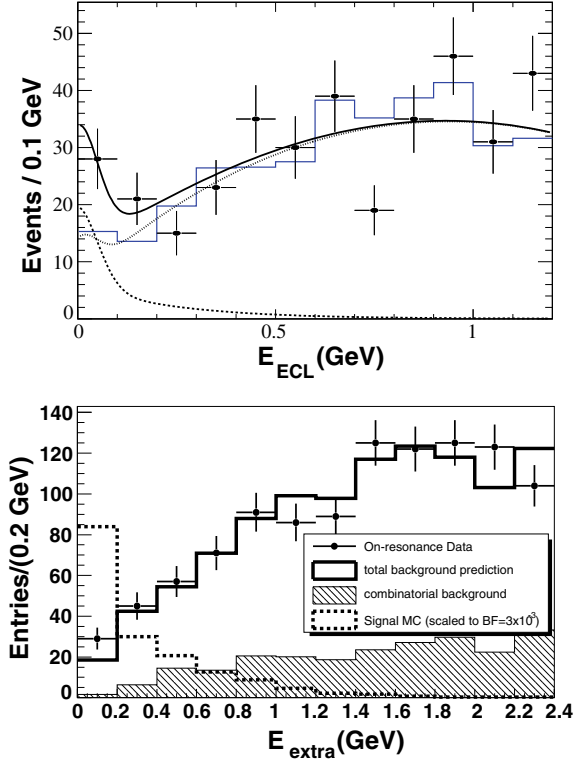


**Fig. 4.5** Illustration of full reconstruction, for tag side  $B^-$  in  $D^0\pi^- \rightarrow K^-\pi^+\pi^-$  final state, and signal  $B^+$  decaying to  $f^+\nu\bar{\nu}'$ , where  $f$  could be  $e, \mu, \pi$  or  $K$ . The dashed line indicates a possible third neutrino

**Fig. 4.6** Data showing evidence for  $B \rightarrow \tau\nu$  (hadronic tag) by Belle [29] and BaBar [30], plotted against extra energy in EM calorimeter after full reconstruction of the other  $B$  [Copyright (2006 and 2008) by The American Physical Society]



As shown in Fig. 4.6, using full reconstruction in hadronic modes and with a data sample of 449M  $B\bar{B}$  pairs, in 2006 Belle reported  $17.2^{+5.3}_{-4.7}$  events, where  $\tau$  decays were studied in the  $e\nu\nu, \mu\nu\nu, \pi\nu$  and  $\rho\nu$  channels. This constituted the first evidence, at  $3.5\sigma$  significance, for  $B^+ \rightarrow \tau^+\nu$ , giving [29]

$$B_{B \rightarrow \tau\nu} = (1.79^{+0.56+0.46}_{-0.49-0.51}) \times 10^{-4} \quad (\text{Belle 449M}). \quad (4.16)$$

Besides full reconstruction tag of the other  $B$ , one needs to make sure that there really is just a single charged track (an extra  $\pi^0$  for the  $\rho$ ) and nothing else. The main tool used to suppress backgrounds is the remaining extra energy in the EM calorimeter, called  $E_{\text{ECL}}$  by Belle (and  $E_{\text{Extra}}$  by BaBar). As seen in Fig. 4.6a, the peaking of

events above background at  $E_{\text{ECL}} \sim 0$  constituted evidence for  $B \rightarrow \tau\nu$ . This, of course assumes that the studies have been careful enough such that there are no other types of peaking background.

With 383M  $B\bar{B}$  pairs and  $D^*\ell\nu$  reconstruction on tag side, however, in the same time frame BaBar saw no clear signal [26], giving  $(0.9 \pm 0.6 \pm 0.1) \times 10^{-4}$ , which is consistent with zero. However, with hadronic tag, BaBar reported some evidence in 2007, at  $(1.8_{-0.8}^{+0.9} \pm 0.4 \pm 0.2) \times 10^{-4}$  (second figure in Fig. 4.6), which is consistent with (4.16) by Belle. The combined result for BaBar is [30],

$$\mathcal{B}_{B \rightarrow \tau\nu} = (1.2 \pm 0.4 \pm 0.36) \times 10^{-4} \text{ (BaBar 383M)}, \quad (4.17)$$

where we follow HFAG to combine background and efficiency related errors. Diluted by the semileptonic tag measurement, the significance of (4.17) is  $2.6\sigma$ , but it is consistent with the Belle result. Between (4.16) and (4.17), the existence of  $B \rightarrow \tau\nu$  became experimentally established.

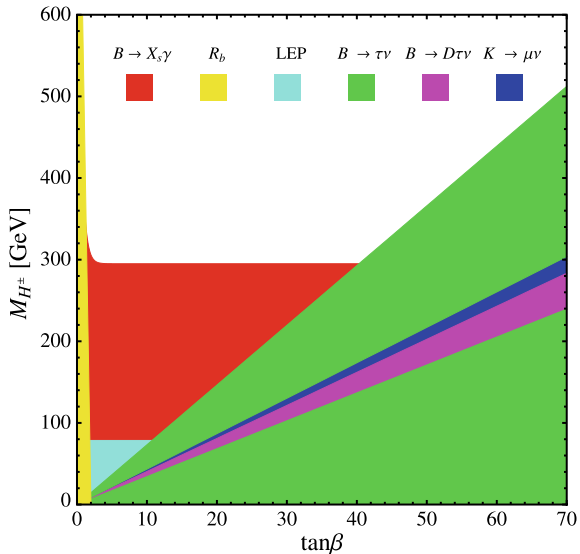
### Impact of $B \rightarrow \tau\nu$ Measurement

Taking central values at the time from lattice for  $f_B$ , and  $|V_{ub}|$  from semileptonic  $B$  decays, the nominal SM expectation was  $(1.6 \pm 0.4) \times 10^{-4}$ . Thus, Belle and BaBar have reached SM sensitivity, and (4.16) and (4.17) together now place a constraint on the  $\tan\beta$ - $m_{H^+}$  plane through  $r_H \sim 1$ . We illustrate the impact of  $B \rightarrow \tau\nu$  in Fig. 4.7, together with the constraint from  $b \rightarrow s\gamma$  of (4.8), as well as a few other processes. It is clear that  $B \rightarrow \tau\nu$ , which excludes a large region on the lower right, and  $b \rightarrow s\gamma$ , which excludes  $m_{H^+}$  below 300 GeV, provide the best constraints, and are complementary to each other. While this is a snapshot from 2008, it illustrates the utility of these two modes as New Physics probes, which can only be measured in the clean  $e^+e^-$  production environment.

Belle and Babar continued their analyses with larger datasets, and with improved analyses. The early null result of BaBar in the semileptonic  $B \rightarrow D^{(*)}\ell\nu$  tag approach might have arisen from higher background from the looser constraint because of an extra neutrino, although it has good efficiency. By 2010 and with full 459M  $B\bar{B}$  data, BaBar finally reported evidence [26] of a signal with semileptonic tag, at  $(1.7 \pm 0.8 \pm 0.2) \times 10^{-4}$ . This was followed by Belle, reporting  $(1.54_{-0.37-0.31}^{+0.38+0.29}) \times 10^{-4}$  in 2010, with the final result of  $(1.25 \pm 0.28 \pm 0.27) \times 10^{-4}$  for 772M  $B\bar{B}$  events given in 2015. For hadronic, or full reconstruction tag approach, one has all information available, but the efficiency at a few per mille is rather low, and adding more tag modes eventually reaches diminished return. Final results were reported in 2013:  $(0.72_{-0.25}^{+0.27} \pm 0.11) \times 10^{-4}$  for Belle with 772M  $B\bar{B}$  events, and  $(1.83_{-0.49}^{+0.53} \pm 0.24) \times 10^{-4}$  for BaBar with 468M. Note that BaBar finds larger numbers compared with Belle in both cases, but with larger errors. Combining the four measurements, the PDG average is

$$\mathcal{B}_{B \rightarrow \tau\nu} = (1.09 \pm 0.24) \times 10^{-4} \text{ (PDG 2014)}, \quad (4.18)$$

**Fig. 4.7** Impact of  $B \rightarrow \tau\nu$  on  $\tan\beta$ - $m_{H^+}$  plane ca. 2008, together with  $b \rightarrow s\gamma$  and other constraints. [Taken from [31], courtesy U. Haisch]



which is dominated by Belle, but brought above  $1 \times 10^{-4}$  by BaBar numbers. This is within  $1.4\sigma$  of the SM value,

$$\mathcal{B}_{B \rightarrow \tau\nu}^{\text{SM}} = \left(0.75^{+0.10}_{-0.05}\right) \times 10^{-4} \quad (\text{CKMfitter 2015}), \quad (4.19)$$

obtained by the CKMfitter group [32] by combining all available information at the time, including lattice. We note that the agreement would be better with Belle data taken alone, while for BaBar taken alone, there is a bit more tension, with experiment on the high side.

At the Super B Factory, together with refinements from lattice QCD,  $B \rightarrow \tau\nu$  will remain a superb probe of the  $H^+$  boson, which would complement the direct  $H^+$  searches at the LHC. Even if a  $H^+$  boson is discovered, the  $B \rightarrow \tau\nu$  process will provide us with useful information. Unlike the ever refined theory calculation that would be necessary for the  $b \rightarrow s\gamma$  dialogue, the particularly nice feature for  $B \rightarrow \tau\nu$  is its theoretical cleanliness, all hadronic effects being contained in  $f_B$ .

#### A Sidetrack: New Physics in $D_s^+ \rightarrow \mu^+\nu, \tau^+\nu$ ?

Can effects analogous to  $B \rightarrow \tau\nu$  be competitive in other systems? For lighter meson systems, it was pointed out that [27] charged Higgs effects are in general more subdued. Simply put, the  $m_B^2$  in the  $r_H$  factor of (4.12) would be replaced by a much smaller mass. For example, replacing  $m_B^2$  by  $m_K^2$  for  $K$  mesons, the effect is much smaller, as one can see from Fig. 4.7. But since the measurements are rather precise, it could still provide interesting constraints. However, to be competitive with  $B \rightarrow \tau\nu$ , usually further theoretical model assumptions [33] need to be made.

The process  $D_s^+ \rightarrow \ell^+\nu$ , where  $\ell = \mu, \tau$ , proceeds via  $c\bar{s}$  annihilation, and  $m_B^2$  in (4.12) is replaced by  $(m_s/m_c)m_{D_s}^2$ . The impact of  $H^+$  on  $D_s^+ \rightarrow \ell^+\nu_\ell$  decay is in general rather small [27]. Furthermore, this is a tree level process proceeding without any CKM suppression, hence it seems rather hard for New Physics effects to compete with SM. The rate is usually used to measure  $f_{D_s}|V_{cs}|$  in a rather clean way.

Two developments caused a stir around 2008. The experimental measurements by CLEO-c and Belle, at different energy thresholds hence with different systematic errors, were in good agreement [34, 35], combining to give

$$f_{D_s}|\text{expt}| = (277 \pm 9) \text{ MeV} \quad (\text{CLEO-c + Belle, 2008}), \quad (4.20)$$

assuming  $|V_{cs}| = 1$ . However, the BaBar measurement [36] gave a somewhat higher central value, though not inconsistent with (4.20). It is not included in (4.20) because it is not an absolute branching ratio measurement.

In a similar time frame, a *very precise* result came from lattice [37],

$$f_{D_s}|\text{latt}| = (241 \pm 3) \text{ MeV} \quad (\text{lattice "rooting", 2008}), \quad (4.21)$$

with % level errors for a nonperturbative result! This precision arises in the "improved" staggered fermion approach in lattice QCD, with the assumption called "rooting" to simplify the computation of the fermion determinant. By taking the fourth root of the quark determinant (a very complicated quantity that is in large part the gist of the lattice sea, or dynamical, quark effects), it drastically reduces the amount of computation needed. No other approach was able to compete in the numerical precision reached. Arguing that the precision of (4.21) can stand scrutiny, and that experiment and lattice could not be reconciled (aggravated by larger BaBar value), it was claimed [38] that this discrepancy suggests New Physics, and models such as leptoquarks were offered.

We will not comment further on lattice QCD computations, except that important results need independent measurements using different approaches. In Sect. 3.1.2 we have in fact used the discrepancy of the above two equations to argue, in an intuitive way, that  $B_s$  mixing in SM is likely to be larger than the experimental measurement of (3.13). From the fact that even the quite sensible fourth generation seems ruled out by data, it can be said that the claim of [38] borders on the incredulous. The New Physics "models" proposed by [38], unlike our general arguments [27] for  $H^+$  effects, are rather constructed and ad hoc, and not what one would *normally* contemplate.

If the tree dominant and Cabibbo-allowed  $D_s^+ \rightarrow \ell^+\nu$  is the chosen mode to reveal to us the first signs of New Physics, then, to paraphrase Einstein, "the Lord would be malicious".<sup>5</sup> Sure enough, the experimental value gradually came down,<sup>6</sup> while lattice numbers moved up a little, and the "discrepancy" faded away to below  $2\sigma$ . See [39] for a chronicle.

<sup>5</sup>As commented to the CLEO speaker at FPCP2008 Conference.

<sup>6</sup>For example, HFAG [13] brought the BaBar number down drastically in 2010, by using a more reasonable normalization.

### $B \rightarrow D^{(*)}\tau\nu$ Rate Measurement

Soon after  $B \rightarrow \tau\nu$ , the semitauonic  $B \rightarrow D^{(*)}\tau\nu$  modes, with large branching ratios, also emerged. In 2007 Belle announced the observation of [40]

$$\mathcal{B}_{D^{*-}\tau^+\nu} = (2.02_{-0.37}^{+0.40}) \pm 0.37\% \quad (\text{Belle 535M}), \quad (4.22)$$

based on  $60_{-11}^{+12}$  reconstructed signal events, which is a  $5.2\sigma$  effect. Subsequently, based on  $232M B\bar{B}$  pairs, BaBar announced the observation ( $5.3\sigma$ ) of  $B^- \rightarrow D^{*0}\tau^-\nu$ , and evidence (over  $3\sigma$ ) for  $\bar{B}^0 \rightarrow D^+\tau^-\nu$  [41]

$$\begin{aligned} \mathcal{B}_{D^{*0}\tau^-\nu} &= (2.25 \pm 0.48 \pm 0.22 \pm 0.17)\% \\ \mathcal{B}_{D^+\tau^-\nu} &= (1.04 \pm 0.35 \pm 0.15 \pm 0.10)\% \quad (\text{BaBar 232M}), \end{aligned} \quad (4.23)$$

where the last error is from normalization. Note that these values are on the large side compared to the inclusive measurement of (4.10), even if  $B \rightarrow D^*\tau\nu$  and  $D\tau\nu$  saturate the inclusive rate.

It is rather curious that, almost 25 years after the first B meson was reconstructed, we have new modes measured with  $\sim 1\text{--}2\%$  branching fractions! Furthermore, one may feel at first sight that  $B \rightarrow D^{(*)}\tau\nu$  measurement should be easier than  $B \rightarrow \tau\nu$ , given the much larger branching ratio (they are not really rare decays), and the fact that one is resorting to full-reconstruction tag. The problem is that  $B \rightarrow D^{(*)}\tau\nu$  suffers from an enormous peaking background from  $B \rightarrow D^{(*)}\ell\nu$  for the leptonic  $\tau$  decay modes. Belle used a modified missing mass to suppress this special peaking background. Both experiments continued to refine measurement, and we give the PDG result

$$\mathcal{B}_{D\tau\nu} = (0.98 \pm 0.13)\%, \quad \mathcal{B}_{D^*\tau\nu} = (1.58 \pm 0.12)\%, \quad (\text{PDG 2016}) \quad (4.24)$$

which combines both  $B^+$  and  $B^0$  decays. Note that (4.24) still saturates the inclusive measurement, (4.10), but is not inconsistent with it.

The SM branching ratios for  $B \rightarrow D^{(*)}\tau\nu$  were poorly estimated when it was first measured. Furthermore, though the  $H^+$  could hardly affect the  $B \rightarrow D^*\tau\nu$  rate, it could leave its mark on the  $D^*$  polarization. The  $B \rightarrow D\tau\nu$  rate, like  $B \rightarrow \tau\nu$  itself, is more directly sensitive to  $H^+$  effect [42], although  $B \rightarrow \tau\nu$  has some advantage from our previous discussion. More theoretical work, as well as polarization information, would be needed for BSM (in particular,  $H^+$  effect) interpretation. Note that  $B \rightarrow \tau\nu$  decay probes the pseudoscalar coupling of  $H^+$ , while  $B \rightarrow D\tau\nu$  probes the scalar coupling since  $B \rightarrow D$  is a  $0^- \rightarrow 0^-$  transition. The effect of  $B \rightarrow D\tau\nu$  measurement is also shown in Fig. 4.7, where one can see that its impact is weaker than  $B \rightarrow \tau\nu$ .

The purely leptonic and semileptonic  $B$  decays to  $\tau$  would provide complementary information at Belle II. But BaBar pulled a bombshell on the  $B \rightarrow D^{(*)}\tau\nu$  modes, quite a few years after PEP-II shutdown.

### 4.3 $R_D, R_{D^*}$ Anomaly

As mentioned, the  $B \rightarrow D^{(*)}\tau\nu$  measurement suffers from a rather large peaking background from  $B \rightarrow D^{(*)}\ell\nu$  for the leptonic  $\tau$  decay modes. The B factories turned this peaking background into some advantage: the results in (4.24) were extracted from taking the ratios of  $B \rightarrow D^{(*)}\tau\nu$  modes with the corresponding  $B \rightarrow D^{(*)}\ell\nu$  modes, with the former reconstructed via  $\tau \rightarrow \ell\nu\bar{\nu}$  decay, where  $\ell = e, \mu$ .<sup>7</sup> Taking such ratios have the advantage that many experimental and theoretical uncertainties or common factors cancel.

#### 4.3.1 BaBar Bombshell

In part motivated by the desire to reduce the  $B \rightarrow D^*\tau\nu$  feed-down to  $B \rightarrow D\tau\nu$  when the final state  $D^*$  is not completely reconstructed, BaBar developed [41, 43] a multimode, ratio approach. This is because, as we have stated,  $B \rightarrow D\tau\nu$  is more sensitive to  $H^+$  effects than  $B \rightarrow D^*\tau\nu$ . The strategy was to fully (hadronic) reconstruct the  $B_{\text{tag}}$  on tag side, and select one  $D^*$  plus one  $\ell$  for the signal side, from which one constructs the missing four-momentum  $p_{\text{miss}}$ . To distinguish  $B \rightarrow D^{(*)}\tau\nu$  signal events from the normalization modes of  $B \rightarrow D^{(*)}\ell\nu$ , the latter would lead to a large peak at  $m_{\text{miss}}^2 = p_{\text{miss}}^2 \cong 0$  because of one single missing neutrino, while signal events arising from  $\tau \rightarrow \ell\nu\nu$  would lead to broad  $m_{\text{miss}}^2$  distribution extending out to about  $9 \text{ GeV}^2$ , because of three missing neutrinos. Making a multidimensional combined fit, one extracts

$$R_{D^{(*)}} \equiv \mathcal{B}_{D^{(*)}\tau\nu} / \mathcal{B}_{D^{(*)}\ell\nu}, \quad (4.25)$$

where  $B^+$  and  $B^0$  modes are combined assuming isospin symmetry. The approach utilizes the  $|\mathbf{p}_\ell^*|$  ( $B$ -frame) and  $q^2 = (p_B - p_{D^{(*)}})^2$  distributions in the fit, hence can provide more information. With 232M  $B\bar{B}$  events, the extracted  $R_{D^*}$ , hence  $\mathcal{B}_{D^*\tau\nu}$ , was more than [41]  $6\sigma$  in significance.

We cannot do justice to this sophisticated analysis. While Belle was somewhat oblivious, BaBar continued to improve the analysis, including event reconstruction improvements that increased signal efficiency by a factor of 3, and exploiting BDT techniques to separate signal from background. BaBar announced [44], simultaneous with posting to arXiv [45], the result

$$R_D = 0.440 \pm 0.071, \quad R_{D^*} = 0.332 \pm 0.029, \quad (\text{BaBar 2012}) \quad (4.26)$$

---

<sup>7</sup>It is understood that the ratio is taken for  $e$  and  $\mu$  individually, but with both modes included in the measurement.

at FPCP 2012 in Hefei, China. BaBar updated input parameters to theory [46] work developed since first observations,<sup>8</sup> to give the SM prediction

$$R_D^{\text{SM}} = 0.297 \pm 0.017, \quad R_{D^*}^{\text{SM}} = 0.252 \pm 0.003. \quad (\text{BaBar 2012}) \quad (4.27)$$

The measurements therefore exceeded SM expectations by 2.0 and  $2.7\sigma$ , respectively, combining to  $3.4\sigma$ .

### BaBar Statement

The statement of  $3.4\sigma$  by itself should not raise an eyebrow by too much. The real bombshell is the statement [45]

*the combination of  $R_D$  and  $R_{D^*}$  excludes the  $H^+$  boson of type II 2HDM with a 99.8% confidence level for any value of  $\tan\beta/m_{H^+}$ .*

While sounding a bit strong compared with the  $3.4\sigma$  significance (of deviation from SM), let us see where this astounding statement came from.

BaBar was checking against the possible interpretation with 2HDM-II. The differential decay rate formula is [44, 46],

$$\begin{aligned} \frac{d\Gamma_\tau}{dq^2} &= \frac{G_F^2 |V_{cb}|^2 |\mathbf{p}| q^2 \left(1 - \frac{m_\tau^2}{q^2}\right)^2}{96\pi^3 m_B^2} \\ &\times \left[ \left( |H_{++}|^2 + |H_{--}|^2 + |H_{00}|^2 \right) \left( 1 + \frac{m_\tau^2}{2q^2} \right) + \frac{3}{2} \frac{m_\tau^2}{q^2} |H_{0t}|^2 \right], \quad (4.28) \end{aligned}$$

where  $q^2 = (p_B - p_{D^{(*)}})^2$  is the  $\tau\nu$  lepton-pair mass,  $|\mathbf{p}|$  is a momentum defined in [46] for defining lepton-pair helicities,  $H_{mn}$  are helicity amplitudes with  $D^*$  and lepton-pair helicities  $+$ ,  $-$  and  $0$ , plus a 4th component  $t$  for the latter; for  $B \rightarrow D\tau\nu$ ,  $H_{\pm\pm}$  is absent. The charged Higgs  $H^+$  effect enters only through the last term of (4.28), via

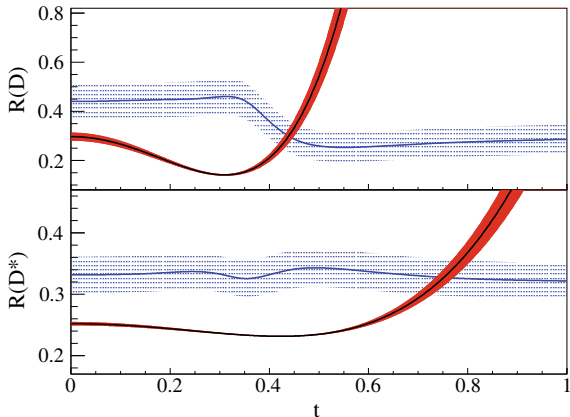
$$H_{0t}^{2\text{HDM}} = H_{0t}^{\text{SM}} \left[ 1 - \frac{m_b \tan^2 \beta}{m_b \mp m_c} \frac{q^2}{m_{H^+}^2} \right], \quad (4.29)$$

where  $- (+)$  sign is for  $B \rightarrow D^{(*)}\tau\nu$ . Compared with  $r_H$  in (4.12), the  $m_b/(m_b \mp m_c)$  factor brings in some hadronic uncertainties. We note that the numerator and denominator are of different origins. Note also that  $H_{0t}^{\text{SM}}$  contains the scalar form factor that does not appear in  $\bar{B} \rightarrow D\ell\nu$ .

Accounting for difference in efficiency for  $R_D$  and  $R_{D^*}$  measurement for twenty different  $\tan\beta/m_{H^+}$  values, the BaBar result is plotted in Fig. 4.8 versus  $t = \tan\beta/m_{H^+}$ , compared with the expected theoretical values. The two intersections are [44, 45]

<sup>8</sup>To show the progress in lattice QCD, an almost concurrent result [47] with BaBar paper gave  $R_D^{\text{latt}} = 0.316 \pm 0.012 \pm 0.007$ , in suitable agreement with (4.27).

**Fig. 4.8** Comparison of BaBar's  $B \rightarrow D^{(*)}\tau\nu$  results [45] with  $H^+$  effect from 2HDM-II (the narrow band). The  $x$ -axis is  $\tan \beta/m_{H^+}$  in  $\text{GeV}^{-1}$  units, with SM at  $\tan \beta/m_{H^+} = 0$  [Copyright (2012) by The American Physical Society]



$$\tan \beta/m_{H^+} = 0.44 \pm 0.02 \quad (0.75 \pm 0.04) \text{ GeV}^{-1}, \quad \text{for } R_D \text{ (} R_{D^*} \text{)} \quad (4.30)$$

with impressive precision because many uncertainties cancel. The two numbers are incompatible with each other, leading to the aforementioned statement.

*What if the two values met!?* Actually, whether they would meet at either value, or any value in between, it would be in very strong conflict with the measured  $B \rightarrow \tau\nu$  rate: *the  $\tan \beta/m_{H^+}$  values seem too large*, when seen in the light of the  $m_B^2$  factor in (4.12). Within 2HDM-II, if we take  $\tan \beta/m_{H^+} \simeq 0.44$  or  $0.75 \text{ GeV}^{-1}$  from (4.30), the  $B \rightarrow \tau\nu$  rate would be enhanced by  $r_H \sim 19$  or  $215$ , respectively, which is ruled out by direct measurement [26], including the inclusive measurement of (4.10). This would make the interpretation of (4.27) difficult, hence the deviation in  $R_{D^*}$  is even more problematic than  $R_D$ . Put another way, given that  $B \rightarrow \tau\nu$  rate is of order SM expectation, either  $\tan \beta/m_{H^+}$  is small compared with  $1/m_B$ , or it is close to  $\sqrt{2}/m_B \simeq 0.27 \text{ GeV}^{-1}$ . In any case it would be considerably less than (4.30), hence should give smaller  $R_D$  and  $R_{D^*}$  values compared to (4.27).  $B \rightarrow \tau\nu$  is the most sensitive of the three processes to charged Higgs boson of 2HDM-II, which was a point emphasized in [27].

### LHCb Joins the Fray

Aside from a long followup paper with more details [26], BaBar had exhausted its data. By 2015, Belle caught up with the  $B_{\text{tag}} + D^{(*)}\ell$  reconstruction and ratio method, and measured [26]  $R_D = 0.375 \pm 0.064 \pm 0.026$ ,  $R_{D^*} = 0.293 \pm 0.038 \pm 0.015$  with 772M  $BB$  events, which is consistent with both (4.26) and (4.27), i.e. both BaBar and SM, hence tension is weaker.<sup>9</sup> A year later, using semileptonic tag for the  $B_{\text{tag}}$ , Belle measured [26]  $R_{D^*} = 0.302 \pm 0.030 \pm 0.011$ . Though tagging efficiency is higher, the extra  $\nu$  on tag side required  $D^*$  reconstruction on signal side, and degraded the  $m_{\text{miss}}$  resolution.

<sup>9</sup>Belle found  $R_D$  and  $R_{D^*}$  compatible around  $\tan \beta/m_{H^+} \sim 0.5 \text{ GeV}^{-1}$ , but this is still in conflict with measured  $B \rightarrow \tau\nu$  and  $b \rightarrow \tau\nu + X$  rates within 2HDM-II.



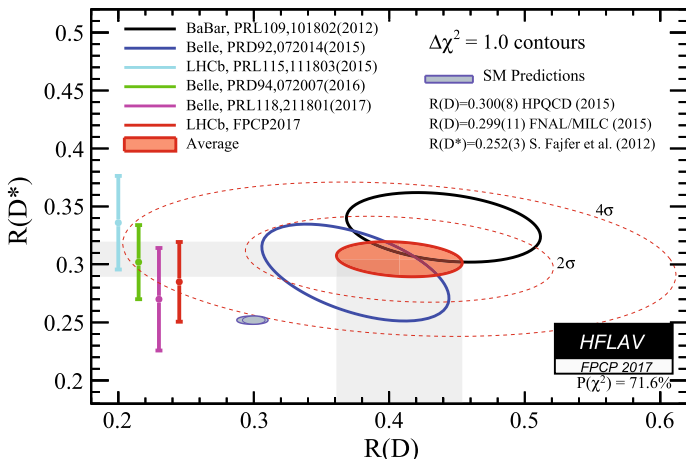


**Fig. 4.9** HFLAV plot for  $R_D - R_{D^*}$  as of FPCP 2017 Conference. [from HFLAV, <http://www.slac.stanford.edu/xorg/hflav/>]

What upped the ante was the surprise announcement [48] by LHCb in 2015, that they could measure  $R_{D^*}$  with  $D^*\mu$  signal reconstruction<sup>10</sup> in *hadronic production environment*. LHCb reconstructed  $D^{*+} \rightarrow D^0\pi^+$  (conjugate included), with  $D^0 \rightarrow K^+\pi^-$ . With excellent PID and tracking, one could then select a muon that comes from the same  $B$  decay vertex (SV), which is displaced from the primary vertex (PV). Taking the SV to PV direction as the  $B$  meson momentum direction, and making a reasonable approximation on the  $B$  momentum projection onto the beam axis, the excellent vertex resolution allowed sufficient resolution for an analysis similar to BaBar’s for  $m_{\text{miss}}$ . With full Run 1 data of  $3 \text{ fb}^{-1}$ , LHCb measured [48]

$$R_{D^*} = 0.336 \pm 0.027 \pm 0.030, \quad (\text{LHCb } 3 \text{ fb}^{-1}, D^{*-}\mu^+) \quad (4.31)$$

which is more consistent with BaBar value in (4.26). Combining all data, the significance (of deviation from SM) hovered around  $4\sigma$ . Together with its persistence, this made  $R_{D^{(*)}}$  a leading “anomaly” in flavor physics, a highlight from the combined data from B factory and LHCb Run 1, with the backdrop that “No New Physics” was uncovered at LHC direct search. This led to a further ballooning of theory work.

We give in Fig. 4.9 the  $R_D - R_{D^*}$  plot, prepared by HFLAV (name changed from HFAG at Moriond 2017) for the FPCP 2017 Conference, which contains two further data entries compared with what we have discussed so far. The two large ellipses are the fully hadronic  $B_{\text{tag}} + D^{(*)}\ell$  reconstruction measurements of BaBar [45] and Belle [26], which are visually away from the tiny SM ellipse on lower-left. The leftmost “bar” (light blue in original HFLAV plot) is the LHCb measurement [48] of  $R_{D^*}$  using  $\tau \rightarrow \mu\nu\nu$  decay, which is more consistent with the BaBar ellipse, the

<sup>10</sup>Performance for electron is poorer.

bar to its right (bright green) is the Belle measurement of  $R_{D^*}$  with semileptonic tag [26], which is consistent with the Belle ellipse. This summarizes the situation before summer 2017.

### 4.3.2 Assessment: Towards Belle II + LHCb Era

Perhaps offering a glimpse of the LHCb plus Belle II era to come, the two other bars in Fig. 4.9 are the new measurements, by Belle [49] with<sup>11</sup>  $\tau \rightarrow \pi\nu, \rho\nu$ , and by LHCb [50, 51] with  $\tau \rightarrow \pi\pi\pi(\pi^0)\nu$ , respectively. The  $\tau$  lepton is reconstructed in final states with only hadrons. While one can still take the ratio with  $B \rightarrow D^*\mu\nu$ , the latter is not part of the analysis. The good thing is that systematic errors are quite independent of all previous analyses.

The two measurements with  $\tau$  reconstructed in hadronic final states give

$$R_{D^*} = 0.270 \pm 0.035_{-0.025}^{+0.028} \quad (\text{Belle 772M, one prong}), \quad (4.32)$$

$$R_{D^{*\ast}} = 0.285 \pm 0.019 \pm 0.029 \quad (\text{LHCb 3 fb}^{-1}, \text{ three prong}). \quad (4.33)$$

While (4.33) has the best statistical error so far, both measurements give lower values than previous ones by the individual experiments. Most notably, both numbers are consistent with SM expectation! In fact, the LHCb presentation [50] emphasized that the result pulls down the world average, but increases slightly the discrepancy with SM (to  $4.08\sigma$ ). But taken by themselves, the 2017 measurements are quite consistent with SM, and there would be *no* anomaly in  $R_{D^{*\ast}}$ .

While the Belle measurement, via  $B_{\text{tag}}$  plus  $D^*\tau$ (1-prong) in the clean  $e^+e^-$  B factory environment is relatively straightforward, the LHCb three-prong measurement has huge backgrounds to face [50, 51] in the hadronic production environment. One reconstructs  $D^{*\ast} \rightarrow D^0(\rightarrow K^+\pi^-\pi^+)$ , plus  $\pi^+\pi^+\pi^-(\pi^0)$  ( $\pi^0$  ignored, and as usual, conjugate included). But  $B^0 \rightarrow D^*\pi\pi\pi + X$  is about 100 times larger than the targeted signal of  $B^0 \rightarrow D^*\tau_{3\text{-prong}}\nu$ . However, as we have seen, with precise vertex resolution, one could demand the three pions to emerge from a vertex rather detached from the  $B$  vertex. This use of  $\tau$  decay time,  $t_\tau$ , as a discriminating variable, results in 3 orders of magnitude suppression of the “prompt” background. But the  $D$  (in order of  $D^0, D_s^+$  and  $D^+$  in longevity) mesons have comparable lifetime to  $\tau$ , thus the next background to deal with is  $B \rightarrow D^{*\ast}D_q + X$ , with  $D_q \rightarrow \pi\pi\pi + X$ , where  $D_s^+$  is the leading menace. An “anti- $D_s$  BDT” multivariate classifier was built to handle this, and in the end it was the poorly known  $D^+ \rightarrow K^+\pi\pi\pi\pi^0$  decay that left a loose end. To cancel uncertainties as much as possible,  $B \rightarrow D^{*\ast}\pi\pi\pi$  was taken as normalization mode, where the ratio was extracted from the fit. (4.33) is then derived by multiplying by the LHCb measurement of the normalization mode [26] and dividing by the world average for  $B^0 \rightarrow D^{*\ast}\mu^+\nu$ . LHCb expects to increase statistics by a

<sup>11</sup>The preliminary Belle result was reported by the plenary speaker on B physics at ICHEP 2016 Conference, but the conference paper became public only afterwards.

factor of 3 by adding Run 2 data. It would be interesting to see how the result, and significance, would evolve.

### Awaiting the Next Round

Although from the same dataset, it is clear that the LHCb three-prong measurement of  $R_{D^{*-}}$  is independent of the  $D^{*-}\mu^+$  measurement [48], and so is the one-prong measurement of  $R_{D^*}$  by Belle independent from B factory measurements with  $\tau \rightarrow \ell\nu\nu$ . Given that the anomaly is more apparent with the actual ratio analysis, where both the  $\tau$  and normalization modes are reconstructed in the same charged lepton final state, one should be concerned with possible common systematic effects in the measurements inspired by the pioneering BaBar approach, which in any case seems to over-saturate<sup>12</sup> the inclusive measurement of (4.10). We also note that Belle measurements have always been more consistent with SM than BaBar and the first LHCb measurement. Furthermore, while the significance of discrepancy with SM has hovered around  $4\sigma$  since 2015, it is not much above BaBar’s original  $3.4\sigma$ , and did not improve with more measurements. Given that Belle II would start to have B physics data by 2019, we view it prudent to let both experiment and theory develop more, and see how this “ $R_D, R_{D^*}$  anomaly” pans out in the Belle II era, while LHCb can add further information on analogously defined  $R_{J/\psi}$  [52] and  $R_{A_c}$  measurements from  $B_c$  and  $A_b$  decays.

With anomalies as such, theory has been abuzz. While the Higgs sector of MSSM would not be abandoned as yet, with the provocative statement from BaBar that 2HDM-II is ruled out [45], alternative models have been proposed (we give only the initial reference, as the literature is large): general 2HDM with flavor-changing neutral Higgs (FCNH) couplings [53] and beyond, leptoquarks [54], and  $W'$  [55]. These reflect possible new  $b\bar{c}\bar{\nu}\tau$  four-fermion operators, with corresponding scalar or vector boson exchange, where leptoquarks can be either scalar or vector. Beyond usual constraints, various hurdles or challenges have been raised, such as the  $B_c$  lifetime [56, 57] (from  $B_c \rightarrow \tau\nu$  etc. decays),  $q^2$  distributions [58], and high  $p_T$   $\tau$  direct search signatures at the LHC [59], which make model building rather difficult.  $W'$  is disfavored by high  $p_T$   $\tau$ 's at LHC. The combined effect of the three challenges rule out charged scalars. Even the “flavored” leptoquark (LQ) that seemed to survive better, can evade the various challenges only by constructing, e.g. cancellation mechanisms between two scalar leptoquarks [60], or vector leptoquarks [61] with other concoctions, such as extending the Pati-Salam gauge group to three copies [62], or imbedding [63] it in a Randall-Sundrum background. While such constructions appear to be getting a little out of hand, the follow up by CMS [64] with search for  $b$ - $\tau$  LQ [61] lends credence to the flavor anomalies.

But the challenge to (and perhaps extravagance in) model building supports our caution that one should “wait and see” how the  $R_{D^{(*)}}$  anomaly pans out in the next round with Belle II data competing with LHCb. We would also remark that a charged

<sup>12</sup>This is echoed, and exasperated (given  $\sim 1.5$  GeV available phase space), by a major source of uncertainty in the analysis, i.e. modeling of  $B \rightarrow D^{**}\ell\nu$  background, where  $D^{**}$  stands for all resonant and nonresonant effects beyond  $D^*$ .

Higgs, even if beyond 2HDM-II, is still more conservative than leptoquarks. After all, the 125 GeV boson seems to complete a Higgs boson doublet, but we have no inkling for leptoquarks so far. One could either discuss the “prior” for each to appear at or below the TeV scale (and in particular in the  $b \rightarrow c\tau\nu$  process), or we recall Einstein’s maxim, “Subtle is the Lord, but malicious He is not.”

As we wait for more data, and especially for Belle II to turn on, let us turn and look ahead. The difference between  $B \rightarrow D^{(*)}\tau\nu$  and  $B \rightarrow \tau\nu$  is that the semitauonic modes are not really rare, neither are they simple two-body decays. These two facts allowed the methods of signal extraction to develop, despite the background. In addition, the large number of signal events (as compared with the very rare  $B \rightarrow \tau\nu$  decay, which is in addition inaccessible to LHCb) imply that various distributions associated with the process are extracted through the analysis, and provide further information. We have already cited the usage of the  $q^2$  distribution. These distributions would not only help clarify the  $R_{D^{(*)}}$  anomaly, but also offer to probe, e.g.  $H^+$  effects further. It is the pioneering effort of BaBar that led the way.

The Belle one-prong  $\tau^\pm \rightarrow \pi^\pm\nu, \rho^\pm\nu$  study [49] gives another illustration of possible future developments. Besides measuring  $R_{D^*}$  in a mode independent from the BaBar-initiated method, it was in part motivated by the ability to measure  $\tau$ -polarization, by the  $\theta_{\text{hel}}$  angular distribution of the meson in the  $\tau$  rest frame. The  $\tau$ -polarization,  $P_\tau$ , as a probe of charged Higgs effects in  $B \rightarrow D^{(*)}\tau\nu$  decays, was discussed [65, 66] as early as the 1990s, whereas  $D^*$  polarization<sup>13</sup> was emphasized, e.g. in [46]. One again uses fully hadronic tag for  $B_{\text{tag}}$  reconstruction. Given that the  $\tau$  is reconstructed only via  $\pi^\pm$  or  $\pi^\pm\pi^0$ , reconstructing an accompanying  $D^*$  gives better handle. With enough kinematic constraints to define the helicity angle  $\theta_{\text{hel}}$ , Belle simultaneously fits [49] for  $R_{D^*}$  and  $P_\tau$ , finding (4.32) and

$$P_\tau(D^*) = -0.38 \pm 0.51^{+0.21}_{-0.16} \quad (\text{Belle 772M, one prong}), \quad (4.34)$$

where the  $D^*$  labels the accompanying meson to  $\tau\nu$ . This is the first measurement of  $P_\tau(D^*)$  in  $\bar{B} \rightarrow D^*\tau\nu$  decay, which provides a new dimension in the search for New Physics. In the long run, one might contemplate New Physics probes such as triple product correlations.

## References

1. Alam, M.S., et al.: [CLEO Collaboration]: Phys. Rev. Lett. **74**, 2885 (1995)
2. Bertolini, S., Borzumati, F., Masiero, A.: Phys. Rev. Lett. **59**, 180 (1987)
3. Deshpande, N.G., Lo, P., Trampetic, J., Eilam, G., Singer, P.: Phys. Rev. Lett. **59**, 183 (1987)
4. Grinstein, B., Wise, M.: Phys. Lett. B **201**, 274 (1988)
5. Hou, W.-S., Willey, R.S.: Phys. Lett. B **202**, 591 (1988)
6. Misiak, M., et al.: Phys. Rev. Lett. **98**, 022002 (2007)

---

<sup>13</sup>Analogous to  $B \rightarrow D\tau\nu$  being more sensitive to  $H^+$  [20, 42], the charged Higgs can only affect the decay into longitudinally polarized  $D^*$ .

7. Misiak, M., et al.: Phys. Rev. Lett. **114**, 221801 (2015)
8. Ammar, R., et al.: [CLEO Collaboration]: Phys. Rev. Lett. **71**, 674 (1993)
9. Aubert, B., et al.: [BaBar Collaboration]: Phys. Rev. D **72**, 052004 (2005)
10. Lange, B.O., Neubert, M., Paz, G.: Phys. Rev. D **72**, 073006 (2005)
11. Koppenburg, P., et al.: [Belle Collaboration]: Phys. Rev. Lett. **93**, 061803 (2004)
12. For standard practice, see Buchmüller, O.L., Flücher, H.U.: Phys. Rev. D **73**, 073008 (2006)
13. Heavy Flavor Averaging Group (HFLAV; acronym changed from HFAG to HFLAV in March 2017). <http://www.slac.stanford.edu/xorg/hflav>
14. Buras, A.J., Czarnecki, A.i, Misiak, M., Urban, J.: Nucl. Phys. B **631**, 219 (2002)
15. Becher, T., Neubert, M.: Phys. Rev. Lett. **98**, 022003 (2007)
16. Limosani, A., et al.: Belle Collaboration. Phys. Rev. Lett. **103**, 241801 (2009)
17. Aubert, B., et al.: [BaBar Collaboration]: Phys. Rev. D **77**, 051103 (2008)
18. Abdesselam, A., et al.: [Belle Collaboration]: [arXiv:1608.02344](https://arxiv.org/abs/1608.02344) [hep-ex]
19. Misiak, M., Steinhauser, M.: Eur. Phys. J. C **77**, 201 (2017)
20. Grzadkowski, B., Hou, W.-S.: Phys. Lett. B **272**, 383 (1991)
21. Hou, W.-S., Willey, R.S.: Nucl. Phys. B **326**, 54 (1989)
22. Coan, T.E., et al.: [CLEO Collaboration]: Phys. Rev. Lett. **80**, 1150 (1998)
23. Hou, W.-S.: Nucl. Phys. B **308**, 561 (1988)
24. Krawczyk, P., Pokorski, S.: Phys. Rev. Lett. **60**, 182 (1988)
25. Buskulic, D., et al.: [ALEPH Collaboration]: Phys. Lett. B **298**, 479 (1993)
26. Tanabashi, M., et al.: [Particle Data Group]: Phys. Rev. D **98**, 030001 (2018). <http://pdg.lbl.gov/>
27. Hou, W.-S.: Phys. Rev. D **48**, 2342 (1993)
28. The paper only appeared in 1995, Artuso, M., et al.: [CLEO Collaboration]: Phys. Rev. Lett. **75**, 785 (1995)
29. Ikado, K., et al.: [Belle Collaboration]: Phys. Rev. Lett. **97**, 251802 (2006)
30. Aubert, B., et al.: [BaBar Collaboration]: Phys. Rev. D **77**, 011107 (2008)
31. Haisch, U.: [arXiv:0805.2141](https://arxiv.org/abs/0805.2141) [hep-ph]
32. CKMfitter group. <http://ckmfitter.in2p3.fr>
33. See e.g. Masiero, A., Paradisi, P., Petronzio, R.: Phys. Rev. D **74**, 011701 (2006)
34. Artuso, M., et al.: [CLEO Collaboration]: Phys. Rev. Lett. **99**, 071802 (2007)
35. Widhalm, L., et al.: [Belle Collaboration]: Phys. Rev. Lett. **100**, 241801 (2008)
36. Aubert, B., et al.: [BaBar Collaboration]: Phys. Rev. Lett. **98**, 141801 (2007)
37. Follana, E., Davies, C.T.H., Lepage, G.P., Shigemitsu, J.: Phys. Rev. Lett. **100**, 062002 (2008)
38. Dobrescu, B.A., Kronfeld, A.S.: Phys. Rev. Lett. **100**, 241802 (2008)
39. Kronfeld, A.S.: Ann. Rev. Nucl. Part. Sci. **62**, 265 (2012)
40. Matyja, A., Rozanska, M., et al.: [Belle Collaboration]: Phys. Rev. Lett. **99**, 191807 (2007)
41. Aubert, B., et al.: [BaBar Collaboration]: Phys. Rev. Lett. **100**, 021801 (2008)
42. Grzadkowski, B., Hou, W.-S.: Phys. Lett. B **283**, 427 (1992)
43. For more details, see Aubert, B., et al.: [BaBar Collaboration]: Phys. Rev. D **79**, 092002 (2009)
44. Talk by Lüth, V.G.: [arXiv:1209.4674](https://arxiv.org/abs/1209.4674) [hep-ex], at FPCP2012, Hefei, China, May 21–25, 2012
45. Lees, J.P., et al.: [BaBar Collaboration]: Phys. Rev. Lett. **109**, 101802 (2012). [[arXiv:1205.5442](https://arxiv.org/abs/1205.5442) [hep-ex]]
46. Fajfer, S., Kamenik, J.F.: Nišandžić. I. Phys. Rev. D **85**, 094025 (2012)
47. Bailey, J.A., et al.: [Fermilab Lattice and MILC Collaborations]: Phys. Rev. Lett. **109**, 071802 (2012)
48. Aaij, R., et al.: [LHCb Collaboration]: Phys. Rev. Lett. **115**, 111803 (2015)
49. Hirose, S., Iijima, T., et al.: [Belle Collaboration]: Phys. Rev. Lett. **118**, 211801 (2017)
50. Talk by Wormser, G.: At FPCP2017, Prague, Czech, June 5–9, 2017
51. Aaij, R., et al.: [LHCb Collaboration]. [arXiv:1708.08856](https://arxiv.org/abs/1708.08856) [hep-ex]
52. Aaij, R., et al.: [LHCb Collaboration]. [arXiv:1711.05623](https://arxiv.org/abs/1711.05623) [hep-ex]
53. Crivellin, A., Greub, C., Kokulu, A.: Phys. Rev. D **86**, 054014 (2012)
54. Fajfer, S., Kamenik, J.F., Nišandžić. I., Zupan, J.: Phys. Rev. Lett. **109**, 161801 (2012)
55. Greljo, A., Isidori, G., Marzocca, D.: JHEP **1507**, 142 (2015)

56. Li, X.-Q., Yang, Y.-D., Zhang, X.: JHEP **1608**, 054 (2016)
57. Alonso, R., Grinstein, B., Martin Camalich, J.: Phys. Rev. Lett. **118**, 081802 (2017)
58. Freytsis, M., Ligeti, Z., Ruderman, J.T.: Phys. Rev. D **92**, 054018 (2015)
59. Faroughy, D.A., Greljo, A., Kamenik, J.F.: Phys. Lett. B **764**, 126 (2017)
60. See e.g. Crivellin, A., Müller, D., Ota, T.: JHEP **1709**, 040 (2017)
61. Buttazzo, D., Greljo, A., Isidori, G., Marzocca, D.: JHEP **1711**, 044 (2017)
62. Bordone, M., Cornella, C., Fuentes-Martin, J., Isidori, G.: Phys. Lett. B **779**, 317 (2018)
63. Blanke, M., Crivellin, A.: Phys. Rev. Lett. **121**, 011801 (2018)
64. Sirunyan, A.M., et al.: [CMS Collaboration]: JHEP **1807**, 115 (2018)
65. Kalinowski, J.: Phys. Lett. B **245**, 201 (1990)
66. Tanaka, M.: Z. Phys. C **67**, 321 (1995)

# Chapter 5

## Electroweak Penguin: $b \rightarrow s\ell\ell$ , Anomalies, $Z'$



In Sect. 2.2, we discussed the effects of the  $b \rightarrow s\bar{q}q$  electroweak penguin interfering with the strong penguin and tree amplitudes. The quintessential electroweak penguin would be  $b \rightarrow s\ell^+\ell^-$  decay, or  $b \rightarrow s\nu\nu$  that has no photonic contribution. We now discuss how the study of these processes, present already in SM, could help us probe New Physics. Besides presenting some background development, we begin with the forward-backward asymmetry  $A_{\text{FB}}(B \rightarrow K^*\ell^+\ell^-)$  as a probe of the  $bsZ$  vertex, and the subsequent unfolding of the  $P'_5$  and  $R_{K^{(*)}}$  anomalies. We comment briefly on a possible  $Z'$  boson as a source for generating effective  $[\bar{s}b][\bar{\ell}\ell]$  (and  $[\bar{s}b][\bar{\nu}\nu]$ ) four-fermi interactions. The  $b \rightarrow s\nu\nu$  process has the same signature as  $b \rightarrow s + \text{nothing}$ . A later chapter extends the signature as a probe of *light* Dark Matter (DM).

### 5.1 $A_{\text{FB}}(B \rightarrow K^*\ell^+\ell^-)$

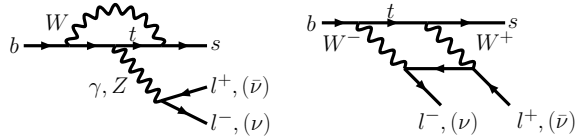
Ever since its observation early on at the B factories, the  $B \rightarrow K^*\ell^+\ell^-$  process has been a favorite pursuit, including later on at LHCb. Essentially 4-body with exquisite signatures starting with polarization of  $\ell^+\ell^-$  that have less hadronic dependence, together with  $B \rightarrow K\ell^+\ell^-$ , they have provided a treasure trove of New Physics probes.

#### 5.1.1 Observation of $m_t$ -enhanced $b \rightarrow s\ell^+\ell^-$

In SM, the  $B \rightarrow K^{(*)}\ell^+\ell^-$  process ( $b \rightarrow s\ell^+\ell^-$  at inclusive level) arises from photonic penguin, Z penguin and box diagrams, as shown in Fig. 5.1.

At first sight, one would think that the photonic penguin is at  $\alpha G_{\text{rf}}$  order ( $\alpha$  from QED,  $G_{\text{F}}$  from one  $W$ ), while the Z penguin and box diagrams, which have *two* heavy vector boson propagators, are effectively at  $G_{\text{F}}^2$  order of weak interactions. Since  $G_{\text{F}} \sim 10^{-5} \text{ GeV}^{-2}$  is small compared to the physical decay scale

**Fig. 5.1** Photonic penguin, Z penguin, and the box diagram for  $b \rightarrow s\ell^+\ell^-$ ,  $s\nu\bar{\nu}$



of  $m_b^2$ , it seems intuitive to drop the Z penguin and box diagrams. This was in fact what was first [1] done, but it was soon pointed out [2] that the Z penguin (gauge related to both the photon penguin and box diagrams) would in fact dominate for large  $m_t$ ! We have already discussed this “nondecoupling” phenomenon of the SM heavy  $t$  quark in Sect. 3.2.2, but it is worthwhile to understand the origins of this.

### Nondecoupling: $m_t$ Enhancement of $bsZ$ Coupling

A heuristic way to see Z penguin dominance of  $b \rightarrow s\ell^+\ell^-$  is to observe that the above “ $G_F$  power counting” has a loophole. Comparing  $\alpha G_F$  of the photonic penguin with  $G_F^2$  of the Z penguin, the two factors actually have different mass dimensions. To compensate, the latter should be written as  $G_F^2 m^2$ . This has been used in our simple power counting above, where we have tacitly used  $m_b^2$ . However, from subtleties of the diagrams involved, and supported by a full calculation, one finds  $m_t^2$  instead of  $m_b^2$  as the outcome.  $G_F m_t^2$  is certainly not negligible compared to  $\alpha$  for  $m_t$  above 100 GeV or so.

Nondecoupling of heavy quarks in SM is due to their large Yukawa couplings. Note that heavy particle propagators in general lead to decoupling, i.e. heavy mass effects are normally decoupled, with  $G_F$  power counting as a good example.<sup>1</sup> So, one would have thought that the effect of a heavy top would also be decoupled. In pure QED and QCD processes, this would indeed be the case. However, the  $SU(2) \times U(1)$  weak interaction is more delicate:

$$\lambda_t \equiv \sqrt{2} \frac{m_t}{v}, \quad (5.1)$$

is the dynamical Yukawa coupling, where  $v$  is the v.e.v. scale. The heaviness of  $m_t$  is a dynamical effect. It turns out that two powers of Yukawa couplings remain for the Z loop calculation, which results in *nondecoupling*. So why does this not happen for the photonic penguin?

It is not our purpose to present any diagrammatic calculations. However, it would be elucidating to give an account of the subtleties that distinguishes the  $\gamma$  and Z penguins, i.e.  $\bar{s}b\gamma$  and  $\bar{s}bZ$  couplings. So let us try to be as lucid as possible, and explain in a language that hopefully even experimenters can grasp (see also Footnote 3 of Chap. 4). In attempting the calculations for the diagrams of Fig. 5.1, one would like to ignore external masses and momenta as much as possible, since  $m_b^2/M_W^2$  is

<sup>1</sup>Technically this statement is actually not true. For low energy tree level effects, it is the process mass scale versus  $M_W$  scale that provides suppression. See below.



small (i.e.  $G_F m_b^2$  is negligible). In so doing, one then discovers that the  $\bar{s}b\gamma$  vertex would vanish in the  $m_b^2/M_W^2 \rightarrow 0$  limit. Hence, to extract the  $\bar{s}b\gamma$  vertex, extra care needs to be taken, and one needs to make an expansion in small external masses and momenta, before setting them to zero. Put differently, one recalls that the photon, even if off-shell, couples to conserved currents, which is a requirement of gauge invariance. A vanishing vertex is of course trivially conserved, but to have a non-trivially conserved  $\bar{s}b\gamma$  vertex, the effective vertex would depend on the *external* momentum and mass(es). The point is that  $m_b$  and  $m_s$  are of unequal mass, so  $\bar{s}\gamma_\mu b$  (unlike e.g.  $\bar{e}\gamma_\mu e$ ) cannot by itself be a conserved current.

In the notation of Inami and Lim [3], we write the effective  $\bar{s}b\gamma$  vertex as

$$\bar{s} \left[ (q^2 \gamma_\mu - q_\mu \not{q}) \mathcal{F}_1 + i \sigma_{\mu\nu} q^\nu (m_b R + m_s L) \mathcal{F}_2 \right] b, \quad (5.2)$$

where  $q$  is the 4-momentum carried off by the photon. It is clear that (5.2) is explicitly conserved, i.e. contracting with  $q^\mu$ , both terms vanish. Note that the  $q_\mu$  term, when contracting with another conserved current (e.g.  $\bar{\ell}\gamma_\mu \ell$  in our case, or an external photon polarization vector), would vanish. Furthermore, the contribution of the  $\mathcal{F}_1$  “form factor” would vanish for on-shell ( $q^2 = 0$ ) photons. So, it is the  $\mathcal{F}_2$  term that contributes to physical  $b \rightarrow s\gamma$  decay, but both  $\mathcal{F}_1$  and  $\mathcal{F}_2$  contribute to  $b \rightarrow s\ell^+\ell^-$ .

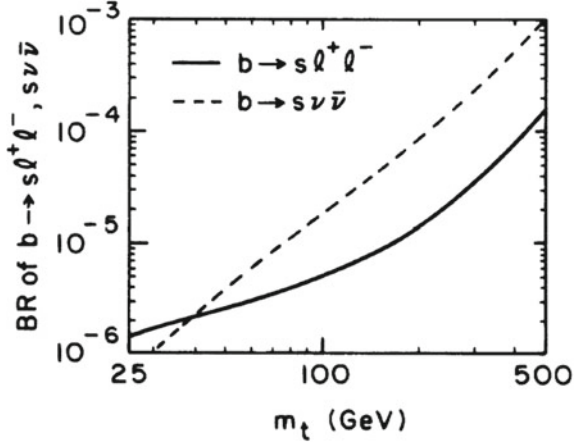
We see now what must be collected in expanding the  $\bar{s}b\gamma$  vertex of Fig. 5.1: we must collect  $q^2 \gamma_\mu$ ,  $q_\mu \not{q}$ , as well as  $\sigma_{\mu\nu} q^\nu m_{b,s}$  terms. That they come together to give the form of (5.2) is a check on the calculation. In contrast, the  $\bar{s}bZ$  vertex is not conserved, because electroweak gauge invariance is spontaneously broken down to electromagnetism. Thus, in computing the  $\bar{s}bZ$  vertex of Fig. 5.1, one does not need to put the vertex in the form of (5.2), and one could set  $m_b^2/M_W^2$  to zero from the outset. It is this subtlety, that the electromagnetic current is conserved, but the charge and neutral currents are not, that sets apart the behavior (in  $m_t$  dependence) of the  $\bar{s}b\gamma$  and  $\bar{s}bZ$  couplings.

The result above is of course gauge invariant. In the physical gauge, the longitudinal components of the  $W^+$  boson lead to  $m_t$  in the numerator in the  $\bar{t}bW^+$  coupling. In gauges with unphysical scalars  $\phi_W^+$ , these are the would-be Goldstone bosons that got “eaten” by the  $W^+$  boson to make it heavy, and, as a partner to the SM neutral Higgs boson, it couples to top via (5.1). The whole picture works consistently for the  $\bar{s}bZ$  vertex, which is not conserved, but for the  $\bar{s}b\gamma$  vertex, the requirement of (5.2) by current conservation replaces the possible  $m_t^2$  factors by  $q^2$  and  $m_{b(s)q}$ , and the  $m_t$  effect for  $\bar{s}b\gamma$  is closer to the decoupling kind,<sup>2</sup> as already commented on in Sect. 3.2.2.

We have thus argued why the  $m_t$  dependence of photonic and  $Z$  penguins are so different, and how the latter could dominate for large enough  $m_t$ . It is intricately related to spontaneous symmetry breaking and mass generation in electroweak theory. A full calculation of course bears all this out. We plot in Fig. 5.2 the 30 years

<sup>2</sup>For the  $\bar{s}b\gamma$  vertex, the photon can also radiate off the  $W^+$  (not shown in Fig. 5.1). But for the  $\bar{s}b\gamma$  vertex, the gluon can only radiate off the top. With always two top propagators, the  $\bar{s}b\gamma$  vertex has even weaker  $m_t$  dependence.

**Fig. 5.2** Large  $m_t$  enhancement [2] of  $b \rightarrow s\ell^+\ell^-$ ,  $s\nu\bar{\nu}$  rates [Copyright (1987) by The American Physical Society]



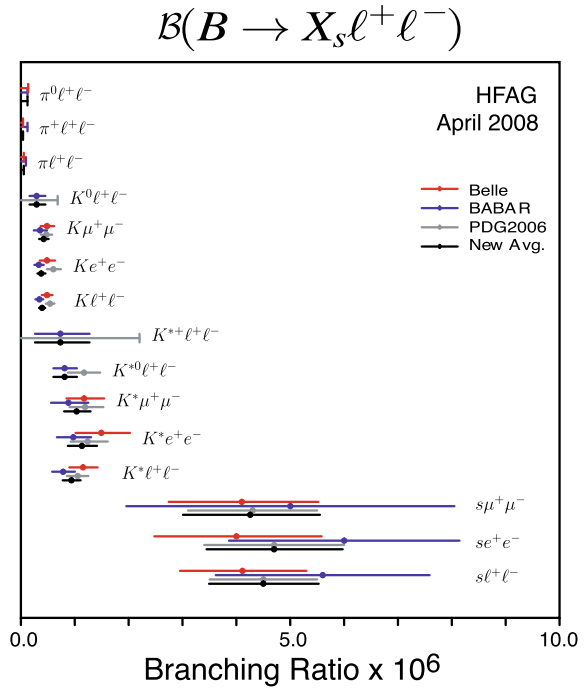
old result from the original observation [2] of large  $m_t$  enhancement of  $b \rightarrow s\ell^+\ell^-$ ,  $s\nu\bar{\nu}$  decay rates. Note that  $b \rightarrow se^+e^-$  would be slightly larger than  $b \rightarrow s\mu^+\mu^-$  because of low  $q^2$  enhancement from the photonic penguin. The strong, almost  $m_t^2$  dependence is most apparent for  $b \rightarrow s\nu\bar{\nu}$ , which has no photonic contribution, and we have summed over 3 neutrinos. Much progress has been made in sophisticated calculations of the rates of  $b \rightarrow s\ell^+\ell^-$ ,  $s\nu\bar{\nu}$ . However, the results of Fig. 5.2 capture the main effect, and all subsequent calculations are corrections.

### Observation of $B \rightarrow K^{(*)}\ell^+\ell^-$ and $b \rightarrow s\ell^+\ell^-$

Although  $b \rightarrow s\gamma$  was already observed by CLEO in the 1990s, the first observation of an electroweak penguin decay was only made by Belle in 2001. With 31.3M  $B\bar{B}$  pairs, combining  $B \rightarrow Ke^+e^-$  and  $K\mu^+\mu^-$  events ( $K$  stands for both charged and neutral kaons), Belle observed [4]  $\sim 14$  events with a combined statistical significance of  $5.3\sigma$  for  $B \rightarrow K\ell^+\ell^-$ . The result was consistent with SM, but subject to  $B \rightarrow K$  form factors, so the interpretation is less interesting. Observation of  $B \rightarrow K^*\ell^+\ell^-$  [5] soon followed. Repeating the  $b \rightarrow s\gamma$  history, the inclusive  $b \rightarrow s\ell^+\ell^-$  measurement ( $B \rightarrow X_s\ell^+\ell^-$  experimentally) was subsequently observed a year or so later, by Belle in summer 2002. With 65.4M  $B\bar{B}$  pairs and again combining  $e^+e^-$  and  $\mu^+\mu^-$ , a total of  $\sim 60$  events were observed [6] with  $5.4\sigma$  statistical significance, and  $b \rightarrow s\ell^+\ell^-$  became experimentally established.

In the experimental studies, one cuts out the  $J/\psi$  and  $\psi'$  resonance regions in  $q^2$ , as these produce the same final states, and are in fact much larger. These charmonium regions actually provide large control samples to test the fit models for the electroweak penguin study. A snapshot of measurements of electroweak penguins by Belle and Babar as of Spring 2008 are summarized in Fig. 5.3. Rates for exclusive modes depend on form factors, and are less interesting. The inclusive rate (not so different for PDG2016) is consistent with SM expectations (see e.g. [7]), hence confirming the large  $m_t$  enhancement [2]. Note that the latter observation was made in 1986, predating the ARGUS discovery [8] of large  $B_d$  mixing, which led to the change in mindset that the top quark is uniquely heavy.

**Fig. 5.3** HFAG plot for various  $B \rightarrow X \ell^+ \ell^-$  measurements



Many modes, including exclusive  $B \rightarrow \pi \ell \ell$ ,  $\rho \ell \ell$  (replacing  $s$  by  $d$  in Fig. 5.2), have been searched for. A study based on 657M  $B\bar{B}$  pairs by Belle [9] pushed the limit on  $B^+ \rightarrow \pi^+ \ell^+ \ell^-$  down to the  $5 \times 10^{-8}$  level, which is only a factor of 1.5 above SM expectations [10]. But one did not have to wait for a Super B Factory for the measurement. With just  $1 \text{ fb}^{-1}$  data,  $B^+ \rightarrow \pi^+ \mu^+ \mu^-$  was observed by LHCb [11] in 2012,  $\mathcal{B}_{\pi^+ \mu^+ \mu^-} = (2.3 \pm 0.6 \pm 0.1) \times 10^{-8}$ , which is one of the rarest decays ever measured. Its ratio with  $\mathcal{B}_{K^+ \mu^+ \mu^-}$  is consistent with  $|V_{ts} V_{tb}|^2$ .

Given that the top quark is a v.e.v. scale fermion, we could say that TeV scale physics influenced the  $b \rightarrow s \ell \ell$  rate, as a prime example of the flavor-TeV link. Since electroweak symmetry breaking is the main theme for the LHC to probe as a machine, to go above the v.e.v. scale, the complementary nature of  $b \rightarrow s \ell \ell$  with the high energy approach again resonates with the cartoon of Fig. 1.1. Our special interest in the 4th generation can also be seen from this perspective [2]. The  $t'$  quark, being a SM type chiral quark with mass generated through the analogue of (5.1) can also affect the  $bsZ$  coupling, so  $b \rightarrow s \ell \ell$  is also a sensitive probe of  $t'$ .

### 5.1.2 $A_{\text{FB}}(B \rightarrow K^* \ell^+ \ell^-)$ Problem and Its Demise

The top quark exhibits nondecoupling in the Z penguin and box diagrams, which is analogous to the electroweak penguin effect in  $B^+ \rightarrow K^+ \pi^0$ , and the box

diagrams for  $B_s^0\text{-}\bar{B}_s^0$  mixing. Due to this nondecoupling of the top quark, the  $Z$  penguin dominates the  $b \rightarrow s\ell^+\ell^-$  decay amplitude.

### Forward-backward Asymmetry in $B \rightarrow K^*\ell^+\ell^-$

Not long after the large  $m_t$  enhancement was pointed out, it was noted that interference between the vector ( $\gamma$  and  $Z$ ) and axial vector ( $Z$  only, box as an appendage) contributions in  $b \rightarrow s\ell^+\ell^-$  production gives rise to a forward-backward asymmetry [12], similar to the  $\mathcal{A}_{\text{FB}}$  in  $e^+e^- \rightarrow f\bar{f}$  found in textbooks. But the *enhancement of  $bsZ$  coupling effectively brings the  $Z$  from  $M_Z$  down to below the  $B$  mass, much closer to the  $\gamma$* . Furthermore, *one now probes potential New Physics in the  $b \rightarrow s$  loop*. Since interference between amplitudes is the essence of quantum physics,  $\mathcal{A}_{\text{FB}}$  is of great interest. In particular, for the differential  $d\mathcal{A}_{\text{FB}}(q^2)/dq^2$  asymmetry, the variation over  $q^2 \equiv m_{\ell\ell}^2$  probes different regions of interference between  $bs\gamma$  and  $bsZ$ .

It is more than a figure of speech to say that the  $\ell^+\ell^-$  pair in the final state, much like an electron microscope that scatters an electron wave off the material being probed, actually provides us with a ‘‘microscope’’ to look back at what is happening inside the loop-induced  $bs\gamma$  and  $bsZ$  vertices.

With both the inclusive  $B \rightarrow X_s\ell^+\ell^-$  and exclusive  $B \rightarrow K^{(*)}\ell^+\ell^-$  decays measured [5, 13] (see Fig. 5.3), experimental interest turned to  $\mathcal{A}_{\text{FB}}$  for  $B \rightarrow K^*\ell^+\ell^-$ . While inclusive  $\mathcal{A}_{\text{FB}}$  is also pursued, it is more challenging because of background issues, and largely impossible in a hadronic environment. The experimentally defined forward-backward asymmetry is

$$\frac{d\mathcal{A}_{\text{FB}}(q^2)}{dq^2} \equiv \frac{d\mathcal{B}/dq^2|^{+} - d\mathcal{B}/dq^2|^{-}}{d\mathcal{B}/dq^2|^{+} + d\mathcal{B}/dq^2|^{-}}, \quad (5.3)$$

where  $d\mathcal{B}/dq^2$  is the differential rate, and the  $\pm$  superscript indicates forward and backward moving  $\ell^+$  versus the  $B$  meson direction in the  $\ell^+\ell^-$  frame.

As the process is easy to visualize, we give the quark level amplitude [10],

$$\mathcal{M}_{b \rightarrow s\ell^+\ell^-} \propto V_{cs}^* V_{cb} \left\{ -2 \frac{m_b m_B}{q^2} C_7^{\text{eff}} [\bar{s} i\sigma_{\mu\nu} \hat{q}^\nu Rb][\bar{\ell}\gamma^\mu \ell] + C_9^{\text{eff}} [\bar{s}\gamma_\mu Lb][\bar{\ell}\gamma^\mu \ell] + C_{10} [\bar{s}\gamma_\mu Lb][\bar{\ell}\gamma^\mu \gamma_5 \ell] \right\}, \quad (5.4)$$

where short distance physics, including within SM, is isolated in the Wilson coefficients  $C_7^{\text{eff}}$ ,  $C_9^{\text{eff}}$  and  $C_{10}$ , which can be systematically computed. The  $1/q^2$  term carries the  $C_7$  effective photon contribution, which comes from the  $\sigma_{\mu\nu}$  term in (5.2), while  $C_9^{\text{eff}}$  and  $C_{10}$  are from the  $Z$  penguin (as well as the  $q^2\gamma_\mu$  term of (5.2), and the box diagram). We have factored out  $V_{cs}^* V_{cb}$  instead of the usual  $V_{ts}^* V_{tb}$ . This has the advantage of being the product of CKM elements that are already measured, and real by standard convention [5].

A commonly used formula for the differential  $A_{\text{FB}}$  is

$$\frac{dA_{\text{FB}}(q^2)}{dq^2} \propto C_{10} \xi(q^2) \left[ \text{Re}(C_9^{\text{eff}}) F_1 + \frac{1}{q^2} C_7^{\text{eff}} F_2 \right], \quad (5.5)$$

where  $\xi(q^2)$  and  $F_1, F_2$  can be found in [10]. Within SM, the Wilson coefficients are practically real, as has been ingrained into the formula. This form has somehow influenced the development of the subject, as we will discuss. Actually,  $C_9^{\text{eff}}$  receives some long distance  $c\bar{c}$  effect that can be absorptive [2], hence the real part is taken since it is not a CPV observable.

### Early Measurements and Complex Wilson Coefficients

Belle reported its first  $A_{\text{FB}}$  measurement in  $B \rightarrow K^* \ell^+ \ell^-$  with 386M  $B\bar{B}$  pairs [14], and the results were consistent with SM, ruling out the possibility of flipping the sign of  $C_9$  or  $C_{10}$  separately from SM value, but flipping the two signs together, equivalent to flipping sign of  $C_7$ , was not ruled out. With 229M  $B\bar{B}$ , BaBar gave [5]  $A_{\text{FB}}$  in just two  $q^2$  bins in 2006, below and above  $m_{J/\psi}^2$ . The higher  $q^2$  bin was consistent with SM and disfavored BSM scenarios. For the lower  $q^2$  bin ( $4m_\mu^2$  to  $6.25 \text{ GeV}^2$ ), the value was  $\sim 2\sigma$  away from SM, which was not inconsistent with the Belle result, while sign-flipped BSM's are less favored. Updating with 384M  $B\bar{B}$  pairs [15], the high  $q^2$  bin was consistent with SM as before, but BaBar measured  $A_{\text{FB}}|_{\text{low } q^2} = 0.24^{+0.18}_{-0.23} \pm 0.05$  for the low  $q^2$  bin. The SM expectation in this region is  $A_{\text{FB}}|_{\text{low } q^2}^{\text{SM}} = -0.03 \pm 0.01$ . Viewed together with the Belle result, it seemed that the low  $q^2$  behavior was not quite SM-like, though SM was not excluded.

In part motivated by the suggestive deviations at lower  $q^2$ , and in anticipation of LHCb turn-on, it was pointed out [16] that (5.5), used already by Belle and Babar in their analyses, may be an over-interpretation: there is no reason a priori why the Wilson coefficients should be kept real when probing BSM physics! This can be seen most easily by inspection of (5.4): the Wilson coefficients are effective couplings of 4-fermi interactions, and in a theory that allows for CPV phases, in general they should be complex. In contrast to the oftentimes tacitly assumed Minimal Flavor Violation (or MFV [17]) mindset, where one postulates that New Physics conforms with observed CKM flavor structure, hence implying (5.5), one should use the proper form,

$$\frac{dA_{\text{FB}}(q^2)}{dq^2} \propto \text{Re}(C_9^{\text{eff}} C_{10}^*) F'_1 + \frac{1}{q^2} \text{Re}(C_7^{\text{eff}} C_{10}^*) F'_2, \quad (5.6)$$

when interpreting data, where we have absorbed  $\xi(q^2)$  into the  $F'_i$  form factor combinations. Here, one is not concerned with  $CP$  conserving long distance effects such as in  $C_9^{\text{eff}}$ , but the possibility that the  $C_i$ s may pick up BSM weak ( $CP$  violating) phases. If present, they could enrich the interference pattern through (5.6), in contrast to the usual form of (5.5), which basically takes the short distance Wilson coefficients as real *by fiat*.

Assuming New Physics enters through effective  $bsZ$  and  $bs\gamma$  couplings, and allowing the Wilson coefficients to be only constrained by the measured radiative ( $b \rightarrow s\gamma$ ) and electroweak ( $b \rightarrow s\ell\ell$ ) penguin rates, it was shown [16] that  $d\mathcal{A}_{\text{FB}}/dq^2$  could in fact vary more prominently for  $q^2 < m_{j/\psi}^2$ , where  $\hat{s} \equiv q^2/m_B^2$ . Conventional wisdom at the time emphasized that the precise position of the zero,  $q_0^2$ , is less form factor dependent hence of interest. But allowing for sizable weak phases for the Wilson coefficients, the position of the zero could be [16] anywhere around or below the SM expectation.

One motivation behind (5.6) at the time was, if  $P_{\text{EW}}$  is the culprit for the  $\Delta\mathcal{A}_{K\pi}$  problem discussed in Sect. 2.2, the equivalent  $C_9$  and  $C_{10}$  for  $B^+ \rightarrow K^+\pi^0$  decay seem to carry *large* weak phases, and one should let Nature speak through  $B \rightarrow K^*\ell^+\ell^-$  data. The fourth generation with parameters as determined from  $\Delta m_{B_s}$ ,  $\mathcal{B}(B \rightarrow X_s\ell^+\ell^-)$  and  $\Delta\mathcal{A}_{K\pi}$  indeed belongs to the class of BSM models where  $C_9$  and  $C_{10}$  coefficients would be complex. Using the MC study with  $2 \text{ fb}^{-1}$  data by LHCb [18] for  $d\mathcal{A}_{\text{FB}}/d\hat{s}$ , it was illustrated [16] that LHCb has the ability to distinguish between SM and the 4th generation, or other New Physics models, but it was not clear whether the B factories would have enough resolution.

### $\mathcal{A}_{\text{FB}}(B \rightarrow K^*\ell^+\ell^-)$ Problem and LHCb “Countermeasure”

Let us return to measurements at the B factories. The aforementioned results from Belle [14] and BaBar [15] both indicated that  $\mathcal{A}_{\text{FB}} > 0$  is preferred for the low  $q^2$  region  $\in (4m_\mu^2, 6.25 \text{ GeV}^2)$ . This was sometimes phrased as “ $C_7 = -C_7^{\text{SM}}$  seems preferred from  $\mathcal{A}_{\text{FB}}$  data”, but it had already been pointed out [19] that  $C_7 = -C_7^{\text{SM}}$ , i.e. flipping the sign of the photonic penguin, would lead to too large a  $B \rightarrow X_s\ell^+\ell^-$  rate as compared with experiment. As stated, the SM expectation is  $\mathcal{A}_{\text{FB}}|_{\text{low } q^2}^{\text{SM}} \sim -0.03$  for the low  $q^2$  bin of BaBar. This can be understood from the crossing of zero at  $q_0^2 \sim 4 \text{ GeV}^{-1}$  in SM, and that  $\mathcal{A}_{\text{FB}}$  would have to vanish at  $q^2 = 0$ . Since the region below the zero is larger than the region above, the mutual compensation gives the SM expectation at slightly negative. The hint of positive value therefore lead to much anticipation towards the large dataset update from Belle.

Belle announced their  $657M B\bar{B}$  pair result at ICHEP2008 [22]. Separating into 6  $q^2$  bins, *all* turned out positive, so the deviation from SM became even more acute. Published in 2009 [20], this became the “ $\mathcal{A}_{\text{FB}}$  problem”, as we illustrate in left panel of Fig. 5.4. There is no indication of zero crossing (dotted line corresponds to  $C_7 = -C_7^{\text{SM}}$ ), and suggestive of sizable deviations from SM in the low  $q^2$  bins. In particular, for  $1 < q^2 < 6 \text{ GeV}^2$ , Belle measures

$$\mathcal{A}_{\text{FB}}|_{1-6 \text{ GeV}^2} = 0.26_{-0.30}^{+0.27} \pm 0.07 \quad (\text{Belle 2009}), \quad (5.7)$$

while  $\mathcal{A}_{\text{FB}}|_{1-6 \text{ GeV}^2}^{\text{SM}} = -0.04 \pm 0.03$ . The longitudinal fraction  $F_L$  and isospin asymmetry<sup>3</sup>  $A_I$  are also plotted.

<sup>3</sup>BaBar had found some significance for  $A_I$  below  $m_{j/\psi}^2$  [5], which was not confirmed by the Belle paper. Subsequent measurement by LHCb with  $3 \text{ fb}^{-1}$  data found isospin asymmetries for  $B \rightarrow K^{(*)}\mu^+\mu^-$  to be consistent with SM.

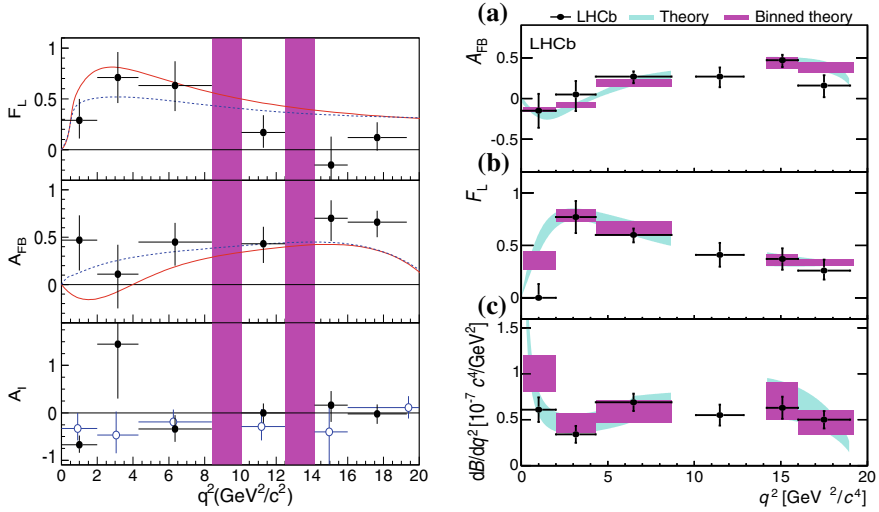


**Fig. 5.4**  $A_{\text{FB}}(B \rightarrow K^* \ell^+ \ell^-)$  [left] measured by Belle [20] (center), with  $J/\psi$  and  $\psi'$  mass regions excluded, [Copyright (2009) by The American Physical Society] where upper (lower) plot is for longitudinal fraction  $F_L$  (isospin symmetry  $A_I$ ); [right] measured by LHCb [21] (upper), together with  $F_L$  and  $d^2B/dq^2$ , with two different representations of SM expectation

With  $6.8 \text{ fb}^{-1}$   $p\bar{p}$  collision data at  $\sqrt{s} = 1.96 \text{ TeV}$ , CDF gave [23]  $\mathcal{A}_{\text{FB}}|_{1-6 \text{ GeV}^2} = 0.29^{+0.20}_{-0.23} \pm 0.07$  in summer 2011. While individually not significant enough, the three measurements by Belle, CDF and BaBar all gave positive  $\mathcal{A}_{\text{FB}}$  values for low  $q^2$ , and the “ $\mathcal{A}_{\text{FB}}$  problem” smelled real. It also illustrates our point of using (5.6) rather than (5.5) in fitting data. Given that  $C_7 = -C_7^{\text{SM}}$  sign-flip is not tenable, one could even claim that data favored somewhat the 4th generation case, where the zero crossing point has moved to much lower  $q^2$ , with a drop in peak value as well. Thus, in the 4th generation model motivated by the  $\Delta\mathcal{A}_{K\pi}$  problem (Sect. 2.2.2), we have  $\mathcal{A}_{\text{FB}} > 0$  for the low  $q^2$  bin, which is in better agreement with data. With the emergent hint for large and negative  $\sin 2\Phi_{B_s}$ , as well (Sect. 3.2), it appeared that the 4th generation model with sizable  $b \rightarrow s$  CPV phase should be taken seriously!

Alas, the shelf life of the  $\mathcal{A}_{\text{FB}}$  problem did not last long. While the hint for sizable  $\sin 2\Phi_{B_s}$  was dashed by LHCb at Lepton-Photon 2011 in Mumbai (see Sect. 3.2), the  $\mathcal{A}_{\text{FB}}$  problem was eliminated already at EPS-HEP 2011 held in Grenoble. With just  $0.37 \text{ fb}^{-1}$   $pp$  collision data at  $\sqrt{s} = 7 \text{ TeV}$ , LHCb found [21] (see right panel of Fig. 5.4)

$$\mathcal{A}_{\text{FB}}|_{1-6 \text{ GeV}^2} = -0.06^{+0.13}_{-0.14} \pm 0.04 \quad (\text{LHCb } 0.37 \text{ fb}^{-1}, 2011), \quad (5.8)$$

which does not confirm prior measurements, but is in good agreement with SM. This was a precursor to  $\sin 2\Phi_{B_s}$  turning out consistent with SM. With full 7 TeV data taken in 2011, at  $1 \text{ fb}^{-1}$ , LHCb measured [24]  $\mathcal{A}_{\text{FB}}|_{1-6 \text{ GeV}^2} = -0.17^{+0.06}_{-0.06} \pm 0.01$ ,

which is a little more negative than SM expectation. But the first measurement of zero-crossing point for  $\mathcal{A}_{\text{FB}}$  gave  $q_0^2 = 4.9 \pm 0.9 \text{ GeV}^2$  (systematic error at 0.05  $\text{GeV}^2$  order), which is consistent with a typical [25] prediction of  $4.36_{-0.31}^{+0.33} \text{ GeV}^2$ . The prediction for position of zero-crossing point is largely free from form factor uncertainties [10], but the experimental measurement is not trivial [24], as there are only six  $q^2$  bins.

## 5.2 $P'_5$ and $R_{K^{(*)}}$ Anomalies

With  $\mathcal{A}_{\text{FB}}$  problem eliminated, before long LHCb had its own ‘‘anomaly’’:  $P'_5$ . Subsequently, another anomaly,  $R_K$  and  $R_{K^*}$ , emerged.

### 5.2.1 $P'_5$ Anomaly

As stated,  $B \rightarrow K^*\ell^+\ell^-$ , in the form of  $B^0 \rightarrow K^{*0}\mu^+\mu^-$  followed by  $K^{*0} \rightarrow K^+\pi^-$  that is studied in detail by LHCb, is a four-body final state rich with observables. Besides  $q^2$ , the angular distribution is described by three angles (see e.g. [26] for definition): the helicity angle  $\theta_K$  of the  $K^{*0}$  candidate (angle between  $K^+$  and  $B^0$  three-momenta in the  $K^{*0}$  rest frame), the helicity angle  $\theta_\ell$  of the dimuon system (angle between  $\mu^+$  and  $B^0$  three-momenta in the  $\mu^+\mu^-$  rest frame), and the angle  $\phi$  between the  $K^{*0} \rightarrow K^+\pi^-$  decay plane and dimuon plane in the  $B^0$  rest frame. Averaging over  $B^0$  and  $\bar{B}^0$ , the differential distribution can be expressed as,

$$\begin{aligned} \frac{1}{d\Gamma/dq^2} \frac{d^4\Gamma}{d\Theta dq^2} = & \frac{9}{32\pi} \left[ \frac{1}{4} (1 - F_L) \sin^2 \theta_K \cos 2\theta_\ell - F_L \cos^2 \theta_K \cos 2\theta_\ell \right. \\ & + \frac{3}{4} (1 - F_L) \sin^2 \theta_K + F_L \cos^2 \theta_K + S_3 \sin^2 \theta_K \sin^2 \theta_\ell \cos 2\phi \\ & + S_4 \sin 2\theta_K \sin 2\theta_\ell \cos \phi + S_5 \sin 2\theta_K \sin \theta_\ell \cos \phi \\ & + \frac{4}{3} A_{\text{FB}} \sin^2 \theta_K \cos \theta_\ell + S_7 \sin 2\theta_K \sin \theta_\ell \sin \phi \\ & \left. + S_8 \sin 2\theta_K \sin 2\theta_\ell \sin \phi + S_9 \sin^2 \theta_K \sin^2 \theta_\ell \sin 2\phi \right], \quad (5.9) \end{aligned}$$

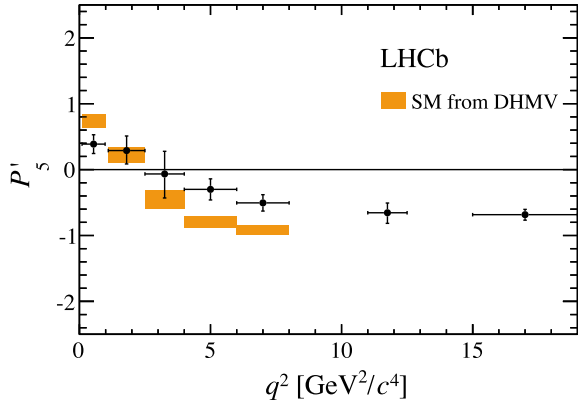
where, besides  $F_L$  and  $\mathcal{A}_{\text{FB}}$ , one has additional angular observables  $S_n$  ( $n = 3, 4, 5, 7, 8, 9$ ) from the  $B^0 \rightarrow K^{*0}\mu^+\mu^-$  decay amplitude, which are functions of the Wilson coefficients and form factors (hence functions of  $q^2$  as well).

As suggested by [27], the combinations of  $S_i$  and  $F_L$

$$P'_{4,5,6,8} = \frac{S_{4,5,7,8}}{\sqrt{F_L(1 - F_L)}}, \quad (5.10)$$



**Fig. 5.5** Measurement of  $P'_5$  by LHCb experiment [31] with  $3 \text{ fb}^{-1}$  data



(in the LHCb definition [28]) are largely free from form factor uncertainties, especially at low  $q^2$  (large  $K^{*0}$  recoil). With 7 TeV data, LHCb performed an angular analysis to measure  $P'_{4,5,6,8}$ , each in six  $q^2$  bins. Not surprisingly, given that  $\mathcal{A}_{\text{FB}}$  agreed with SM, most measured values are also consistent. However, LHCb found [28] a local discrepancy of  $3.7\sigma$  for one out of 24 observables, namely the  $P'_5$  observable in  $4.30 < q^2 < 8.68 \text{ GeV}^2$  bin. Thus commenced the “ $P'_5$  anomaly”. It was quickly pointed out (see [29, 30] for earliest references) that a negative shift  $\Delta C_9 \simeq -1$  of the  $C_9$  Wilson coefficient, achievable by a new  $Z'$  boson, could account for the discrepancy.

An obvious question is whether this could be a fluctuation among many measurables, which was addressed by LHCb in their 2013 paper: for 24 independent measurements, “the probability that at least one varies from the expected value by  $3.7\sigma$  or more is approximately 0.5%” [28]. The question was also raised whether the effect could be due to the  $c\bar{c}$  threshold [32], which lies precisely in this particular bin.

A full angular analysis [31] of full Run 1 data of  $3 \text{ fb}^{-1}$ , largely confirmed<sup>4</sup> the  $1 \text{ fb}^{-1}$  results, but the discrepancy remained, as can be seen from Fig. 5.5. With higher statistics, LHCb refined the  $4.30 < q^2 < 8.68 \text{ GeV}^2$  bin into two separate bins of  $4.0 < q^2 < 6.0 \text{ GeV}^2$  and  $6.0 < q^2 < 8.0 \text{ GeV}^2$ , with deviation from SM expectation (shaded) at  $2.8\sigma$  and  $3.0\sigma$ , respectively. To determine the level of compatibility with SM, LHCb followed the suggestion [29, 30] that a shift in  $C_9$  could suffice, and developed a  $\chi^2$  fit for the purpose. The best fit was found with  $\Delta C_9 = -1.04 \pm 0.25$ , with significance of deviation at  $3.4\sigma$ . While one cannot make a direct comparison to the  $1 \text{ fb}^{-1}$  significance of  $3.7\sigma$  in a single, broader bin, it is of some concern that the significance did not improve with tripling the dataset. Basically, while the larger dataset allowed separating into two bins, compared with the  $1 \text{ fb}^{-1}$  result, the central values of each bin have moved closer towards SM expectation. Had this occurred in the opposite direction, the significance clearly would have jumped up.

<sup>4</sup>An  $S$ -wave  $K^+\pi^-$  component, treated as systematic uncertainty in  $1 \text{ fb}^{-1}$  analysis, was now measured to be not more than 5%.

## Prognosis

The  $P'_5$  anomaly uncovered by LHCb is certainly intriguing, but it may be too soon to claim New Physics. On theory side, the  $c\bar{c}$  threshold (around  $q^2 \simeq 6.8 \text{ GeV}^2$ ) issue was studied further, and it was claimed [33] that the observed effect could arise from *sizable*, non-factorized power corrections, that even optimized observables [27] can get affected by such “hadronic uncertainties”. On experimental side, Belle performed [34] an angular analysis on  $B \rightarrow K^*\ell^+\ell^-$  (i.e. using (5.9)) with 772M  $B\bar{B}$  pairs. In the  $4 < q^2 < 8 \text{ GeV}^2$  bin, a deviation of  $2.6\sigma$  with SM was found for the  $P'_5$  variable of the muon mode, and  $1.3\sigma$  for electron mode, with combined effect of  $2.5\sigma$ . However, using  $20.5 \text{ fb}^{-1}$  data at 8 TeV  $pp$  collision energy and following an analysis similar to LHCb on  $B^0 \rightarrow K^{*0}\mu^+\mu^-$ , the CMS experiment finds [35] agreement with SM expectations. That is, for the two bins of  $4.3 < q^2 < 6.0 \text{ GeV}^2$  and  $6.0 < q^2 < 8.68 \text{ GeV}^2$ , the measured  $P'_5$  values are compatible with the corresponding shaded regions in Fig. 5.5.

We clearly need more data, both from LHCb in Run 2 onwards, as well as the anticipated large dataset from Belle II in the near future, to shed further light on the  $P'_5$  anomaly. The issue of possible large hadronic effect due to  $c\bar{c}$  threshold may be harder to tackle.

As for New Physics that may affect the  $[\bar{s}b][\bar{\ell}\ell]$  4-fermion operator, for example  $Z'$  models with effective FCNC couplings are relatively easy to construct. Normally,  $Z'$  models have too much freedom in picking U(1) charges, hence somewhat arbitrary. But one type of  $Z'$  model, that of gauged  $L_\mu - L_\tau$  symmetry, has a special appeal, which we will discuss later.

### 5.2.2 $R_K, R_{K^*}$ Anomaly

Although  $B \rightarrow K^*\mu^+\mu^-$ ,  $K^*e^+e^-$  decay rates differ because of the photon pole at low  $q^2$  and the difference in dilepton thresholds, it was already pointed out in early papers such as [7] that the two decays are practically the same, hence the SM expectation for muon to electron ratio,  $R_K^{\text{SM}} \cong 1$ . Thus, for instance in their  $\mathcal{A}_{\text{FB}}$  paper, Belle measured [20] (ignoring the distinction between  $4m_\mu^2$  and  $4m_e^2$ )  $R_K = 1.03 \pm 0.19 \pm 0.06$ , and  $R_{K^*} = 0.83 \pm 0.17 \pm 0.08$ , where the latter is also consistent with expectation of  $R_{K^*}^{\text{SM}} \cong 0.75$ .

It was then pointed out [36] that the muon to electron ratio can in itself be a probe of New Physics. Originally defined as the ratio of  $B \rightarrow K^{(*)}\mu^+\mu^-$  and  $B \rightarrow K^{(*)}e^+e^-$  decay rates for  $q^2$  from dimuon threshold up to a common  $q_{\text{max}}^2$ , it was stressed that  $R_K^{\text{SM}} \cong 1$  to rather high accuracy, while  $R_{K^*}^{\text{SM}}|_{\text{no cut}} \simeq 0.73$  (“no cut” meaning ratio of full rates), also with high accuracy. Since these expected values are much higher in precision than individual rates, they offer sensitive probes of New Physics. Further studies, including even lattice studies [37], predicted  $R_K = 1$  to better than per mille accuracy.

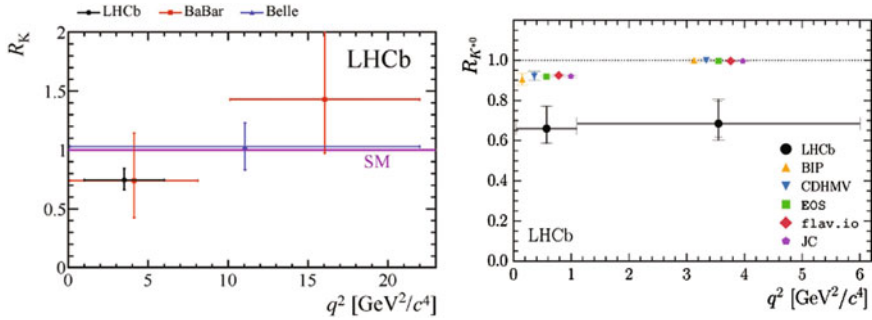


**Fig. 5.6**  $R_K$  [38] (figure taken from LHCb public webpage) and  $R_{K^*}$  [39] measured by LHCb with  $3 \text{ fb}^{-1}$  data

LHCb took this suggestion seriously. It is in fact straightforward for experiments to present measurements of ratio of decay rates in fixed bins of  $q^2 \in [q_{\min}^2, q_{\max}^2]$ . With  $3 \text{ fb}^{-1}$  data and for  $q^2 \in [1, 6] \text{ GeV}^2$ , LHCb studied  $B^+ \rightarrow K^+ \ell^+ \ell^-$ , where only the  $Z$ -penguin contributes, measuring [38]

$$R_K^{[1, 6]} = 0.745_{-0.074}^{+0.090} \pm 0.036 \quad (\text{LHCb } 3 \text{ fb}^{-1}, 2014), \quad (5.11)$$

( $q^2$  in  $\text{GeV}^2$  units) amounting to  $2.6\sigma$  deviation from 1, the expectation from *lepton universality* (LUV). As can be seen from the left panel of Fig. 5.6, earlier Belle and BaBar results, with larger errors, are not in disagreement. Although by itself not yet significant, the attractive phrase of LUV test—*New Physics coupling differently to muons versus electrons*—and the eye-catching central value, together with the  $R_{D^{(*)}}$  and  $P'_5$  anomalies, enticed theorists into action. There were no other indications of New Physics!

Measurement of  $R_{K^*}$  was called for. Missing the Moriond 2017 conferences, the  $3 \text{ fb}^{-1}$  result was announced in a seminar at CERN. Two  $q^2$  bins were studied: the central- $q^2$  bin of  $q^2 \in [1.1, 6] \text{ GeV}^2$ , and low- $q^2$  bin of  $q^2 \in [0.045, 1.1] \text{ GeV}^2$ . The photon peak, absent in the  $R_K$  study, allows enough statistics for the latter bin. The boundary at  $1.1 \text{ GeV}^2$ , rather than  $1 \text{ GeV}^2$  as in the  $R_K$  study, is to include  $\phi \rightarrow \ell^+ \ell^-$  in the low- $q^2$  bin, which itself starts at the lower boundary of  $0.045 \text{ GeV}^2$ , just above  $4m_\mu^2$  threshold. In measuring the ratio of dimuon versus dielectron modes, a double ratio method of normalizing the  $B^0 \rightarrow K^{*0} \ell^+ \ell^-$  rate by the corresponding  $B^0 \rightarrow K^{*0} J/\psi (\rightarrow \ell^+ \ell^-)$  rate was used to control and reduce uncertainties. LHCb measured [39]

$$\begin{aligned} R_{K^*}^{[0.045, 1.1]} &= 0.66_{-0.07}^{+0.11} \pm 0.03, \\ R_{K^*}^{[1.1, 6]} &= 0.69_{-0.07}^{+0.11} \pm 0.05, \quad (\text{LHCb } 3 \text{ fb}^{-1}, 2017), \end{aligned} \quad (5.12)$$

i.e. same trend as  $R_K$ , and each beyond  $2\sigma$  in significance, which excited many theorists. Indeed, a chorus and flourish of theorists and theory papers announced

(see e.g. [40, 41])—appearing in arXiv on the same day<sup>5</sup> as the famed LHCb seminar at CERN—that the  $P'_5$  and  $R_K, R_{K^*}$  anomalies can be commonly accounted for by the aforementioned shift in  $C_9$ . We have commented earlier that this can be achieved by some  $Z'$  boson.

### Prognosis

A plot similar to the left panel of Fig. 5.6 could be shown (see [39]), where Belle and BaBar results are not in disagreement. Instead, we show in right panel of Fig. 5.6 the  $R_{K^*}$  measurements by LHCb compared with various theory estimates, where we refer to the LHCb paper for the references. For the central- $q^2$  bin, the result is quite similar to  $R_K$ . The same could be said for the low- $q^2$  bin, that the experimental result is similarly below theory values clustered around 0.92 (reflecting the phase space difference between dimuon and dielectron modes). But herein lies the caution.

At very low  $q^2$ , we have dipole dominance from  $B \rightarrow K^*\gamma^*$ , where the parent  $B \rightarrow K^*\gamma$  decay is already very well measured [5], while  $\gamma^* \rightarrow \ell^+\ell^-$  certainly respects lepton universality. That LHCb finds exactly similar lower trend compared with  $R_{K^*}^{[1.1, 6]}$  and  $R_K^{[1.1, 6]}$  is a cause of concern. In a way, measuring the low- $q^2$  bin is a “sanity check”; had the result concurred with theory expectation, it would make the other two  $R_K$  and  $R_{K^*}$  results much more convincing. It is likely for this reason, of a “control measurement”, that LHCb took the pain to measure the lower- $q^2$  bin. This is reflected in shifting the boundary from 1 to 1.1 GeV<sup>2</sup> to include the  $\phi$  in the low- $q^2$  bin, since by vector meson dominance lepton universality is respected.

Once again we see the need for both more data from LHCb, and perhaps more importantly, an independent measurement from Belle II, where the production hence final state environment is very different.

### $Z'$ of Gauged $L_\mu - L_\tau$ ?

Grains of salt aside, the  $P'_5$  and the  $R_K, R_{K^*}$  anomalies, all arising from  $B \rightarrow K^{(*)}\ell^+\ell^-$  decays and in particular in the dimuon final state, are certainly intriguing. The theory chorus line that a shift [40, 41] of order  $-1$ , or 30%, in the SM operator coefficient  $C_9$  could account for all three discrepancies, points to a possible  $Z'$  boson. As we have toyed with extending quark generations (Chaps. 2 and 3), extra Higgs doublets (Chap. 4), it is certainly reasonable to ponder<sup>6</sup> extra  $U(1)$  bosons.

We have already mentioned the  $Z'$  boson of the gauged  $L_\mu - L_\tau$  symmetry when discussing the  $P'_5$  anomaly in the previous section. The lepton numbers  $L_i$  are conserved for each  $i = e, \mu, \tau$ , and one could consider promoting some combination to a gauge symmetry. In this context,  $L_i - L_j$  symmetry is appealing because they are anomaly free, and the  $L_\mu - L_\tau$  symmetry [42], with the  $Z'$  coupling only to muon and tauon (and associated neutrinos) is special because it is poorly constrained, hence have a better chance to be “hidden” so far by Nature.

<sup>5</sup>At least 6 papers (of which we cite only the lucky first two) and altogether 30 authors, not to mention the string of continuing papers.

<sup>6</sup>We have already commented in the previous chapter that, while possible to account for some anomalies, we view (flavored) leptiquarks as more exotic.

While the gauged  $L_\mu - L_\tau$  symmetry singles out the muon against the electron, how does it couple to quarks? [43] introduced new vector-like quarks  $Q$  that carry  $U(1)'$  charge, which mix with SM quarks via Yukawa couplings  $Y_{Qj}$  to a complex singlet scalar  $\phi$ , the v.e.v. of which breaks the  $L_\mu - L_\tau$  symmetry. Effective  $[bs]_L[\mu\mu]$  operators of same form as SM could be constructed at tree level, and with  $m_Q$  at 10 TeV order while  $m_\phi$  and associated v.e.v. below TeV, the needed  $\Delta C_9$  could be generated.

The gauged  $L_\mu - L_\tau$  symmetry is motivated in itself by being relatively hidden. With exotic  $Q$  (doublets), or  $U$  and  $D$  (singlets) vector-like quarks, phenomenology could touch upon not just the  $B$  sector, but also muon, kaon and even top sector, which we would mention in the proper sections. As a tribute yet again to flavor anomalies, the CMS experiment has made a search [44] of the  $L_\mu - L_\tau$  gauge boson in  $Z \rightarrow \mu^+\mu^-Z' \rightarrow \mu^+\mu^-\mu^+\mu^-$  events, setting bounds on  $\mu\mu Z'$  coupling strength versus  $m_{Z'}$ .

### 5.3 $B \rightarrow K^{(*)}\nu\nu$

The subject of  $B \rightarrow K^{(*)}\nu\bar{\nu}$  is still in its infancy, and the SM sensitivity is not yet reached. The  $B \rightarrow K^{(*)}\nu\nu$  (and  $b \rightarrow s\nu\nu$ ) decay mode is attractive from the theory point of view, since the photonic penguin does not contribute, nor do  $J/\psi$  or  $\psi'$  decay to  $\bar{\nu}\nu$ . It can arise only from short distance physics, such as  $Z$  penguin and box diagram contributions [2] in Fig. 5.1, hence the decay rates are better predicted. Note that the SM expectation for  $B^+ \rightarrow K^+\nu\bar{\nu}$ , at  $4 \times 10^{-6}$  level [45], is about an order of magnitude larger than  $B^+ \rightarrow K^+\ell^+\ell^-$ , as can be roughly seen from Fig. 5.2, where a factor of  $\sim 6$  comes from [2] counting 3 neutrinos, and  $Z$  charge of  $e$  versus  $\nu$ .

The search for these processes allow us to probe, in principle, what happens in the  $bsZ$  loop in a clean way. Since the neutrinos go undetected, what is of special interest is that the process also allows us to probe light dark matter (DM), which is complementary to the DAMA/CDMS type of direct searches. The latter experiments rely on detecting special electronic signals arising from a nucleus mildly displaced by a DM particle. But this means that the approach loses sensitivity for light DM particles. Such DM pairs could arise from exotic Higgs couplings to the  $b \rightarrow s$  loop. The topic may gain in importance, given that traditional WIMP-type heavy DM particles have not been found, despite refined searches. As we will see, there may even be effectively-dark light particles lurking in  $B \rightarrow K^{(*)} + \text{nothing}$  decays.

#### 5.3.1 Experimental Search

Though clean theoretically, with two missing neutrinos, the experimental signal is rather poor, hence not as well studied as  $B \rightarrow K^{(*)}\ell^+\ell^-$  modes. In fact, it is complementary to  $B^+ \rightarrow \tau^+\nu$  search with semileptonic  $\tau$  decays. We shall focus on

$B^+ \rightarrow K^+\nu\nu$  decay as the experimental benchmark. A simple estimate shows that  $B^+ \rightarrow \tau^+\nu \rightarrow K^+\nu\nu$  is subdominant to the direct  $B^+ \rightarrow K^+\nu\nu$  electroweak penguin decay, while the CKM-suppressed  $B^+ \rightarrow \pi^+\nu\nu$  electroweak penguin decay is subdominant compared to  $B^+ \rightarrow \tau^+\nu \rightarrow \pi^+\nu\nu$ . As we have seen in Sect. 4.2, compounded with a larger  $B^+ \rightarrow \tau^+\nu \rightarrow \pi^+\nu\nu$  rate, with the addition of the leptonic  $\tau \rightarrow \ell\bar{\nu}_\ell\nu_\tau$  decay modes, it is  $B^+ \rightarrow \tau^+\nu$  that is already measured.

BaBar pioneered  $B^+ \rightarrow K^+\nu\nu$  search, using the approach of full reconstruction of the other charged  $B$  meson (see Fig. 4.5). With 89M  $B\bar{B}$  pairs, the 90% C.L. limit of  $5.2 \times 10^{-5}$  was obtained [46] for  $B^+ \rightarrow K^+\nu\nu$ , which is more than an order of magnitude above SM. As a companion study to  $B \rightarrow \tau\nu$  search, Belle searched in many modes with a larger dataset of 535M  $B\bar{B}$  pairs [47], also with full reconstruction of the other  $B$ . No signal was found, and a stringent limit of  $1.4 \times 10^{-5}$  is placed on  $B^+ \rightarrow K^+\nu\nu$ , which is still a factor of 3 above the SM expectation. With 459M  $B\bar{B}$ s, but using semileptonic  $B \rightarrow D^{(*)}\ell\nu$  to tag the other  $B$ , BaBar managed [48] to improve the  $K^+\nu\nu$  limit to  $1.3 \times 10^{-5}$ , slightly better than Belle. Note that the semileptonic tag has higher efficiency than full hadronic tag, and constitutes a statistically independent data sample.

BaBar's semileptonic tag study separated the neutrino pair mass  $q^2 \equiv m_{\nu\bar{\nu}}^2$  into two regions, below or above  $0.4m_B^2$ . With 471M  $B\bar{B}$ s, and using full hadronic tag of other  $B$ , BaBar reported [49] some intriguing results in 2013. With better control of signal information, and making a thorough study of backgrounds, BaBar separated into 10 bins of  $s_B \equiv q^2/m_B^2$ . The main result<sup>7</sup> is plotted in Fig. 5.7. The solid histograms are the backgrounds, which is dominated by the peaking kind, with combinatorial background (shaded) increasing with  $q^2$ . Noticeable is some excess in the lowest  $s_B$  bin for  $B^+ \rightarrow K^+\nu\bar{\nu}$ , and to a lesser extent,  $B^0 \rightarrow K^{*0}\nu\bar{\nu}$ . Because overall background uncertainty, the significance of excess is only  $1.4\sigma$  and not considered significant, but it does give rise to a *two-sided* 90% confidence interval of

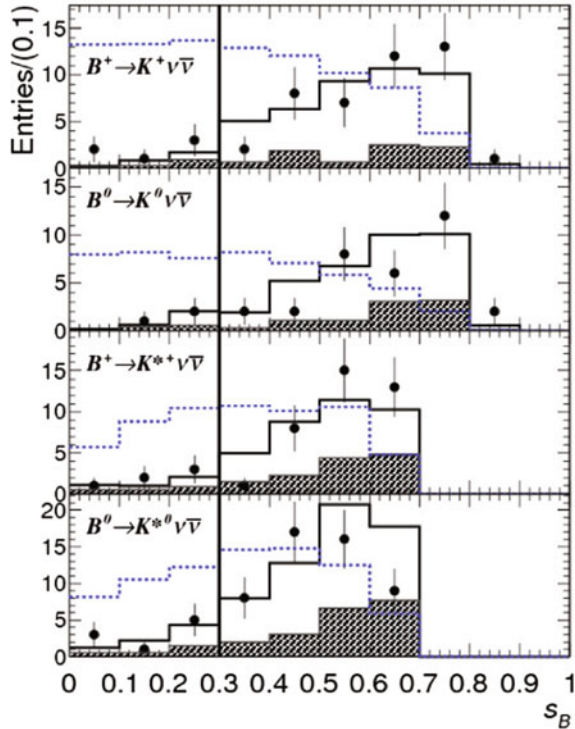
$$\mathcal{B}(B^+ \rightarrow K^+\nu\bar{\nu}) \in [0.4, 3.7] \times 10^{-5} \quad (\text{BaBar 2013, had. tag}), \quad (5.13)$$

which is reduced to  $\mathcal{B}(B \rightarrow K\nu\bar{\nu}) \in [0.2, 3.2] \times 10^{-5}$  when combined with the lower efficiency  $B^0 \rightarrow K^0\nu\bar{\nu}$  mode. Combining with the statistically independent semileptonic tag result of [48], BaBar finds  $\mathcal{B}(B^+ \rightarrow K^+\nu\bar{\nu}) < 1.6 \times 10^{-5}$ , with  $\mathcal{B}(B \rightarrow K\nu\bar{\nu}) = (0.8_{-0.6}^{+0.7}) \times 10^{-5}$ , or the bound of  $1.7 \times 10^{-5}$ , which is not too different.

With 772M  $B\bar{B}$  pairs and using hadronic tag, Belle found [50]  $2.0\sigma$  significance for  $B^+ \rightarrow K^+\nu\bar{\nu}$ , or the bound of  $5.5 \times 10^{-5}$  when  $2.2 \times 10^{-5}$  was expected. But  $B^0 \rightarrow K_S^0\nu\bar{\nu}$  showed little excess, and there were no sign of  $K^{*0}\nu\bar{\nu}$  modes. Interestingly, both charged and neutral  $B \rightarrow \pi\nu\bar{\nu}$  modes showed excess of  $2\sigma$  order, and  $B^+ \rightarrow \rho^+\nu\bar{\nu}$  was at  $1.7\sigma$ , but little excess appeared in  $B^0 \rightarrow \rho^0\nu\bar{\nu}$ . Although the hadronic tag was improved by neural network techniques, and there were improvements in background suppression and signal extraction, unfortunately, this Belle update with hadronic tag did not separate into  $q^2$  bins. What is worse, with a larger

<sup>7</sup>The BaBar paper also placed bounds on  $J/\psi, \psi' \rightarrow \nu\bar{\nu}$  decays.

**Fig. 5.7** Distribution in  $s_B \equiv q^2/m_B^2$  for  $B \rightarrow K^{(*)}\nu\bar{\nu}$  search by BaBar with 471M  $B\bar{B}$  pairs [49], where some excess is seen in lowest  $s_B$  bin for  $B^+ \rightarrow K^+\nu\bar{\nu}$  above total background (solid). See text and [49] for further explanation of figure. [Copyright (2013) by American Physical Society]



data set and with improved efficiencies, Belle still maintained the same  $2.5 \text{ GeV}/c^2$  momentum cut (in  $B_{\text{sig}}$  frame) used in [47], the first Belle analysis, to “reject radiative two-body modes such as  $B \rightarrow K^*\gamma$ ”. No  $q^2$  distribution was shown, such that there is no way to assess whether the excess comes from low  $q^2$ . A few years later, and also with 772M  $B\bar{B}$  pairs, Belle reported [51] the statistically independent semileptonic tag result. No  $q^2$  binning was made, and no mention of whether there was a  $B \rightarrow K^*\gamma$  veto. The  $B^+ \rightarrow K^+\nu\bar{\nu}$  mode again had  $1.9\sigma$  significance, but no excess is seen in the less efficient  $B^0 \rightarrow K_S^0\nu\bar{\nu}$  mode. This time,  $B^+ \rightarrow K^{*+}\nu\bar{\nu}$  showed  $2.3\sigma$  significance, but it was not corroborated by the  $B^0 \rightarrow K^{*0}\nu\bar{\nu}$  mode with similar efficiency.

To summarize, we have not yet seen firm evidence for  $B \rightarrow K^{(*)}\nu\bar{\nu}$ , in contrast with  $B \rightarrow \tau\nu$ , which has  $e\bar{\nu}_e\nu_\tau$  and  $\mu\bar{\nu}_\mu\nu_\tau$  final states to aid its discovery. What appears consistent between different measurements is some excess in  $B^+ \rightarrow K^+\nu\bar{\nu}$  mode, and perhaps dominated by the lowest  $q^2$  bin, if (5.13) and Fig. 5.7 are to be taken seriously.  $B \rightarrow K^{(*)} + \text{nothing}$  should be a main goal at Belle II.

LHCb cannot access this mode. To measure  $B \rightarrow K^{(*)}\nu\bar{\nu}$  modes at the Super B Factory, one would really need to improve background suppression, which seems challenging. The issues for improving the measurements are common between  $B \rightarrow \tau\nu$  and  $B \rightarrow K^*\nu\bar{\nu}$ , i.e. the challenge of modes with missing mass. Even with full reconstruction of the other  $B$ , it is desirable to improve on detector hermeticity at the Super B Factory.

### 5.3.2 Constraint on Light Dark Matter

With  $b \rightarrow s\ell\ell$  measurement in good agreement with SM, one would infer that  $B \rightarrow K\nu\nu$  cannot deviate from SM expectation. However, besides sheer experimental prowess and for sake of confirmation, a bigger motivation for studying  $B \rightarrow K + \text{nothing}$  is to search for light Dark Matter (DM). As Dark Matter is demanded by astrophysical and cosmological evidence, this highlights the importance of the search for the  $B \rightarrow K + \text{nothing}$  signature (see e.g. [52]). Complementary approaches for search of light DM, light exotic Higgs bosons, “dark photons”, etc., are discussed further in Chap. 7, and in Sect. 8.2 for kaon physics.

#### Light DM and $B \rightarrow K + \text{Nothing}$

There are several aspects as to why *light* DM is important. By “light” we mean GeV or even sub-GeV scale, rather than the more typical weak scale DM, as the quintessential particle physics candidate for DM would be WIMPs<sup>8</sup> (Weakly Interacting *Massive* Particles, which is one of the big motivations for SUSY). But as a motivation for light DM, there are puzzling 0.511 MeV lines from the galactic bulge [54], and suggestions have been made that annihilation of sub-GeV WIMPs near galactic center could lead to positron abundance. Second, for typical underground experiments such as DAMA or CDMS, one detects the electronic signals from DM-nucleus collisions. Denoting the DM particle as  $S$ , because the energy transfer to the nucleus scales as  $m_S^2/m_{\text{Nuc}}^2$ , there is little sensitivity to  $m_S$  below a few GeV for these experiments. On the other hand, if light DM does exist, they could be the end products of Higgs decay (Higgs “portal”),  $h \rightarrow SS$ , where  $h$  is the SM-like Higgs boson. This has implications for Higgs property studies at the LHC as well. Thus, it is imperative to gain access to the possibility of light DM.

So how does light DM become relevant in  $b \rightarrow s$  transitions? If one had a light Higgs boson  $h^0$ , then  $b \rightarrow sh^0$  would be rather sizable [55], again because of the Higgs affinity (now with direct Higgs boson emission) of the top quark in the loop, and being a two-body decay process. This possibility is now ruled out.<sup>9</sup> The simplest light DM arises from having a singlet Higgs boson. In these models, the singlet Higgs can have both a bare mass and a component generated by a Higgs coupling  $\lambda$  to the v.e.v. scale. If it so happens that the singlet Higgs mass  $m_S$  is light, though fine-tuned, its coupling to the SM-like Higgs boson could still be large. Combining  $b \rightarrow sh^*$  production, where  $h^*$  is a virtual SM-like Higgs boson, followed by  $h^* \rightarrow SS$ , because of the aforementioned coupling, one has  $b \rightarrow sSS$  (see Fig. 5.8), which leads to  $B \rightarrow KSS$  and gives a  $B \rightarrow K + \text{nothing}$  signature, because the decay of  $S$  is inhibited. The point is, with  $m_t$  enhancement of  $htt$  coupling (common with  $Ztt$ ), and with

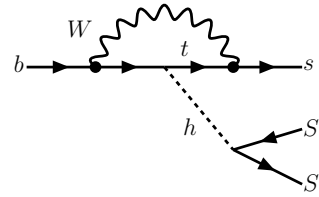
---

<sup>8</sup>The rise with energy, then apparent plateauing above 200 GeV, of the positron fraction in primary cosmic rays observed [53] by AMS experiment on International Space Station, could point to a WIMP close to TeV in mass.

<sup>9</sup>Though lacking further support, the possibility that the HyperCP events [56] are due to a very light exotic Higgs boson will be discussed in Sect. 7.1. It has actually been ruled out by the 2018 LHCb measurement [57] of  $\Sigma^+ \rightarrow p\pi^+\pi^-$ .



**Fig. 5.8** Diagram for  $b \rightarrow sh^* \rightarrow sSS$ , where  $h$  is the SM-like Higgs boson, and  $S$  is a light singlet Higgs boson that is a Dark Matter candidate



$\lambda$  enhancement of  $hSS$  coupling, the  $b \rightarrow sSS$  process in general dominates over  $b \rightarrow s\nu\nu$ , so long that it is kinematically allowed.

Experimental bounds on  $B^+ \rightarrow K^+\nu\bar{\nu}$  can therefore be used to constrain [52] Higgs portal DM models. With relative generous assumptions on strong interaction uncertainties that affect the DM annihilation cross section, and in the assessment of consistency with cosmological abundance requirements, even the earlier BaBar and Belle results imply that  $m_S < 1.5$  GeV is unlikely in the above picture. There is, however, a catch for heavier  $m_S$ , which reflects the  $p_K$  cut employed by the experimental study to reject  $b \rightarrow c$  background. The stiffer the  $p_K$  cut, the earlier one loses sensitivity to heavier  $m_S$  because of phase space for the  $KSS$  final state. Earlier CLEO [5] analysis has lower  $p_K$  cut. But as we progress through the more and more stringent BaBar [46] and Belle [47] searches, since these studies aim at more stringent bound on  $B^+ \rightarrow K^+\nu\bar{\nu}$ , a larger  $p_K$  cut is needed to suppress background. If one targets singlet Higgs DM search, then the  $p_K$  and other cuts should be re-optimized for different  $m_S$  assumptions. There may therefore be room for improvement even with the same data set. On the other hand, given the observed bound seems to be above expectation, perhaps there is some extra process feeding  $B^+ \rightarrow K^+ + \text{nothing}$ , so more novel handling of background should be explored for the case of  $m_S$  between 1.5 to 2 GeV.

Note that the singlet Higgs scenario is the simplest for light DM. One can certainly enlarge the model with further assumptions, or consider fermionic DM. There is no lack of other, more elaborate models, and our discussion is only meant as an illustration. With much more data, Belle II should have more say on this important subject, which is quite complementary to LHC studies and direct DM search.

### Vector Portals and Effective Darkness

We mention one such somewhat constructed scenario for illustration, in connection with the  $R_K$  and  $R_{K^*}$  anomaly. It was pointed out [58] that a vector boson  $V$  with  $m_V \sim 2.5$  GeV that induces  $b \rightarrow s$  and couples to muon, could account for the  $R_K$  and  $R_{K^*}$  anomaly (it fails to account for  $P'_5$  because of constraints [59] from Drell-Yan production). But to evade the absence of narrow dimuon peaks,  $V$  needs to decay dominantly invisibly to give sizable  $\Gamma_V$ , which motivates the invisible decay being into a pair of (fermion or scalar) DM. That is, one replaces  $h^* \rightarrow SS$  in Fig. 5.8 by  $V^* \rightarrow \chi\bar{\chi}$ , where  $\chi$  is the DM particle. Independent of DM detail, however, the scenario predicts  $q^2$ -dependent deviation from  $e$ - $\mu$  universality because  $m_V < m_B$ , though it does not alleviate the issue with lower bin of  $R_{K^*}$ . Furthermore,  $B \rightarrow K +$

*nothing* would be not far from current limit, and the scenario could possibly explain the muon  $g - 2$  “anomaly” (Chap. 9).

We note, however, that the current bound for  $B \rightarrow K^+ + \textit{nothing}$  hints at a possible excess, which is seemingly driven by the lowest  $q^2$  bin (see Fig. 5.7), which the scenarios above cannot address. If one takes the lowest  $s = q^2/m_B^2$  bin “excess” and two-sided bound of (5.13) as hint, a different scenario was pointed out. One could have  $B^+ \rightarrow K^+ + Z'$ , where the  $Z'$  could be the gauge boson of  $L_\mu - L_\tau$ . If  $m_{Z'}$  is below the dimuon threshold, then  $Z' \rightarrow \nu\bar{\nu}$  decay is at 100% level, and could give rise to the excess without any narrow dimuon peak. Such a scenario [60], though too light in mass to account for the  $b \rightarrow s\ell^+\ell^-$  decay anomalies (though it can explain  $g - 2$ ), could evade existing  $K^+ \rightarrow \pi^+\nu\nu$  and  $K_L \rightarrow \pi^0\nu\nu$  bounds [5], iff  $m_{Z'} \sim m_\pi$ . We would therefore discuss in a little more detail in Sect. 8.2 in relation to KOTO experiment. This scenario illustrates that excess in  $B^+ \rightarrow K^+ + \textit{nothing}$  need not be related to DM, but only *effectively* “dark”. The lack of further signatures means the number of possibilities is large (for example, invisibly decaying axion-like particles [61]), enhancing the need to perform the search as best as one can at Belle II, including separating into  $q^2$  bins.

## References

1. Eilam, G., Soni, A., Kane, G.L., Deshpande, N.G.: Phys. Rev. Lett. **57**, 1106 (1986)
2. Hou, W.-S., Willey, R.S., Soni, A.: Phys. Rev. Lett. **58**, 1608 (1987)
3. Inami, T., Lim, C.S.: Prog. Theor. Phys. **65**, 297 (1981)
4. Abe, K., et al.: [Belle Collaboration]: Phys. Rev. Lett. **88**, 021801 (2002)
5. Tanabashi, M., et al.: [Particle Data Group]: Phys. Rev. D **98**, 030001 (2018). <http://pdg.lbl.gov/>
6. Kaneko, J., et al.: [Belle Collaboration]: Phys. Rev. Lett. **90**, 021801 (2003)
7. Ali, A., Lunghi, E., Greub, C., Hiller, G.: Phys. Rev. D **66**, 034002 (2002)
8. Albrecht, H., et al.: [ARGUS Collaboration]: Phys. Lett. B **192**, 245 (1987)
9. Wei, J.-T., Chen, K.-F., et al.: [Belle Collaboration]: Phys. Rev. D **78**, 011101 (2008)
10. Ali, A., Ball, P., Handoko, L.T., Hiller, G.: Phys. Rev. D **61**, 074024 (2000)
11. Aaij, R., et al.: [LHCb Collaboration]: JHEP **1212**, 125 (2012)
12. Ali, A., Mannel, T., Morozumi, T.: Phys. Lett. B **273**, 505 (1991)
13. Heavy Flavor Averaging Group (HFLAV; acronym changed from HFAG to HFLAV in March 2017). <http://www.slac.stanford.edu/xorg/hflav>
14. Ishikawa, A., et al.: [Belle Collaboration]: Phys. Rev. Lett. **96**, 251801 (2006)
15. Aubert, B., et al.: [BaBar Collaboration]: Phys. Rev. D **79**, 031102 (2009)
16. Hovhannisyan, A., Hou, W.-S., Mahajan, N.: Phys. Rev. D **77**, 014016 (2008)
17. D’Ambrosio, G., Giudice, G.F., Isidori, G., Strumia, A.: *ibid.* B **645**, 155 (2002)
18. Dickens, J., Gibson, V., Lazzeroni, C., Patel, M.: CERN-LHCB-2007-039
19. Gambino, P., Haisch, U., Misiak, M.: Phys. Rev. Lett. **94**, 061803 (2005)
20. Wei, J.T., Chang, P., et al.: [Belle Collaboration]: Phys. Rev. Lett. **103**, 171801 (2009)
21. Aaij, R., et al.: [LHCb Collaboration]: Phys. Rev. Lett. **108**, 181806 (2012)
22. Talk by Wei, J.T.: [for the Belle Collaboration]: At the 34th International Conference on High Energy Physics (ICHEP2008), Philadelphia, U.S.A., 29 July – 5 August
23. Aaltonen, T., et al.: [CDF Collaboration]: Phys. Rev. Lett. **108**, 081807 (2012)
24. Aaij, R., et al. [LHCb Collaboration]: JHEP **1308**, 131 (2013)
25. Beneke, M., Feldmann, T., Seidel, D.: Eur. Phys. J. C **41**, 173 (2005)

26. Altmannshofer, W., et al.: JHEP **0901**, 019 (2009)
27. Descotes-Genon, S., Matias, J., Ramon, M., Virto, J.: JHEP **1301**, 048 (2013)
28. Aaij, R., et al.: [LHCb Collaboration]: Phys. Rev. Lett. **111**, 191801 (2013)
29. Descotes-Genon, S., Matias, J., Virto, J.: Phys. Rev. D **88**, 074002 (2013)
30. Altmannshofer, W., Straub, D.M.: Eur. Phys. J. C **73**, 2646 (2013)
31. Aaij, R., et al.: [LHCb Collaboration]: JHEP **1602**, 104 (2016)
32. Lyon, J., Zwicky, R.: [arXiv:1406.0566](https://arxiv.org/abs/1406.0566) [hep-ph]
33. Ciuchini, M., et al.: JHEP **1606**, 116 (2016)
34. Wehle, S., Niebuhr, C., Yashchenko, S., et al.: [Belle Collaboration]: Phys. Rev. Lett. **118**, 111801 (2017)
35. Sirunyan, A.M., et al.: [CMS Collaboration]: Phys. Lett. B **781**, 517 (2018)
36. Hiller, G., Krüger, F.: Phys. Rev. D **69**, 074020 (2004)
37. Boucharad, C., et al.: [HPQCD Collaboration]: Phys. Rev. Lett. **111**, 162002 (2013)
38. Aaij, R., et al.: [LHCb Collaboration]: Phys. Rev. Lett. **113**, 151601 (2014)
39. Aaij, R., et al.: [LHCb Collaboration]: JHEP **1708**, 055 (2017)
40. Capdevila, B., Crivellin, A., Descotes-Genon, S., Matias, J., Virto, J.: JHEP **1801**, 093 (2018)
41. Altmannshofer, W., Stangl, P., Straub, D.M.: Phys. Rev. D **96**, 055008 (2017)
42. He, X.-G., Joshi, G.C., Lew, H., Volkas, R.R.: Phys. Rev. D **43**, 22 (1991)
43. Altmannshofer, W., Gori, S., Pospelov, M., Yavin, I.: Phys. Rev. D **89**, 095033 (2014)
44. Sirunyan, A.M., et al.: [CMS Collaboration]: [arXiv:1808.03684](https://arxiv.org/abs/1808.03684) [hep-ex]
45. Buchalla, G., Hiller, G., Isidori, G.: Phys. Rev. D **63**, 014015 (2000)
46. Aubert, B., et al.: [BaBar Collaboration]: Phys. Rev. Lett. **94**, 101801 (2005)
47. Chen, K.F., et al.: [Belle Collaboration]: Phys. Rev. Lett. **99**, 221802 (2007)
48. del Amo Sanchez, P., et al.: [BaBar Collaboration]: Phys. Rev. D **82**, 112002 (2010)
49. Lees, J.P., et al.: [BaBar Collaboration]: Phys. Rev. D **87**, 112005 (2013)
50. Lutz, O., Neubauer, S., Heck, M., Kuhr, T., et al.: [Belle Collaboration]: Phys. Rev. D **87**, 111103 (2013)
51. Grygier, J., Goldenzweig, P., Heck, M., et al.: [Belle Collaboration]: Phys. Rev. D **96**, 091101 (2017)
52. Bird, C., Jackson, P., Kowalewski, R.V., Pospelov, M.: Phys. Rev. Lett. **93**, 201803 (2004)
53. Accardo, L., et al.: [AMS Collaboration]: Phys. Rev. Lett. **113**, 121101 (2014)
54. Jean, P., et al.: Astron. Astrophys. **407**, L55 (2003)
55. Willey, R.S., Yu, H.-L.: Phys. Rev. D **26**, 3086 (1982)
56. Park, H., et al.: [HyperCP Collaboration]: Phys. Rev. Lett. **94**, 021801 (2005)
57. Aaij, R., et al.: [LHCb Collaboration]: Phys. Rev. Lett. **120**, 221803 (2018)
58. Sala, F., Straub, D.M.: Phys. Lett. B **774**, 205 (2017)
59. Bishara, F., Haisch, U., Monni, P.F.: Phys. Rev. D **96**, 055002 (2017)
60. Fuyuto, K., Hou, W.-S., Kohda, M.: Phys. Rev. Lett. **114**, 171802 (2015)
61. Izaguirre, E., Lin, T., Shuve, B.: Phys. Rev. Lett. **118**, 111802 (2017)

# Chapter 6

## Scalar Interactions and Right-Handed Currents



It should be clear from the previous chapters that loop-induced  $b \rightarrow s$  transitions offer many good probes of New Physics at the TeV scale, and remains the current frontier of flavor physics. As last examples of their usefulness, we discuss the search for enhanced  $B_s \rightarrow \mu^+ \mu^-$  decay as probe of BSM Higgs boson effects, and probing for right-handed (RH) interactions via time-dependent CPV in  $B^0 \rightarrow K_S^0 \pi^0 \gamma$  decay. The observation of the former is a triumphant highlight of flavor physics at LHC Run 1, although the consistency with SM reflects the dashed hopes at the Tevatron that the process might get greatly enhanced. The analogous  $B^0 \rightarrow \mu^+ \mu^-$  decay, not yet firmly observed, is the next pursuit. Combining signature versus the raw cross sections, the TCPV study of  $B^0 \rightarrow K_S^0 \pi^0 \gamma$  is best done at the Super B factory, where Belle II data would soon arrive.

The question of right-handed interactions has been with us since the establishment of left-handedness of the weak interactions. The TCPV probe of  $B^0 \rightarrow K_S^0 \pi^0 \gamma$  decay, or more generally  $B^0 \rightarrow X^0 \gamma$ , utilizes a beautiful refinement of the TCPV discussed in Chap. 2, that allow us to probe RH interactions involving  $b$  to  $s$  flavor conversion. It also utilizes a special experimental environment that is rather unique to the asymmetric energy B factories. For  $B_s \rightarrow \mu^+ \mu^-$ , though the signature is straightforward, the actual effect that occurs at large  $\tan \beta$  (the ratio of vacuum expectation values of multi-Higgs models) is rather subtle, compared with the straightforward charged Higgs effect in  $B^+ \rightarrow \tau^+ \nu$ .

### 6.1 $B_s \rightarrow \mu^+ \mu^-$ (and $B^0 \rightarrow \mu^+ \mu^-$ )

Because of the possibility of rather large  $\tan \beta$  enhancement, and because of its straightforward signature, the  $B_s \rightarrow \mu^+ \mu^-$  decay mode has been a favorite mode for probing exotic Higgs sector effects in MSSM at hadron colliders.

The process proceeds in SM just like  $b \rightarrow s \ell^+ \ell^-$ , except  $s$  is now in the initial state as the  $\bar{s}$  spectator quark that annihilates with the  $b$  quark. Since  $B_s$  is a pseudoscalar, the photonic penguin (as well as the vector part of  $b \rightarrow s$  current) does

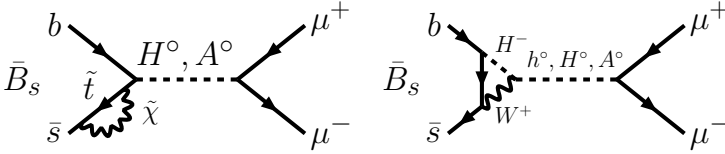


**Fig. 6.1** Diagrams illustrating neutral Higgs mediated FCNC for  $B_s \rightarrow \mu^+ \mu^-$  in supersymmetry

not contribute. With loop,  $f_{B_s}$  and helicity suppression, the SM expectation is only  $\sim 3.4 \times 10^{-9}$  [1], with  $B^0 \rightarrow \mu^+ \mu^-$  further CKM-suppressed by roughly a factor of 1/20. Much like  $B^+ \rightarrow \tau^+ \nu$ , the process is basically sensitive to (pseudo)scalar operators. In MSSM, one has both neutral scalar and pseudoscalar bosons arising from a 2HDM-II framework. But these bosons are flavor-conserving at tree level, and naively they cannot mediate  $\bar{s}b \rightarrow \mu^+ \mu^-$ . However, at the loop level, and for large  $\tan \beta$ , one can “no longer diagonalize the masses of the quarks in the same basis as their Yukawa couplings” [2–5], and enhancement effect could be dramatic.

We illustrate this in Fig. 6.1 with a diagram involving the  $sb$  self-energy. A second diagram is shown where a  $t$ - $W$ - $H^+$  loop emits exotic neutral Higgs bosons that turn into muon pairs. It is argued that [2–5] both type of diagrams lead to amplitudes  $\propto \tan^3 \beta$  for large  $\tan \beta$ , hence a possible enhancement by  $\tan^6 \beta$  in rate! Showing two diagrams also serves the purpose to illustrate that the effective  $bs\mu\mu$  coupling depends on how SUSY is broken, and can differ substantially between different scenarios. This is in contrast with the simple clarity of the  $\tan \beta$  dependence of the charged  $H^+$  boson effect in  $B^+ \rightarrow \tau^+ \nu_\tau$ , (4.13) and (4.14), which arises at the tree level. Of course, there could be more drastic theories for  $B_s \rightarrow \mu^+ \mu^-$ , such as  $R$ -parity violating SUSY, which we do not go into. Experimental measurement of  $B_q \rightarrow \mu^+ \mu^-$  seem straightforward enough, and one need not be concerned with model details here.

### Early Experimental Measurement

The first search for  $B^0 \rightarrow \mu^+ \mu^-$  was by [6] CLEO in the early days of  $B$  physics, setting the 90% C.L. upper limit of 0.02%, which is derived from the two track search bound of 0.05% for  $B^0 \rightarrow \pi^+ \pi^-$ . The early CLEO detector did not have PID ability that is sensitive to charged particle mass, but the limit is improved by the rudimentary lepton ID capabilities, in the dimuon case by requiring both muons penetrate the iron yoke. After some improvement by ARGUS,<sup>1</sup> it was UA1 at  $Spp\bar{p}S$  that broke [8] the  $10^{-5}$  barrier, although the admixture of  $B_d$  and  $B_s$  was not separated. The next milestone of  $10^{-6}$  was broken [9] by CDF at the Tevatron, after an initial study with a smaller dataset in 1996. Thanks to improved tracking with Si vertex detectors hence better dimuon mass resolution, though they still cannot be fully separated, CDF could provide the separate bounds of  $8.6 \times 10^{-7}$  and  $2.6 \times 10^{-6}$  for  $B^0 \rightarrow \mu^+ \mu^-$  and  $B_s \rightarrow \mu^+ \mu^-$ , respectively, at 95% C.L.

<sup>1</sup>We refer to older versions of [7] here, and similarly below. More recent PDG issues only give listing since the start of LHC era.

By now it should be clear that  $B_q \rightarrow \mu^+ \mu^-$  search belongs to the domain of hadronic machines, because of sheer cross section for  $b$ -hadron production, which simultaneously includes  $B_s$  and  $\Lambda_b$ , etc. Development of detector capabilities added to the momentum, and the LHCb experiment that specialize on  $B$  physics went on track at the LHC, while the BTeV project, formed slightly later, also went along at the lower energy Tevatron.<sup>2</sup> CDF and DØ also went through upgrades with  $B$  physics in mind for Tevatron Run II. In contrast,  $e^+e^-$  colliders are limited by production cross section in pursuing ultra-rare decays. Furthermore, the aim was to run on  $\Upsilon(4S)$ , while for  $B_s$  production, one needs to run at  $\Upsilon(5S)$  (or higher).

The CLEO II experiment did manage to reach below  $10^{-6}$  for  $B^0 \rightarrow \mu^+ \mu^-$ , before becoming CLEO-c to pursue charm physics (due to competition from the B factories). Early on with the B factories, Belle searched for  $B^0 \rightarrow \mu^+ \mu^-$  with 85M  $B\bar{B}$  pairs, setting a limit [10] that approached  $10^{-7}$ , but Belle never returned to the subject again. Slightly later, BaBar made the search with a slightly larger data set and improved on the Belle limit, but a result from CDF in the same time frame was comparable. By 2008 and with 384M  $B\bar{B}$  pairs, BaBar did reach [11] the 90% C.L. bound of  $5.2 \times 10^{-8}$  for  $B^0 \rightarrow \mu^+ \mu^-$ . However, a few years prior, CDF had already reached [12] a better limit, and even the bound for  $B_s \rightarrow \mu^+ \mu^-$  was approaching  $10^{-7}$ . The game was in the court of hadronic machines, while Belle and BaBar dropped the pursuit.

### 6.1.1 Tevatron Versus LHC

It was during the period of Tevatron upgrade, and before turn on of B factories, that the suggestion [2–5] of possible  $\tan^6 \beta$  enhancement arose, which certainly upped the ante. The limit on  $B_s \rightarrow \mu^+ \mu^-$  at the turn of the millennium was still three orders of magnitude above SM expectation. Could it be enhanced by orders of magnitude? In any case one had 3 orders of magnitude for a “discovery zone”, and this is probing SUSY and associated scalar bosons from flavor sector, and gave Tevatron people a great impetus. Attention now turned to  $B_s \rightarrow \mu^+ \mu^-$ , as most likely  $B^0 \rightarrow \mu^+ \mu^-$  is at least an order of magnitude smaller. With the ease of trigger and the large number of  $B$  mesons produced,  $B_q \rightarrow \mu^+ \mu^-$  thus became a subject vigorously pursued at hadron facilities, with enormous range for search. There is much at stake, since prior to observing the Higgs, the bound on  $B_s \rightarrow \mu^+ \mu^-$  put stringent constraints on SUSY models. If exotic Higgs are observed in the future,  $B_s \rightarrow \mu^+ \mu^-$  measurement would still be rather invaluable.

The two-track nature makes the search relatively straightforward, although the issue is background control. One has to be careful with muon identification, checking for fakes, e.g. from  $K^\pm$  penetrating to the muon system. DØ employed a likelihood ratio cut, while CDF used a neural network for separation of signal versus background. To avoid bias, a blind analysis is done by both experiments, i.e.

---

<sup>2</sup>Unfortunately, BTeV was terminated in early 2005 for budgetary reasons.

event selection is optimized prior to unveiling the signal region. For the estimate of branching fraction, a well known mode such as  $B^+ \rightarrow J/\psi K^+$  (where  $J/\psi \rightarrow \mu^+ \mu^-$ ) is used for normalization.

With Run II data taking good shape, the Tevatron experiments improved the limits considerably. The  $2 \text{ fb}^{-1}$  limits from CDF and  $D\bar{0}$  are  $4.7 \times 10^{-8}$  [13] and  $7.5 \times 10^{-8}$  [14] respectively at 90% C.L., combining to give<sup>3</sup>

$$\mathcal{B}(B_s \rightarrow \mu^+ \mu^-) < 4.7 \times 10^{-8} \quad (\text{HFAG Winter 2008}), \quad (6.1)$$

at 90% C.L. While still an order of magnitude away from SM, the CDF limit is an improvement by about factor of 2 over the previous one.

The expected reach for the Tevatron is about  $2 \times 10^{-8}$  at  $\sim 7 \text{ pb}^{-1}$  per experiment, assuming improvements in the 2010 run, which is still more than a factor of 6 above SM. Further improvement would have to come from LHCb, which claimed [15] it would overtake the Tevatron in this mode with just  $0.05 \text{ fb}^{-1}$  data. With  $2 \text{ fb}^{-1}$ ,  $3\sigma$  evidence could be attained for SM signal strength, and  $5\sigma$  observation with  $10 \text{ fb}^{-1}$ . Thus, the expectation was that LHCb could probe down to SM expectation by 2010 or so. But before that, the race between Tevatron and LHC was still to unfold. On top of that, there is the expected progress to come with the turning on of LHC, where direct search for Higgs particles and charginos would also be vigorously pursued.

Thus, expectation was in the air in 2008, that some excitement

could arrive soon. But history went through a twist [16]: the LHC magnet accident occurred during September 2008, not long after first beam, which delayed the actual start of LHC data taking by more than a year. In turn, Tevatron extended its Run II, shutting down only in 2011 when LHC performance appeared promising by late 2010.

The showdown came at the EPSHEP conference held at Grenoble in summer 2011, where CDF gave the exciting hint [17] beforehand that  $\mathcal{B}(B_s \rightarrow \mu^+ \mu^-) = (1.8_{-0.9}^{+1.1}) \times 10^{-8}$ . The central value was more than 5 times larger than SM expectation! This measurement was based on the aforementioned  $7 \text{ fb}^{-1}$  data collected by CDF for Run II, giving a two-sided bound of  $0.46 \times 10^{-8} < \mathcal{B}(B_s \rightarrow \mu^+ \mu^-) < 3.9 \times 10^{-8}$  at 90% C.L. But the results of CMS and LHCb reported at the meeting refuted the CDF result, where the ‘‘LHC combination’’ is [18]

$$\mathcal{B}(B_s \rightarrow \mu^+ \mu^-) < 1.1 \times 10^{-8} \quad (\text{LHC Combo, EPSHEP 2011}), \quad (6.2)$$

at 95% C.L. (note the change in convention from 90%). The published 95% limits are  $1.9 \times 10^{-8}$  [19] for CMS with  $1.14 \text{ fb}^{-1}$ , and  $1.6 \times 10^{-8}$  [20] for LHCb<sup>4</sup> with  $0.37 \text{ fb}^{-1}$ , both taken in 2011 at 7 TeV. Such is the prowess of a new  $pp$  collider at higher energy. CDF did add  $3 \text{ fb}^{-1}$  data from the Run II extension, bringing the num-

<sup>3</sup>The 90% C.L. limit on  $B^0 \rightarrow \mu^+ \mu^-$  by CDF was  $1.5 \times 10^{-8}$ . Also, the 95% C.L. limit on  $B_s \rightarrow \mu^+ \mu^-$  was  $5.8 \times 10^{-8}$ .

<sup>4</sup>LHCb had published [7] an earlier result based on  $0.037 \text{ fb}^{-1}$  collected in 2010, indeed already reaching comparable sensitivity with Tevatron.

ber [7] down to  $(1.3_{-0.7}^{+0.9}) \times 10^{-8}$ , suggesting the  $7 \text{ fb}^{-1}$  result might be a fluctuation. The ball is now in the LHC court.

With its large solenoid and strong magnetic field, and excellent muon detection, CMS emerged as a welcome dark horse in the  $B_s \rightarrow \mu^+\mu^-$  game. We have skipped the discussion of  $B^0 \rightarrow \mu^+\mu^-$  here, as the limits continued to improve and there were no surprises. We have also not mentioned  $D\theta$ , nor ATLAS at the LHC, as their measurements were not the drivers.

### 6.1.2 Observation of $B_s \rightarrow \mu^+\mu^-$ at LHC

The next episode is the measurement with full 2011 data. Presented at the Winter 2012 conferences and based on  $5 \text{ fb}^{-1}$  at 7 TeV collision energy, CMS published [21] the 95% C.L. bound of  $7.7 \times 10^{-9}$  for  $B_s \rightarrow \mu^+\mu^-$ , where the median expected limit was at  $8.4 \times 10^{-9}$ , suggesting a mild deficit of observed events. Furthermore, this “deficit” was more indicative in the barrel detector alone. More enticing is the LHCb measurement [22] of  $\mathcal{B}(B_s \rightarrow \mu^+\mu^-) = (0.8_{-1.3}^{+1.8}) \times 10^{-9}$ , which is based on  $1.0 \text{ fb}^{-1}$  at 7 TeV. There appears to be *some deficit* from SM expectation [23] of  $\mathcal{B}(B_s \rightarrow \mu^+\mu^-)|^{\text{SM}} = (3.2 \pm 0.2) \times 10^{-9}$ , which had become more precise. Though a downward fluctuation is possible, the fact that CMS mildly supports it carries some weight. We have moved from possible enhancements by orders of magnitude, and entered the era of SM sensitivity. We defer physics discussion until a little later.

As the LHC was performing rather well, observation of  $B_s \rightarrow \mu^+\mu^-$  (if at SM strength) was clearly in sight! Because of proximity to announcement of the Winter result, ICHEP2012 (where Higgs boson discovery was announced!) had to be missed. LHCb managed to analyze half the data from 2012, and presented first evidence (see Fig. 6.2 [left]) for  $B_s \rightarrow \mu^+\mu^-$  at the HCP symposium held November 2012 in Kyoto.<sup>5</sup> With  $1.0 \text{ fb}^{-1}$  at 7 TeV and  $1.1 \text{ fb}^{-1}$  at 8 TeV, LHCb measured [24]

$$\mathcal{B}(B_s \rightarrow \mu^+\mu^-) = \left(3.2_{-1.2}^{+1.5}\right) \times 10^{-9} \quad (\text{LHCb@HCP2012}), \quad (6.3)$$

with  $3.4\sigma$  statistical significance, while the 95% C.L. bound for  $B^0 \rightarrow \mu^+\mu^-$  was pushed down to  $9.4 \times 10^{-10}$  at 95% C.L. CMS was held back by issues of peaking background and  $K^+$  penetration to muon system etc., which of course need to be dealt with.

The results of CMS and LHCb analyzing the full 2011–2012 dataset were presented at the EPSHEP conference held in Stockholm in July 2013, which were submitted to Physical Review Letters on the same day, and published back to back [26, 27]. The results are,

---

<sup>5</sup>At the Kyoto meeting, HCP merged with another conference to become the LHCP (LHC Physics) conference.



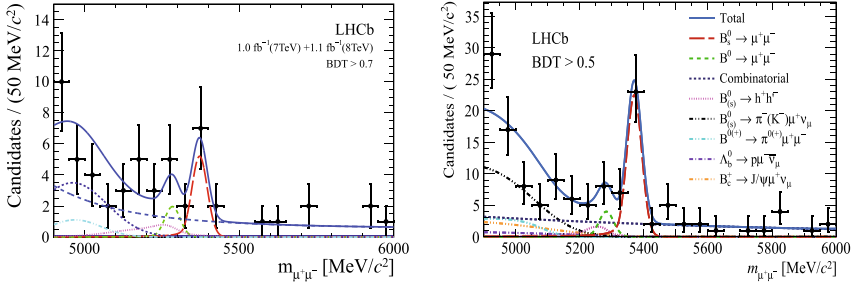


**Fig. 6.2** [left] Dimuon  $m_{\mu\mu}$  distribution [24] showing first evidence for  $B_s \rightarrow \mu^+\mu^-$  (long dashed) and hint for  $B^0 \rightarrow \mu^+\mu^-$  (adjacent shorter dashed); [right] first single experiment observation [25] of  $B_s \rightarrow \mu^+\mu^-$ . Both are by LHCb

$$\begin{aligned} \mathcal{B}(B_s \rightarrow \mu^+\mu^-) &= \left(3.0_{-0.9}^{+1.0}\right) \times 10^{-9} && \text{(CMS Summer 2013),} \\ \mathcal{B}(B_s \rightarrow \mu^+\mu^-) &= \left(2.9_{-1.0}^{+1.1}\right) \times 10^{-9} && \text{(LHCb Summer 2013),} \end{aligned} \quad (6.4)$$

with 4.3 and 4.0 $\sigma$ , respectively. The CMS (LHCb) result is based on 5 (1) fb $^{-1}$  at 7 TeV and 20 (2) fb $^{-1}$  at 8 TeV. Both experiments have found strong evidence for  $B_s \rightarrow \mu^+\mu^-$ , and it was clear that a combination would yield a discovery above 5 $\sigma$ . Note that there seems some deficit with respect to SM, which echoes the 2012 Winter result, [21, 22], although it was less evident in the LHCb “evidence” paper [24]. Another interesting point is that both experiments find some events in  $B^0 \rightarrow \mu^+\mu^-$  that imply somewhat larger rate than SM expectation. We do not quote the numbers here, because they are not significant enough individually, while the experiments are a little ambivalent since it has not been the target of measurement.

As (6.4) was unveiled during LS1 (Long Shutdown 1 of LHC running), data was not forthcoming until 2015, so CMS and LHCb went ahead to combine their datasets, an effort that took more than a year. This was quite an undertaking, to synchronize between two rather large but different experiments, from apparatus and methodological detail, to organizational structure and sociology. The combination was announced at end of 2014, and finally published [28] in June 2015 in Nature with some fanfare:

$$\begin{aligned} \mathcal{B}(B_s \rightarrow \mu^+\mu^-) &= \left(2.8_{-0.6}^{+0.7}\right) \times 10^{-9}, \\ \mathcal{B}(B^0 \rightarrow \mu^+\mu^-) &= \left(3.9_{-1.4}^{+1.6}\right) \times 10^{-10} \quad \text{(CMS&LHCb Run 1 Combo),} \end{aligned} \quad (6.5)$$

with significance of 6.2 and 3.2 $\sigma$ , respectively. These numbers should be compared with the new reference standard for SM expectation [29],

$$\begin{aligned}\mathcal{B}(B_s \rightarrow \mu^+\mu^-)|^{\text{SM}} &= \left(3.65 \pm 0.23\right) \times 10^{-9}, \\ \mathcal{B}(B^0 \rightarrow \mu^+\mu^-)|^{\text{SM}} &= \left(1.06 \pm 0.09\right) \times 10^{-10} \quad (\text{SM 2014}),\end{aligned}\quad (6.6)$$

which collects significant improvements in  $\mathcal{O}(\alpha)$ ,  $\mathcal{O}(\alpha_s^2)$  corrections and lattice form factors. The experimental value for  $B_s \rightarrow \mu^+\mu^-$  seems on the low side, while for  $B^0 \rightarrow \mu^+\mu^-$  the central value appears 3 times higher. Put differently, assuming SM values, the expected significance [28] were  $7.8$  and  $0.8\sigma$ , respectively. Thus, the  $B_s \rightarrow \mu^+\mu^-$  “deficit” is more than  $1\sigma$ , while the excess in  $B^0 \rightarrow \mu^+\mu^-$  is less than  $3\sigma$ , hence the deviations are not yet established.

More data is needed. Indeed, by Moriond 2017, LHCb could add  $1.4 \text{ fb}^{-1}$  data at 13 TeV (higher  $B$  production cross section), i.e. from Run 2, to the previous Run 1 data ( $1 \text{ fb}^{-1}$  at 7 TeV and  $2 \text{ fb}^{-1}$  at 8 TeV), and reported [25] the first observation of  $B_s \rightarrow \mu^+\mu^-$  by a single experiment (see Fig. 6.2 [right]),

$$\begin{aligned}\mathcal{B}(B_s \rightarrow \mu^+\mu^-) &= \left(3.0 \pm 0.6_{-0.2}^{+0.3}\right) \times 10^{-9}, \\ \mathcal{B}(B^0 \rightarrow \mu^+\mu^-) &= \left(1.5_{-1.0-0.1}^{+1.2+0.2}\right) \times 10^{-10} \quad (\text{LHCb 2017}),\end{aligned}\quad (6.7)$$

with significance of  $7.8$  and  $1.6\sigma$ , respectively, where the “excess” in  $B^0 \rightarrow \mu^+\mu^-$  seems to have receded. It would be interesting to see what CMS has to say, but unfortunately, CMS has not updated so far. Although data has increased significantly, the high pile-up environment at Run 2 poses challenges to the central collider detector environment. In contrast, LHCb uses luminosity leveling as currently dictated by the trigger (which is a focus for upgrade improvement), and benefits from it for now.

LHCb made also a first attempt at measuring the  $B_s \rightarrow \mu^+\mu^-$  effective lifetime [25], finding no significance of deviation from expectation. In SM, only the heavier  $B_s$  state can decay to  $\mu^+\mu^-$ , and the effective lifetime measurement has been suggested [30] as a new probe for physics beyond SM, by disentangling the presence of the lower  $B_s$  state (through mass eigenstate rate asymmetry  $A_{\Delta\Gamma}$ ).

## Interpretation and Prognosis

Where do we stand on  $B_q \rightarrow \mu^+\mu^-$  pursuit?

We have given a brief, but relatively exhaustive recount of experimental measurements, because the saga is a triumph of experimentation, culminating in the observation [28] of  $B_s \rightarrow \mu^+\mu^-$  mode. Looking back, the first search by CLEO [6] was more or less a byproduct of two-track search, and likewise for some time onwards for the various players in the field. There was practically no expectation from the theory perspective, as the  $B_q \rightarrow \mu^+\mu^-$  is much more suppressed even than  $B^+ \rightarrow \tau^+\nu$ ,  $\mu^+\nu$ , which is exactly how GIM was conceived. In the earlier days, so rare a decay rate seemed so far out of reach.

Even for specialized facilities such as (super) B factories, one is limited by the number of  $B$  or  $B_s$  mesons available, from running at  $\Upsilon(4S)$  or  $\Upsilon(5S)$ , while early efforts for fixed target hadronic production facilities for  $B$  physics were not successful. The idea was of course there to cash in on the much larger hadronic production cross section for  $b$  hadrons. It was the successful implementation of Si detectors at hadron colliders, as well as the innovation of a *forward* collider detector that moved the field ahead, not just for  $B_q \rightarrow \mu^+ \mu^-$  pursuit, but for a good fraction of  $B$  physics studies. Thus, Tevatron went for its Run II upgrades, while LHCb (and BTeV for a time) pushed ahead. It was in this time frame that  $B_q \rightarrow \mu^+ \mu^-$ , though still very challenging, no longer seemed totally remote, which in turn provided stimulus for theory, and the insight [2–5] of large  $\tan \beta$  enhancement via loop effects emerged. This further galvanized the experimental effort. It captures the mind that  $B_q \rightarrow \mu^+ \mu^-$  rate could be enhanced by several orders of magnitude, and basically within the popular and leading theory framework of SUSY. It gave flavor experimentalists great hope that they might get the first glimpse of SUSY before the LHC even started!

If Nature was willing, CDF could have captured the prize up until 2011. Indeed, CDF thought for a while that it was seeing something [17]: the experimental central value was sizable compared with SM expectation. Because of tight  $b \rightarrow s \ell^+ \ell^-$  constraints (as effective operators are the same as SM), hence order of magnitude enhancement was outside the realm for the 4th generation, it was noticed that  $B_q \rightarrow \mu^+ \mu^-$  measurements were now within target range. Indeed, when the indications for  $B_s \rightarrow \mu^+ \mu^-$  from CMS and LHCb hinted at sub-SM rate values, it was pointed out [31] that a 4th generation could readily account for it. This was, unfortunately soon drowned out by the Higgs boson discovery, which resulted in the 4th generation falling out of favor.

Alas, once again Nature was stingy with giving out New Physics. The triumphant LHCb and CMS (i.e. (6.5), from [28]) carry with them the sorrow of no real discovery.

But it was interesting to note that, from 2014 to 2015, the two experiments were relatively quiet on the apparent large central value of  $B^0 \rightarrow \mu^+ \mu^-$ , as if they did not “believe” in their own finding, and theorists seem to concur with them. Although the 2017 LHCb result [25] may have vindicated this stance, it does seem a little odd. Basically, this may be because a factor of two or three enhancement would run against MFV (Minimal Flavor Violation), which had become entrenched. It was dutifully pointed out [32] that a 4th generation could account for a factor of three enhancement of  $B^0 \rightarrow \mu^+ \mu^-$  relatively easily, and could be its “revenge” for the Higgs interpretation of the 125 GeV boson, but little attention was given to it. The only accompanying theory work [33] for enhancing  $\mathcal{B}(B^0 \rightarrow \mu^+ \mu^-)/\mathcal{B}(B_s \rightarrow \mu^+ \mu^-)$  was SUSY GUTS with nonstandard (Georgi-Jarlskog) Higgs representations, which also received scant attention.

Instead, theoretical focus is still on  $B_s \rightarrow \mu^+ \mu^-$ , which has really turned into precision measurement. There has been emphasis on the efficacy of  $B_s \rightarrow \mu^+ \mu^-$  as a future probe [34] of New Physics, or utilizing it as a constraint [35] on  $B_{s,d} \rightarrow \tau^+ \tau^-$ ,  $e^+ e^-$ . To be true, it should be noted that only BaBar (but not Belle) has so far pursued  $B^0 \rightarrow \tau^+ \tau^-$  [36], which has been followed up by LHCb [37] for both  $B_s$

and  $B^0 \rightarrow \tau^+ \tau^-$ , hence there is still much to explore, while  $B_{s,d} \rightarrow e^+ e^-$  should also be taken up seriously as a pursuit of its own. But we would still like to emphasize that  $B_d \rightarrow \mu^+ \mu^-$  ought not be taken lightly by LHCb and CMS. Although one would eventually measure it at the High-Luminosity LHC, there has been insufficient interest from theory community, which has affected the appetite of the experimental community. It would be interesting to see the full Run 2 results from both LHCb and CMS, which may take a couple of years.

## 6.2 TCPV in $B \rightarrow K_S^0 \pi^0 \gamma, X^0 \gamma$

Let us turn to a very different kind of physics, with ball in court for Belle II.

With large QCD enhancement [38, 39], the  $b \rightarrow s \gamma$  rate is dominated by the SM. The left-handedness of the weak interaction dictates that the  $\gamma$  emitted in  $\bar{B}^0 \rightarrow \bar{K}^{*0} \gamma$  decay has left-handed helicity (defined somewhat loosely), where the emission of right-handed (RH) photons is suppressed by  $\sim m_s/m_b$ , as can be read off from (5.2). This reflects the need for a mass insertion for helicity flip, and the fact that a power of  $m_b$  or  $m_s$  is required for the  $b \rightarrow s \gamma$  vertex by gauge invariance (or current conservation). For  $B^0 \rightarrow K^{*0} \gamma$  decay that involves  $\bar{b} \rightarrow \bar{s} \gamma$ , the opposite is true, and the emitted photon is dominantly of RH kind.

The fact that photon helicities do not match for  $\bar{B}^0 \rightarrow \bar{K}^{*0} \gamma$  versus  $B^0 \rightarrow K^{*0} \gamma$  in SM has implications for a conceptually very interesting probe [40]. Mixing-dependent CPV, i.e. TCPV, involves the interference of  $\bar{B}^0$  and  $\bar{B}^0 \xrightarrow{\text{mix}} B^0$  decays to a common final state that is not flavor-specific (i.e. no definite flavor). For radiative  $\bar{B}^0 \rightarrow \bar{K}^{*0} \gamma$  decay versus  $\bar{B}^0 \xrightarrow{\text{mix}} B^0 \rightarrow K^{*0} \gamma$  decay, the common final state is  $K_S^0 \pi^0$ . As illustrated in Fig. 6.3, since within the SM the  $\bar{B}^0 \rightarrow \bar{K}^{*0} \gamma$  process leads to  $\gamma_L$ , while the  $B^0 \rightarrow K^{*0} \gamma$  process gives rise to  $\gamma_R$ , these two processes cannot interfere as the final states are orthogonal to each other! This is in contrast to, say TCPV in the common  $CP$  eigenstate of  $\phi K_S$  from  $\bar{B}^0$  decay and  $\bar{B}^0 \xrightarrow{\text{mix}} B^0$  decays. The interference requires RH photons from  $\bar{B}^0 \rightarrow \bar{K}^{*0} \gamma$  decay, which is suppressed by the helicity flip factor of  $m_s/m_b \sim \text{few } \%$  [40] within SM, although (the curse of) hadronic corrections might [41] enhance this.

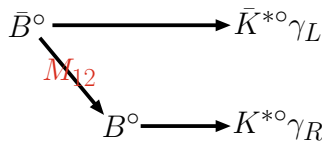


**Fig. 6.3** Mismatch in photon helicity for  $\bar{B}^0 \rightarrow \bar{K}^{*0} \gamma$  decay versus  $\bar{B}^0 \xrightarrow{\text{mix}} B^0 \rightarrow K^{*0} \gamma$  decay in the SM. To have TCPV in the  $K^{*0} \gamma$  final state ( $K^{*0} \rightarrow K_S^0 \pi^0$ ), Nature needs to provide a sizable right-handed photon component for  $\bar{B}^0 \rightarrow \bar{K}^{*0} \gamma$  decay

However, if there are RH interactions that also induce  $b \rightarrow s\gamma$  transition, then  $\bar{B}^0 \rightarrow \bar{K}^{*0}\gamma$  would acquire a  $\gamma_R$  component to interfere with the  $\bar{B}^0 \implies B^0 \rightarrow K^{*0}\gamma$  amplitude [40, 42]. Thus, *TCPV in  $B^0 \rightarrow K^{*0}\gamma$  decay mode probes RH interactions!* This does not require the RH interaction, which is necessarily New Physics, to carry extra CPV phase, since there is already the measured SM phase  $\Phi_{B_d} = \phi_1/\beta$  in  $B_d^0\text{-}\bar{B}_d^0$  mixing, although extra CPV phase can also be probed.

A formula at this point may help us grasp the physics. Analogous to the TCPV  $S$  parameter discussed in Chap. 2, we have [40, 43]

$$\mathcal{S}_{X^0\gamma} = \xi_{X^0} \frac{2|C_{11}C'_{11}|}{|C_{11}|^2 + |C'_{11}|^2} \sin(2\Phi_{B_d} - \phi_{11} - \phi'_{11}), \quad (6.8)$$

where  $\xi_{X^0}$  is the  $CP$  eigenvalue of the state  $X^0$ , and  $|C_{11}|$  and  $\phi_{11}$  are the strength and CPV phase of the left-handed  $b \rightarrow s\gamma$  Wilson coefficient,<sup>6</sup> with a prime indicating the right-handed counterpart. As (6.8) makes clear, TCPV would vanish with  $|C'_{11}|$  (up to  $m_s/m_b$ -suppressed SM effect), and that the CPV phase of the decay amplitudes can affect the measured value. It should be noted that a RH component in  $\bar{B}^0 \rightarrow \bar{K}^{*0}\gamma$  decay is rather easy to hide in  $b \rightarrow s\gamma$  inclusive rate, since the LH and RH components add in quadrature. We have commented that the 2015 result of (4.7) for theory and 2014 HFAG result of (4.6) seem to have moved closer to each other from the previous episode, (4.5) versus (4.3). If one takes the deficit of the NNLO prediction of (4.5) in 2007 versus the experimental measurement of (4.3) seriously, however, one could actually say that data calls for some extra contribution to the inclusive  $b \rightarrow s\gamma$  rate. For the more recent (4.7) versus (4.6), some extra contribution is still allowed. In any case, these measurements would be revisited by Belle II.

Alas, Nature plays a trick on us for the search of TCPV in  $B^0 \rightarrow K^{*0}\gamma$  decay. As mentioned,  $K^{*0}\gamma$  has to be in a  $CP$  eigenstate, such as  $K^{*0} \rightarrow K_S^0\pi^0$ , so the final state is  $K_S^0\pi^0\gamma$ . The  $\pi^0$  and  $\gamma$  certainly do not give vertices. For the  $K_S^0$ , though “short-lived”, it is produced with high momentum hence typically decays at the outer layers of the silicon detector, and vertex information is poor. Since one needs  $\Delta z$  to convert to  $\Delta t$  for a TCPV measurement, it seems impossible to study TCPV in the  $K_S^0\pi^0\gamma$  final state. The intriguing suggestion of [40], beautiful as it is, appeared to be just an impossible dream. Such was the impression from (at least some of us on) the Belle side.

Fortunately, with a larger silicon vertex detector and with an extra silicon layer compared to Belle, BaBar was not deterred, and pushed forward a technique called “ $K_S$  vertexing”. It was demonstrated [44] that, though degraded, the  $K_S \rightarrow \pi^+\pi^-$  decay does give some vertex information. The key point is the availability of the beam direction information because of the boost (thanks to the asymmetric beam energies of the B factories), providing a “beam profile” for the somewhat rudimentary  $K_S$  momentum vector to point back to. The closeness of  $m_B$  to half the  $\Upsilon(4S)$  mass

---

<sup>6</sup>Because one has counted 7–10 for the electroweak penguin four-quark operators, the label is 11 rather than 7, where it refers to the term that can radiate an on-shell photon.

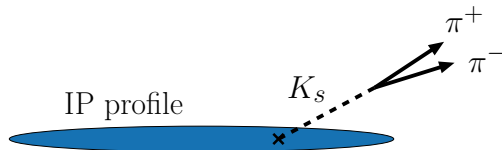


**Fig. 6.4** Figure illustrating  $K_S$  vertexing. The  $B^0\text{-}\bar{B}^0$  system is boosted in the  $z$  direction, leading to an elongated “IP profile”, where IP stands for Interaction Point. Although the decay lifetime of  $K_S$  from  $B$  decay is not optimal for the silicon vertex detector, intersecting the  $K_S$  momentum with the IP profile gives some information of the  $B$  meson decay vertex

implies that the transverse motion is small. The method, illustrated in Fig. 6.4, was validated with gold plated modes like  $B^0 \rightarrow J/\psi K_S$ , by removing the  $J/\psi \rightarrow \ell^+ \ell^-$  tracks. Using 124M  $B\bar{B}$  events, the first measurement [44] gave  $\mathcal{S}_{K_S^0 \pi^0} = 0.48^{+0.38}_{-0.47} \pm 0.06$ . Though errors are large, this was the proof of principle for  $K_S$  vertexing. BaBar then demonstrated [45] that the technique could be applied to  $B^0 \rightarrow K^{*0} \gamma$  decay, finding  $\mathcal{S}_{K^{*0}[K_S^0 \pi^0] \gamma} = 0.25 \pm 0.63 \pm 0.14$ . The method has been extended to other TCPV studies such as in  $B^0 \rightarrow K_S K_S K_S$ .

Subsequent to the pioneering TCPV study in  $B^0 \rightarrow K^{*0} \gamma$  decay by BaBar, Belle [46] followed (after a pilot study with smaller data [7]) with 535M  $B\bar{B}$  pairs, finding  $\mathcal{S}_{K^{*0}[K_S^0 \pi^0] \gamma} = -0.32^{+0.36}_{-0.33} \pm 0.05$ . The final BaBar update with 467M (full data) gave [47]  $\mathcal{S}_{K_S \pi^0 \gamma} = -0.03 \pm 0.29 \pm 0.03$ . All results are consistent with zero, hence with SM as well. The BaBar measurement was also done in  $B^0 \rightarrow K_S \pi^0 \gamma$  mode without requiring the  $K_S \pi^0$  to reconstruct to a  $K^{*0}$ . Other decay modes have also been explored by both experiments, especially to overcome the shortcoming of vertex finding. For example, both the  $B^0 \rightarrow \phi K_S \gamma$  [48] and  $\eta K_S \gamma$  [49] modes have been studied with the full 772M  $B\bar{B}$  pairs of Belle data. Though measurements are consistent with SM, errors are statistics-dominated, thus establishing these for further exploration at Belle II.<sup>7</sup> The additional tracks allow for probing the photon polarization by angular distributions of final state hadrons.

This is a very interesting direction to explore, again highlighting the need for a Super B factory, to seriously probe for RH interactions. At the LHCb, one lacks the “beam profile” technique for  $K_S$  vertexing, since one does not know the original  $B$  direction. The  $B_s \rightarrow \phi \gamma$  mode may be used, although the  $\phi$  is also not so good in providing a vertex, since the  $K^+ K^-$  pair is rather colinear because of  $2m_K \sim m_\phi$ , especially with the large boost for LHCb. But  $B^0 \rightarrow \phi K_S \gamma$  might be pursued. Probably the LHCb upgrade would be needed to be competitive with a Super B factory. Other ideas to probe RH currents in  $b \rightarrow s \gamma$  are  $\gamma \rightarrow e^+ e^-$  conversion in detector [50],  $\Lambda$  polarization in  $\Lambda_b \rightarrow \Lambda \gamma$  decay [51], and angular measurables in  $B \rightarrow K^* \ell^+ \ell^-$  decay mentioned in the previous chapter. If an observation is made, one would need multiple measurables to clarify, since one can see from (6.8) that  $\mathcal{S}_{K^{*0}[K_S^0 \pi^0] \gamma}$  involves not only the strength, but also the phase of  $C'_{11}$ .

<sup>7</sup>Belle II improves on Belle with larger SVD, pixel detector to improve low momentum tracking, and improved CDC with better lever arm.

We have not gone into possible New Physics models that could generate TCPV in  $B^0 \rightarrow K^{*0} \gamma$  since this is an existence proof by experiment, and current data is still far away from giving any hint. That is, the key measurements are to come in the Belle II era. One particular model we are fond of, an interesting case that combines SUSY and flavor, is with maximal  $\tilde{s}_R\text{-}\tilde{b}_R$  RH squark mixing [52]. It is motivated in approximate Abelian flavor symmetry models [53] together with SUSY, which provides also the strong dynamics. In this model, the flavor-mixed light  $\tilde{s}\tilde{b}_{1R}$  squark could be driven light by the large flavor mixing, even if SUSY is above the TeV scale (hence might still be relevant). If a “solo  $\tilde{b}$ ” squark is eventually discovered at the LHC, while little else is seen as far as SUSY is concerned, one should test whether this new  $\tilde{b}$  squark also has a large  $\tilde{s}$  component.

## References

1. Buras, A.J.: Phys. Lett. B **566**, 115 (2003)
2. Huang, C.S., Liao, W., Yan, Q.S.: Phys. Rev. D **59**, 011701 (1999)
3. Hamzaoui, C., Pospelov, M., Toharia, M.: Phys. Rev. D **59**, 095005 (1999)
4. Choudhury, S.R., Gaur, N.: Phys. Lett. B **451**, 86 (1999)
5. Babu, K.S., Kolda, C.: Phys. Rev. Lett. **84**, 228 (2000)
6. Giles, R., et al.: [CLEO Collaboration]: Phys. Rev. D **30**, 2279 (1984)
7. Tanabashi, M., et al.: [Particle Data Group]: Phys. Rev. D **98**, 030001 (2018). <http://pdg.lbl.gov/>
8. Albajar, C., et al.: [UA1 Collaboration]: Phys. Lett. B **262**, 163 (1991)
9. Abe, F., et al.: [CDF Collaboration]: Phys. Rev. D **57**, R3811 (1998)
10. Chang, M.-C., Chang, P., et al.: [Belle Collaboration]: Phys. Rev. D **68**, 111101 (2003)
11. Aubert, B., et al.: [BaBar Collaboration]: Phys. Rev. D **77**, 032007 (2008)
12. Abulencia, A., et al.: [CDF Collaboration]: Phys. Rev. Lett. **95**, 221805 (2005)
13. Aaltonen, T., et al.: [CDF Collaboration]: Phys. Rev. Lett. **100**, 101802 (2008)
14. Abazov, V.M., et al.: [DØ Collaboration]: DØ Note 5344
15. Eisenhardt, S.: Talk at 2007 Europhysics Conference on High Energy Physics. Manchester, England (2007)
16. Nielsen, H.B., Ninomiya, M.: Int. J. Mod. Phys. A **23**, 919 (2008). [arXiv:0707.1919](https://arxiv.org/abs/0707.1919) [hep-ph]
17. Aaltonen, T., et al.: [CDF Collaboration]: Phys. Rev. Lett. **107**, 191801 (2011)
18. Wilkinson, G.: Plenary talk at 2011 Europhysics Conference on High Energy Physics. Grenoble, France (2007)
19. Chatrchyan, S., et al.: [CMS Collaboration]: Phys. Rev. Lett. **107**, 191802 (2011)
20. Aaij, R., et al.: [LHCb Collaboration]: Phys. Lett. B **708**, 55 (2012)
21. Chatrchyan, S., et al.: [CMS Collaboration]: JHEP **1204**, 033 (2012)
22. Aaij, R., et al.: [LHCb Collaboration]: Phys. Rev. Lett. **108**, 231801 (2012)
23. Buras, A.J.: Acta Phys. Polon. B **41**, 2487 (2010)
24. Aaij, R., et al.: [LHCb Collaboration]: Phys. Rev. Lett. **110**(2), 021801 (2013)
25. Aaij, R., et al.: [LHCb Collaboration]: Phys. Rev. Lett. **118**, 191801 (2017)
26. Chatrchyan, S., et al.: [CMS Collaboration]: Phys. Rev. Lett. **111**, 101804 (2013)
27. Aaij, R., et al.: [LHCb Collaboration]: Phys. Rev. Lett. **111**, 101805 (2013)
28. Khachatryan, V., et al.: [CMS and LHCb Collaborations]: Nature **522**, 68 (2015)
29. Bobeth, C., Gorbahn, M., Hermann, T., Misiak, M., Stamou, E., Steinhauser, M.: Phys. Rev. Lett. **112**, 101801 (2014)
30. De Bruyn, K., Fleischer, R., Knegjens, R., Koppenburg, P., Merk, M., Pellegrino, A., Tuning, N.: Phys. Rev. Lett. **109**, 041801 (2012)

31. Hou, W.-S., Kohda, M., Xu, F.: Phys. Rev. D **85**, 097502 (2012)
32. Hou, W.-S., Kohda, M., Xu, F.: Phys. Rev. D **87**, 094005 (2013)
33. Dutta, B., Mimura, Y.: Phys. Rev. D **91**, 095011 (2015)
34. Altmannshofer, W., Niehoff, C., Straub, D.M.: JHEP **1705**, 076 (2017)
35. Fleischer, R., Jaarsma, R., Tetlalmatzi-Xolocotzi, G.: JHEP **1705**, 156 (2017)
36. Aubert, B., et al.: [BaBar Collaboration]: Phys. Rev. Lett. **96**, 241802 (2006)
37. Aaij, R., et al.: [LHCb Collaboration]: Phys. Rev. Lett. **118**, 251802 (2017)
38. Bertolini, S., Borzumati, F., Masiero, A.: Phys. Rev. Lett. **59**, 180 (1987)
39. Deshpande, N.G., Lo, P., Trampetic, J., Eilam, G., Singer, P.: Phys. Rev. Lett. **59**, 183 (1987)
40. Atwood, D., Gronau, M., Soni, A.: Phys. Rev. Lett. **79**, 185 (1997)
41. Grinstein, B., Grossman, Y., Ligeti, Z., Pirjol, D.: Phys. Rev. D **71**, 011504 (2005)
42. Atwood, D., Gershon, T., Hazumi, M., Soni, A.: Phys. Rev. D **71**, 076003 (2005)
43. Chua, C.-K., He, X.-G., Hou, W.-S.: Phys. Rev. D **60**, 014003 (1999)
44. Aubert, B., et al.: [BaBar Collaboration]: Phys. Rev. Lett. **93**, 131805 (2004)
45. Aubert, B., et al.: [BaBar Collaboration]: Phys. Rev. Lett. **93**, 201801 (2004)
46. Ushiroda, Y., Sumisawa, K., et al.: [Belle Collaboration]: Phys. Rev. D **74**, 111104(R) (2006)
47. Aubert, B., et al.: [BaBar Collaboration]: Phys. Rev. D **78**, 071102 (2008)
48. Sahoo, H., Browder, T.E., et al.: [Belle Collaboration]: Phys. Rev. D **84**, 071101 (2011)
49. Nakano, H., Ishikawa, A., Sumisawa, K., Yamamoto, H., et al.: [Belle Collaboration]: Phys. Rev. D **97**, 092003 (2018)
50. Grossman, Y., Pirjol, D.: JHEP **0006**, 029 (2000)
51. Mannel, T., Recksiegel, S.: J. Phys. G **24**, 979 (1998)
52. Chua, C.-K., Hou, W.-S., Nagashima, M.: Phys. Rev. Lett. **92**, 201803 (2004)
53. Leurer, M., Nir, Y., Seiberg, N.: Nucl. Phys. B **420**, 468 (1994)



# Chapter 7

## Probes of the Dark Sector at Flavor Facilities



Before we turn to non-B physics probes, we detour from our main theme of  $b \rightarrow s$  loop probes of New Physics, and give some account of a special arena for probing the Dark Sector, starting with the decays of bottomonium, namely  $\Upsilon(nS)$ ,  $n = 1 - 3$ . As we have mentioned in Sect. 5.3, the CDMS/DAMA type of approaches to Dark Matter (DM) search are not sensitive to light DM. The bottomonium system offers to (partially) cover such a window. At the same time, the related exotic Higgs sector can also be probed. These suggestions have led the Belle and BaBar experiments to make dedicated data runs on  $\Upsilon(nS)$  resonances below the  $\Upsilon(4S)$ .

Even before the fact that no evidence for supersymmetry were revealed at the LHC, developments in astrophysics opened up new avenues for DM search, leading the B factories to further pursuits in probing the Dark Sector with ever sophistication. The remainder of the chapter does not aim for completeness, just for illustration.

### 7.1 $\Upsilon$ Decay Probes

DM particles could be as light as the GeV order. Part of the motivation is the 0.511 MeV  $\gamma$  rays [1] coming from the galactic center that indicate slow positrons, which suggest a particle lighter than 100 MeV if the source is DM annihilation. Combined with the insensitivity of DAMA/CDMS experiments to low mass DM, it is imperative for us to gain probes of light DM. Such low mass DM may not be so easy to see at the LHC.

#### 7.1.1 $\Upsilon(3S) \rightarrow \pi^+\pi^-\Upsilon(1S) \rightarrow \pi^+\pi^- + \text{Nothing}$

Assuming light DM  $\chi$ , the pair annihilation cross section of dark matter particles,  $\sigma(\chi\chi \rightarrow q\bar{q})$ , is estimated [2] from cosmological data. Assuming time-reversal invariance, this is applied to  $b\bar{b} \rightarrow \chi\chi$ , and the estimate is that  $\mathcal{B}(\Upsilon(1S) \rightarrow \chi\chi) \sim$

0.6%. The mass of  $\chi$  of course has to be lighter than  $m_b$ , and the details depend on whether the “mediator”, or nature of coupling, is of scalar, pseudoscalar, or vector type. The suggestion from theory was to use radiative return (or ISR), i.e.  $\Upsilon(4S) \rightarrow \gamma_{\text{ISR}} \Upsilon(nS)$ , followed by meticulous studies of many decay channels of  $\Upsilon(nS)$  down to  $\Upsilon(1S)$ , to tag and search for  $\Upsilon(1S) \rightarrow \text{nothing}$ . It was argued that, with  $400 \text{ fb}^{-1}$  on the  $\Upsilon(4S)$ , a bound of 0.1% could be attained [2].

Here, the Belle experiment showed their prowess. Rather than doing a meticulous  $\Upsilon(4S)$  radiative return study, by assessing the situation and studying tagging efficiencies to optimize the trigger, the Belle experiment took instead a dedicated 4-day run *directly* on the  $\Upsilon(3S)$  in 2006, collecting  $2.9 \text{ fb}^{-1}$ , corresponding to 11M  $\Upsilon(3S)$  events. The idea [3] bears some similarity to the full reconstruction tag method for getting a “B beam”. That is, using kinematics of  $\Upsilon(3S) \rightarrow \Upsilon(1S)\pi^+\pi^-$  decay, where one knows the energy of the initial state (in CM frame), by reconstructing the  $\pi^+\pi^-$  system, one looks for a peak in the recoil mass distribution at the  $\Upsilon(1S)$ , *but observing no signal in the detector* ( $\Upsilon(1S) \rightarrow \text{nothing}$ ). Combining cross section versus pion efficiency, Belle concluded that a  $\Upsilon(3S)$  run is the best.

Of course, as always, it is a matter of control of signal over background, and optimization of the two-track trigger was crucial. Since the pions are on the soft side, both need to be able to reach an appreciable portion of the tracker (CDC). The trigger was studied further and verified with the control sample of  $\Upsilon(3S) \rightarrow \Upsilon(1S)\pi^+\pi^-$ , where  $\Upsilon(1S) \rightarrow \mu^+\mu^-$ . The main background comes from two-photon events, i.e.  $e^+e^- \rightarrow e^+e^-\pi^+\pi^-$ , where the  $e^+$  and  $e^-$  escape detection. To suppress these, one uses the fact that for these events, the two pions tend to have balanced  $p_T$ , and the  $\pi\pi$  system would be rather boosted, in contrast to signal events. Peaking background arise from  $\Upsilon(3S) \rightarrow \Upsilon(1S)\pi^+\pi^-$  events where  $\Upsilon(1S) \rightarrow \ell^+\ell^-$ , and the leptons go outside of detector acceptance. These backgrounds can be remedied only when “cracks” or holes of the detector are plugged. For the combinatoric, two-photon background, a very forward photon tagger might help.

The result of the Belle study is shown in Fig. 7.1. Fitting with combinatoric and peaking backgrounds as described, Belle extracted  $38 \pm 39$  signal events, which is consistent with no signal. The expected number of events with  $\mathcal{B}(\Upsilon(1S) \rightarrow \chi\chi) = 0.6\%$  is 244. The limit of

$$\mathcal{B}(\Upsilon(1S) \rightarrow \text{invisible}) < 0.25\%, \quad (\text{Belle } 2.9 \text{ fb}^{-1} \Upsilon(3S) \text{ run}), \quad (7.1)$$

at 90% C.L. rules out the original theory expectation [2]. But of course, the case should not be viewed as closed, both because of the importance, but also because the theory could certainly be refined.

The Belle study was followed by a search by CLEO [4], using  $1.2 \text{ fb}^{-1}$  on the  $\Upsilon(2S)$  for  $\pi^+\pi^-\Upsilon(1S)$  decay where the  $\Upsilon(1S)$  decays invisibly. A limit slightly poorer than that of Belle’s is set. This is because of the softer pions from  $\Upsilon(2S)$  decay as compared to  $\Upsilon(3S)$ , and though CLEO has better understanding of their detector because of long and steady experience, trigger efficiency that drove Belle to study  $\Upsilon(3S)$  does matter. In a different mass domain, the BES experiment also

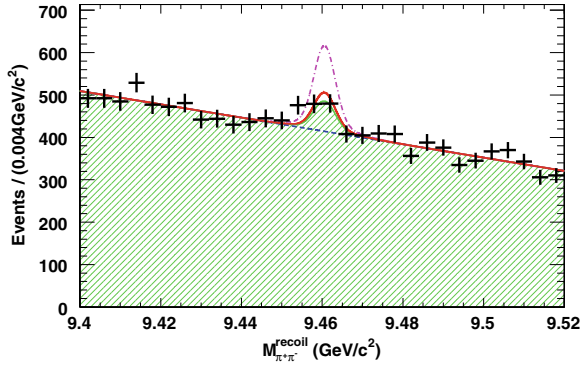


**Fig. 7.1** Recoil mass  $M_{\pi^+\pi^-}^{\text{recoil}}$  against the  $\pi^+\pi^-$  tag in the Belle search [3] for dark matter via  $\Upsilon(3S) \rightarrow \Upsilon(1S)[\rightarrow \text{nothing}]\pi^+\pi^-$  [Copyright (2004) by The American Physical Society]. Dashed (lower solid) line is the combinatoric (peaking) background; see text for description. The other solid line fits to data, while the dot-dash line is the expectation from  $\mathcal{B}(\Upsilon(1S) \rightarrow \chi\chi) = 0.6\%$

searched for the invisible decay of  $J/\psi$  [2] in  $\psi(2S) \rightarrow \pi^+\pi^-J/\psi$  transitions [5], again turning out a null result.

When the PEP-II accelerator had to be terminated earlier than scheduled because of the US funding situation, the BaBar experiment decided to take  $\sim 30 \text{ fb}^{-1}$  on the  $\Upsilon(3S)$  (10 times Belle data) in early 2008, followed by  $\sim 15 \text{ fb}^{-1}$  on  $\Upsilon(2S)$  (12 times CLEO data). The purpose is at least three-fold. The first is for bottomonium spectroscopy, in particular the  $\eta_b$ , which BaBar has subsequently announced discovery [6] in the inclusive  $\gamma$  data in  $\Upsilon(1S) \rightarrow \gamma\eta_b$ . This is quite some triumph, since the  $\eta_b$  has been hiding ever since the  $\Upsilon$  discovery for 30 years. A second motivation is for the potential to search for the exotic pseudoscalar Higgs boson  $a_1$  via  $\Upsilon(1S) \rightarrow \gamma a_1$ , followed by  $a_1 \rightarrow \tau^+\tau^-$ , where the light  $a_1$  could even be behind the 214.3 MeV  $\mu^+\mu^-$  events observed [7] by the HyperCP experiment in  $\Sigma^+ \rightarrow p\mu^+\mu^-$ , which provides further motivation. This will be covered next. A third motivation is to push down on the bound of (7.1). Having 10 times Belle data certainly helps. But inspection of Fig. 7.1 suggest that one may need to reduce the background. Something like an Extreme Forward Calorimeter (EFC, see Fig. 2.2) of Belle needs to be active for MIPs (minimum ionizing particle) and electron rejection.

**Remark on Forward Detector Improvement**

The EFC [8] was an integral part of the Belle detector, precisely plugging the forward (and backward) holes caused by the QCS final focusing magnet. It was designed for three purposes: (i) a (relative) luminosity monitor; (ii) a photon tagger for two photon events when one photon is off-shell; (iii) improve hermeticity. For the first role, it gave important contributions to the KEKB collider commissioning, and the EFC remained a useful instrument for the KEKB accelerator. The design with radiation-hard BGO [9] was in part for the second role of tagging the  $\gamma^*$  with  $e^-/e^+$ . For the third role,

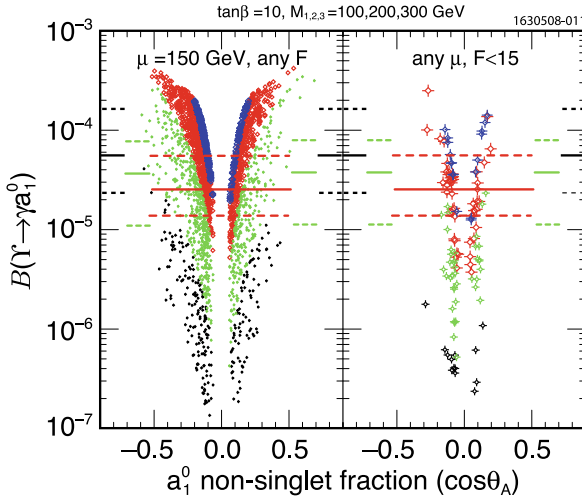


**Fig. 7.2** CLEO upper limits (solid line) on  $\Upsilon(1S) \rightarrow \gamma a_1^0 \rightarrow \gamma \tau^+ \tau^-$ , based on 21.5M  $\Upsilon(1S)$  events [16]. The underlying theory plot is from [13], which corresponds to NMSSM model parameters, where the figure on the right with fewer models is for “less fine-tuning (F)”. [Copyright (2007) by The American Physical Society] Different grey shades correspond to different  $a_1^0$  mass, with the black points corresponding to the heaviest  $a_1^0$ , where CLEO loses sensitivity. The CLEO bounds have respective shading

a major motivation was to help the pursuit of  $B \rightarrow \tau \nu$  because of the difficult missing-mass signature. A proof of principle was conducted [10] to show that MIP detection was possible with the rad.-hard BGO crystal design.

However, an early study [11] found that the Belle detector has too many holes already. Furthermore, the service and cabling of SVD and inner CDC detectors not only took up space in the forward and backward cones, they also give rise to material in front of the EFC. The power of the EFC to improve hermeticity, though providing a factor of two improvement in  $S/B$ , was by far insufficient for the  $B \rightarrow \tau \nu$  cause, and this direction was not actively pursued. As we have seen, the B factories took the punishment of  $10^{-3}$  in efficiency to finally use the full reconstruction tag approach to measure the  $B \rightarrow \tau \nu$  mode.

With interest gaining in missing-energy and especially missing-mass events, there were renewed interest in designing a “super-EFC” for the Belle II experiment. With much improved coverage in the forward-backward directions, with both calorimetry and muon detection capabilities, a limit of  $\mathcal{B}(\Upsilon(1S) \rightarrow \text{invisible}) < 2 \times 10^{-4}$  was in reach with  $500 \text{ fb}^{-1}$  running on the  $\Upsilon(3S)$ . But the SM expectation of  $\mathcal{B}(\Upsilon(1S) \rightarrow \nu \bar{\nu}) \sim 10^{-5}$  remains out of reach. Such a “Super Forward Detector” eventually was not built.

### 7.1.2 $\Upsilon(1S) \rightarrow \gamma a_1^0$ Search

Let us turn to elucidate the physics of a light  $a_1^0$  pseudoscalar.

The popular Minimal SuperSymmetric Standard Model (MSSM) came under stress, mainly from the Higgs mass limit,  $m_H > 114.4$  GeV from LEP [12]. A Higgs boson, or SM-like Higgs boson  $h^0$ , around 100 GeV would be most natural. In general, some fine-tuning of parameters need to be done to accommodate this. A natural way to avoid fine-tuning of parameters is to go to NMSSM, N standing for ‘‘Next (to)’’. Besides the Higgs sector of 2HDM-II, one adds an additional singlet Higgs field. Assuming  $CP$  invariance in the Higgs sector, the Higgs particle spectrum consists of 3 neutral scalars, two neutral pseudoscalars, and a pair of charged Higgs. That is, an extra scalar and pseudoscalar compared to a 2HDM. To make a long story short, one of the pseudoscalars, called the  $a_1^0$ , is light, and the region of parameter space reduces much of the fine-tuning of MSSM, by allowing the SM-like Higgs boson to evade the LEP-II bound. The  $a_1^0$  should have enough non-singlet content, i.e. fraction  $\cos \theta_A$  of the pseudoscalar  $A^0$  of MSSM, such that the  $h^0 \rightarrow a_1^0 a_1^0$  width is large, thereby suppressing the  $h^0 \rightarrow b\bar{b}$  decay and evade the bound from  $e^+e^- \rightarrow Zb\bar{b}$ . Since the latter bound extends to  $Z4b$ , one further needs  $m_{a_1^0} < 2m_b$  such that  $a_1^0 \rightarrow b\bar{b}$  decay is itself forbidden.

To sum it up, let us take  $\tan \beta = 10$  as example. One needs  $\cos \theta_A > 0.05$  to give  $\mathcal{B}(h^0 \rightarrow a_1^0 a_1^0) > 0.7$ , and  $m_{a_1^0} < 2m_b$ . By evading the  $Zh^0 \rightarrow Zb\bar{b}$  bound on  $h^0$  with  $a_1^0 \rightarrow \tau^+\tau^-$ , one notes that the signature of  $Za_1^0 \rightarrow Z\tau^+\tau^-$  and  $Zh^0 \rightarrow Z4\tau$  have not been well studied at LEP. It was suggested [13] that a subdued  $h^0 \rightarrow b\bar{b}$  (at  $\sim 10\%$ ) could in fact account for an excess of  $Zb\bar{b}$  events just below 100 GeV.

So why are we going into this theory detail? Even if NMSSM softens the fine-tuning of MSSM, it seems to be quite contrived in itself. The answer is several fold. Chiefly for our concern is that, with  $m_{a_1^0} < 2m_b$ , the  $a_1^0$  can be accessed in  $\Upsilon(nS)$  decay. There are two other concerns that heighten the importance for the search of a light  $a_1^0$ . The scenario outlined in the previous paragraph [13] may be difficult, perhaps even impossible, to unravel at a hadronic collider. However, the light  $a_1$  can precisely be searched for in  $\Upsilon \rightarrow \gamma a_1$  decay, where a lower bound on this rate is argued [13]. This search could turn out to be of utmost importance if the SM-like Higgs does not show up at the LHC. Note that even  $h^0 \rightarrow \gamma\gamma$  might get diluted away by the  $h^0 \rightarrow a_1^0 a_1^0$  mode. If this is what is realized in Nature, then even with an ILC (International Linear Collider), which could observe  $h^0 \rightarrow a_1^0 a_1^0$ , information from  $\mathcal{B}(\Upsilon \rightarrow \gamma a_1)$  would still be valuable and complementary.

A second data-based motivation is for an  $a_1^0$  lighter than  $2m_s$ , which would be rather light indeed. If this is the case, then  $a_1 \rightarrow \mu^+\mu^-$  would dominate.<sup>1</sup> It has been suggested that the 3  $\mu^+\mu^-$  events at 214.3 MeV as seen [7] by the HyperCP experiment at Fermilab, in the  $\Sigma^+ \rightarrow p\mu^+\mu^-$  process, could be [14] such a light pseudoscalar. Admittedly, having three events in a narrow mass region just above

---

<sup>1</sup>Between  $2m_s$  and  $2m_\tau$ , the  $a_1^0$  would decay hadronically and would be a rather difficult object to study at the LHC. However, it seems hard for this case to survive  $B$  decay bound, since most likely  $b \rightarrow s a_1^0$  would be too large.

threshold, and appearing only in the  $\Sigma^+ \rightarrow p\mu^+\mu^-$  mode in these latter days rather than much earlier, seem to challenge our senses. However, it is claimed that *this is possible in the NMSSM*, while all  $K$  and  $B$  constraints are satisfied. Let us not go into the detailed theoretical intricacies [14], but to note that the HyperCP events must be followed up experimentally. One suggestion [15] is  $\Upsilon(1S) \rightarrow \gamma a_1^0 \rightarrow \gamma\mu^+\mu^-$  search.

Besides  $\eta_b$  and DM search, the possibility for  $a_1^0$  search was one of the major motivations for BaBar's end run on the  $\Upsilon(3S)$  and  $\Upsilon(2S)$  just before shutting down. Besides direct radiative decay of  $\Upsilon(3S)$  and  $\Upsilon(2S)$  to  $a_1^0$ , the stronger recommendation [13], maybe influenced by the Belle special run on  $\Upsilon(3S)$  for DM search discussed already, was to use  $\Upsilon(3S)$ ,  $\Upsilon(2S) \rightarrow \pi^+\pi^-\Upsilon(1S)$ , followed by  $\Upsilon(1S) \rightarrow \gamma a_1^0$ , using the  $\pi^+\pi^-$  as tag for the  $\Upsilon(1S)$ .

But the CLEO experiment had already collected  $1.1 \text{ fb}^{-1}$  on the  $\Upsilon(1S)$  (and  $1.2 \text{ fb}^{-1}$  each on the  $\Upsilon(2S)$  and  $\Upsilon(3S)$ ) with the CLEO III detector, before scaling down the energy to CLEO-c. With 21.5M  $\Upsilon(1S)$  events at hand, CLEO found [16] that much of the parameter space for  $2m_\tau < m_{a_1^0} < 7.5 \text{ GeV}$ , and for light  $a_1 \rightarrow \mu^+\mu^-$  ( $m_{a_1} < 2m_s$ ), are ruled out.

$\Upsilon(1S) \rightarrow \gamma a_1^0$  decay is nothing but the Wilczek process [17] for a pseudoscalar Higgs particle, with the  $a_1^0 bb$  coupling modulated by  $\tan\beta \cos\theta_A$ , where  $\tan\beta$  is the usual enhancement factor for down-type quarks (and charged leptons) in 2HDM-II, and  $\cos\theta_A$  expresses the 2HDM-II fraction of  $a_1^0$ . Thus,

$$\mathcal{B}_{\Upsilon(1S) \rightarrow \gamma a_1^0} = \tan^2\beta \cos^2\theta_A \times \mathcal{B}_{\Upsilon(1S) \rightarrow \gamma A^0}^{\text{Wilczek}}, \quad (7.2)$$

where  $\mathcal{B}_{\Upsilon(1S) \rightarrow \gamma A^0}^{\text{Wilczek}}$  includes kinematics and all corrections. For both  $a_1^0 \rightarrow \tau^+\tau^-$  and  $\mu^+\mu^-$  search, CLEO [16] selected two tracks with opposite charge, with at least one  $\gamma$ , but applying a  $\pi^0$  veto.

For  $a_1^0 \rightarrow \tau^+\tau^-$  candidates, a missing energy between 2 and 7 GeV was required. The two tracks were demanded to be  $e^\pm\mu^\mp$  or  $\mu^\pm\mu^\mp$ . Events with  $e^+e^-$  are discarded because of severe Bhabha background. The signal is then a near monochromatic peak in  $E_\gamma$  over the background. The background comes mainly from continuum  $e^+e^- \rightarrow (\gamma)\tau^+\tau^-$ , where possibly one photon from a  $\pi^0$  daughter of a  $\tau$  lepton was not constructed. The continuum background was estimated by scaling from data collected at, or near, the  $\Upsilon(4S)$ , which described the  $\Upsilon(1S)$  data rather well. No significant peak was observed. Plotting with the NMSSM result of [13], the CLEO limits on  $\Upsilon(1S) \rightarrow \gamma a_1^0 \rightarrow \gamma\tau^+\tau^-$  are given in Fig. 7.2. For the medium grey region of  $2m_\tau < m_{a_1^0} < 7.5 \text{ GeV}$ , most models are ruled out, except when the non-singlet fraction  $|\cos\theta_A|$  is small. For the light grey region, corresponding to  $7.5 \text{ GeV} < m_{a_1^0} < 8.8 \text{ GeV}$ , some models, or parameter space, are allowed, as CLEO is losing sensitivity. For the models marked in black, corresponding to  $8.8 \text{ GeV} < m_{a_1^0} < 9.2 \text{ GeV}$ , CLEO has little sensitivity.

For  $a_1^0 \rightarrow \mu^+\mu^-$  search [16], both tracks must pass muon ID, and the total observed energy of the  $\gamma\mu^+\mu^-$  should be consistent with the  $\Upsilon(1S)$ . One searches for peaks in  $m_{\mu^+\mu^-}$ , as it has better resolution than  $E_\gamma$ . The background arises from

radiative (ISR)  $e^+e^- \rightarrow \gamma\mu^+\mu^-$  with a rather hard photon, with  $e^+e^- \rightarrow \gamma J/\psi \rightarrow \gamma\mu^+\mu^-$  providing a control mode to check things such as resolution. The  $\Upsilon(1S)$  data is well described by scaling from  $\Upsilon(4S)$  data (adjusting for  $J/\psi$  position). The special interest is for  $m_{a_1^0} = 214.3$  MeV, i.e. the region of HyperCP events. A fit in this region gives  $7.5_{-4.5}^{+5.3}$  events, giving the bound of  $\mathcal{B}(\Upsilon(1S) \rightarrow \gamma a_1^0) < 2.3 \times 10^{-6}$  at 90% C.L. Translated to  $\tan\beta \cos\theta_A$ , the bound disfavors the claim by [14], and CLEO “calls for a reevaluation of the  $a_1^0$  hypothesis for the HyperCP events.”

BaBar pursued [18]  $\Upsilon(2S, 3S) \rightarrow \gamma a_1^0$ , followed by  $a_1^0 \rightarrow \mu^+\mu^-$  decay, with 98.6M and 121.8M  $\Upsilon(2S)$  and  $\Upsilon(3S)$  mesons, respectively. It set upper limits on  $a_1^0$  coupling to  $b$  quark that are analogous to the CLEO result, and in particular finding no evidence in support of the  $a_1^0$  explanation [14] of the HyperCP events [7]. Using this data and the  $\pi^+\pi^-$  tagging approach, BaBar placed various bounds on  $a_1^0 \rightarrow \mu^+\mu^-$ ,  $\tau^+\tau^-$ ,  $gg$  and  $s\bar{s}$  in various mass ranges, which we refer to PDG [12] for further reference.

We remark that  $a_1^0$ - $\eta_b$  mixing [19] has been considered for the heavy mass  $m_{a_1^0} > 9.2$  GeV case. But with BaBar observation [6] of  $\eta_b$  in the recoil photon from  $\Upsilon(3S) \rightarrow \gamma\eta_b$ , based on 109M  $\Upsilon(3S)$  events, the likelihood for  $a_1^0$ - $\eta_b$  mixing effect is not a high one. BaBar finds  $m_{\eta_b} \simeq 9389$  MeV, with  $\Upsilon(1S)$ - $\eta_b(1S)$  hyperfine splitting at 71 MeV. The latter is not much higher than expected from QCD.

BaBar did follow through with the  $\pi^+\pi^-$  tagging [3] of  $\Upsilon(1S) \rightarrow$  invisible using their  $\Upsilon(3S)$  special run data, setting the limit [20] of

$$\mathcal{B}(\Upsilon(1S) \rightarrow \text{invisible}) < 3.0 \times 10^{-4}, \quad (\text{BaBar 91.4M } \Upsilon(3S)), \quad (7.3)$$

at 90% C.L., improving (7.1) by almost an order of magnitude.

It is interesting that  $\Upsilon(1S)$ ,  $\Upsilon(2S)$ ,  $\Upsilon(3S)$  studies have turned into a new arena on New Physics, and plugs a potential weak spot for LHC. More may follow at Belle II in a similar vein.

## 7.2 The Quest for Dark Photons

The early result on 0.511 MeV lines from the galactic bulge [1] observed by the INTEGRAL satellite became firm by 2006 [21]. But as CLEO and BaBar competed on the  $\Upsilon(1S) \rightarrow \gamma a_1^0$  search, the observation [22] by PAMELA (Payload for Antimatter Matter Exploration and Light-nuclei Astrophysics) satellite made major impact on our view of DM. In particular, PAMELA found a rapid rise in  $e^+$  fraction above 10 GeV, even up to 100 GeV, suggesting a primary source, either from an astrophysical object (e.g. pulsar), or from  $DM$  annihilation. For the latter case, it was advocated [23] that a new force may be operating on the Dark Sector, with Compton wavelength not less than  $\text{GeV}^{-1}$ . As we have alluded to, given that the INTEGRAL signature is in positrons, it suggests a sub-GeV “mediator”, although the PAMELA results, later confirmed by AMS [24] to even higher energies, suggest the DM parti-

cle is TeV scale in mass. Suggestions soon followed [25, 26] for search of the Dark Photon,  $A'$ , the mediator with GeV or sub-GeV mass, at flavor factories. The  $A'$  may provide a “portal” to the Dark Sector, which may be no less rich in structure/forces as compared with our Matter world.

It is not our purpose to review the developments in DM, but just discuss the efforts made at flavor facilities. The framework, as outlined clearly in an early work [27], is the “kinetic” mixing between  $A'$  and the usual photon via  $\varepsilon F_{\mu\nu}F'^{\mu\nu}$ , where  $\varepsilon$  is likely generated at the loop order hence small. Note that this kinetic mixing term is gauge invariant, but may require loop generation if the extra U(1) is embedded in some larger (Dark Sector) gauge symmetry. In this context, in general [25] the Dark Photon  $A'$  receives mass via the Higgs mechanism, hence there is an associated Dark Higgs,  $h'$ .

### 7.2.1 Exotic Higgs-Strahlung: $e^+e^- \rightarrow A'h', h' \rightarrow A'A'$

The first suggested search at B factories is via multi-leptons by exotic Higgs-strahlung [25], i.e.  $e^+e^- \rightarrow A'^* \rightarrow A'h'$ , followed by  $h' \rightarrow A'A'$ , if  $m_{h'} > 2m_{A'}$ . The advantage of this process is that it depends only on a single power of  $\varepsilon$  at the amplitude level. With the fact that the PAMELA signal is in positron (and electron) excess, it is reasonable that a light  $A'$  decays via  $\ell^+\ell^-$ , where  $\ell = e, \mu$ , which can be pursued in an analogous way at fixed target experiments [28].

The event topology at low energy, high intensity  $e^+e^-$  colliders depends on the  $h'$  and  $A'$  masses. For  $m_{h'} > 2m_{A'}$ , the produced  $h'$  would decay promptly, but the lifetime could become large enough to escape detection for  $m_{h'} < m_{A'}$ . Since the dark photon width  $\Gamma_{A'} \propto m_{A'}\varepsilon^2$ , which could decay promptly, or lead to displaced vertex. At B factory energies, dark photon decay is prompt for  $m_{A'} > 250$  MeV and  $\varepsilon > 10^{-4}$ .

The BaBar experiment took up [29] the task for  $e^+e^- \rightarrow A'^* \rightarrow A'h', h' \rightarrow A'A'$  search, for the mass range  $0.25 \text{ GeV} < m_{A'} < 3.0 \text{ GeV}$  and  $0.8 \text{ GeV} < m_{h'} < 10.0 \text{ GeV}$ , assuming  $m_{h'} > 2m_{A'}$ . BaBar used 10% of all available data (not just on  $\Upsilon(4S)$ , but also  $\Upsilon(3S)$ ,  $\Upsilon(2S)$ , as well as off-resonance) for optimizing selection criteria, and used the remaining  $516 \text{ fb}^{-1}$  for the analysis. BaBar defined signal with six charged tracks as *exclusive*:  $3(\ell^+\ell^-)$ ,  $2(\ell^+\ell^-)\pi^+\pi^-$ ,  $\ell^+\ell^-2(\pi^+\pi^-)$ , but not  $3(\pi^+\pi^-)$ . The partially reconstructed *inclusive* modes consist of  $2(\ell^+\ell^-) + X$  (but not  $2(e^+e^-) + X$ ), where  $X$  denotes any final state other than  $\ell^+\ell^-$  or  $\pi^+\pi^-$ . The charged tracks were required to originate from the same primary vertex, and the multiple oppositely charged pairs were required to be all consistent in mass. Besides events originating from  $\rho/\omega \rightarrow \pi^+\pi^-$  decays near  $m_{A'} \sim 0.7\text{--}0.8 \text{ GeV}$ , the observed events are consistent with the two events expected from optimization sample. With detailed studies of efficiencies, BaBar placed bounds on  $\alpha_D \varepsilon^2$  down to below  $10^{-9}$  for  $m_{h'}$  lighter than a few GeV, rising with  $m_{h'}$  as well as with  $m_{A'}$ . Assuming  $\alpha_D = \alpha$



for the Dark sector gauge coupling, this corresponds to  $\varepsilon \in (10^{-4}, 10^{-3})$ . Note that one could have  $\alpha_D \sim 1$ , then the limit on  $\varepsilon$  would be much more stringent.

Belle took the time to make a comprehensive study [30], using altogether  $977 \text{ fb}^{-1}$ , corresponding to data collected from  $\Upsilon(1S)$  to  $\Upsilon(5S)$  resonances and in the nearby continua. Belle extended the mass range to  $0.1 \text{ GeV} < m_{A'} < 3.5 \text{ GeV}$  and  $0.2 \text{ GeV} < m_{h'} < 10.5 \text{ GeV}$  for exclusive modes, keeping the assumption that  $m_{h'} > 2m_{A'}$ , i.e. prompt  $h'$  and  $A'$  decays. They also added the  $3(\pi^+\pi^-)$  mode, hence altogether 10 modes with six charged tracks originating from primary vertex. For  $2(\ell^+\ell^-) + X$  inclusive modes, Belle added  $2(e^+e^-) + X$ , constraining  $X$  by missing mass, and studied the mass range  $1.1 \text{ GeV} < m_{A'} < 3.5 \text{ GeV}$  (following the discussion of [25]), and  $0.2 \text{ GeV} < m_{h'} < 10.5 \text{ GeV}$ . Belle chose to optimize signal selection by MC simulation, and devised ways to build up sidebands from data for background, such as “opposite sign” dileptons, and large mass difference between heaviest and lightest Dark Photon candidates in an event. They also included ISR and vacuum polarization corrections, which are significant. Inclusion of  $3(\pi^+\pi^-)$  mode in the study improved the limits around  $\rho/\omega$  resonances dramatically.

In all cases, the number of observed events is consistent with background estimates, i.e. no significant signal was observed. The extracted bounds were compared with the result from BaBar, which turned out to be almost a factor of 2 smaller, and more so for heavier  $A'$ . For  $\alpha_D = \alpha$ ,  $m_{h'} < 8 \text{ GeV}$  and  $m_{A'} < 1 \text{ GeV}$ , Belle excludes  $\varepsilon > 8 \times 10^{-4}$ . Because the backgrounds were found to be rather low, an encouraging outcome is that future improvements should scale nearly linearly with integrated luminosity. This of course ought to be validated by early Belle II data when it becomes available.

### 7.2.2 Dark Photon from ISR: $e^+e^- \rightarrow \gamma_{\text{ISR}}A'$

Analogous to  $e^+e^- \rightarrow \gamma\gamma$ , one could have  $e^+e^- \rightarrow \gamma A'$ , followed by  $A' \rightarrow e^+e^-$ ,  $\mu^+\mu^-$ . Given that  $\Gamma_{A'}$  is suppressed by  $\varepsilon^2$  hence rather narrow, one could search for narrow  $\ell^+\ell^-$  resonances in radiative  $e^+e^- \rightarrow \gamma\ell^+\ell^-$ . BaBar took up such a study [31] with  $514 \text{ fb}^{-1}$  data, using 5% data for optimization of selection criteria. Using the theoretical results for  $A'$  decay from [25], BaBar combined the two channels into a single measurement. Bounds on  $\varepsilon$  were set at the  $10^{-4}$ – $10^{-3}$  level for  $20 \text{ MeV} < m_{A'} < 10.2 \text{ GeV}$ , improving significantly from previous constraints, including the earlier [20] result from BaBar. In particular, the BaBar result ruled out almost all of the remaining parameter space, at the time of publication, for the simplest [32] Dark Sector explanation of muon  $g - 2$  discrepancy.

While Belle has yet to follow up on the  $e^+e^- \rightarrow \gamma A', A' \rightarrow \ell^+\ell^-$  analysis, BES III has taken up the task for a smaller mass range, for 1.5–3.4 GeV, also finding no evidence [33]. Though not the most competitive, we use their plot (Fig. 7.3) to illustrate the strong interest from multiple experiments.

Independent of the astrophysics hints for TeV-scale WIMPs, a sub-GeV Dark Photon  $A'$  is motivated [32] by the persistence of the muon  $g - 2$  “anomaly” [34].

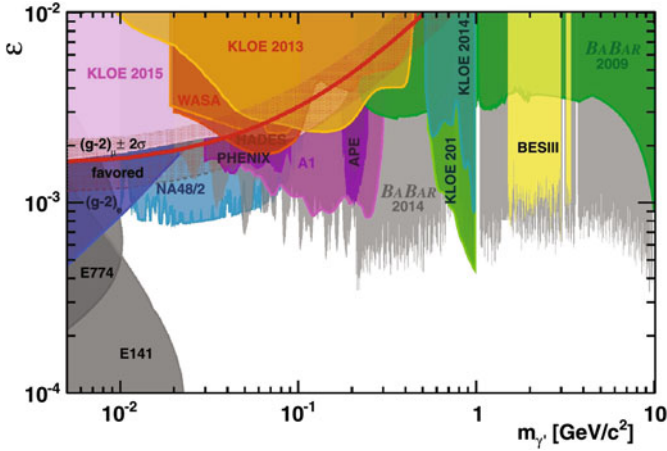


**Fig. 7.3** Upper limits at 90% C.L. from the BESIII experiment [33] (shaded between 1.5 and 3.4 GeV) on kinetic mixing strength  $\varepsilon$ , as a function of Dark Photon mass  $m_{\gamma^*}$  (which most studies denote as  $m_{A'}$ ). Different experiments give different bounds with respective shading

A low mass  $A'$  could alleviate the discrepancy with a rather small coupling, hence the extra U(1) is “secluded”, i.e. it has otherwise not been probed much. If there are low mass DM states  $\chi$  in the Dark Sector, then  $A' \rightarrow \chi\chi$  decay can invalidate the previous narrow  $\ell^+\ell^-$  resonance search by BaBar [31] in  $e^+e^- \rightarrow \gamma A'$ , as well as other analogous searches. In planning for the end run on  $\Upsilon(2S)$  and  $\Upsilon(3S)$ , BaBar had the foresight in preparing for a *single photon trigger*, which now came in handy for the  $e^+e^- \rightarrow \gamma A', A' \rightarrow \text{invisible}$  search [35]. Assuming the emitted  $A'$  is on-shell and with the invisible decay predominant, the signature is a single monoenergetic photon, with energy  $E_\gamma^*$  in  $e^+e^-$  C.M. frame related to  $m_{A'}$  via  $m_{A'}^2 = s - 2E_\gamma^*\sqrt{s}$ , and there is no further dependence on  $m_\chi$  nor its coupling to  $A'$ .

We do not go into any details of the single photon trigger, but in their final running period, BaBar managed to take  $48 \text{ fb}^{-1}$  data for “high  $m_{A'}$ ” (low  $E_\gamma$ ) trigger, mostly on  $\Upsilon(2S)$  and  $\Upsilon(3S)$ , and  $53 \text{ fb}^{-1}$  for “low  $m_{A'}$ ” trigger by adding  $5 \text{ fb}^{-1}$  on  $\Upsilon(4S)$ . The two main backgrounds are two photon  $e^+e^- \rightarrow \gamma\gamma(\gamma)$  annihilation, and radiative Bhabha  $e^+e^- \rightarrow \gamma e^+e^-$  scattering events. The former, of more concern for “low  $m_{A'}$ ” trigger as it peaks towards zero mass, cannot be reliably estimated. It suffers from alignment of ECAL (EMC) crystals with collision point, hence inefficient in the gaps. Radiative Bhabha affects “high  $m_{A'}$ ” trigger more when both  $e^+$  and  $e^-$  escape detection. In the end, BaBar found no evidence for monochromatic photons recoiling against an invisibly decaying  $A'$ , setting limits on  $\varepsilon$  for  $m_{A'} < 8 \text{ TeV}$ . In particular, the BaBar result of  $\varepsilon < 10^{-3}$  for  $m_{A'} < 1.5 \text{ GeV}$  rules out the possibility of invisibly decaying Dark Photon as the explanation for the muon  $g - 2$  anomaly. For heavier  $m_{A'}$ , the limit is mostly more stringent, except for a window around 5.5–6.4 GeV.

### 7.2.3 Inclusive $A' \rightarrow \mu^+ \mu^-$ Search at LHC

With strong interest in the Dark Photon  $A'$ , and in view of the increase in luminosity and especially the migration from hardware to software-based trigger in Run 3 for LHCb, an *inclusive*  $A' \rightarrow \mu^+ \mu^-$  search [36] was proposed, where the production process of  $A'$  need not be specified. The point is, with  $\gamma$ - $A'$  mixing, the production and decay kinematics for an off-shell photon  $\gamma^*$  and  $A'$  in  $pp$  collisions are identical for  $m_{\gamma^*} = m_{A'}$ .

The expected  $A' \rightarrow \mu^+ \mu^-$  signal yield is given by [36, 37]

$$n_{\text{ex}}^{A'}[m_{A'}, \varepsilon^2] = \varepsilon^2 \left( \frac{n_{\text{ob}}^{\gamma^*}[m_{A'}]}{2\Delta m} \right) \mathcal{F}[m_{A'}] \epsilon_{\gamma^*}^{A'}[m_{A'}, \tau_{A'}], \quad (7.4)$$

where  $n_{\text{ob}}^{\gamma^*}[m_{A'}]$  is the observed prompt  $\gamma^* \rightarrow \mu^+ \mu^-$  yield in a small  $\pm\Delta m$  window around  $m_{A'}$ ,  $\mathcal{F}[m_{A'}]$  include phase space and other factors, and  $\epsilon_{\gamma^*}^{A'}[m_{A'}, \tau_{A'}]$  is the ratio of detection efficiencies for  $A' \rightarrow \mu^+ \mu^-$  and  $\gamma^* \rightarrow \mu^+ \mu^-$ , which depends on  $\tau_{A'}$ . If  $A' \rightarrow \text{invisible}$  decay is negligible, then  $\Gamma_{A'} \propto m_{A'} \varepsilon^2$ , which can either lead to displaced vertex, e.g. when  $m_{A'}$  is not far above  $2m_\mu$ , or when  $\tau_{A'}$  is small compared with detector resolution, then the prompt (or prompt-like)  $A' \rightarrow \mu^+ \mu^-$  decay cannot be distinguished from prompt  $\gamma^* \rightarrow \mu^+ \mu^-$  production, and  $\epsilon_{\gamma^*}^{A'}[m_{A'}, \tau_{A'}] \approx 1$ . This means most systematic effects cancel, and one can conduct a data-driven search to constrain  $\varepsilon^2$  by comparing  $n_{\text{ob}}^{A'}[m_{A'}]$  with  $n_{\text{ex}}^{A'}[m_{A'}, \varepsilon^2]$ .

LHCb conducted a proof of principle study [37] with  $1.6 \text{ fb}^{-1}$  data taken at 13 TeV collision energy in 2016, with results that are already promising. The promptlike search was performed from  $2m_\mu$  up to 70 GeV (above which the  $Z$  boson dominates). For long-lived  $A'$ , the mass range was restricted to  $214 \text{ MeV} < m_{A'} < 350 \text{ MeV}$ . For promptlike  $A'$  search, prompt  $\gamma^* \rightarrow \mu^+ \mu^-$  production constitutes irreducible background. For resonances that decay to  $\mu^+ \mu^-$ , the mass peak regions are avoided. Misreconstructions are of three types: double misreconstruction of prompt hadrons as muons ( $hh$ ), misidentifying a prompt hadron together with a muon from heavy quark  $Q$  decay ( $h\mu_Q$ ), or both muons from  $Q$  decay ( $\mu_Q\mu_Q$ ). In between  $m_\phi$  and  $m_\gamma$ , misreconstruction overwhelms signal-like  $\gamma^* \rightarrow \mu^+ \mu^-$  contribution, and an isolation requirement is applied, but otherwise the misreconstruction backgrounds are suppressed by stringent  $\mu$ -ID and promptlike requirements in the trigger.

The value of  $n_{\text{ob}}^{\gamma^*}[m_{A'}]$  for given  $m_{A'}$  is extracted from data by binned extended maximum likelihood fit. The observed  $A' \rightarrow \mu^+ \mu^-$  yield is determined from fits to the  $m(\mu^+ \mu^-)$  spectrum, and normalized with (7.4) to obtain constraint on  $\varepsilon^2$ . Regions of  $[m_{A'}, \varepsilon^2]$  parameter space where the upper limit on  $n_{\text{ob}}^{\gamma^*}[m_{A'}]$  is less than  $n_{\text{ex}}^{A'}[m_{A'}, \varepsilon^2]$  are excluded at 90% C.L. With 2016 data alone, LHCb finds constraints on promptlike  $A'$  to be comparable with existing best (BaBar, see Fig. 7.3) limits for  $m_{A'} < 0.5 \text{ GeV}$ , and since above 10.5 GeV has not been probed before, the LHCb limits are most stringent for  $10.6 \text{ GeV} < m_{A'} < 70 \text{ GeV}$ .

For long-lived  $A'$  search, stringent trigger criteria make prompt muon contamination negligible. Background events from photon conversion in silicon vertex detec-

tor are suppressed by precision knowledge of the material map, while  $b$  decays and the  $K_S \rightarrow \pi^+\pi^-$  tail were also dealt with. Although only small regions of  $m_{A'}$  are excluded for  $\varepsilon^2$  around  $10^{-9}$  by 2016 data, it would rapidly improve with more data. This search for long-lived  $A'$  is also the first [37] to achieve sensitivity with displaced-vertex signature.

The 2016 data sample was collected with a trigger that is inefficient for low mass  $A' \rightarrow \mu^+\mu^-$ , so the analysis helped improve the software trigger efficiency significantly for 2017 data. The increase in luminosity in Run 3, and in particular the removal of hardware trigger and move to fully software trigger, would increase the number of expected  $A' \rightarrow \mu^+\mu^-$  in low mass region by a factor of 100–1000, and there is much to look forward to.

### 7.2.4 Muonic Dark Force: $e^+e^- \rightarrow \mu^+\mu^-Z'$ , $Z' \rightarrow \mu^+\mu^-$

All previous discussions of Dark Photon  $A'$  search rely on its kinetic mixing with the photon, which itself couples universally with electric charge, and so far no evidence for  $A'$  has been found. The strong constraints by existing searches (see Fig. 7.3) utilizing coupling to electron and light quarks somewhat reflects the situation with direct WIMP search, as well as at the LHC. But what if a new gauge boson  $Z'$  couples preferentially with heavy-flavor leptons? It would then evade the previous search bounds.

The muon  $g - 2$  anomaly provides motivation [32] for some muonic force, such as the gauged  $L_\mu - L_\tau$  symmetry mentioned in Sect. 5.2.2 in the context of the  $P'_S$ ,  $R_K$  and  $R_{K^*}$  anomalies. The model with vector-like quarks that aim [38] for the latter cannot explain muon  $g - 2$  discrepancy. But turning around, the same authors found [39] that such a  $Z'$  that can explain muon  $g - 2$  by preferentially coupling to muons, is constrained by neutrino trident production, or neutrino scattering off a nucleus that brings out an accompanying muon pair, excludes  $m_{Z'} > 400$  MeV, but a light  $Z'$  with correspondingly weak coupling  $g'$  could still explain muon  $g - 2$ , which is fascinating in itself. We return to this in the kaon subsection.

With these and other motivations, BaBar embarked on a search [40] for the muonic-coupled  $Z'$ , via  $e^+e^- \rightarrow \mu^+\mu^-Z'$ ,  $Z' \rightarrow \mu^+\mu^-$ . Again,  $514 \text{ fb}^{-1}$  data was used, with 5% used for optimization and validation. Backgrounds are mainly from QED produced  $e^+e^- \rightarrow \mu^+\mu^-\mu^+\mu^-$ , which was modeled with ISR taken into account. Event selection starts with 4 charged tracks from primary vertex, with a pair of same sign muons,  $\mu^\pm\mu^\pm$  identified. For data on  $\Upsilon(3S)$  and  $\Upsilon(2S)$  peaks, opposite sign dimuons with mass within 100 MeV of  $\Upsilon(1S)$  and with two oppositely charged tracks are vetoed to suppress  $\Upsilon(3S, 2S) \rightarrow \pi^+\pi^-\Upsilon(1S)$ . A band around  $J/\psi$  was also excluded. The result is interpreted in the model of [39], where one has equal strength of vector couplings to muons, taons and corresponding neutrinos, providing the strongest bound below  $\sim 3$  GeV, down to the dimuon threshold. It should be noted that the measurement probes also models where [41] couplings to neutrinos are absent.

## Prognosis

The coverage in this chapter is not exactly related to flavor physics. However, it shows the interconnection of flavor physics facilities with other subfields. The high-intensity, low(er) energy nature of flavor facilities allows one to probe lighter Dark Matter, which is increasing in importance, both because of absence so far of traditional WIMPS in direct and collider searches, but also because of astrophysics hints, such as positron excess near the galactic bulge.

BaBar has taken the lead in covering the terrain, in particular the single photon trigger that allowed the study of  $e^+e^- \rightarrow \gamma A'$ ,  $A' \rightarrow \text{invisible}$ . Belle has not yet followed up on  $e^+e^- \rightarrow \gamma A'$  search for narrow  $\ell^+\ell^-$  resonances, nor on BaBar's search for muonic dark boson  $Z'$ . However, Belle II has started running, and a single photon trigger has been prepared, with lower threshold than BaBar, as well as a more hermetic ECAL. The single photon trigger is especially usefully in earlier runs, before it gets run over by trigger rate at high luminosity. The above modes, as well as Higgs-strahlung, would be followed up by Belle II [42], which also intends to study muonic  $Z'$  that decays invisibly. LHCb is also well prepared now for the inclusive  $A' \rightarrow \mu^+\mu^-$  search with full Run 2, and eventually, Run 3 data. But can LHCb study  $\mu^+\mu^-Z'$ ,  $Z' \rightarrow \mu^+\mu^-$ ? Let us hope for further development, since the proton size problem, the difference between muonic atom measurement [43] and traditional measurements, adds further impetus to a light muonic force [44].

In any case, the Belle II era looks quite interesting for light Dark Photon or Dark Boson search, where invisible  $\Upsilon(1S)$  decays would also be probed. We have not covered Axion-like particle (ALP) search, which is a Belle II theme (e.g. in  $e^+e^- \rightarrow \gamma\gamma\gamma$ ). See [45] for a recent discussion.

## References

1. Jean, P., et al.: *Astron. Astrophys.* **407**, L55 (2003)
2. McElrath, B.: *Phys. Rev. D* **72**, 103508 (2005)
3. Tajima, O., et al.: [Belle Collaboration]: *Phys. Rev. Lett.* **98**, 132001 (2006)
4. Rubin, P., et al.: [CLEO Collaboration]: *Phys. Rev. D* **75**, 031104 (2007)
5. Ablikim, M., et al.: [BES Collaboration]: *Phys. Rev. Lett.* **100**, 1920011 (2008)
6. Aubert, B., et al.: [BaBar Collaboration]: *Phys. Rev. Lett.* **101**, 071801 (2008)
7. Park, H., et al.: [HyperCP Collaboration]: *Phys. Rev. Lett.* **94**, 021801 (2005)
8. Wang, M.-Z., et al.: *Nucl. Instrum. Meth. A* **455**, 319 (2000)
9. Sahu, S.K., et al.: *Nucl. Instrum. Meth. A* **388**, 144 (1997); Akhmetshin, R., et al.: *ibid. A* **455**, 324 (2000)
10. Ueno, K., et al.: *Nucl. Instrum. Meth. A* **396**, 103 (1997)
11. Wang, C.H., et al.: A Study of  $B \rightarrow \tau\nu$  Search at BELLE, Belle (internal) Note **180** (1997)
12. Tanabashi, M., et al. [Particle Data Group]: *Phys. Rev. D* **98**, 030001 (2018). <http://pdg.lbl.gov/>
13. Dermisek, R., Gunion, J.F., McElrath, B.: *Phys. Rev. D* **76**, 051105 (2007)
14. He, X.G., Tandean, J., Valencia, G.: *Phys. Rev. Lett.* **98**, 081802 (2007)
15. Mangano, M.L., Nason, P.: *Mod. Phys. Lett. A* **19**, 1373 (2007)
16. Love, W., et al.: [CLEO Collaboration]: *Phys. Rev. Lett.* **101**, 151802 (2008)
17. Wilczek, F.: *Phys. Rev. Lett.* **39**, 1304 (1977)

18. Aubert, B., et al.: [BaBar Collaboration]: Phys. Rev. Lett. **103**, 081803 (2009)
19. Fullana, E., Sanchis-Lozano, M.A.: Phys. Lett. B **653**, 67 (2007)
20. Aubert, B., et al.: [BaBar Collaboration]: Phys. Rev. Lett. **103**, 251801 (2009)
21. Weidenspointner, G., et al.: Astron. Astrophys. **450**, 1012 (2006)
22. Adriani, O., et al.: [PAMELA Collaboration]: Nature **458**, 607 (2009)
23. Arkani-Hamed, N., Finkbeiner, D.P., Slatyer, T.R., Weiner, N.: Phys. Rev. D **79**, 015014 (2009)
24. Accardo, L., et al.: [AMS Collaboration]: Phys. Rev. Lett. **113**, 121101 (2014)
25. Batell, B., Pospelov, M., Ritz, A.: Phys. Rev. D **79**, 115008 (2009)
26. Essig, R., Schuster, P., Toro, N.: Phys. Rev. D **80**, 015003 (2009)
27. Holdom, B.: Phys. Lett. **166B**, 196 (1986)
28. Bjorken, J.D., Essig, R., Schuster, P., Toro, N.: Phys. Rev. D **80**, 075018 (2009)
29. Lees, J.P., et al.: [BaBar Collaboration]: Phys. Rev. Lett. **108**, 211801 (2012)
30. Jaegle, I., et al.: [Belle Collaboration]: Phys. Rev. Lett. **114**, 211801 (2015)
31. Lees, J.P., et al.: [BaBar Collaboration]: Phys. Rev. Lett. **113**, 201801 (2014)
32. Pospelov, M.: Phys. Rev. D **80**, 095002 (2009)
33. Ablikim, M., et al.: [BESIII Collaboration]: Phys. Lett. B **774**, 252 (2017)
34. Bennett, G.W., et al.: [Muon g-2 Collaboration]: Phys. Rev. D **73**, 072003 (2006)
35. Lees, J.P., et al.: [BaBar Collaboration]: Phys. Rev. Lett. **119**, 131804 (2017)
36. Ilten, P., Soreq, Y., Thaler, J., Williams, M., Xue, W.: Phys. Rev. Lett. **116**, 251803 (2016)
37. Aaij, R., et al.: [LHCb Collaboration]: Phys. Rev. Lett. **120**, 061801 (2018)
38. Altmannshofer, W., Gori, S., Pospelov, M., Yavin, I.: Phys. Rev. D **89**, 095033 (2014)
39. Altmannshofer, W., Gori, S., Pospelov, M., Yavin, I.: Phys. Rev. Lett. **113**, 091801 (2014)
40. Lees, J.P., et al.: [BaBar Collaboration]: Phys. Rev. D **94**, 011102 (2016)
41. Batell, B., McKeen, D., Pospelov, M.: Phys. Rev. Lett. **107**, 011803 (2011)
42. Hearty, C.: Talk at the U.S. Cosmic Visions: New Ideas in Dark Matter Workshop, College Park, USA (2017)
43. Pohl, R., et al.: Nature **466**, 213 (2010)
44. Barger, V., Chiang, C.-W., Keung, W.-Y., Marfatia, D.: Phys. Rev. Lett. **106**, 153001 (2011)
45. Dolan, M.J., Ferber, T., Hearty, C., Kahlhoefer, F., Schmidt-Hoberg, K.: JHEP **1712**, 094 (2017)

## Chapter 8

# *D* and *K* Systems: Box and EWP Redux



We shall highlight only  $D^0$  mixing and rare  $K \rightarrow \pi\nu\bar{\nu}$  decays.

$D^0$  mixing was observed in 2007, 31 years after the observation of  $D$  mesons (see Table 8.1). Being the smallest in (relative) strength, and the last one to be observed, one has come full circle from the original insight by Gell-Mann and Pais [1], on possible quantum-mechanical mixing in the neutral kaon–anti-kaon system. It also demonstrates that the B factories are charm factories as well (the  $\sim 1.3$  nb cross section for  $e^+e^- \rightarrow c\bar{c}$  production is larger than  $\sim 1.1$  nb for  $e^+e^- \rightarrow B\bar{B}$  production), while the study of charm at  $D\bar{D}$  threshold would still play a key role. Though veiled by hadronic effects, the observation of  $D^0$  mixing opens a new avenue for probing New Physics, especially in the pursuit of CPV at the Super B (rather, Flavor) Factory, and at LHCb.

On the other hand, being the forebearer of FCNC and CPV studies, limits in the kaon system have been pushed down to the extreme, but facilities have dwindled. The pursuit of  $K_L \rightarrow \pi^0\nu\bar{\nu}$  (CPV) and  $K^+ \rightarrow \pi^+\nu\bar{\nu}$  modes illustrates the effort to reach down to SM level, and hopefully discover New Physics along the way.

### 8.1 $D^0$ Mixing

Thirty one years after the  $D^0$  meson was first observed, between the Belle and BaBar experiments, and with quite some feat of experimental effort,  $D^0$ – $\bar{D}^0$  mixing was finally observed in 2007. This is the last neutral meson mixing to be measured (see Table 8.1).

While the measurements of mixing for  $K^0$ – $\bar{K}^0$  and  $B_d^0$ – $\bar{B}_d^0$  systems were rather soon after the mesons were discovered, measurement of meson mixings was much more challenging for the  $B_s^0$ – $\bar{B}_s^0$  and  $D^0$ – $\bar{D}^0$  systems. For  $B_s$ , the challenge was the ultra fast oscillations, while there is also the mixing in lifetime (width mixing), or lifetime difference, which is now also established. For  $D^0$ , the challenge was the sheer smallness of  $x_D$  and  $y_D$ , i.e. the smallness of mass and lifetime differences. We are still not firmly sure whether  $x_D$  is nonzero. Curiously, the observation of  $B_s^0$ – $\bar{B}_s^0$

**Table 8.1** Current measured values of meson mixing, in mass and lifetime, ordered in first year of measurement, where  $x = \Delta m/\Gamma$ ,  $y = \Delta\Gamma/2\Gamma$ . The number in parenthesis in the last column is the year the meson was discovered. We use May 2018 CPV-allowed result from HFLAV for  $D$ -mixing

|         | $x$                          | $y$                          | Date        |
|---------|------------------------------|------------------------------|-------------|
| $K^0$   | 0.474                        | 0.997                        | 1956 (1950) |
| $B_d^0$ | 0.770                        | $-0.002 \pm 0.005$           | 1987 (1983) |
| $B_s^0$ | 26.7                         | $0.066 \pm 0.004$            | 2006 (1992) |
| $D^0$   | $0.0036^{+0.0021}_{-0.0016}$ | $0.0067^{+0.0006}_{-0.0013}$ | 2007 (1976) |

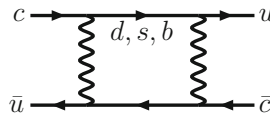


**Fig. 8.1** A SM box diagram for  $D^0$ - $\bar{D}^0$  mixing. The  $q'\bar{q}$  contributions (where  $q^{(\prime)} = d, s$ ), though negligible at short distance, could generate  $\Gamma_{12}^D$  at hadron level, since  $c \rightarrow q'u\bar{q}$  and  $c\bar{u} \rightarrow q'\bar{q}$  generate  $D^0$  decays

and  $D^0$ - $\bar{D}^0$  mixings came in such close succession, in 2006 and 2007 respectively. It reflects the maturity of the Tevatron and the B factories, as well as the complementary nature, and some level of competition, between them. Furthermore, the measurement of meson mixing is the prelude to the even more interesting CPV studies. The epic is still ongoing for these two relative newborns.

### 8.1.1 SM Expectations and Observation at B Factories

Just like the  $K^0$ ,  $B_d^0$  and  $B_s^0$  meson systems, the box diagrams shown in Fig. 8.1 govern the short distance contributions to  $D^0$  mixing. But this is the only case<sup>1</sup> where one has the down-type quarks in the loop.

From our previous discussions of box diagrams, because the  $d$  and  $s$  quark masses are so small, their contribution is negligible at short distance, so only the  $b$  quark contribution matters in the box diagram. But even  $m_b$  is tiny compared to  $m_t$  (or  $M_W$ ), which leads to suppression factors of  $m_b^2/M_W^2$ . In addition,  $V_{ub}V_{cb}^*$  is extremely small compared to the leading  $V_{ud}V_{cd}^* \simeq -V_{us}V_{cs}^* \simeq -0.22$  in the CKM triangle relation

$$V_{ud}V_{cd}^* + V_{us}V_{cs}^* + V_{ub}V_{cb}^* = 0. \quad (8.1)$$

<sup>1</sup>For the unaware, the top decay width is of order 1.4 GeV, so the top lifetime is much shorter than the strong interaction time scale of  $10^{-23}$  s for it to pair with light quarks to form bound states. There are no  $T$  mesons, charged or neutral.



Thus, in the SM, because of lack of “Higgs affinity” in the loop,  $D^0$  mixing receives very tiny short distance (SD) contributions. Normally this implies that it is an excellent probe of New Physics. But the smallness of SD effects makes it susceptible to long distance (LD) contributions of hadronic origins.

Cutting across the light  $s$  and  $d$  quark lines in the box diagram, the resulting diagrams are the squared amplitudes of  $c \rightarrow su\bar{d}$ ,  $su\bar{s}$ ,  $du\bar{d}$ ,  $du\bar{s}$ , as well as  $c\bar{u} \rightarrow s\bar{d}$ ,  $s\bar{s}$ ,  $d\bar{d}$ ,  $d\bar{s}$  processes. Note that the annihilation type of diagrams are not suppressed compared to spectator diagrams, because the charm mass is not too far above the hadronic scale. These squared amplitudes correspond to, for example, “right-sign” (RS) or Cabibbo-favored (CF)  $D^0 \rightarrow K^- \pi^+$ , Cabibbo-suppressed (CS)  $D^0 \rightarrow K^- K^+$ ,  $\pi^- \pi^+$ , and “wrong-sign” (WS) or doubly Cabibbo-suppressed (DCS)  $D^0 \rightarrow K^+ \pi^-$  hadronic processes. Put another way,  $D^0$  and  $\bar{D}^0$  decay to common final states can interfere and generate the absorptive part of the hadronic level box amplitude, or a *width difference*, much like in  $K^0-\bar{K}^0$  and  $B_s^0-\bar{B}_s^0$  systems.

It has been argued [2] that SU(3) breaking effects in  $PP$  and  $4P$  (where  $P$  stands for  $K$  or  $\pi$ ) final states can generate a percent level  $y_D \equiv \Delta\Gamma_D/2\Gamma_D$ , the parameter usually used in place of the width difference  $\Delta\Gamma_D$ . It was further shown that a  $y_D$  at the percent level can generate, via a dispersion relation, the dispersive mass mixing  $x_D = \Delta m_D/\Gamma_D$  that is comparable in size to  $y_D$ . Unfortunately, the hadronic uncertainties are uncontrollable. These estimates concur with earlier arguments [3] that  $x_D \sim y_D \sim 1\%$  is possible from long distance SM, or hadronic, effects. With the observation of  $D^0-\bar{D}^0$  mixing in 2007,  $x_D, y_D$  are below 1% and finite, i.e. consistent with long distance effects.

### Observation at B Factories

The 2007 observation of  $D^0$  mixing is the combined result of

1. Belle analysis of  $540 \text{ fb}^{-1}$  data for  $D^0 \rightarrow K^+ K^-, \pi^+ \pi^-$  ( $CP$  eigenstates) versus  $K^- \pi^+$ , to extract  $y_{CP}$  [4];
2. Both Belle [5] and BaBar [6] analyzed  $D^0 \rightarrow K^\mp \pi^\pm$  (Cabibbo-favored versus doubly Cabibbo-suppressed), with  $400 \text{ fb}^{-1}$  and  $384 \text{ fb}^{-1}$  data respectively, to extract  $x'_D$  and  $y'_D$ , where  $(x'_D, y'_D)$  is a rotation from  $(x_D, y_D)$  by a strong phase  $\delta$  between the Cabibbo allowed and suppressed  $D^0 \rightarrow K^\mp \pi^\pm$  decays;
3. A time-dependent Dalitz analysis of  $D^0 \rightarrow K_S \pi^+ \pi^-$  by Belle [7] with  $540 \text{ fb}^{-1}$ , that allows one to extract  $x_D$  and  $y_D$  directly.

The main progress, almost concurrent, were the evidence shown separately in [4, 6]. These analyses are rather complicated and technical. We highlight only very briefly the key points.

Let us first mention three general aspects for conducting  $D^0$  mixing studies. To tag the flavor of  $D^0$ , one uses the slow pion (denoted as  $\pi_s^+$ ) in  $D^{+*} \rightarrow D^0 \pi^+$ . A slow  $\pi_s^-$  that forms a  $D^*$  would tag a  $\bar{D}^0$  (analogous to same side tagging). Second, the intersection of the reconstructed  $D^0$  track and the beam profile gives vertex information, similar to “ $K_S$  vertexing”. Finally, almost every  $B$  decay has  $D$  mesons in the final state, but the  $B$  lifetime would severely smear the timing

information. To cut out  $B\bar{B}$  background, one typically requires  $p_{D^0} > 2.5 \text{ GeV}$  in the  $e^+e^-$  c.m. frame. Thus, in the language of  $B_d$  and  $B_s$  mixing studies at hadronic machines, at B factories one uses prompt  $D^{*+}$  production with “same side tagging”. Indeed, as we shall see, after the evidence of  $D^0$  mixing were announced separately by Belle [4] and BaBar [6], CDF also measured [8]  $D^0$  mixing.

$y_{\text{CP}}: D^0 \rightarrow K^-K^+, \pi^-\pi^+$  Versus  $K^-\pi^+$

The  $K^-K^+$  and  $\pi^-\pi^+$  are  $CP$  even final states. In the limit of no CPV, which is a good approximation since there is still<sup>2</sup> no evidence of CPV in  $D^0$  system,  $\tau_{P-P^+}$  gives the lifetime of the  $CP$  even  $D^0$  and  $\bar{D}^0$  meson eigenstate. One can measure the difference between the “flavor-specific” lifetime versus the lifetime in  $CP$  eigenstate,

$$y_{\text{CP}} \equiv \frac{\tau_{K^-\pi^+}}{\tau_{K^-K^+}} - 1 \cong y_D \cos \phi \cong y_D. \quad (8.2)$$

The first approximation is analogous to (3.10) for  $B_s$  system, where we have dropped a term related to CPV in mixing. That is, setting  $|q/p| \cong 1$  in

$$|D_{1,2}\rangle = p|D^0\rangle \pm q|\bar{D}^0\rangle. \quad (8.3)$$

which is defined similarly to (A.11). The second approximation in (8.2) follows from absence of CPV, which is borne out by data so far. The measurement of  $y_{\text{CP}}$  probes  $D^0$  meson width mixing, or  $\Gamma_{12}$ .

The FOCUS experiment reported a  $y_{\text{CP}}$  at several percent level in 2000 [10], which aroused much interest at the B factories. The FOCUS value was soon put to rest by Belle, BaBar and CLEO [10]. To measure a smaller value, one needs much more data. By early 2007, using  $540 \text{ fb}^{-1}$  data collected on the  $\Upsilon(4S)$  resonance, Belle found 111 K, 1.22 M and 49 K events in the  $K^-K^+$ ,  $K^-\pi^+$  and  $\pi^-\pi^+$  final states, respectively, with high purity. Fitting both the  $\pi^-\pi^+$  and  $K^-K^+$  modes versus  $K^-\pi^+$  mode, Belle found [4]  $y_{\text{CP}} = 1.31 \pm 0.32 \pm 0.25\%$ , which constitutes  $3.2\sigma$  ( $4.1\sigma$  statistical) evidence. The effect is visible to the eye from the ratio of decay-time distributions, that the  $CP$  even mixture of  $D^0$  and  $\bar{D}^0$  meson state decays slightly faster, just like the case of  $K_S^0$ . Of course, unlike the striking difference in lifetime for  $K_S^0$  and  $K_L^0$ , the small % level lifetime difference is due to many more open channels for both the  $CP$  even and odd states in the  $D^0$ - $\bar{D}^0$  system.

The Belle  $y_{\text{CP}}$  result was subsequently confirmed by BaBar using  $384 \text{ fb}^{-1}$  data, with slightly lower significance. Combined together,  $y_{\text{CP}}$  became the most precisely measured  $D^0$  mixing parameter [10, 11], and still is. At this high precision, there is currently no indication for  $t$ -dependent nor time-integrated CPV in the lifetime of  $D^0$  versus  $\bar{D}^0 \rightarrow K^+K^-$ . Because of the smallness of  $x_D$  and  $y_D$  themselves, it would require even higher statistics for CPV phases to be profitably probed.

<sup>2</sup>For a more complete treatment considering CPV in  $D$  mixing, we refer to [9] (and PDG). The formalism bears much similarity with our limited discussion of the  $B_s$  system. Although unequivocal indication for New Physics has to come with observation of TCPV in  $D^0$  system, we are still not yet there.

$y'_D: D^0 \rightarrow K^- \pi^+$  **Versus**  $K^+ \pi^-$

$D^0 \rightarrow K^- \pi^+$  is a CF (Cabibbo-favored) decay, hence it is called the right-sign (RS) decay when associated with a  $\pi_s^+$  tag. For the  $K^+ \pi^-$  final state (called WS) with a  $\pi_s^+$  tag, it could either come from DCS decay, or through  $D^0 \rightarrow \bar{D}^0$  oscillation, then the  $\bar{D}^0 \rightarrow K^+ \pi^-$  decay. Thus, this is nothing but TCPV, except that, like the  $B_s$  system, width mixing is possibly present. In addition, since the CF versus DCS  $D^0 \rightarrow K^\mp \pi^\pm$  amplitudes could have a strong phase difference  $\delta_{K\pi}$  (i.e. they mix via final state rescattering) between them, one actually measures

$$x'_D = x_D \cos \delta_{K\pi} + y_D \sin \delta_{K\pi}, \quad y'_D = -x_D \sin \delta_{K\pi} + y_D \cos \delta_{K\pi}. \quad (8.4)$$

Because  $x_D$  and  $y_D$  are so small, the exponential time dependence of mass and width mixing can be approximated linearly in amplitude, hence are up to quadratic terms when comparing rates. That is, the probability for a  $\pi_s^+$  tagged  $D^0(t=0) \equiv D^0$  at time zero to be detected at time  $t$  in the WS final state  $K^+ \pi^-$  is,

$$|\langle K^+ \pi^- | D^0(t) \rangle|^2 e^{\hat{t}} \propto R_D + \sqrt{R_D} y'_D \hat{t} + \frac{1}{4} (x_D'^2 + y_D'^2) \hat{t}^2, \quad (8.5)$$

where  $\hat{t} \equiv t/\tau$  is normalized by the mean lifetime  $\tau$  of  $D^0/\bar{D}^0$  mesons, and once again we have ignored CPV. In (8.5),  $R_D$  is the ratio of the DCS to CF decay rates, the  $x_D'^2 + y_D'^2$  term arises from mixing alone, while the term linear in  $t$  is due to interference between the DCS and mixing amplitudes, which is the main term of interest. In the limit that  $x'_D$  and  $y'_D$  are small, it is this interference term that has the best sensitivity.

With 400 fb<sup>-1</sup> data, the Belle study [5] gave approximately  $2\sigma$  exclusion from zero in the  $(x_D'^2, y_D')$  plane, with  $R_D$  consistent with SM expectation. Subsequently, and almost concurrent with the Belle evidence [4] for  $y_{CP}$ , the BaBar experiment announced  $3.9\sigma$  evidence [6] for  $D^0$  mixing with a data of 384 fb<sup>-1</sup>. Identifying about 4000 WS events versus 1.14M RS events, the best fit value assuming no CPV (again with  $R_D$  consistent with SM) was  $(x_D'^2, y_D') \times 10^3 = (-0.22 \pm 0.30 \pm 0.21, +9.7 \pm 4.4 \pm 3.1)$ . The negative  $x_D'^2$  value is unphysical, but still consistent with zero, while  $y_D'$  is at the % level. The sensitivity is clearly in  $y_D'$ , as the  $x_D'^2$  measurement does not translate too well into  $x_D'$ .

The BaBar result for  $y_D'$  was later confirmed by CDF [8] with 1.5 fb<sup>-1</sup> data, finding  $(x_D'^2, y_D') \times 10^3 = (-0.12 \pm 0.35, +8.5 \pm 7.6)$ , claiming  $3.8\sigma$  deviation from zero in  $(x_D'^2, y_D')$  plane. In principle, this could have been achieved in the same time frame as the BaBar study, but in any case it demonstrates clearly that  $D^0$  mixing can be pursued in a hadronic environment.

$x_D, y_D: \mathbf{t-dep.} D^0 \rightarrow K_S \pi^+ \pi^-$  **Dalitz Analysis**

The unique feature of time-dependent Dalitz analysis in  $D^0/\bar{D}^0$  decay to the self-conjugate  $K_S \pi^+ \pi^-$  final state, is its ability to *probe both  $x_D$  and  $y_D$  directly*,

including the sign of  $x_D$ . At the starting point, it is like extending the  $y_p$  program to  $D^0/\bar{D}^0 \rightarrow K^{*\pm}\pi^\mp$  in the  $K_S\pi^+\pi^-$  final state. But the self-conjugate nature of the final state means the CF and DCS decays populate the same Dalitz plot, with a flip of  $m_{K_S\pi^-}^2 \leftrightarrow m_{K_S\pi^+}^2$ , allowing them to interfere. Combining with the time evolution (i.e.  $x_D$  and  $y_D$ ) of the  $D^0$  versus  $\bar{D}^0$  tagged states, there is such prowess in the  $t$ -dependent Dalitz analysis method that one can in principle extract much information, including information on  $q/p$  and CPV in the long run. There is considerable similarity with the formalism for study of mixing-dependent CPV in  $B_s$  system, where one also has  $\Delta\Gamma_{B_s} \neq 0$ . The difference is, of course,  $\Delta m_{B_s}/\bar{\Gamma}_{B_s}$  is so large, while  $\Delta m_D/\bar{\Gamma}_{D^0}$  and  $\Delta\Gamma_D/2\bar{\Gamma}_{D^0}$  are so tiny.

Note that the  $D^0 \rightarrow \rho^0 K_S$  decay to  $CP$  eigenstate, just like the CF  $D^0 \rightarrow K^{*-}\pi^+$  decay and DCS  $D^0 \rightarrow K^{*+}\pi^-$  decay, also populates different bands in the  $K_S\pi^+\pi^-$  Dalitz plot. In fact, one models the quasi-two-body as well as nonresonant contributions (treated as a complex constant term), and these bring in many fitting parameters, including strong phases, but one enjoys large number of events in the Dalitz plot signal region. The methodology is quite similar to the “ $DK$  Dalitz” program [12] for  $\phi_3/\gamma$  extraction, where one utilizes the analyzing power of interference of  $D^0/\bar{D}^0 \rightarrow K_S\pi^+\pi^-$  in the  $K_S\pi^+\pi^-$  Dalitz plot. Although in principle (limit of infinite statistics) the approach is model independent, in practice, one also models resonant and nonresonant  $D$  decay to  $K_S\pi\pi$ .

Using the  $t$ -dep. Dalitz analysis approach in  $K_S\pi^+\pi^-$ , in Spring 2007, Belle came out with the result [7] using a dataset of  $540 \text{ fb}^{-1}$ . With  $\sim 0.5$  M signal events in the  $K_S\pi^+\pi^-$  Dalitz plot and assuming negligible CPV, the fitted numbers were  $x_D = 0.80 \pm 0.29_{-0.07}^{+0.09+0.10} \%$  and  $y_D = 0.33 \pm 0.24_{-0.12}^{+0.08+0.06} \%$ , where the last error is the systematic error due to the Dalitz decay model. The result disfavors  $(x_D, y_D) = (0, 0)$  by  $2.2\sigma$ , which may seem less significant than the  $y_{CP}$  and  $y'_D$  results. But this is the first result with real significance for  $x_D$ , indicating that  $x_D$  is positive and of similar strength to  $y_D$ .

This method is by far the most sophisticated, hence most complicated of all approaches to  $D^0$  mixing. But it also means that a detailed exposition is beyond the scope of this book. In any case, there was no indication for New Physics, a situation which persists.

### Observation of $D^0$ Mixing in 2007 and Current Status

By late Spring 2007, the pursuit of the above three methods had produced measurements that, when combined, excluded  $(x_D, y_D) = (0, 0)$  at the  $5\sigma$  level (see Fig. 8.2), thereby  $D^0$  mixing became established. This does not include the BaBar confirmation of  $y_{CP}$ , nor the CDF confirmation of  $y'_D$ . The best fit by HFAG, assuming  $CP$  invariance, gives,

$$x_D = 0.87_{-0.34}^{+0.30} \%, \quad y_D = 0.66_{-0.20}^{+0.21} \% \quad (\text{May 2007}), \quad (8.6)$$

with  $\delta_{K\pi} = 0.33_{-0.29}^{+0.26}$  rad, or  $(18.9_{-16.6}^{+14.9})^\circ$ . While  $y_D$  is more solid, a finite % level  $x_D$  is indicated.

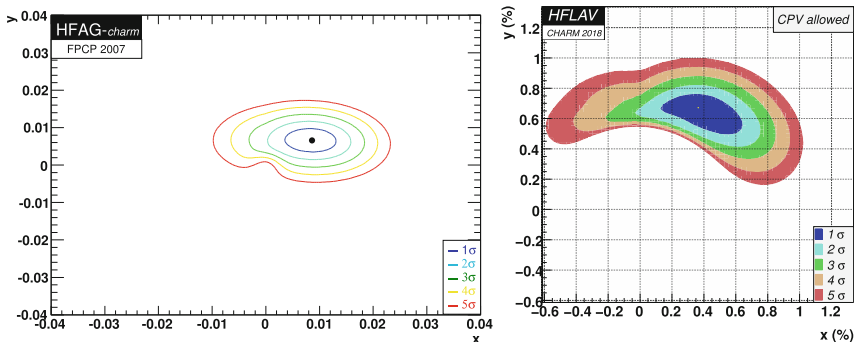


**Fig. 8.2** [left] Combined fit observation of  $D^0$  mixing in Spring 2007 with (8.6) as best fit result, together with  $\delta_{K\pi} = (18.9^{+14.9}_{-16.6})^\circ$  and assuming  $CP$  invariance; [right] CPV-allowed fit result in May 2018, (8.7), with  $\delta_D = (14.7^{+8.4}_{-17.6})^\circ$

There has been much progress since summer 2007. Rather than going into any further detail, we just quote the CHARM 2018 results from HFLAV [11]. Although data is *still consistent with no CPV*, as significance has been quite improved, we quote the fit that allows for CPV,

$$x_D = 0.36^{+0.21}_{-0.16}\%, \quad y_D = 0.67^{+0.06}_{-0.13}\% \quad (\text{May 2018}), \quad (8.7)$$

with  $\delta_D = (14.7^{+8.4}_{-17.6})^\circ$ . The major difference from 2007 is the reduced value for  $x_D$ , which is even less significant, i.e. we have not yet established that  $x_D$  is non-vanishing.

### 8.1.2 Interpretation, $\Delta A_{CP}$ Interlude, and Prospects

As we have already discussed,  $|x_D| \sim y_D \sim 1\%$ , which is observed by experiment, can arise in the SM by hadronic final state effects. Note that the short distance effect for  $x_D$  is negligible. It is of some interest to note that, if the  $4P$  final state dominates the long distance contribution, which is consistent with  $y_D \sim 1\%$ , then  $x_D^{\text{LD}}$  and  $y_D$  (necessarily long distance) should be of the opposite sign [13], while data show the same sign. Although it has been checked [2] that changing hadronic parameters does not change this conclusion, unfortunately the hadronic effects are not well under control for one to make a definite statement. In any case, one should remember the  $\Delta m_K$  enterprise. Although the observed strength could arise from charm and even long distance effects, comparable BSM at even twice the observed  $\Delta m_K$  is always allowed. The same can in principle be applied to  $\Delta m_D$ .

We have spent some time covering what it took to bring forth the observation of  $D^0$  mixing, but what we are really interested in is the New Physics impact, rather than hadronic physics. Although one has made great experimental stride, but a decade

after observation, one still cannot say that there is indication for New Physics in  $D^0$  mixing. A rather comprehensive study for New Physics implications can be found in [14]. Ultimately it seems, one would need to measure CPV, expected to be tiny within SM (with or without long distance dominance), to find unequivocal evidence for BSM. We stress again that CPV effects in  $D^0$  mixing appear to be small at present. Put another way, had CPV effects been observed with present sensitivities, we would have found convincing BSM physics. For instance, correlated with  $\Delta\mathcal{A}_{K\pi}$  (Sect. 2.2), by having the  $b'$  in the box diagram,<sup>3</sup> a 4th generation could lead to sizable [16]  $\Delta m_D$  and even  $CP$  violating phase. This possibility, of course, became diminished when  $\sin 2\Phi_{B_s}$  was found to be consistent with 0 in 2011 by LHCb (Sect. 3.1), and went out of favor with the discovery of the 125 GeV boson that is rather consistent with SM.

### The $\Delta A_{CP}$ Interlude

Curiously, in late 2011, the LHCb experiment at the LHC announced [17] an *unexpectedly large direct CPV difference* of its own,

$$\begin{aligned}\Delta A_{CP} &\equiv A_{CP}(D^0 \rightarrow K^+ K^-) - A_{CP}(D^0 \rightarrow \pi^+ \pi^-) \\ &= -0.82 \pm 0.21 \pm 0.11\% \quad (0.62 \text{ fb}^{-1}, \text{ LHCb 2011}),\end{aligned}\quad (8.8)$$

based on  $0.62 \text{ fb}^{-1}$  data taken in 2011, with significance of  $3.5\sigma$ . The large value, even before the “confirmation” ( $2.7\sigma$ ) by CDF [18], lead theorists into a frenzy, and divided between cherry-picking on possible enhancement of neglected hadronic operators (*déjà vu?*), or inventing *New Physics*. Because  $\sin 2\Phi_{B_s}$  is consistent with 0 hence with SM, and we have no choice but to accept an enhanced  $C$  amplitude, if  $\Delta A_{CP}$  turned out true, it is even more likely to be due to hadronic effect, although the large value would really stretch things. Sure enough, by adding more data, the effect petered away. By 2014, LHCb announced [19] that, with  $3 \text{ fb}^{-1}$  accumulated during Run 1 of LHC, the measure value became:

$$\Delta A_{CP} = 0.14 \pm 0.16 \pm 0.08\% \quad (3 \text{ fb}^{-1}, \text{ LHCb 2014}), \quad (8.9)$$

and the “ $\Delta A_{CP}$  problem” was no more. The result of (8.9) was further improved [10] with  $D^*$  tagging with same data set to  $(-0.10 \pm 0.08 \pm 0.03)\%$ , reaching per mille error. This was further improved by factor of two for individual asymmetries by including time-dependence [20], with still no indication for CPV.

---

<sup>3</sup>It is advantageous to use a  $4 \times 4$  parametrization [15] that follows SM3 to put one weak phase in  $V_{ub}$ , but the two other phases in  $V'_{ts}$ ,  $V'_{td}$ , respectively, and choosing the three new rotation angles as  $|V'_{tb}|$ ,  $|V'_{ts}|$ ,  $|V'_{td}|$ . Full unitarity can be implemented, and the correlation of  $\Delta\mathcal{A}_{K\pi}$  and  $D$ -mixing easily demonstrated.

## Prognosis

Though efforts have been heroic, there is so far no indication for New Physics in  $D$  meson mixing, nor in decay. There are good reasons for this, as already given in Sect. 8.1.1 for  $D$  mixing. As for decay, the reason is similar: the dominant tree level decays, unlike for  $K$  and  $B$  mesons, are Cabibbo allowed, while for loop processes, there is lack of ‘‘Higgs affinity’’ in the smallness of  $m_d, m_s, m_b$ , which in fact leads to effective GIM cancellation. Even if one finds some unexpected effect, one would always have to struggle with possible hadronic enhancements. While the experimental effort should certainly continue, one should not keep the hope high for uncovering New Physics in the  $D$  meson system.

Besides continued progress, there are two things to watch in regards  $D^0$  mixing. One is to follow up on the Dalitz analysis of Belle [7] that saw an indication for  $x_D$ . Second, to unravel some of the hadronic physics in the decay final state, one needs to gain independent access to the strong phases. Employing quantum coherence just like in TCPV studies in  $\Upsilon(4S) \rightarrow B^0\bar{B}^0$  decays, by a tagged Dalitz analysis in  $\psi(3770) \rightarrow D^0\bar{D}^0$  decays, one can [21] extract the strong phase  $\delta_D$ , which would in turn feedback on  $x_D$  and  $y_D$  extraction. It is here where BESIII could aid the  $D^0$  mixing program considerably through this type of studies. Basically, the Dalitz type of analysis, with the help of quantum coherence, holds the power for the future.

This is an area where Belle II can compete well with LHCb because of its diversity.

## 8.2 Rare $K$ Decays: $K \rightarrow \pi\nu\bar{\nu}$ Pursuit

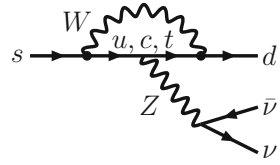
Kaon physics is the wellspring from which the SM flavor structure sprang out, giving forth ideas of GIM cancellation (hence charm), box diagrams, strong and electroweak penguins, as well as the experimental discovery of CPV, which lead to the KM postulate of 3 generations, before two generations were even complete. But despite its years, kaon physics is not yet a spent force. For New Physics, the focus is on the electroweak penguin processes  $K^+ \rightarrow \pi^+\nu\bar{\nu}$  and  $K_L \rightarrow \pi^0\nu\bar{\nu}$ , where the latter is  $CP$  violating. As depicted in Fig. 8.3, these are the original electroweak penguins where strong heavy quark mass dependence was uncovered by Inami and Lim [22]. The advantage of pursuing this program is the rather small theoretical uncertainties, thanks to the long history of kaon physics. Unlike  $D^0$  mixing of the previous section, these processes are short distance dominated, the main hadronic dependence is in the transition form factors, which can be extracted from similar charged current decays. A representative theoretical prediction [23] is

$$\mathcal{B}^{\text{SM}}(K^+ \rightarrow \pi^+\nu\bar{\nu}) = (9.11 \pm 0.72) \times 10^{-11}, \quad (8.10)$$

$$\mathcal{B}^{\text{SM}}(K_L \rightarrow \pi^0\nu\bar{\nu}) = (3.00 \pm 0.31) \times 10^{-11}, \quad (8.11)$$

where theoretical uncertainties are at the 10% level.

**Fig. 8.3** SM  $Z$  penguin diagram for  $s \rightarrow d\bar{\nu}\nu$  decay, which generates  $K^+ \rightarrow \pi^+\nu\bar{\nu}$  and  $K_L \rightarrow \pi^0\nu\bar{\nu}$  transitions



The other useful measurement, again because of short distance dominance, is the venerable and well measured  $\varepsilon_K$  parameter, which depends on  $f_K^2 B_K$ , and is a focus of lattice studies. If 10% measurement of the SM prediction for the  $K^+ \rightarrow \pi^+\nu\bar{\nu}$  and  $K_L \rightarrow \pi^0\nu\bar{\nu}$  modes can be achieved, then whether these two measurements would meet together with  $\varepsilon_K$  on the  $\bar{\rho}-\bar{\eta}$  plane is both a test of (3 generation) CKM structure, and a probe of BSM. The path is longer for the  $K_L \rightarrow \pi^0\nu\bar{\nu}$  mode, but there is also more reach for New Physics discovery.

### 8.2.1 Path to $K \rightarrow \pi\nu\nu$

The measurement of  $\varepsilon'/\varepsilon$  at the turn of the millennium [10] was a highlight of kaon physics. Despite the top effect through the electroweak penguin, which allowed  $\varepsilon'/\varepsilon$  to nearly vanish, unfortunately, the interpretation of  $\varepsilon'/\varepsilon$  is almost completely clouded by long-distance effects. For New Physics probes, we concentrate only on modes that are not marred by hadronic effects, but will return to a brief discussion of  $\varepsilon'/\varepsilon$  later.

#### $K^+ \rightarrow \pi^+\nu\bar{\nu}$

There was a long standing hint of 3 events for  $K^+ \rightarrow \pi^+\nu\bar{\nu}$  decay at BNL by the E787/949 experiments (an effort extending 20 years). These 3 events were based on  $7.7 \times 10^{12}$  (!) stopped  $K^+$ s at the BNL AGS proton accelerator, with pion momentum in the range  $211 < p_{\pi^+} < 229$  MeV/c, which is above the  $K^+ \rightarrow \pi^+\pi^0$  peak. With background estimated at  $0.44 \pm 0.05$  events, the measured branching ratio is  $\mathcal{B}(K^+ \rightarrow \pi^+\nu\bar{\nu}) = (1.47^{+1.30}_{-0.89}) \times 10^{-10}$  [10], which should be compared with the SM prediction, (8.10).

E949 extended the search to  $140 < p_{\pi^+} < 195$  MeV/c, which is *below* the  $K^+ \rightarrow \pi^+\pi^0$  peak, using a smaller sample of  $1.7 \times 10^{12}$  stopped  $K^+$  decays. Similar to the previous study above  $K^+ \rightarrow \pi^+\pi^0$  peak, one detects the incoming charged kaon, its decay at rest, together with an outgoing charged pion with no other detector activity in coincidence.

Active degraders were used for the final stage slow down of the incoming kaon, which gives coincidence with the decay in the target. For the emitted  $\pi^+$ , besides measuring its momentum, it is further brought to rest in a “range stack”, for sake of both positive identification as well as measurement of the energy. It is important to veto all other activity, especially photons, e.g. from the  $\pi^0$  in  $K^+ \rightarrow \pi^+\pi^0$  decay, which is the dominant background. Another background to deal with is  $\pi^+$



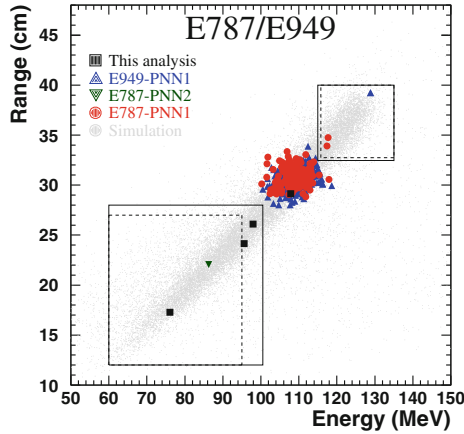


**Fig. 8.4** Measured energy versus range plot for events passing  $K^+ \rightarrow \pi^+\nu\bar{\nu}$  cuts. The 3 events in the smaller box at larger  $E_\pi$  are from the higher momentum  $\pi^+$  study, and the lower  $E_\pi$  box is for the update study below  $K^+ \rightarrow \pi^+\pi^0$  peak (the downward-pointing triangle is from earlier E787 data). The latter gives rise to the cluster of events around  $E_\pi \simeq 108$  MeV. The fine grey dots are simulated  $K^+ \rightarrow \pi^+\nu\bar{\nu}$  events. [From [24], used with permission]

rescattering in the target. The extended study to below the  $K^+ \rightarrow \pi^+\pi^0$  peak was possible by improvements made in background rejection via the active degrader and the range stack. A blind analysis was used, i.e. the “signal box” was opened only after the signal selection criteria, acceptance, and background estimates were all completed.

The pion energy versus range plot [24] of the final E949 analysis is given in Fig. 8.4. Although the signal region is smaller for the previously published analysis above the  $K^+ \rightarrow \pi^+\pi^0$  peak, it carries 4.2 times the sensitivity than the new analysis below the  $K^+ \rightarrow \pi^+\pi^0$  peak, due both to lower  $S/B$  as well as statistics for the latter. From the 3 events in the lower box of Fig. 8.4 alone, one gets  $\mathcal{B}(K^+ \rightarrow \pi^+\nu\bar{\nu}) = (7.89_{-5.10}^{+9.26}) \times 10^{-10}$ . Combining with the earlier result of E787/949 using the upper box, the final result is,

$$\mathcal{B}(K^+ \rightarrow \pi^+\nu\bar{\nu}) = (1.73_{-1.05}^{+1.15}) \times 10^{-10}, \quad (\text{E787/E949, 2008}) \quad (8.12)$$

where the central value is higher than, but still consistent with, SM prediction of (8.10). There may be some hint, but one cannot say there is a strong indication for New Physics.

### $K_L \rightarrow \pi^0\nu\bar{\nu}$

The E391a experiment, which ran at KEK PS, is the first dedicated experiment on  $K_L \rightarrow \pi^0\nu\bar{\nu}$ . It produced its first limit [25] of  $\mathcal{B}(K_L \rightarrow \pi^0\nu\bar{\nu}) < 6.7 \times 10^{-8}$  in 2008, and reached its final limit [26] of

$$\mathcal{B}(K_L \rightarrow \pi^0\nu\bar{\nu}) < 2.8 \times 10^{-8}, \quad (\text{E391a, 2010}) \quad (8.13)$$

at 90% C.L., by adding another dataset equivalent in size. The limit is of course very far away from the SM expectation of (8.10). But this also means that there is great potential for discovery of BSM physics. Note that this decay is intrinsically  $CP$  violating, since the decay amplitude is the *difference* between  $K^0$  and  $\bar{K}^0$  decay because of the  $K_L$  wavefunction. This adds to the interest in this mode as a probe of New Physics.

$K_L \rightarrow \pi^0 \nu \bar{\nu}$  search is considerably more challenging than  $K^+ \rightarrow \pi^+ \nu \bar{\nu}$ . The beam is more difficult, while the signal is just 2 photons (from  $\pi^0$ ) and *nothing else*. Besides measuring these two photons well but not even demanding  $m_{\gamma\gamma} = m_{\pi^0}$  while vetoing everything else, one needs to reconstruct the  $K_L$  decay vertex along the beam direction. This requires a ‘‘pencil’’ beam. The discriminant is then missing  $p_T$  (carried away by  $\nu \bar{\nu}$ ) versus  $Z_{\text{vertex}}$ , which forms the fiducial region that must be studied very carefully.

To reduce backgrounds from beam-gas interaction, the  $K_L$  decay region is maintained at the high vacuum of  $10^{-5}$  Pa, while separated from the detector region by a thin membrane. The main background is from  $K_L \rightarrow \pi^0 \pi^0 (\pi^0)$ , where two (four) photons escape detection, and neutron halo of the beam that interact with the detector and produce  $\pi^0$  and  $\eta$  mesons. The latter turned out to dominate for E391a. In fact, for the three run periods at the 12 GeV PS, the first period suffered from serious neutron-induced backgrounds that were caused by the drooping of the membrane. Having fixed this, for the second run period, the  $K_L \rightarrow \pi^0 \pi^0$  background was estimated by MC simulation, and verified with reconstructed  $4\gamma$  events. To understand neutron halo background, a dedicated run with an inserted aluminum plate was undertaken.

The signal box was opened only after all selection criteria and background estimates were determined. No events were seen in the neutral pion  $p_T$  versus  $Z_{\text{vertex}}$  signal region. The number of  $K_L$  decays were estimated at  $5.1 \times 10^9$  (this is considerably smaller than  $N_{K^+} \sim 10^{13}$  of  $K^+$  study) by measuring the number of  $K_L \rightarrow \pi^0 \pi^0$  events. Together with signal acceptance estimated at 0.67% and background estimate of  $0.41 \pm 0.11$  events (neutron dominant), the single event sensitivity is found to be  $\sim 2.9 \times 10^{-8}$ . With no events in the signal box, the limit of  $6.7 \times 10^{-8}$  was extracted. The limit was improved by adding data from the third run, equivalent in statistics to the second, where again no signal events were found, and the limit of (8.13) was reached.

It is useful now to bring in the Grossman–Nir bound. The following model-independent and solid relation holds [27] due to isospin symmetry,

$$\mathcal{B}(K_L \rightarrow \pi^0 \nu \bar{\nu}) < 4.3 \times \mathcal{B}(K^+ \rightarrow \pi^+ \nu \bar{\nu}), \quad (8.14)$$

where 4.3 is largely from  $K_L$  versus  $K^+$  lifetime ratio. Using the 90% C.L. upper limit of E949 derived from (8.12), one gets the ‘‘Grossman–Nir bound’’ of

$$\mathcal{B}(K_L \rightarrow \pi^0 \nu \bar{\nu}) < 1.4 \times 10^{-9}, \quad (\text{‘‘GN bound’’}) \quad (8.15)$$

which is 20 times more stringent than the E391a bound of (8.13). One can imagine the frustration with the  $K_L$  worker! A common conception is that one starts to probe

New Physics with  $K_L \rightarrow \pi^0\nu\nu$  only *after* one crosses the “GN bound”, a point which we shall return to in the next subsection.

### 8.2.2 Pushing the Frontier: NA62 and KOTO

After the  $\varepsilon'/\varepsilon$  measurement, the U.S. somehow dismantled its kaon program, which still has not recovered. In Europe, while  $\phi$  factory efforts like KLOE continued, the main effort at CERN was to develop towards  $K^+ \rightarrow \pi^+\nu\bar{\nu}$  observation. The NA48 experiment first went through the transformation of NA48/1 and NA48/2, pursuing several kinds of rare  $K$  and hyperon studies. But by the late 2000s, a new experiment, NA62, was formed, where the first phase was the  $R_K = K_{e2}/K_{\mu2}$  program, or the ratio of  $K^+ \rightarrow e^+\nu$  versus  $K^+ \rightarrow \mu^+\nu$  (the original “ $R_K$ ”), which was in part motivated by the  $B^+ \rightarrow \tau^+\nu$  “excess” at the B factories.

We have already mentioned E391a working in Japan at the KEK PS. This was in part due to the attraction of developing the J-PARC (Japan Proton Accelerator Research Complex) facility with the 30 GeV (50 GeV capable) Main Ring. E391a could be viewed as the pilot study for the more ambitious KOTO experiment (originally the E14 proposal) for  $K_L \rightarrow \pi^0\nu\bar{\nu}$  search. A bit unfortunately, this was a time where budget limitations started to set in even for Japan, which e.g. affected the construction schedule of the  $K_L$  beam-line.

#### NA62: $K^+ \rightarrow \pi^+\nu\nu$ at CERN

The aim of the NA62 experiment [28] is to observe  $K^+ \rightarrow \pi^+\nu\bar{\nu}$ . Assuming the SM branching ratio of (8.10) at  $10^{-10}$  level, NA62 aims at reaching  $\mathcal{O}(100)$   $K^+ \rightarrow \pi^+\nu\bar{\nu}$  events, or 10% precision, running at the North Area of SPS. Unlike E787/E949, NA62 uses 75 GeV/c  $K^+$  mesons decaying in flight, to provide better kinematic constraints for signal selection. The existing beam-line as well as the NA48 detector are modified and upgraded. For background rejection, the  $K^+$  momentum is measured by pixel detectors upstream to improve the kinematic constraint, photons (from  $\pi^0$ ) are vetoed, and the  $\pi^+$  momentum is measured with precision and positive PID. The benefit of a full fledged detector and beam-line program is a long list of rare  $K^+$ ,  $\pi^+$  and  $\pi^0$  decays that one could study. There were further thoughts to upgrade NA62 and the CERN proton complex to reach  $\sim 1000$   $K^+$  events, followed by  $\sim 100$   $K_L$  events with further upgrades.

After approval and construction, the pilot run finally started in 2014, followed by commissioning run in 2015, which extended into 2016, but physics data taking did start. The remaining LHC Run 2 years, 2017 and 2018, were full data taking years. The first physics result, based on 2016 data, came out in 2018.

We have already mentioned kinematic constraints. Whether decay at rest or in-flight, both E787/E949 and NA62 try to measure the  $K^+$  and  $\pi^+$  momenta as precisely as possible. This is because the biggest background concern is  $K^+ \rightarrow \pi^+\pi^0$ , which has 20.7% branching fraction, and sits between the two signal boxes of Fig. 8.4.

Between the two signal boxes,  $m_{\text{miss}}^2 = (p_{K^+} - p_{\pi^+})^2$  in the 0.01–0.025 GeV<sup>2</sup> range, i.e. roughly 100 to 160 MeV mass window around  $\pi^0$ , are effectively blocked out. This kinematic exclusion is not an active veto, but is a crucial element in detector setup for collecting  $K^+ \rightarrow \pi^+ \nu \bar{\nu}$  events but rejecting the most threatening background,<sup>4</sup> which we will come back to. Put another way, the  $\pi^0$  window is “too bright to behold”.

The two signal regions are similar to E787/E949. One of course needs to contend with backgrounds such as  $K^+ \rightarrow \pi^+ \pi^+ \pi^-$  and  $\mu^+ \nu$ . For instance, the latter restricts the signal box to  $p_{\pi^+} < 35$  GeV in lab frame. The first  $K^+ \rightarrow \pi^+ \nu \nu$  data set, corresponding to one month in 2016, was analyzed and reported at Summer 2018 conferences [29]. With a blind analysis, the single event sensitivity was determined to be  $\text{SES} = (3.15 \pm 0.01 \pm 0.24) \times 10^{-10}$ , with e.g.  $K^+ \rightarrow \pi^+ \pi^0, \mu^+ \gamma, \pi^+ \pi^- e^+ \nu$  and upstream backgrounds under control. The expected SM signal event was found at 0.27 level, and total background expectation at  $0.15 \pm 0.09 \pm 0.01$ . Upon open box, one event was found, with clear  $\pi^+$ -ID in RICH detector. The preliminary upper limit [29] was set at  $\mathcal{B}(K^+ \rightarrow \pi^+ \nu \bar{\nu}) < 10 (14) \times 10^{-10}$  at 90% (95%) C.L., which is consistent with SM, (8.10), as well as E787/E949, (8.12). But perhaps a bit unfortunately, the observed event sits at the corner of the signal box in Region 2, which may cause NA62 to further scrutinize their analysis approach.

The 2017 data is 20 times the size of 2016, and 2018 data should be comparable, with improvements in background control. One should expect, therefore, a major improvement (20 events for SM expectation) in the measurement of  $\mathcal{B}(K^+ \rightarrow \pi^+ \nu \bar{\nu})$ , concurrent with Belle II data taking. Of course, after Long Shutdown 2 (LS2) of the LHC, NA62 would certainly continue to take data during LHC Run 3.

### **KOTO: $K_L \rightarrow \pi^0 \nu \nu$ at J-PARC**

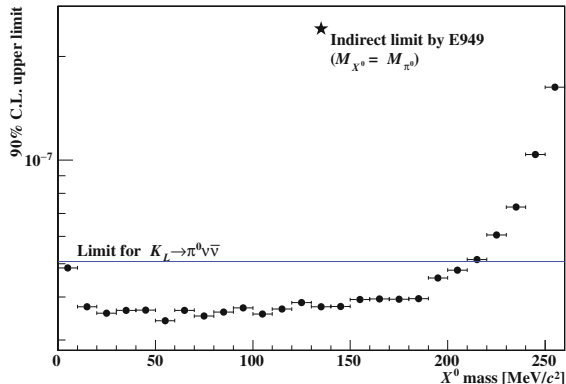
The KOTO experiment [30] got its name from “KO at TOKai”, as Tokai is where J-PARC is located. The KOTO detector is modified from the E391a detector. The  $K_L$  yield and run period at J-PARC will gain quite significantly from KEK PS. One key upgrade of the detector is the reuse of the KTeV CsI calorimeter, which is longer and finer segmented than the one used in E391a. Together with new readout (waveform digitization), better resolution can be achieved. The beam-line is newly designed based on experience gained from E391a to reduce beam halo, and allows further improvement. The vetoes are also improved. Overall, the aim for KOTO is to reach 10 events, assuming SM expectation of  $3 \times 10^{-11}$ , (8.11). If there is New Physics enhancement, discovery could come earlier, but if SM persists, then a 10% measurement requires  $\mathcal{O}(100)$  events, which would probably take another decade or more to reach, in J-PARC Phase 2.

After the 2011 earthquake and tsunami, which caused some damage at J-PARC, physics run finally started in 2013. The run, however, was shutdown at 100h (!) due to the “incident” at J-PARC, and did not restart until 2015. But this may have been a

---

<sup>4</sup>Background rejection at  $> 10^{12}$  is necessary.

**Fig. 8.5** Upper limit on  $\mathcal{B}(K_L \rightarrow \pi^0 \nu \bar{\nu})$  (horizontal line) at 90% C.L. from KOTO based on 2013 data [31], together with bound on  $\mathcal{B}(K_L \rightarrow \pi^0 X^0)$  versus  $m_{X^0}$ , compared with the indirect limit [32] from E949 ( $\star$ ). [Courtesy KOTO Collaboration]



mixed blessing, as detailed studies helped improve the detector and software for the 2015 run and onwards.

The major physics background, like  $K^+ \rightarrow \pi^+ \pi^0$  for NA62, is  $K_L \rightarrow \pi^0 \pi^0$  for KOTO, so there is hermetic veto around the decay volume. Since just two photons are detected, the  $p_T$  and decay point along  $Z$  direction defines the signal region. Even if the run time was very limited, three types of backgrounds emerged at the 2013 run. Two were due to beam halo neutrons, either producing upstream  $\pi^0$ s, or scattering off the detector downstream, producing two hits that mimic signal. A third type is a  $K_L \rightarrow \pi^+ \pi^- \pi^0$  decay where the  $\pi^+ \pi^-$  both pass through the beamhole. Methods that were developed to mitigate these backgrounds, both in added hardware and in software improvements, were tested with the first equivalent amount of data in 2015, leading to further improved understanding and control of background. When signal box was finally opened just before KAON2016, one event was observed against the expectation of 0.34 events, and the upper limit [31] is  $5.1 \times 10^{-8}$  at 90% C.L., almost a factor of two worse than the E391a result of (8.13). This limit is shown in Fig. 8.5, where further discussion of bound on  $K_L \rightarrow \pi^0 X^0$ , in relation with a result from E949 [32], is given in the next subsection.

But the improvements helped facilitate the 2015 run, which accumulated 20 times the data of the 2013 run, and its analysis. KOTO reported [33] the result based on 2015 data at 2018 summer conferences,

$$\mathcal{B}(K_L \rightarrow \pi^0 \nu \bar{\nu}) < 3.0 \times 10^{-9}, \quad (\text{KOTO prelim., 2018}) \quad (8.16)$$

at 90% C.L., which improves the E391a result, (8.13), by an order of magnitude. Besides the data increase and analysis methods developed through the study of 2013 data [31], it reflects zero events in the signal box.

As illustrated, KOTO is an experiment based on vetoing background, so the approach is to learn along the way. The data from the 2016–2018 physics run should allow KOTO to push SES from  $1.3 \times 10^{-9}$ , achieved in analysis of 2015 data [33], down to  $5 \times 10^{-10}$ . There would be further detector upgrades in 2018, and

beam power would increase from 50 to 90 kW gradually. The planned 3-year run for 2019–2021 would push SES down to  $10^{-11}$  level, towards SM sensitivity. The effort is painstakingly slow, but steady.

### 8.2.3 *Kaon Prospects*

The years after LHC Run 2 appear particularly ripe for flavor physics. Not only we have the myriad  $B$  anomalies while Belle II emerges on the scene, both  $K^+ \rightarrow \pi^+ \nu \bar{\nu}$  and  $K_L \rightarrow \pi^0 \nu \bar{\nu}$  measurements also have rather good prospects, and discoveries could be made.

What New Physics could there be? Since  $K \rightarrow \pi \nu \bar{\nu}$  decay arises from the electroweak penguin (Fig. 8.3), which has strong  $m_t$  dependence for the 3 generation Standard Model, it allows great sensitivity to the 4th generation, and *rather large enhancements of  $K_L \rightarrow \pi^0 \nu \bar{\nu}$  decay was predicted* [16], in correlation with  $\Delta \mathcal{A}_{K\pi}$  (Sect. 2.2). Alas,  $\sin 2\Phi_{B_s} \sim 0$  as measured by LHCb (Sect. 3.2), together with the observed 125 GeV boson behaving just like the SM Higgs boson, have made the 4th generation effect unlikely.

#### $K \rightarrow \pi X^0$ and Grossman–Nir Bound

To illustrate that kaon physics is not a “spent” field, we offer the case of  $K \rightarrow \pi X^0$  decay [34], where  $X^0$  is a dark-like object with  $m_{X^0} \sim m_{\pi^0}$  that could have so far evaded detection, but could in fact be lurking all this time since the E787/E989 era.

The two signal boxes of Fig. 8.4 is in fact rather familiar: in between the two signal regions,  $K^+ \rightarrow \pi^+ \pi^0$  has 20.7% branching fraction and needs to be excluded kinematically, because it is “too bright to behold”. Could Nature, therefore, trick us by “hiding” a dark-like object in this blinding spot? The E949 experiment, the successor of E787, was aware of this, and set the task to measure  $\pi^0 \rightarrow \nu \nu$  by tagging the  $\pi^+$  in  $K^+ \rightarrow \pi^+ \pi^0$  decay. A study showed  $\sim 3$  non- $K\pi 2$  background events, but upon open box, 99 events were found. These were attributed to photon detection *inefficiency*, which is amusing, as one usually strives to understand detection efficiency. Patching up the result, E949 gave the rather poor limit [32],

$$\mathcal{B}(\pi^0 \rightarrow \nu \bar{\nu}) < 2.7 \times 10^{-7}, \quad (\text{E949, 2005}) \quad (8.17)$$

at 90% C.L., which gives rise to [32]

$$\mathcal{B}(K^+ \rightarrow \pi^+ X^0) < 5.6 \times 10^{-8}, \quad (\text{E949, 2005}) \quad (8.18)$$

for  $m_{X^0} = m_{\pi^0}$  and assumed stable. This limit is a factor 200 poorer than the one from (8.12) for  $K^+ \rightarrow \pi^+ \nu \nu$  from the same data.

This episode was somewhat forgotten in the arduous pursuit of  $K \rightarrow \pi \nu \nu$ . In particular, E391a and KOTO were preoccupied with the thought that the “GN bound”

of (8.15) marks the starting point for them to get into the business of probing New Physics. As NA62 continues the practice of kinematic exclusion of the  $\pi^0$  window, KOTO in fact does not have such luxury. One is unable to measure the incoming  $K_L$  momentum, and one does not fully “ID” the two observed photons as forming a  $\pi^0$ . Thus, one cannot have kinematic control. Instead, much like a blind man, KOTO’s approach is based on “feeling”, i.e. understanding background, and design methods to reject them. As such, KOTO in fact can [34] “feel the presence” of a non-decaying or invisible  $X^0$ , in the  $\pi^0$  mass window.

Realizing this, in their first published physics paper, KOTO gave [31] also the bounds on  $\mathcal{B}(K_L \rightarrow \pi^0 X^0)$  versus  $m_{X^0}$ , as efficiency and acceptance vary (see Fig. 8.5). Shown also is the E949 result of (8.18), now reverse-scaled by the isospin relation of (8.14), which, unlike the “GN bound” of (8.15), is the essence of the Grossman–Nir bound. Thus, even with the meager amount of 2013 data, KOTO was able to improve upon the E949 result by roughly a factor of 6! This opens up a new avenue for New Physics search.

While the notion [34] discussed above should have emerged from the  $K_L$  proposal or its review process, it was unveiled quite inadvertently. In Sect. 7.2, we have mentioned the model [35] built around the gauged  $L_\mu - L_\tau$  symmetry to account for the  $P'_5$  anomaly, where vector-like quarks were introduced that mix with SM quarks to generate effective  $bsZ'$  coupling at tree level. Turning to investigate the muon  $g - 2$  anomaly, the same authors of [35] discovered that the so-called neutrino trident process rules out the  $Z'$  above 400 MeV in mass [36]. This then motivated a study of  $K \rightarrow \pi Z'$  and  $B \rightarrow K^{(*)} Z'$  phenomenology (published later as [37]), which are induced by analogous  $tcZ'$  or  $ttZ'$  couplings at loop level. But with BaBar [38] practically ruling out a muonic dark force above the dimuon threshold, the remaining thing to check is  $Z' \rightarrow \nu\nu$  below  $m_{Z'} < 2m_\mu$ . It was through this investigation that the “ $\pi^0$  loophole” was uncovered [34]. Although this somewhat built-up model provides just an existence proof, it serves as a reminder for us to stay on the alert and check our premises and working assumptions, such that we do not miss out on experimental opportunities that may be right before us.

So,  $K_L \rightarrow \pi^0 + \text{nothing}$  search<sup>5</sup> is also a search for  $K_L \rightarrow \pi^0 X^0$ , where  $X^0$  is a dark or dark-like object (the  $Z'$  example decays to  $\nu\nu$  promptly hence cannot be DM). This search defies the traditional “GN bound” constraint, even as the latter changes with new measurements by NA62. But what about NA62 and  $K^+ \rightarrow \pi^+ + \text{nothing}$  search? Recall the E949 search [32] for  $\pi^0 \rightarrow \nu\nu$  by tagging the  $\pi^+$  from  $K^+ \rightarrow \pi^+ \pi^0$ , the issue is the understanding of photon detection inefficiency. One needs to study/understand calorimeter sampling fluctuations for lower energy photons, and photonuclear interactions, such as with neutrons, for higher energy photons. This is no easy feat, but is needed for NA62 to be able to compete with KOTO on the new front of  $K \rightarrow \pi + X^0$  search. Given that the path is long for both experiments, we are optimistic that NA62 would follow up on this.

---

<sup>5</sup>A parallel holds for  $B \rightarrow K^{(*)} + \text{nothing}$  search at Belle II. Recall the mild excess in lowest  $q^2$  bin of BaBar’s  $B \rightarrow K^{(*)} \nu\nu$  study (Sect. 5.3.1).

## Resurgent $\varepsilon'/\varepsilon$ and Other New Physics

There has been renewed interest in whether  $\varepsilon'/\varepsilon$  probes New Physics, if not already providing a strong hint. When  $\varepsilon'/\varepsilon$  was observed at the turn of the millennium, despite its tiny value, people were disillusioned by the constraint provided by  $\varepsilon'/\varepsilon$ , as the process suffers from very large hadronic uncertainties. The various hadronic matrix elements seem too hard to evaluate precisely. Lattice workers, however, have taken up the challenging tasks. After several decades of efforts, there has been a recent measurement [39] by RBC+UKQCD collaboration,

$$\begin{aligned} \text{Re}(\varepsilon'/\varepsilon)|_{\text{latt}} &= \text{Re} \left\{ \frac{i\omega e^{i(\delta_2 - \delta_0)}}{\sqrt{2}\varepsilon} \left[ \frac{\text{Im}A_2}{\text{Re}A_2} - \frac{\text{Im}A_0}{\text{Re}A_0} \right] \right\} \\ &= (1.38 \pm 5.15 \pm 4.59) \times 10^{-4}, \quad (\text{RBC/UKQCD}) \quad (8.19) \end{aligned}$$

where  $A_0$  and  $A_2$  are the  $I = 0, 2$  decay amplitudes, respectively,  $\delta_I$  are the strong phase shifts, and  $1/\omega = \text{Re}A_0/\text{Re}A_2 \simeq 22.5$  is from experiment. The RBC-UKQCD value is considerably smaller than the observed  $\text{Re}(\varepsilon'/\varepsilon)|_{\text{exp}} \simeq 17 \times 10^{-4}$ . This has drawn interests from some theorists (see e.g. [40], and references therein). We shall not go into this. On one hand, the theory efforts that followed were not genuine predictions, but stimulated by the lattice result. On the other hand, the discrepancy so far is not much more than  $2\sigma$ , and RBC+UKQCD needs to improve on their errors, which they are working on. But, would there be a second, independent lattice effort to confirm (8.19)? And, would a new experiment eventually form to remeasure  $\varepsilon'/\varepsilon$ ?

What other New Physics may be probed by kaon physics? One example is searching for the Dark Photon, where e.g. a bound by NA48/2 [41] appears in Fig. 7.3. Since NA62 is the successor of NA48/2, it would of course continue to pursue this subject, as well as axion-like particles, heavy neutral leptons, etc. Some of these New Physics are discussed from theory perspective, e.g. in [40]. NA62 also plans for future upgrades, for example the KLEVER project [42] to measure  $\mathcal{B}(K_L \rightarrow \pi^0 \nu\nu)$  at CERN SPS.

Rare kaon decays are an integral part of the flavor program, where prospects look good for the next decade.

## References

1. Gell-Mann, M., Pais, A.: Phys. Rev. **97**, 1387 (1955)
2. Falk, A.F., et al.: Phys. Rev. D **69**, 114021 (2004)
3. Bigi, I.I., Uraltsev, N.: Nucl. Phys. B **592**, 92 (2001)
4. Starič, M., et al. [Belle Collaboration]: Phys. Rev. Lett. **98**, 211803 (2007)
5. Zhang, L.M., et al. [Belle Collaboration]: Phys. Rev. Lett. **96**, 151801 (2006)
6. Aubert, B., et al. [BaBar Collaboration]: Phys. Rev. Lett. **98**, 211802 (2007)
7. Zhang, L.M., et al. [Belle Collaboration]: Phys. Rev. Lett. **99**, 131803 (2007)
8. Aaltonen, T., et al. [CDF Collaboration]: Phys. Rev. Lett. **100**, 121802 (2008)
9. Bergmann, S., et al.: Phys. Lett. B **486**, 418 (2000)



10. Tanabashi, M., et al. [Particle Data Group]: Phys. Rev. D **98**, 030001 (2018). <http://pdg.lbl.gov/>
11. Heavy Flavor Averaging Group (HFLAV; acronym changed from HFAG to HFLAV in March 2017). <http://www.slac.stanford.edu/xorg/hflav>
12. Poluektov, A., et al. [Belle Collaboration]: Phys. Rev. Lett. **70**, 072003 (2004)
13. Falk, A.F., Grossman, Y., Ligeti, Z., Petrov, A.A.: Phys. Rev. D **64**, 054034 (2002)
14. Golowich, E., Hewett, J., Pakvasa, S., Petrov, A.A.: Phys. Rev. D **76**, 095009 (2007)
15. Hou, W.-S., Soni, A., Steger, H.: Phys. Lett. B **192**, 441 (1987)
16. Hou, W.-S., Nagashima, M., Soddu, A.: Phys. Rev. D **76**, 016004 (2007)
17. Aaij, R., et al. [LHCb Collaboration]: Phys. Rev. Lett. **108**, 111602 (2012)
18. Aaltonen, T., et al. [CDF Collaboration]: Phys. Rev. Lett. **109**, 111801 (2012)
19. Aaij, R., et al. [LHCb Collaboration]: JHEP **1407**, 041 (2014)
20. Aaij, R., et al. [LHCb Collaboration]: Phys. Rev. Lett. **118**, 261803 (2017)
21. Asner, D.M., Sun, W.M.: Phys. Rev. D **73**, 034024 (2006)
22. Inami, T., Lim, C.S.: Prog. Theor. Phys. **65**, 297 (1981)
23. Buras, A.J., Buttazzo, D., Girrbach-Noe, J., Knegjens, R.: JHEP **1511**, 033 (2015)
24. Artamonov, A.V., et al. [E949 Collaboration]: Phys. Rev. Lett. **101**, 191802 (2008)
25. Ahn, J.K., et al. [E391a Collaboration]: Phys. Rev. Lett. **100**, 201802 (2008)
26. Ahn, J.K., et al. [E391a Collaboration]: Phys. Rev. D **81**, 072004 (2010)
27. Grossman, Y., Nir, Y.: Phys. Lett. B **398**, 163 (1997)
28. See <http://test-na62.web.cern.ch/test-NA62/>
29. See e.g. Engelfried, J.: Talk Presented at Flavor Physics and CP Violation Conference (FPCP2018), Hyderabad, India, July 2018
30. See <http://koto.kek.jp/>
31. Ahn, J.K., et al. [KOTO Collaboration]: PTEP **2017**, 021C01 (2017)
32. Artamonov, A.V., et al. [E949 Collaboration]: Phys. Rev. D **72**, 091102 (2005)
33. See e.g. Shiomu, K.: Talk Presented at ICHEP2018 Conference, Seoul, Korea, July 2018
34. Fuyuto, K., Hou, W.-S., Kohda, M.: Phys. Rev. Lett. **114**, 171802 (2015)
35. Altmannshofer, W., Gori, S., Pospelov, M., Yavin, I.: Phys. Rev. D **89**, 095033 (2014)
36. Altmannshofer, W., Gori, S., Pospelov, M., Yavin, I.: Phys. Rev. Lett. **113**, 091801 (2014)
37. Fuyuto, K., Hou, W.-S., Kohda, M.: Phys. Rev. D **93**, 054021 (2016)
38. Lees, J.P., et al. [BaBar Collaboration]: Phys. Rev. D **94**, 011102 (2016)
39. Bai, Z., et al. [RBC+UKQCD Collaboration]: Phys. Rev. Lett. **115**, 212001 (2015)
40. Buras, A.J.: Acta Phys. Polon. B **49**, 1043 (2018)
41. Batley, J.R., et al. [NA48/2 Collaboration]: Phys. Lett. B **746**, 178 (2015)
42. See e.g. Moulson, M.: Talk Presented at ICHEP2018 Conference, Seoul, Korea, July 2018

# Chapter 9

## Lepton Number Violation and $\mu, \tau$ Systems



In this chapter we consider lepton flavor violation (LFV) in the charged lepton sector, which is something we have never observed yet. If they exist, the source has to lie outside of the SM. Before discussing the relative new field of LFV  $\tau$  decay search at the B factories and the future, we briefly discuss  $\mu \rightarrow e$  transitions, such as  $\mu \rightarrow e\gamma$  and  $\mu \rightarrow e$  conversion on nuclei, the search of which has a history as long as particle physics itself. Inevitably, we then also touch upon muon  $g - 2$  and electric dipole moments.

We will cover rare or radiative  $\tau$  decays, which have  $b \rightarrow s$  echoes, and the enigmatic (if found) baryon number violating decays. There should be no doubt that we would have uncovered Beyond the Standard Model physics if any of these are observed. Here, it is again the B factories that have pushed the frontiers. Compared to the 1.1 nb cross section for  $e^+e^- \rightarrow B\bar{B}$  and 1.3 nb for  $e^+e^- \rightarrow c\bar{c}$ , the  $e^+e^- \rightarrow \tau^+\tau^-$  cross section of 0.9 nb is not far behind. Thus, B factories are also tau and charm factories!

Of course, LFV is already observed in neutrino oscillations, despite and probably because of the extreme smallness of neutrino masses. This is a great subject of its own which we have not covered. The study of mixing in the neutrino sector has truly blossomed since 1998. Two unexpectedly large mixing angles were first uncovered, which are in strong contrast to the hierarchical angles seen in the quark sector. A tremendous drive to measure  $\theta_{13}$  mixing angle followed, to hopefully open the chapter on CPV in neutrino sector. This goes hand in hand with lofty ideas such as leptogenesis, the proposal that the baryon asymmetry of the Universe came through some lepton asymmetry in the early Universe at an earlier step. To the surprise of everyone,  $\theta_{13}$  was discovered to be not quite small, and the neutrino field is no less robust than our general flavor field, but discussion of which is outside our scope.

## 9.1 $\mu \rightarrow e$ Transitions, $g - 2$ and EDM

The muon was discovered in  $\mu \rightarrow e\bar{\nu}_e\nu_\mu$  decay, which occurs practically 100% of the time. The fact that the kinematically allowed  $\mu \rightarrow e\gamma$  seemed completely absent was the first indication that the electron and the muon numbers are separately conserved.

With the observation of neutrino oscillations, hence neutrinos have mass,  $\mu \rightarrow e\gamma$  is then in principle generated, through diagrams similar to Fig. 4.1a, but with neutrinos in the loop and the photon radiating off the  $W$  boson. However, because of the extreme smallness of neutrino masses, the rate vanishes as  $|\Delta m_\nu^2|^2/M_W^4$ , and the generated rate is less than  $10^{-50}$ ! In the limit of strictly massless neutrinos, the original definition of SM, then separate lepton numbers are automatically conserved. Turning this around, this means that *any* measurement of  $\mu \rightarrow e\gamma$  would constitute discovery of BSM physics.

### 9.1.1 $\mu \rightarrow e$ Transitions

#### $\mu \rightarrow e\gamma$

The first phase of experiments were conducted in the 1950s. By the mid-1960s, limits on  $\mu \rightarrow e\gamma$  had already reached down to  $10^{-8}$ . A second round of experiments in the 1970s reached  $10^{-10}$ , after which the design and construction of  $\mu \rightarrow e\gamma$  experiments (like most other particle physics experiments) became stretched in time at the turn of the millennium, the MEGA experiment at LAMPF gave the limit [1]

$$\mathcal{B}(\mu \rightarrow e\gamma) < 1.2 \times 10^{-11}, \quad (\text{MEGA, 1999}) \quad (9.1)$$

at 90% C.L.<sup>1</sup> The MEGA result came out around the exciting time of the 1998 observation of  $\nu_\mu$  to  $\nu_\tau$  (“atmospheric”) neutrino oscillations. Together with the near completion of B factories, they inspired many theoretical studies on  $\mu \rightarrow e\gamma$  and  $\tau \rightarrow \ell\gamma$  (see [3] as an example). Not surprisingly, these BSM theories suggest, in the SUSY-GUT context, that  $\mu \rightarrow e\gamma$  could occur in the  $10^{-15}$ – $10^{-11}$  range. Diagrammatically, these processes occur through loop processes similar to Fig. 9.1a shown for  $\tau \rightarrow \mu\gamma$  transitions in the next section, through slepton mixing effects in the loop. A new experiment capable of probing this range, MEG at PSI, aimed at reaching below  $10^{-13}$ , rose to this challenge. Physics runs started in late 2008 and finished in 2013. The upgraded MEG II experiment will enter engineering run in 2019, continuing with physics run until 2021.

As the extremely impressive limit of (9.1) suggests, MEG needs to push hard on background reduction. The signal consists of a 52.8 MeV positron back-to-back with a 52.8 MeV photon in time coincidence, and coming from a common origin. With the muon stopped to decay at rest, positive charge is selected to avoid muon capture

<sup>1</sup>A different type of LFV probe, e.g. that of  $K \rightarrow \pi\mu^\pm e^\mp$ , also have limits reaching below  $10^{-10}$  level [2].

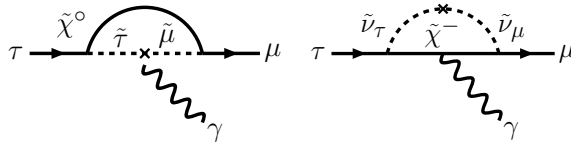


**Fig. 9.1** Diagrams illustrating  $\tau \rightarrow \mu\gamma$  transition induced by SUSY loops. Lepton flavor violation is indicated by the cross, or mixing, of different flavored sleptons

by nucleus. Accidental overlap of events (an  $e^+$  from  $\mu^+ \rightarrow e^+\nu_e\bar{\nu}_\mu$  and a  $\gamma$  from  $\mu^+ \rightarrow e^+\gamma\nu_e\bar{\nu}_\mu$ ) is the dominant background. Thus, a DC muon beam, rather than a pulsed one, is used. The 590 MeV cyclotron at PSI is the world's most powerful proton cyclotron for this purpose.

Several special detector designs are worthy of note. For  $e^+$  detection at the low energy of 52.8 MeV, sensitive but very low mass drift chambers were designed and constructed, together with a timing counter that is the world's best in performance ( $\sigma_t \sim 40$  ps). A special COBRA (COnstant Bending RAdius) magnet was designed with graded, rather than uniform  $B$  field, to provide constant  $e^+$  bending radius, independent of the  $e^+$  emission angle. For a uniform field, a low energy  $e^+$  tends to be swept out too quickly. For photon detection and measurement, liquid Xenon as scintillator was chosen. The light yield is comparable (80%) to NaI, but with fast response (4.2 ns) and short decay time. Because of the narrow temperature range between liquid and solid Xe phases, care must be taken for reliable and stable temperature control.

With these specially designed subdetectors, including the DAQ readout system, MEG went through stages of engineering runs, and took data between 2009 and 2013. The final result of the MEG experiment [4] is

$$\mathcal{B}(\mu \rightarrow e\gamma) < 4.2 \times 10^{-13}, \quad (\text{MEG}, 2016) \quad (9.2)$$

at 90% C.L., which improves the result of MEGA [1], (9.1), by a factor of 30. Earlier MEG results are documented in PDG [2].

From experience gained, MEG pushed for upgrade to Phase II, aiming to probe below  $10^{-14}$ . With absence of SUSY so far at the LHC, traditional MSSM and SUSY-GUT model expectations for  $\mu \rightarrow e\gamma$  are now somewhat mute. But given that pockets or cracks of parameter space do remain, it would be interesting to watch the correlation [5] between  $\mu \rightarrow e\gamma$  and muon  $g - 2$  in SUSY context. Motivated by large neutrino mixing [2] and still in context of SUSY, linking with flavor symmetries suggest [6]  $\mathcal{B}(\mu \rightarrow e\gamma)$  at the  $10^{-13}$  level, while linking [7] with seesaw and baryogenesis-through-leptogenesis still leaves some parameter space to be probed, even if (from this perspective)  $\tau \rightarrow \mu\gamma$  may not be promising at Belle II.

Besides increased beam current, MEG-II detector upgrade basically improves by a factor of two in resolution in all aspects, e.g. changing from 2" PMT to SiPM for the LXe photon detector. The aim is to improve the MEG limit by another order of magnitude, to the  $6 \times 10^{-14}$  level or lower. After pilot runs in 2017 and 2018, it will enter engineering run and take physics data for the 3 years of 2019–2021.

### $\mu \rightarrow e$ Conversion

There are further LFV probes using muons, such as  $\mu \rightarrow e$  conversion on nuclei, and  $\mu \rightarrow eee$ . If  $\mu \rightarrow e\gamma$  probes the dipole transition, these probe different effective contact interactions. The former is related to SUSY and neutrino mixing, but new contact interactions have even broader coverage of possible NP, including  $Z'$ , extra Higgs, heavy neutrinos, leptoquark, compositeness, etc., i.e. similar to the LHC, with higher reach in NP scale, up to  $10^4$  TeV. We cannot do justice to the potential physics contact, but refer the reader to [8] for a review (which probably needs an update with LHC results). We refrain from going into  $\mu^+ \rightarrow e^+e^-e^+$ ,<sup>2</sup> but cover  $\mu \rightarrow e$  conversion on nuclei briefly.

The current limit on  $\mu \rightarrow e$  conversion is held by SINDRUM II [10],

$$R_{\mu e} = \frac{\Gamma(\mu + (A, Z) \rightarrow e + (A, Z))}{\Gamma(\mu + (A, Z) \rightarrow \nu_\mu + (A, Z - 1))} < 7 \times 10^{-13}, \quad (\text{SINDRUM II, 2006}) \quad (9.3)$$

at 90% C.L., with muonic atoms formed on gold nucleus. The conversion electron has energy basically the same as the muon mass. The limit of (9.3) is somewhat dated, but improvement with same method would not be easy, as the SINDRUM II experiment already consumed  $\sim 1$  MW proton beam power. Next generation experiments are based on the idea [11] of using strong solenoidal B fields to confine soft pions for decay, then collect the decay muons, which drastically reduces the required beam power. Thus, two new experiments, aiming for a staggering *4 orders of magnitude* improvement, invest heavily on superconducting solenoids. Background from beam pion capture, followed by nuclear  $\gamma$  decay with  $\gamma$  conversion resulting in  $e^+$ , is mitigated by using pulsed proton beam and waiting out the prompt decay. The main background is from muon decay in orbit, where the tail of energy distribution above  $m_\mu/2$  can enter the signal region, hence detector resolution is key.

The COMET experiment [12] at J-PARC takes a staged approach aiming for fast start. For COMET Phase I, detector and facility preparation is underway, with C-shaped solenoid aiming for run start as early as possible, to reach below  $10^{-14}$ . The 8 GeV accelerator would operate at 3.2 kW. COMET Phase II would use a more sophisticated S-shaped muon transport solenoid, higher beam power (e.g. 56 kW) and improved detector, aiming for run start in 2022 with goal to reach below  $10^{-16}$ . The staged approach of COMET is in part due to the Mu2e experiment [13], which is under construction at Fermilab, and aims for commissioning as early as 2022, and physics run for 3 years. Accumulating a total of  $10^{18}$  stopped muons, the goal is to reach  $R_{\mu e} < 10^{-16}$ .

Both COMET and Mu2e use 8 GeV protons, and muonic atoms formed on Al. As if the competition is not enough, there is another experiment, DeeMe [14] at J-PARC, that is based on a different approach. It would use 3 GeV pulsed proton beam at  $\sim 1$  MW beam power on a thick (light but not too light nuclei, e.g. graphite)

<sup>2</sup>For status of Mu3e experiment at PSI, see e.g. [9].

target for pion production, decay *and* muon stopping, then collect the electrons from  $\mu \rightarrow e$  conversion and use a second beamline as part of the “spectrometer”. DeeMe could start physics run soon [14] and aims to reach below  $10^{-13}$ , with improvement possible by optimizing target (SiC?) and running longer.

The prospects for probing  $\mu \rightarrow e$  transitions look bright. As an explicit example to illustrate the probing power, let us take a recent study [15] of warped extra dimensions, where multi-TeV KK excitations now seems beyond the reach of LHC. The combined constraints of  $\mu \rightarrow e$  transitions discussed here could explore the effects of extra dimensions on LFV beyond  $m_{\text{KK}} > 20$  TeV. It should be clear that  $\mu \rightarrow e$  transition would attract more theoretical interest when the experiments enter data taking.

### 9.1.2 Muon $g - 2$ and EDMs

#### Muon $g - 2$

Though technically not flavor physics exactly (it is a flavor-diagonal effect), one cannot leave out the muon  $g - 2$  “anomaly” from discussion, in as much that it is also not quite “anomalous”. The muon  $g - 2$  “anomaly” is special because of its persistence. From the first “penguin” diagram calculation, that of  $a_e \equiv g_e/2 - 1 = \alpha/2\pi$  at one loop by Schwinger, it remains an active field 70 years later.

The muon  $g - 2$  “anomaly” means deviation between experiment and SM prediction,

$$\Delta a_\mu = a_\mu(\text{Expt}) - a_\mu(\text{SM}) = (274 \pm 76) \times 10^{-11}, \quad (9.4)$$

where the experimental value is measured by BNL-E821 [16] (Muon  $g-2$  Collaboration) in 2006,  $(11659208.0 \pm 5.4 \pm 3.3) \times 10^{-10}$ , and the SM expectation is e.g. from a recent update [17] of hadronic vacuum polarization (HVP) contribution. The more than  $3\sigma$  deviation has persisted for more than a dozen years, and could be handily explained [18] by MSSM. Although SUSY has not been sighted yet at the LHC, the persistent discrepancy has motivated serious efforts to remeasure  $a_\mu$ , as well as to refine the theoretical calculation.

The Fermilab-E989 experiment [19] continues to be called Muon  $g-2$  Collaboration. After relocating and refurbishing the BNL muon storage ring, it has meticulously shimmed the magnetic field to 3 times better uniformity than at BNL, and fully around the 44 m storage ring circumference. With improved detectors and other technologies, and with over 20 times more muons, the aim is to improve the experimental error by a factor of 4, from 540 ppb down to 140 ppb, and hopefully with matching theory improvement. After commissioning run in 2017, initial physics run in 2018 collected [20] twice the data versus BNL-E821, with publication intended for 2019, reaching down to 400 ppb. With 2018–2019 data, the target is to reach 200 ppb, and with 20 times or more BNL data by end of 2020, hopefully the goal of 140 ppb can be attained. This schedule, of course, may be optimistic.

But one also has to improve the theory as well with a concerted effort. Improvement of hadronic uncertainties is critical [21]. A detailed discussion, which heavily depends on lattice improvements [22] to understand hadronic effects, is beyond our scope. We cannot do full justice to this important subject, but look forward to major progress by the early 2020s on this lingering muon  $g - 2$  anomaly.

### Electric Dipole Moments (EDM)

EDM is another subject that we can only touch upon cursorily, as it is rather specialized, especially on the experimental side. EDM is  $T$ -violating hence CPV by the CPT theorem. Measurements of neutron EDM,  $d_n$ , typically utilize trapped ultra-cold neutrons (UCN), while the extraction of electron EDM,  $d_e$ , involves molecular and atomic and even nuclear (e.g. mercury EDM) physics. On the particle physics side, CKM phase contribute only at rather high loop order, and current experiments are many orders of magnitude away from SM expectations, i.e.  $d_n^{\text{SM}} \sim 10^{-32} e \text{ cm}$ ,  $d_e^{\text{SM}} \sim 10^{-40} e \text{ cm}$ . Thus, discovery of EDM would definitely imply NP, albeit in a rather indirect way. We briefly discuss  $d_n$  and  $d_e$  as examples, referring to more specialized reviews [23] for details.

Neutron EDM should have appeared above the  $10^{-24} e \text{ cm}$  level in weak scale SUSY. The current experimental bound [24], from ILL in France, gives (final update from 2006 result [2])

$$d_n^{\text{Expt}} < 3.0 \times 10^{-26} e \text{ cm}, \quad (\text{ILL, 2015}) \quad (9.5)$$

at 90% C.L., which means either CPV phases are small in MSSM, or SUSY breaking scale is considerably above TeV scale. Judging from the absence of SUSY so far at the LHC, the latter is becoming more likely. But it also means that  $d_n$  *could appear at any time*. Of course, the smallness of  $d_n$  already gave the puzzle of an extremely small  $\theta_{\text{QCD}}$ , and the possibility of axion as explanation. However, neutron EDM also probes quark EDMs  $d_u, d_d$  and the corresponding chromo-dipole moments, hence fascinating for theorists.

On the experimental side, there is a world-wide (slow) race to reach below  $10^{-27} e \text{ cm}$  using UCN sources, to improve the bound of (9.5) by two orders of magnitude. The ILL setup was moved to PSI, where a dedicated UCN source was built. The latter moderates spallation neutrons through heavy water, then solid  $\text{D}_2$  crystals. The PSI nEDM experiment [25] has already taken some data, and expected sensitivity should reach below  $10^{-26} e \text{ cm}$ . The upgraded n2EDM experiment to follow at PSI targets reaching below  $10^{-27} e \text{ cm}$ . Across the Atlantic, the SNS nEDM experiment [26] at the Oak Ridge SNS (Spallation Neutron Source) adopts a different and novel [27] approach, using superfluid  $^4\text{He}$  as both the UCN moderator, as well as the high voltage insulator to sustain high electric field. It further uses  $^3\text{He}$  as co-magnetometer and superconducting shield, to control and measure magnetic field systematics. With demonstration phase close to completion, large scale integration and commissioning should converge at Oak Ridge by 2019. The sensitivity, assuming 3 years of running, aims at  $2 \times 10^{-28} e \text{ cm}$  by the early 2020s. These are meticulous and painstaking experiments, so the schedule could easily slip.

There is ongoing R&D to pursue proton EDM,  $d_p$ , measurement using a storage ring [28]. This bears some analogy with muon storage ring study of  $g - 2$  (which would measure  $d_\mu$  parasitically), but would be an “all electric” ring with no B field. The target is to reach sensitivity of  $10^{-29} e \text{ cm}$ , but schedule is not clear.

Somewhat surprisingly, the current leading edge of charged (neutral included) particle EDM search is that of the electron,  $d_e$ , where the limit from the ACME experiment [29] gives,

$$d_e^{\text{Expt}} < 8.7 \times 10^{-29} e \text{ cm}, \quad (\text{ACME, 2013}) \quad (9.6)$$

at 90% C.L. ACME utilizes polar thorium monoxide (ThO) molecule, which has internal effective electric field  $E_{\text{eff}}$  of order 84 GV/cm. We cannot describe the methodology here, which uses molecular beams and lasers, but since this is a first generation experiment of the type, and there are other approaches (e.g.  $^{199}\text{Hg}$ ,  $^{224}\text{Ra}$ , etc.) as well, the result of (9.6) stands further improvement, and should be keenly followed.

As an example of the theories probed, we quote the study [30] of 2HDM-II with CPV in Higgs potential,<sup>3</sup> which induces mixing between  $CP$ -even and  $CP$ -odd neutral Higgs bosons. It is found that, at present, the ThO result on  $d_e$  poses the most stringent constraint, while neutron and mercury constraints are less stringent, and furthermore suffer from hadronic and nuclear matrix element uncertainties. However, given the expected progress, this indirect probe of NP scales would be complementary to the direct search at the LHC. Note that 2HDM-II naturally follows from, but does not necessarily imply, SUSY. Together, these two types of NP provide sufficient motivation for the continued quest of EDMs, and the NP-CPV phases carried by scalar particles are being probed by current EDM searches. If a discovery is made, one would need a lot of improvement in hadronic and nuclear matrix element estimates to disentangle the underlying NP [23] from the multiple probes.

## 9.2 LFV $\tau \rightarrow \ell\gamma, \ell\ell\ell'$ Decays

Like  $\mu \rightarrow e\gamma$  decay,  $\tau \rightarrow \ell\gamma$  decays are extremely suppressed in SM by the very light neutrino masses. The observed near maximal  $\nu_\mu - \nu_\tau$  mixing stimulated a lot of interest in LFV  $\tau \rightarrow \mu$  transitions, as they echo the  $b \rightarrow s$  transitions that have been the dominant theme of our interest. In the context of Grand Unified Theories (GUTs), which in general needs SUSY to make the unification of couplings work, there is clearly  $\tau \rightarrow \mu$  and  $b \rightarrow s$  correspondence. For further discussion, see e.g. [31]. In exploring  $\tau \rightarrow \mu$  transitions, once (if) they are observed, there is great potential to check the link with  $b \rightarrow s$  loop transitions in a given model. This shows the utility of flavor physics in a broad framework.

---

<sup>3</sup>This is in general dangerous, as it would have easily led to rather large  $n_{\text{EDM}}$ .



### 9.2.1 Lepton Universality and $\tau$ Lifetime

It is worthy of mention the ‘‘mundane’’ lepton universality test in  $\tau$  decay. This is in part because LUV, or lepton universality violation, has become an issue due to the  $R_{D^{(*)}}$  and  $R_{K^{(*)}}$  anomalies (Sects. 4.2 and 5.2).

The charged current weak interaction in SM couples with the same strength to all lepton flavors, which should be tested by experiment. Such tests of lepton universality can provide strong constraint on model extensions. The charge current induced leptonic decay width is

$$\Gamma(\tau \rightarrow \ell \nu \bar{\nu}_\ell) = \frac{B(\tau \rightarrow \ell \nu \bar{\nu}_\ell)}{\tau_\tau} = \frac{G_\tau G_\ell m_\tau^5}{192\pi^3} f \left( \frac{m_\ell^2}{m_\tau^2} \right) R_W^\tau R_\gamma^\tau, \quad (9.7)$$

where  $G_\ell = g_\ell^2/4\sqrt{2}M_W^2$  for  $\ell = e, \mu$  are the respective Fermi coupling constants,  $f$  is a phase space factor,  $R_V^\tau$  can be found in [32]. Inserting partial width ratios and the measured  $\tau$  lifetime, where the latter has been significantly improved by a Belle measurement [33], HFAG 2016 obtained [34] the following ratios of coupling constants by using purely leptonic processes,

$$\begin{aligned} \left( \frac{g_\tau}{g_\mu} \right) &= 1.0010 \pm 0.0015, & \left( \frac{g_\tau}{g_e} \right) &= 1.0029 \pm 0.0015, \\ \left( \frac{g_\mu}{g_e} \right) &= 1.0019 \pm 0.0014. & & \text{(HFAG, 2016)} \end{aligned} \quad (9.8)$$

If semi-hadronic processes such as  $\tau \rightarrow (K, \pi)\nu_\tau$  or  $(K, \pi) \rightarrow \mu\bar{\nu}_\mu$  are also considered, the ratio  $g_\tau/g_\mu$  can be further combined to  $1.0000 \pm 0.0014$ , which is in remarkable agreement with lepton universality, providing a very strong constraint to New Physics models in the lepton sector. This is a useful reminder in view of LUV as suggested by  $R_{D^{(*)}}$  and  $R_{K^{(*)}}$  anomalies.

### 9.2.2 $\tau \rightarrow \mu\gamma, \ell\ell\ell'$

Just like the pursuit of  $\mu \rightarrow e$  transitions, observing LFV  $\tau$  decays would be an unambiguous signal of New Physics. LFV  $\tau$  decay processes are absent at tree level in SM, and can occur only through tiny neutrino masses at loop level, highly suppressed by the equivalent of the GIM mechanism. The decay rate for  $\tau \rightarrow \mu\gamma$  is negligible in SM, while the stringent  $\mu \rightarrow e\gamma$  bound of (9.2) dampens one’s hope. But several NP scenarios can in principle increase the rate for this mode, or some other channels, to more accessible values.

With SUSY as the favorite underlying New Physics, models range from sneutrino-chargino or charged slepton-neutralino loops (Fig. 9.1), exotic Higgs,  $R$ -parity violation, to  $\nu_R$  in SO(10) or large extra dimensions (LED). Predictions for  $\tau \rightarrow \ell\gamma, \ell\ell\ell$ ,

$\ell\ell\ell', \ell M^0$  (where  $M^0$  is a neutral meson) could reach the  $10^{-7}$  level, and generally populate  $10^{-8}$ – $10^{-10}$ , which should be compared to the more suppressed range for  $\mu \rightarrow e\gamma$ . These models are often well motivated from observed near maximal  $\nu_\mu$ – $\nu_\tau$  mixing, or from interesting ideas such as seesaw mechanism in SUSY-GUT context, or baryogenesis through leptogenesis. We refrain from getting into details of theory, as the body of literature is rather large, but comment that there may also be the link to muon  $g - 2$  that we have just covered. The long existing discrepancy was another strong motivation for SUSY [18].

On the experimental side, the stars are once again the B factories: With  $\sigma_{\tau^+\tau^-} \sim 0.9$  nb comparable to  $\sigma_{b\bar{b}} \sim 1.1$  nb, B factories are also  $\tau$  (and charm) factories! In the CLEO era of the 1990s, where  $\mathcal{O}(10^7)$   $\tau$ s were collected, the limit on  $\tau \rightarrow \mu\gamma$  had reached  $10^{-6}$ . With the advent of the B factories, and as data accumulated steadily, the limits are approaching the  $10^{-8}$  level, entering the interesting region of potential discovery for the neutrino-SUSY/GUT inspired models. We discuss only  $\tau \rightarrow \ell\gamma$  and  $\tau \rightarrow \ell\ell\ell'$  as examples.

The study of  $\tau$  LFV is in some sense simpler than the study of tau decays in SM: the signal side has low multiplicity, such as  $\tau \rightarrow \mu\gamma$ , and *fully reconstructed*, with  $E_{\text{sig}}$  equal the beam energy ( $E_{\text{beam}}^{\text{CM}}$ ), and  $M_{\mu\gamma}$  equal the tau mass. The main effort is again the control of backgrounds. To pick up a genuine  $e^+e^- \rightarrow \tau^+\tau^-$  event, one tags the other  $\tau$  by one-prong (maybe three-prong also) decays, where missing neutrinos imply that the reconstructed  $E_{\text{tag}} < E_{\text{beam}}^{\text{CM}}$  and  $M_{\text{tag}} < m_\tau$  for tag-side. The two  $\tau$ s are well separated, providing another discriminant. For  $\tau \rightarrow \mu\gamma$  search, to suppress  $e^+e^- \rightarrow \mu^+\mu^-\gamma$  background, the tag side track should not be a muon.

Track energy,  $p_T$ , angular, total CM energy and other cuts are employed to suppress Bhabha,  $\mu^+\mu^-$ , two photon and  $q\bar{q}$  backgrounds. One utilizes further the kinematics of an  $e^+e^- \rightarrow \tau(\rightarrow \mu\gamma)\tau(\rightarrow \text{track} + \nu(\nu))$  event to suppress the remaining  $\tau^+\tau^-$  and  $\mu^+\mu^-$  backgrounds, for example,  $\gamma$  from  $\pi^0$ s,  $\mu$  misidentified as  $\pi$ , or an  $m_{\nu(\nu)}^2$  cut that utilizes the fact that it should be no more than the parent  $\tau$  mass. One then models the final background distributions with the side-band in  $M_{\mu\gamma}$  versus  $\Delta E \equiv E_{\mu\gamma}^{\text{CM}} - E_{\text{beam}}^{\text{CM}}$ , with the signal region blinded. The result is found to be consistent with MC. With a dataset of  $535 \text{ fb}^{-1}$  ( $477\text{M}$   $\tau^+\tau^-$  pairs), Belle found no events in the signal box, setting the limit of [35]

$$\mathcal{B}(\tau \rightarrow \mu\gamma) < 4.5 \times 10^{-8}, \quad (\text{Belle}, 535 \text{ fb}^{-1}) \quad (9.9)$$

A similar study, with higher background because of the  $e^+e^-$  production environment, gives  $\mathcal{B}(\tau \rightarrow e\gamma) < 12 \times 10^{-8}$  at 90% C.L. BaBar published their final result [36] on radiative  $\tau$  decays two years later, finding almost the same bound as Belle for  $\tau \rightarrow \mu\gamma$ , and a better result for  $\tau \rightarrow e\gamma$ .

For  $\tau \rightarrow \ell\ell\ell$  and  $\ell\ell\ell'$  modes, 6 charged lepton combinations ( $e^-e^+e^-$ ,  $\mu^-\mu^+\mu^-$ ,  $e^-\mu^+\mu^-$ ,  $\mu^-e^+e^-$ ,  $\mu^+e^-e^-$  and  $e^+\mu^-\mu^-$ ) have been studied, each with their own special background considerations. The event consists of 4 charged tracks with zero net charge, with one track on the tag side hemisphere, and three tracks on the signal side. As special mode-dependent background studies, for example, one has to

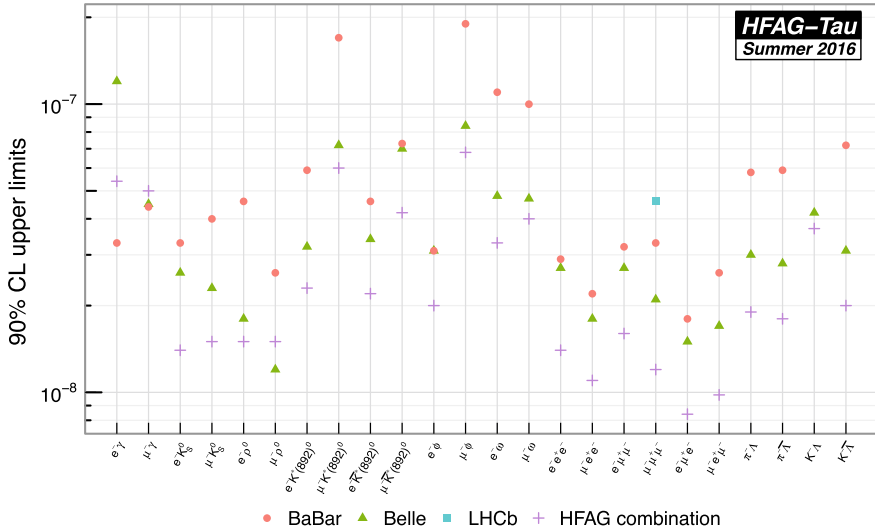


**Fig. 9.2** Published individual upper limits and HFAG combined values (marked by +) on LFV  $\tau$  decays. Because of statistical fluctuations of single results, combined limits are not necessarily tighter. [Source HFAG 2016 [34]]

reject the large  $\gamma \rightarrow e^+e^-$  conversion background for  $\tau \rightarrow \ell e^+e^-$  modes. Because of having like sign muon or electron pairs, the  $\tau^- \rightarrow \mu^+e^-e^-$  and  $e^+\mu^-\mu^-$  modes have the lowest background, hence the best limits were reached for these two modes. With  $535 \text{ fb}^{-1}$  ( $492M \tau^+\tau^-$  pairs<sup>4</sup>) data, Belle set the limit of [37]

$$\mathcal{B}(\tau \rightarrow \bar{\mu}ee (\bar{e}\mu\mu)) < 2.0 (2.3) \times 10^{-8}, \quad (\text{Belle } 535 \text{ fb}^{-1}) \quad (9.10)$$

at 90% C.L., the current best limit for LFV  $\tau$  decays. The limit for  $\tau^- \rightarrow e^-\mu^+\mu^-$  is at  $4.1 \times 10^{-8}$ . Limits from BaBar (using  $376 \text{ fb}^{-1}$ ) are not far behind [38].

Dozens of LFV  $\tau \rightarrow \ell M^0$  decays have been studied, where  $M^0$  is a neutral hadron, be it pseudoscalar, vector, or scalar. The limits have reached below  $10^{-7}$ . For instance, based on a suggestion [39] that  $\tau \rightarrow \mu f_0$  could be more than twice the size of  $\tau \rightarrow \mu\mu\mu$  (a scalar couples to  $s\bar{s}$  versus  $\mu^+\mu^-$ ), using  $671 \text{ fb}^{-1}$  data, Belle sets a limit [40] around  $3.3 \times 10^{-8}$ .

The summary of experimental upper limits from HFAG [34] is given in Fig. 9.2, which shows a plethora of search modes, especially as compared with rare muon decays of the previous section. Most of the existing measurements are from Belle and BaBar. A search for  $\tau^- \rightarrow \mu^-\mu^+\mu^-$  by LHCb [41] based on  $3 \text{ fb}^{-1}$  at LHC Run 1 is getting close, but not yet competitive. But even B factory results just graze the  $10^{-8}$  boundary. *To probe deeper into the parameter space of various LFV rare  $\tau$  decays that are of great interest, we await results from Belle II at SuperKEKB.*

<sup>4</sup>The number of  $\tau^+\tau^-$  pairs is higher than in [35], because an updated calculation of the  $e^+e^- \rightarrow \tau^+\tau^-$  cross section is used; thus, (9.9) should be modified slightly.

### Prognosis

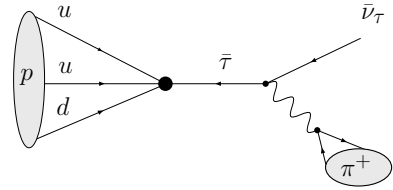
At the dawn of the Belle II era, there has been much progressed at the LHC: No New Physics sighted. Let us mention a few examples of impact of LHC. As we have no evidence for SUSY, LHC results seem to push expectations for  $\tau \rightarrow \mu\mu\mu, e\mu\mu$  towards  $10^{-9}$  [42] in SUSY models, which are not quite within experimental reach in the near future. By introducing additional heavy right-handed Majorana neutrinos, or additional left-handed and right-handed neutral singlets [43], the branching fractions of  $\tau \rightarrow \mu\gamma, e\gamma$  and  $\tau \rightarrow \mu\mu\mu, eee$  can be raised to approximately  $O(10^{-10})$ – $O(10^{-8})$ , and still pertinent. Adding a non-universal gauge boson  $Z'$  in topcolor-assisted technicolor models, the branching fraction of  $\tau \rightarrow eee$  or  $\mu\mu\mu$  can be as large as  $10^{-8}$  within a range of parameter space [44]. But it is not clear whether these old models still stand with LHC data, and correlation with the stringent MEG limit on  $\mu \rightarrow e\gamma$  is a concern. Finally, in the 2HDM-III (i.e. 2HDM model without imposing  $Z_2$  symmetry) that we would discuss in Sect. 10.2 because of flavor changing neutral Higgs (FCNH) couplings and other new Yukawa couplings,  $\tau \rightarrow \mu\gamma$  might be close [45] to the current experimental limit. Suffice it to say that many proposals can raise the LFV branching fractions to the level of  $O(10^{-10})$ – $O(10^{-8})$ , and also generate other possible LFV B meson or Higgs decays. While NP models are now more and more constrained by LHC search and  $\mu \rightarrow e\gamma$ , the experimental study of rare  $\tau$  decays provide complementary information, and should continue in any case.

At SuperKEKB, limits for  $\tau \rightarrow \ell\ell\ell'$  can reach  $10^{-9}$ , but  $\tau \rightarrow \ell\gamma$  suffers from a irreducible background of  $e^+e^- \rightarrow \tau^+\tau^-\gamma$ , and it remains to be seen whether it can reach far below  $10^{-8}$ . Nevertheless, the LFV search program at Belle II is quite unique, and complementary to direct search programs at the LHC. The LHCb experiment can compete in the all charged track modes, but modes with neutrals would be difficult. However, unlike the B factories, the main source of  $\tau$  leptons are in fact  $B$  and  $D$  mesons, so background considerations are quite different, and nontrivial.

### 9.3 $\tau \rightarrow \bar{\Lambda}\pi, \bar{p}\pi^0$ and Baryon Number Violation

A somewhat wild idea is to search for baryon number violation (BNV) in  $\tau$  decay, which certainly violates lepton number as well. The search was started by the ARGUS experiment [46] and followed by CLEO [47] in the 1990s, which searched for  $\tau^- \rightarrow \bar{p}\pi^0, \bar{p}\eta, \bar{p}\pi^0\pi^0, \bar{p}\pi^0\eta, \bar{p}\gamma$  modes. However, before the CLEO paper was published, Marciano pointed out [48] in 1995 that, by using proton decay constraints, the estimated BNV  $\tau$  decay branching ratios are too small to be observed. This, however, did not deter the B factory experiments, and Belle [50] searched for both  $B - L$  conserving  $\tau^- \rightarrow \bar{\Lambda}\pi^-$ , as well as  $B - L$  violating  $\tau^- \rightarrow \Lambda\pi^-$  decays, which was extended by BaBar [51] to  $\bar{\Lambda}K^-$  and  $\Lambda K^-$ . No signal was found, as expected. However, the observation of Marciano was extended [49] to BNV decays involving higher generations (i.e. including  $c, b, t$  as well as  $\tau$ ), with the pessimistic conclusion

**Fig. 9.3** Diagram [49] illustrating virtual  $\tau$  mediating proton decay [Copyright (2006) by The American Physical Society]



that proton decay bounds preclude the possibility of observing any of these decays in any current or future experiments. This seemed to have had a dampening effect on experimental activity.

The experimental signature is, however, rather tantalizing, so let's still explore it. After all, Belle and BaBar have accumulated unprecedented numbers of  $\tau^+\tau^-$  pairs in the clean  $e^+e^-$  production environment. Also, baryon number violation has never been observed so far, while we know it is definitely needed for the early Universe, so all search avenues should be explored.

The Belle study [50] used a data set of  $154 \text{ fb}^{-1}$ , corresponding to  $137\text{M } \tau^+\tau^-$  pairs, while BaBar used [51]  $237 \text{ fb}^{-1}$ , or 50% more. The limits reached are around  $10^{-7}$ . Whether it is slightly above or below this depends on whether a random event turns up in the signal box. The event signature is  $\bar{p}\pi^+(p\pi^-)\pi^-(K^-)$  on signal side, with  $\bar{p}\pi^+$  reconstructing to a  $\bar{\Lambda}$ , and  $\bar{\Lambda} + \text{track}$  reconstructing to tau mass, where PID is used to separate  $\pi^-$  from  $K^-$  track. The  $\bar{\Lambda}$  or  $\Lambda$  pairing with the  $\pi^-$  just determines whether there is  $B - L$  conservation, or not. For the tag side one uses the one-prong  $\tau$  decays as before. So, the signature is 4 charged tracks with zero net charge and missing energy, similar to  $\tau \rightarrow \ell\ell\ell'$  search. The hadronic track nature means that the major remaining background after the usual event selection procedure would be generic  $\tau^+\tau^-$ , or continuum  $q\bar{q}$  events. One can compare MC with side band close to the signal box, which is kept blind until all selections and background rejection procedures are made. The analysis is very similar to LFV searches of the previous section, except one uses proton and  $\Lambda$  identification, instead of electron or muon identification. The limit can in principle improve by at least a factor of two with the data at hand.

So why is the proton lifetime setting such a strong bound on  $\tau$  BNV? To elucidate Marciano's argument, we plot in Fig. 9.3 a diagram [49] for proton decay mediated by a virtual  $\tau$ . On the middle-left side of the diagram, the blob illustrates the BNV  $uud\bar{\tau}$  effective coupling. The virtual tau then decays in some standard way. If the  $uud\bar{\tau}$  coupling exists, it can then induce proton decay. In turn, one can use the proton lifetime to set a bound on  $\tau$  BNV. In this way, one finds that  $\mathcal{B}(\tau \rightarrow \bar{p}\pi^0) < \text{few} \times 10^{-39}$ . For strange baryons, one further involves the weak interaction, and the limit is weakened to

$$\mathcal{B}(\tau \rightarrow \bar{\Lambda}\pi^-) < \text{few} \times 10^{-30}, \quad (9.11)$$

which is depressingly small. In the same vein, for any BNV effective 4-fermi interaction, one can always [49] link with some nucleon decay process, sometimes

by invoking weak interaction loops as one goes to top and beauty quarks. The limits never appear more promising than (9.11), which is surprising, but discouraging.

In the study of [49], however, some really fascinating decay signatures are uncovered, that may be worth contemplating. To name a few:  $D^+ \rightarrow \bar{\Lambda}\ell^+$ ,  $D^0 \rightarrow \bar{\Sigma}^-\ell^+$ ,  $\bar{p}\ell^+$ ;  $B^{0,+} \rightarrow \Xi_{cc}^{+,++}\ell^-$  (probably not suppressed by  $B \rightarrow \Xi_{cc}$  form factor!) and inclusive  $\bar{b} \rightarrow c\ell\bar{\ell}$  (wrong charge combination);  $t \rightarrow \bar{b}\bar{c}\ell^+$ . Experimentalists should be quite attracted to these astounding signatures. But if the argument of Marciano is correct, all these modes cannot exist at an observable level, even if BNV exists!

Our view is, *whenever an experimental search can be conducted, it should be done*, regardless of what the theoretical expectation is. After all, there could be some symmetry and/or cancellation among diagrams, or other wilder ideas, as we know that Nature is more ingenious than we are. With [51] unpublished, there were a trickle of experimental studies: CLEO on  $D^0 \rightarrow \bar{p}e^+, pe^-$  [52], BaBar on  $B \rightarrow \Lambda_{(c)}\ell$  [53], and even  $t \rightarrow \bar{b}\bar{c}\ell^+$  by CMS [54]. The latter was in part motivated by the suggestion [55] that cancellation mechanisms may be at work and the suppression [49] may not be that severe. LHCb has searched for  $\tau \rightarrow p\mu\mu$  [56], and has made an interesting search for  $\Xi_b^0$  oscillations [57] based on six quark operators.

We reiterate that experiments should not hesitate in initiating their search.

## References

1. Brooks, M.L., et al. [MEGA Collaboration]: Phys. Rev. Lett. **83**, 1521 (1999)
2. Tanabashi, M., et al. [Particle Data Group]: Phys. Rev. D **98**, 030001 (2018). <http://pdg.lbl.gov/>
3. Hisano, J., Nomura, D.: Phys. Rev. D **59**, 116005 (1999)
4. Baldini, A.M., et al. [MEG Collaboration]: Eur. Phys. J. C **76**, 434 (2016)
5. Kersten, J., Park, J.H., Stöckinger, D., Velasco-Sevilla, L.: JHEP **1408**, 118 (2014)
6. Blankenburg, G., Isidori, G., Jones-Perez, J.: Eur. Phys. J. C **72**, 2126 (2012)
7. Antusch, S., Arganda, E., Herrero M.J., Teixeira, A.M.: JHEP **0611**, 090 (2006)
8. de Gouvêa, A., Vogel, P.: Prog. Part. Nucl. Phys. **71**, 75 (2013)
9. Papa, A.: Talk Presented at ICHEP2018 Conference, Seoul, Korea, July 2018
10. Bertl, W.H., et al. [SINDRUM II Collaboration]: Eur. Phys. J. C **47**, 337 (2006)
11. Dzhilkibaev, R.M., Lobashev, V.M.: Sov. J. Nucl. Phys. **49**, 384 (1989)
12. Kuno Y. [For the COMET Collaboration]: PTEP **2013**, 022C01 (2013)
13. Bartoszek, L., et al. [Mu2e Collaboration]. [arXiv:1501.05241](https://arxiv.org/abs/1501.05241) [physics.ins-det]
14. See e.g. Natori, H.: Talk Presented at ICHEP2018 Conference, Seoul, Korea, July 2018
15. Beneke, M., Moch, P., Rohrwild, J.: Nucl. Phys. B **906**, 561 (2016)
16. Bennett, G.W., et al. [Muon g-2 Collaboration]: Phys. Rev. D **73**, 072003 (2006)
17. Davier, M.: [arXiv:1612.02743](https://arxiv.org/abs/1612.02743) [hep-ph]
18. For a recent review, see Stöckinger, D.: J. Phys. G **34**, R45 (2007)
19. Grange, J., et al. [Muon g-2 Collaboration]: [arXiv:1501.06858](https://arxiv.org/abs/1501.06858) [physics.ins-det]
20. See e.g. Crnkovic, J.D.: Talk Presented at FPCP2018 Conference, Hyderabad, India, July 2018
21. Jegerlehner, F.: Acta Phys. Polon. B **49**, 1157 (2018)
22. Flavor Lattice Averaging Group. <http://itpwiki.unibe.ch/flag/>
23. Engel, J., Ramsey-Musolf, M.J., van Kolck, U.: Prog. Part. Nucl. Phys. **71**, 21 (2013)
24. Pendlebury, J.M., et al.: Phys. Rev. D **72**, 091102 (2015)

25. See <https://www.psi.ch/nedm/>
26. See <http://www.phy.ornl.gov/nedm/>
27. Golub, R., Lamoreaux, S.K.: Phys. Rept. **237**, 1 (1994)
28. Anastassopoulos, V., et al.: Rev. Sci. Instrum. **87**, 115116 (2016)
29. Baron, J., et al. [ACME Collaboration]: Science **343**, 269 (2014)
30. Inoue, S., Ramsey-Musolf, M.J., Zhang, Y.: Phys. Rev. D **89**, 115023 (2014)
31. Chang, D., Masiero, A., Murayama, H.: Phys. Rev. D **67**, 075013 (2003)
32. Marciano, W., Sirlin, A.: Phys. Rev. Lett. **61**, 1815 (1988)
33. Belous, K., et al. (Belle collaboration): Phys. Rev. Lett. **112**, 031801 (2014)
34. Amhis, Y., et al. [Heavy Flavor Averaging Group]. [arXiv:1612.07233](https://arxiv.org/abs/1612.07233) [hep-ex]
35. Hayasaka, K., et al. [Belle Collaboration]: Phys. Lett. B **666**, 16 (2008)
36. Aubert, B., et al. [BaBar Collaboration]: Phys. Rev. Lett. **104**, 021802 (2010)
37. Miyazaki, Y., et al. [Belle Collaboration]: Phys. Lett. B **660**, 154 (2008)
38. Aubert, B., et al. [BaBar Collaboration]: Phys. Rev. Lett. **99**, 251803 (2007)
39. Chen, C.H., Geng, C.Q.: Phys. Rev. D **74**, 035010 (2006)
40. Miyazaki, Y., et al. [Belle Collaboration]: Phys. Lett. B **672**, 317 (2009)
41. Aaij, R., et al. [LHCb Collaboration]: JHEP **1502**, 121 (2015)
42. Goto, T., Okada, Y., Shindou, T., Tanaka, M., Watanabe, R.: Phys. Rev. D **91**, 033007 (2015)
43. Cvetic, G., Dib, C., Kim, C.S., Kim, J.D.: Phys. Rev. D **66**, 034008 (2002)
44. Yue, C.-X., Zhang, Y.-M., Liu, L.-J.: Phys. Lett. B **547**, 252 (2002)
45. See e.g. Chiang, C.-W., Fuyuto, K., Senaha, E.: Phys. Lett. B **762**, 315 (2016)
46. Albrecht, H., et al. [ARGUS Collaboration]: Z. Phys. C **55**, 539 (1992)
47. Godang, R., et al. [CLEO Collaboration]: Phys. Rev. D **59**, 091303 (1999)
48. Marciano, W.J.: Nucl. Phys. B Proc. Suppl. **40**, 3 (1995)
49. Hou, W.-S., Nagashima, M., Soddu, A.: Phys. Rev. D **72**, 095001 (2006)
50. Miyazaki, Y., et al. [Belle Collaboration]: Phys. Lett. B **632**, 51 (2006)
51. Aubert, B., et al. [BaBar Collaboration]. [arXiv:hep-ex/0607040](https://arxiv.org/abs/hep-ex/0607040) (unpublished)
52. Rubin, P., et al. [CLEO Collaboration]: Phys. Rev. D **79**, 097101 (2009)
53. del Amo Sanchez, P., et al. [BaBar Collaboration]: Phys. Rev. D **83**, 091101 (2011)
54. Chatrchyan, S., et al. [CMS Collaboration]: Phys. Lett. B **731**, 173 (2014)
55. Dong, Z., Durieux, G., Gerard, J.-M., Han, T., Maltoni, F.: Phys. Rev. D **85**, 016006 (2012)
56. Aaij, R., et al. [LHCb Collaboration]: Phys. Lett. B **724**, 36 (2013)
57. Aaij, R., et al. [LHCb Collaboration]: Phys. Rev. Lett. **119**, 181807 (2017)

# Chapter 10

## The Top and The Higgs



The top quark was discovered at the Tevatron in 1995. The Higgs boson was discovered at the LHC in 2012. The top quark is the heaviest of all SM particles. The Higgs boson, the second heaviest, is the last SM particle to be found. The two particles are separately unique.

The top (and bottom) quark was anticipated in the mid-1970s, after the discovery of the  $\tau$  lepton at SLAC. But it took 20 years for it to be discovered by direct production. No one anticipated how heavy it was, and in Sect. 1.3 we illustrated the *nondecoupling* effect of the top Yukawa coupling in electroweak loop diagrams, such that the surprisingly large  $\Delta m_{B_d}$  discovered by the ARGUS experiment [1] harbingered the *heaviness* of the top.

The Higgs boson was “invented” through the Brout-Englert-Higgs mechanism for spontaneous symmetry breaking (SSB), and applied to electroweak symmetry breaking. Thus, vector boson masses are generated by their *gauge couplings* to the vacuum expectation value (v.e.v.),  $v \cong 246 \text{ GeV}$ . It was the brilliance of Weinberg that fermion mass generation came through an analogous mechanism, by their *Yukawa couplings* to v.e.v. of the Higgs field,

$$\lambda_f = \sqrt{2}m_f/v. \tag{10.1}$$

Thus, charged fermions and vector boson couplings to the Higgs particle—predicted by Higgs as remnant of SSB—are proportional to their masses. The Yukawa couplings are the source of flavor physics, including the CPV phase in the CKM matrix of the 3 generation SM. But it took us close to half a century to discover the elusive Higgs boson,  $h$ ,<sup>1</sup> by direct production.

Because of their heaviness, hence production only at very high energy colliders, the top and the Higgs are traditionally not viewed as part of Flavor Physics. But as we illustrate in this chapter, they should be. Not least is the 2018 observation [2, 3] of the  $t\bar{t}h$  production at the LHC, where the production cross section is consistent

---

<sup>1</sup>As will be explained in this chapter, we denote the 125 GeV boson discovered in 2012 as  $h(125)$ , or simply,  $h$ . At about  $v/2$  in mass, it is relatively light.



with  $\lambda_t \simeq 1$ , as implied by (10.1). Thus, we have *directly* measured the source of most loop effects in SM. These loop effects are a prevalent feature in flavor physics, which confirm SM so far, even if there are intriguing “anomalies”.

By now, both ATLAS and CMS have searched directly for  $t \rightarrow ch$  (Sect. 10.1) and  $h \rightarrow \mu\tau$  (Sect. 10.2) decays, which are true frontiers where discovery could emerge at anytime.

## 10.1 Top Changing Neutral Couplings

Because of its heaviness and the Cabibbo-favored nature of the  $t \rightarrow bW^+$  transition, the top quark decays before it can hadronize into a “top meson”. The extremely short lifetime makes rare top decays a somewhat depressed field. We will not treat SM top production and decay, as these indeed do not touch upon flavor physics. Even single top production, which in principle probes  $|V_{tb}|$  directly, we shall still not cover much.

FCNC  $t \rightarrow cZ$  decays, however, have been searched for since [4] the Tevatron discovery of the top. Furthermore, the  $P'_5$  anomaly (Sect. 5.2) suggests there could be analogous top FCNC  $tcZ'$  couplings to a new  $Z'$  boson. With the discovery of  $h(125)$ , it is the top in conjunction with the Higgs that has drawn more attention:  $t \rightarrow ch$  decay [5], which is possible because  $m_h < m_t$ . As these are the particles discovered most recently, from a purely experimental point of view, the flavor-changing neutral Higgs (FCNH)  $tch$  coupling is of fundamental interest, *because it can be probed directly*.

### 10.1.1 TCNC: $t \rightarrow cZ^{(\prime)}$

By the GIM mechanism, there is no  $tcZ$  coupling at tree level in SM, with loop effects further suppressed by GIM cancellation. The case is worse than charm: whatever makes the corresponding  $B$  decays favorable, the situation is turned upsidedown for top. Unlike the prolonged  $B$  lifetime, the top is the shortest-lived of all known particles. If the nondecoupling of the top quark makes rare  $B$  decays interesting, the near degeneracy of the  $d$ ,  $s$  and  $b$  quark masses at the  $M_W$  and  $m_t$  scales means GIM cancellation is *very* effective. Hence  $t \rightarrow cZ$  decay is negligible for all practical purposes within SM. New Physics might have saved the day if new particles appeared at the weak scale. But we have found none so far at the LHC, with scales pushed to a few TeV, i.e. considerably higher than the weak scale.

The long held world best limit is from CMS Run 1 data [6],

$$\mathcal{B}(t \rightarrow cZ) < 0.05\%, \quad (\text{CMS, 2014}) \quad (10.2)$$

at 95% C.L., while the ATLAS Run 1 constraint was slightly weaker. Using  $36.1 \text{ fb}^{-1}$  at 13 TeV, however, ATLAS has now a better limit [7],

$$\mathcal{B}(t \rightarrow cZ) < 2.4 \times 10^{-4}, \quad (\text{ATLAS, 2018}) \quad (10.3)$$

at 95% C.L. Strangely, from a similar sized dataset at the same energy, CMS did not reach much improvement beyond (10.2). The CMS Run 1 paper [6] states that the result translates to “a constraint on the KK gluon to be heavier than 1.1 TeV”, which is actually quite good for a bound coming from an indirect rare top decay, and the new ATLAS result would be an improvement. However, if there were KK gluons just above the TeV scale, they would have been discovered already by direct search. Indeed, compared with pre-LHC estimates, warped extra dimension benchmarks for  $t \rightarrow cZ$  have moved down [8] to  $10^{-5}$  level with LHC Run 1 data, and suppressed by top compositeness scale  $M_*^{-4}$ , which means the number would shrink further with 13 TeV bounds on  $M_*$ . Other models, even in most favorable considerations in say  $R$ -parity violating SUSY, the situation is not better (see e.g. [9]). The projections from theory seem to be beyond reach even at the HL-LHC with  $3000 \text{ fb}^{-1}$ .

The bounds above are from  $t\bar{t}$  pair production, while we have used the notation of  $t \rightarrow cZ$ , even though experimental measurement typically does not know whether it is a  $c$ -jet or not. More proper notation would have been  $t \rightarrow qZ$ . However, were there  $tuZ$  coupling at same level as  $tcZ$  coupling, the large parton density for  $u$  quarks implies we should see enhanced  $ug \rightarrow tZ$  production, which we have not seen. In general, direct bound on  $tuZ$  coupling is stronger than  $tcZ$ , in agreement with the flavor pattern.

We note that limits on  $t \rightarrow cg, c\gamma$  are better. In particular, single top production processes can effectively probe smaller branching fractions than  $t \rightarrow cZ$ , e.g.  $\mathcal{B}(t \rightarrow ug) < 4 \times 10^{-5}$  [10] from ATLAS using 8 TeV data, with  $t \rightarrow cg$  limit weaker. In our view, however, the modeling of FCNC involving gluons or photons are in general more contrived, while  $t \rightarrow u$  transitions do not seem favorable compared to  $t \rightarrow c$  transitions from the known flavor pattern, as we have already stated. Search, of course, should continue.

More interesting may be  $tZ$  associated production,

$$c + g \rightarrow t + Z^{(\prime)}, \quad (10.4)$$

from  $tcZ^{(\prime)}$  coupling. A recent study by CMS [11] using 8 TeV data, sets practically the same limit on  $\mathcal{B}(t \rightarrow cZ)$  as (10.2). In this connection, we remark that there may well exist a weaker coupled  $Z'$  boson associated with  $t \rightarrow c$  transitions. While the left-handed  $tcZ'$  coupling suggested by the  $P'_5$  anomaly is too weak to be directly probed at the LHC, the anomaly has inspired the suggestion of a right-handed  $tcZ'$  coupling that is not much constrained by  $B$  decays [12].<sup>2</sup> A recent study which could be, but not necessarily, related to the gauged  $L_\mu - L_\tau$  model, suggests [14] that  $tZ'$  associated production analogous to (10.4) might lead to discovery with even  $100\text{--}300 \text{ fb}^{-1}$  at 13–14 TeV collision energies. If discovered, this could be called

<sup>2</sup>Reference [12], inspired by and expanded from [13] in the context of the  $P'_5$  anomaly, also emphasized search for  $t \rightarrow cZ' \rightarrow c\mu^+\mu^-$ , away from the  $m_Z$  window, but  $tZ'$  search covers more  $Z'$  mass range.

the “ $P'_5$  anomaly for top”, where one can further study top polarization and angular distributions due to the right-handed nature of the  $t c Z'$  coupling.

Despite some pessimism for the  $t \rightarrow c Z$  probe, the top quark might still be a key to potential New Physics discoveries in the future.

### 10.1.2 TCNH: $t \rightarrow ch$

There is no  $tch$  tree level coupling within SM after mass diagonalization, and the loop-induced effect can again be ignored for all practical purposes. Adding a second Higgs doublet, i.e. in 2HDM extensions, one would have two Yukawa matrices per mass matrix, and in general one cannot simultaneously diagonalize both Yukawa matrices with the mass matrix. This caused great worries, given the spectacular success of the GIM mechanism in removing FCNC. In this vein, prejudice against FCNH couplings led to their removal *by fiat*, via the so-called *Natural Flavor Conservation* (NFC) condition of Glashow and Weinberg [15]: each type of fermion charge receives mass from one and only one Higgs doublet, so the Yukawa and mass matrices are always simultaneously diagonalized. This is usually implemented by invoking a discrete  $Z_2$  symmetry (thereby 2HDM-I and 2HDM-II). The happy situation that, for separate reasons, 2HDM-II is automatic in MSSM, meant that particle physicists are trained to think in terms of 2HDM-II, as reflected in our discussions in previous chapters.

But it was pointed out long ago [16, 17] that, given the “trickle down” flavor pattern observed in quark masses and mixings,<sup>3</sup> Nature does seem to have her schemes of organization and control regarding flavor, while NFC itself appears more “human” than “Natural”. In this context, it was advocated [5] that FCNH involving 3rd generation quarks, namely  $t \rightarrow ch$  (or  $h \rightarrow t\bar{c}$ ,  $\bar{t}c$ , depending on mass), in a 2HDM extension as the most *natural*, hence called 2HDM-III. It should in fact be called the Standard 2HDM, or SM2 for short, as it just follows SM without *ad hoc* assumptions. We will develop towards this theme later in this chapter (Sect. 10.3), after we move from top to Higgs.

With or without the early advocate [5] for  $t \rightarrow ch$  search for  $m_h < m_t$  case, sure enough, efforts within ATLAS [18] on  $t \rightarrow ch(\rightarrow \gamma\gamma)$  search, or in association with CMS [19] on multi-lepton final states, were already ongoing, and within two years of Higgs boson discovery, the limits reached below the percent level [20, 21], which is quite remarkable. Both ATLAS and CMS embarked on  $t \rightarrow ch$  search in  $t\bar{t}$  events with  $h \rightarrow \gamma\gamma$ ,  $WW^*$ ,  $\tau^+\tau^-$ , as well as  $b\bar{b}$ , and the Run 1 combined limits for 8 TeV collisions are,

$$\mathcal{B}(t \rightarrow ch) < 0.46\%, 0.40\% \quad (\text{LHC Run 1}) \quad (10.5)$$

---

<sup>3</sup>For example, the  $\sqrt{m_i m_j}$  pattern of the Fritzsch Ansatz [16]. Of course, this does not work in precise detail, but the general point [17] is well taken.

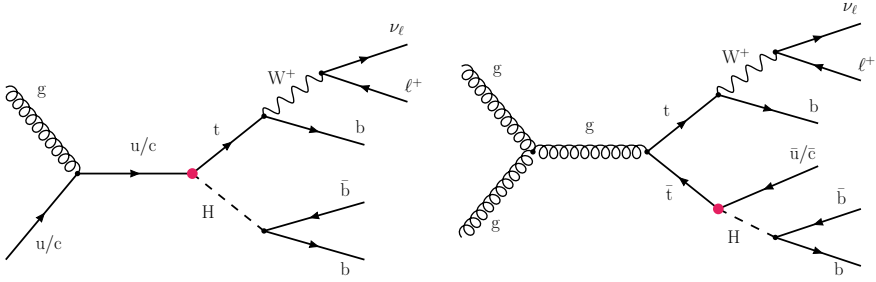


**Fig. 10.1** Diagrams for FCNH  $tch$  search with  $h \rightarrow b\bar{b}$ : [left]  $th^0$  associated production; [right]  $t\bar{t}$  with  $\bar{t} \rightarrow \bar{q}h^0$ . [Figure from CMS experiment [27]]

at 95% C.L. for ATLAS [22] and CMS [23], respectively. Based on  $36.1^{-1}$  data at 13 TeV, ATLAS has further updated with the new 95% C.L. limits of

$$\mathcal{B}(t \rightarrow ch) < 0.22\%, \quad 0.16\% \quad (\text{ATLAS 13 TeV, } 36.1 \text{ fb}^{-1}) \quad (10.6)$$

for  $h \rightarrow \gamma\gamma$  [24] and multileptons [25], respectively. For the dominant  $h \rightarrow b\bar{b}$  decay final state [26], judging from the time it took the experiments to conduct their study, it seems to suffer from more serious background than expected. Based on  $35.9 \text{ fb}^{-1}$  at 13 TeV and combining both single top, i.e.  $th^0$  associated production followed by  $t \rightarrow b\ell^+\nu$  and  $h \rightarrow b\bar{b}$ , together with  $t\bar{t} \rightarrow (b\ell^+\nu)(q\bar{b}\bar{b})$  search (see Fig. 10.1), CMS has published [27] the 95% C.L. limit of  $\mathcal{B}(t \rightarrow ch) < 0.47\%$ , a result which is consistent with (10.5), but not better than (10.6) based on  $h^0 \rightarrow \gamma\gamma$ .

These limits, now approaching  $10^{-3}$ , are rather impressive, as discovery could have occurred along the way if Nature had so desired. And it could in principle *emerge anytime tomorrow*. All this on the backdrop of the prevailing NFC prejudice before Higgs discovery. But the prejudice, i.e. the 2HDM-II mindset, still persists. Based on the cleaner  $h \rightarrow \gamma\gamma$  mode, ATLAS projects [28] a final reach at HL-LHC of  $\mathcal{B}(t \rightarrow ch) < 1.5 \times 10^{-4}$  at 95% C.L. Together with multilepton final states, it seems one should be able to reach below  $10^{-4}$ , if not better. In contrast to  $t \rightarrow cZ$ , there seems to be much better hope for discovery.

It should be noted that all data point towards the decoupling or alignment limit, that  $h^0$  is very close to the SM Higgs boson. In the context of 2HDM, it means that its non-standard couplings, such as  $tch$ , are modulated by a small mixing angle with the exotic  $CP$ -even heavy Higgs boson  $H^0$  (hence the “ $h^0$ ” notation for 125 GeV boson),

$$\rho_{ct} \cos(\beta - \alpha) \bar{c}th^0, \quad (10.7)$$

where we have kept the 2HDM-II notation of  $\cos(\beta - \alpha)$  as the  $h^0$ - $H^0$  mixing angle, and  $\rho_{ct}$  is the FCNH Yukawa coupling of the exotic  $H^0$ . The physical  $ctH^0$  coupling would be modulated by  $|\sin(\beta - \alpha)| \simeq 1$ . Thus, FCNH for  $h^0$  is further “protected”

to be small by alignment, which augments the Cheng-Sher protection of trickle-down mass-mixing.

But it was stressed [29] that  $\rho_{ct} \sim 1$  is possible, while the diagonal element  $\rho_{tt}$  is most reasonably  $O(1)$ , and even  $\rho_{cc}$  is not well constrained. Given our poor handle on  $h \rightarrow c\bar{c}$  measurement, 2HDM-III highlights the importance of precision measurement of  $h \rightarrow \tau\tau$ ,  $c\bar{c}$  with more data. Because  $\cos(\beta - \alpha) \sim 0$ ,  $h \rightarrow WW^*$ ,  $ZZ^*$ ,  $gg$ ,  $\gamma\gamma$  must be close to SM expectation. As for the Yukawa coupling  $\rho_{bb}$  of heavy Higgs  $H^0$ , it enters  $b \rightarrow s\gamma$  loop via the charged Higgs  $H^\pm$ , modulated by CKM matrix elements, receiving also a chiral enhancement factor  $m_t/m_b$ , and has been shown [29] to be  $\sim 0.01$  if  $\rho_{ct}$  is sizable. Thus  $h \rightarrow b\bar{b}$  is also SM-like, but its precision measurement is of interest. The Yukawa pattern discussed here can be checked at LHC Run 2. Note that for large  $\rho_{ct} \sim 1$ , the heavy neutral Higgs bosons  $H^0$  and  $A^0$  could be searched for in  $t\bar{c}$  final states [30], opening up a new search program.

## 10.2 New Yukawa Couplings with Extra Higgs Bosons

With our almost experimental account of  $t \rightarrow ch$  search at the LHC in previous section, it should be clear that ATLAS and CMS would simply do it simply because the Higgs boson is found to be lighter than the top, regardless of “doctrines” such as NFC, or prejudices from MSSM (i.e. 2HDM-II). In this section, we broaden the view and advocate that 2HDM-III [5] with FCNH should in fact be called the “Standard 2HDM”, or SM2 for short, in the same way we treat SM: let Nature have her say. SM2 would be more formally defined in the following section.

### 10.2.1 Flavor Changing Neutral Higgs: $h^0 \rightarrow \mu^\pm \tau^\mp$

After the early suggestion of  $t \rightarrow ch$  [5] in conjunction with the naming of 2HDM-III, i.e. 2HDM with FCNH, impact of FCNH in the lepton sector was explored [31] for  $\mu \rightarrow e\gamma$ , which involves  $\mu\tau h$  and  $\tau e h$  couplings. The importance of two-loop diagrams was emphasized, as these bring in a top loop with  $\rho_{tt}$  coupling (mentioned in the previous section) to heavy Higgs boson  $H^0$ . That is, an effective  $H\gamma^*\gamma$  correction is attached to the  $\mu \rightarrow \tau \rightarrow e$  line, which could compete with the one loop diagram for  $\mu \rightarrow e\gamma$ , as the latter is suppressed by three chirality flips, while the former has only one. The fact that two-loop diagrams may in fact dominate in these type of transitions were originally pointed out by Bjorken and Weinberg [32], but it is often called the Barr-Zee mechanism [33], from an independent but similar diagrammatic discussion for electron EDM.

Motivated in part by the  $tch$  discussion, together with the difficulty of Higgs search at the Tevatron,  $h \rightarrow \mu\tau$  search was suggested [34, 35] as a possibility at the turn of the millennium. Reflecting the times, another motivation was the observation of

large  $\nu_\mu\text{-}\nu_\tau$  mixing in the late 1990s, even though it does not necessarily translate into large  $h \rightarrow \mu\tau$ , as we are not sure that neutrino masses are generated by the (same) Higgs mechanism. But again, Nature can have her say, while the experiments can simply do it.

Further theoretical developments helped motivate  $h \rightarrow \mu\tau$  search at the LHC. This was in part due to the BaBar  $B \rightarrow D^{(*)}\tau\nu$  anomaly, which was announced just before the Higgs discovery. In the earlier phase of discussion, since BaBar stressed the incompatibility with 2HDM-II, people explored [36, 37] the possibility with 2HDM that possessed FCNH, and indeed it seemed to work, running into difficulty only later with other measurables, as discussed in Sect.4.3.2. As the  $h(125)$  had been emerging since late 2011, some theorists turned towards investigating FCNH involving  $h^0$  itself, in particular the importance [38, 39] of  $h \rightarrow \mu\tau$  direct search at the LHC.

With discovery of the  $h^0$  boson in 2012, and following the earlier suggestion [38] that  $h^0 \rightarrow \mu\tau$  is still allowed even at  $O(10\%)$ , the authors of [39] applied the detailed formulas for  $\mu \rightarrow e\gamma$  [31] to the case of  $\tau \rightarrow \mu\gamma$  for a more thorough study. While confirming that  $\mathcal{B}(h^0 \rightarrow \mu\tau)$  at  $O(10\%)$  is indeed still allowed, the authors pointed out further that direct search for  $h^0 \rightarrow \mu\tau$  at the LHC would quickly give rise to a better bound, if not discovery, of finite  $\mu\tau h$  coupling, or

$$Y_{\mu\tau} \bar{\mu}\tau h^0, \quad (10.8)$$

that is more stringent than coming from  $\tau \rightarrow \mu\gamma$ . This gave strong stimulus to the experiments.

Taking up this suggestion and reconstructing  $\tau$  leptons in the electronic and hadronic decay channels, CMS uncovered [40] a remarkable  $2.4\sigma$  excess with 8 TeV data,

$$\mathcal{B}(h \rightarrow \mu\tau) = (0.84^{+0.39}_{-0.37})\%, \quad (\text{CMS 8 TeV, 2015}) \quad (10.9)$$

or  $\mathcal{B}(h \rightarrow \mu\tau) < 1.51\%$  at 95% C.L., which aroused quite some interest. The corresponding 95% C.L. bound [41] from ATLAS with 8 TeV data is 1.85%, which is not inconsistent. The result indeed surpassed the  $\tau \rightarrow \mu\gamma$  constraint, and could be interpreted as a hint for FCNH!

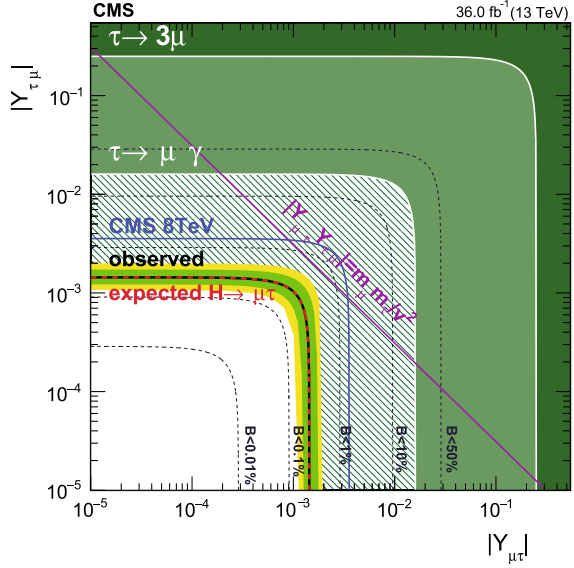
Could  $h^0 \rightarrow \mu\tau$  be at the 1% level?

Comparing (10.8) with (10.7), it is better to write the former as

$$\rho_{\mu\tau} \cos(\beta - \alpha) \bar{\mu}\tau h^0. \quad (10.10)$$

This is because the SM Higgs boson coupling is necessarily diagonal, so the FCNH component of  $h^0$  arises from mixing with the exotic  $H^0$  scalar. Thus,  $|Y_{\mu\tau}| = |\rho_{\mu\tau} \cos(\beta - \alpha)|$  with  $\rho_{\mu\tau}$  being the true exotic Yukawa coupling. The  $Y_{\mu\tau}$  notation of [39], treating the FCNH coupling of  $h^0$  directly, is an oversimplification carried over from the Cheng-Sher Ansatz [17].

**Fig. 10.2** Comparison of CMS result [42] for  $h^0 \rightarrow \mu\tau$  ( $h^0$  marked as  $H$  in plot), based on 13 TeV data taken in 2016, with  $\tau \rightarrow \mu\gamma$ ,  $3\mu$  bounds, in the  $|Y_{\mu\tau}|$ - $|Y_{\tau\mu}|$  coupling plane. The heavy (thin) solid contour is the observed (expected), dashed contours are marked with  $\mathcal{B}(h^0 \rightarrow \mu\tau)$  values, while thin solid diagonal line corresponds to the ‘‘Cheng–Sher’’ value of  $|Y_{\mu\tau}Y_{\tau\mu}| = m_\mu m_\tau/v^2$



From (10.10), we see that, besides a trickle-down flavor suppression in  $\rho_{\mu\tau}$ , exotic  $h^0 \rightarrow \mu\tau$  decay is naturally suppressed by  $h^0$ - $H^0$  mixing angle, which seems to be small, which is the empirical ‘‘alignment’’ phenomenon mentioned earlier. If a sizable rate at the level of (10.9) is confirmed, then  $\rho_{\mu\tau}$  must be sizable, but if the  $h^0 \rightarrow \mu\tau$  hint disappears, it could just be due to a small  $|\cos(\beta - \alpha)|$ , rather than imply the absence of FCNH  $\mu\tau H^0$  coupling.

Alas, after two years of anticipation, the CMS experiment unveiled the 13 TeV result based on 2016 dataset at the LHCP 2017 conference held in Shanghai. With a total of  $35.9 \text{ fb}^{-1}$ , the new 95% C.L. limit [42] is

$$\mathcal{B}(h \rightarrow \mu\tau) < 0.25\%, \quad (\text{CMS 13 TeV, } 35.9 \text{ fb}^{-1}) \quad (10.11)$$

which does not support the 8 TeV result of (10.9). The hint evaporated.

Taking over the original suggestive plot from [39], Fig. 10.2 displays the comparison of the CMS bound, (10.11), with other bounds such as  $\tau \rightarrow \mu\gamma$ ,  $\mu\mu\mu$ , as well as the earlier 8 TeV result [40] of (10.9). Plotted in the  $|Y_{\mu\tau}|$ - $|Y_{\tau\mu}|$  plane (note that we have not distinguished between  $Y_{\mu\tau}$  and  $Y_{\tau\mu}$  for simplicity of discussion), one can see that the  $h \rightarrow \mu\tau$  bound is indeed stronger than rare  $\tau$  decays (see Fig. 9.2), and the naive Cheng-Sher value of  $|Y_{\mu\tau}Y_{\tau\mu}| = m_\mu m_\tau/v^2$  is now ruled out. Put differently, the ‘‘Cheng-Sher’’ Ansatz [17] should be dropped as a guidance for FCNH studies.

### 10.2.2 2HDM-III: Two Higgs Doublets Without $Z_2$

The Cheng-Sher paper [17] treated flavor changing Higgs coupling in multi-Higgs doublet models in a relatively general fashion. In pointing out  $t \rightarrow ch$  process, the “third type of two Higgs doublet model (Model III)” was explicitly defined [5] to have the properties: (1) the NFC condition is not imposed (hence no  $Z_2$  symmetry); (2) low energy FCNC constraints are evaded by mass-dependent couplings of the form [17]

$$M_{ij}^k = \Delta_{ij}^k \sqrt{m_i m_j}, \quad (10.12)$$

“that reflect fermion mass and mixing hierarchies”, where  $k = 1, 2$ , and  $i$  is a generation index. The  $\Delta_{ij}^k$  is viewed as  $O(1)$ , and this has fed the  $Y_{\mu\tau}$  notation in (10.8) and the  $\sqrt{m_\mu m_\tau}/v$  form (see Fig. 10.2). But the definition of  $\Delta_{ij}^k$  is vague, and people generally view (10.12) as the definition for the coupling to  $h^0$  as well. This, however, is a misguidance.

The implementation of Glashow-Weinberg NFC condition is usually by imposing a  $Z_2$  symmetry, where in 2HDM-II the  $u$ -type and  $d$ -type quarks receive mass from different doublets (often labeled as  $\Phi_u, \Phi_d$ ), while in 2HDM-I, all quarks receive mass from the same doublet. There are further variations involving the lepton sector, which we do not get into. Thus, 2HDM-III is a type of 2HDM without  $Z_2$  symmetry. Now that the existence of *one* Higgs doublet is confirmed by observation of  $h(125)$ , it should be clear that imposing a discrete  $Z_2$  symmetry is actually a rather strong, *ad hoc* assumption. The Cheng-Sher Ansatz is more than 30 years old, while the definition of 2HDM-III is only 5 years younger. From the fact that the CMS limit on  $h \rightarrow \mu\tau$  rules out the naive Cheng-Sher Ansatz, it is time to contemplate.

We have by now introduced the flavor changing couplings  $\rho_{ct}$  (10.7),  $\rho_{\mu\tau}$  (10.10), as well as the flavor conserving couplings  $\rho_{cc}, \rho_{tt}$  and  $\rho_{bb}$  of the heavy Higgs boson  $H^0$ . These couplings mix into the coupling of  $h^0$  by the small mixing parameter  $\cos(\beta - \alpha)$ , which means that the  $\rho_{ij}$  couplings of the physical  $H^0$  boson should be modulated by a  $\sin(\beta - \alpha)$  factor. Likewise, the SM couplings of  $h^0$  would pick up a  $\sin(\beta - \alpha)$  factor, while these mix into  $H^0$  with a  $-\cos(\beta - \alpha)$  factor. The  $h^0$ - $H^0$  mixing arises from the Higgs potential, where data indicates that  $|\cos(\beta - \alpha)|$  is quite small (alignment). Our context is a 2HDM, but with NFC cast aside. The observed light  $h^0$  boson (with small  $H^0$  admixture) is the remnant of SSB, or v.e.v. generation. The three Goldstone components of the mass-giving doublet are “eaten” as the longitudinal components of the massive  $W^\pm, W^0$  gauge bosons.

The apparent decoupling/alignment indicates that the second Higgs doublet is considerably heavier, with a scalar  $H^0$ , a pseudoscalar  $A^0$ , and charged scalar  $H^\pm$  that are not too far apart in mass. We shall assume  $CP$  is conserved within the Higgs sector, otherwise it could have easily resulted in sizable neutron EDM. The key point is that, with the simultaneous diagonalization of the fermion mass matrices and Yukawa matrices of the mass-giving doublet, the  $\sin(\beta - \alpha)$ -dependent couplings of  $h^0$  are flavor diagonal. For the second Higgs doublet, however, the Yukawa matrices



cannot be simultaneously diagonalized with the mass matrices, hence are naturally flavor changing. This general phenomenon of FCNH is now being probed at the LHC, as described above. But Nature seems to have been hiding it by a small  $|\cos(\beta - \alpha)|$ .

### 10.3 SM2: SM, But with Two Higgs Doublets

We would now like to introduce the Lagrangian of the Yukawa couplings in SM2, which is elevated from 2HDM-III of the previous section.

2HDM-III was invoked [36, 37] for the  $B \rightarrow D^{(*)}\tau\nu$  anomaly, but fell out of favor by challenges from other data (Sect. 4.3.2). It offered guidance [29] for  $t \rightarrow ch$  search, as discussed in Sect. 10.1, though  $t \rightarrow ch$  has not yet emerged at the  $10^{-3}$  level. It also motivated [39]  $h \rightarrow \mu\tau$  search, but the initial hint [40] with 8 TeV LHC data did not firm up at LHC Run 2 [42].

We note the contrast between  $B \rightarrow D^{(*)}\tau\nu$  versus  $t \rightarrow ch$  and  $h \rightarrow \mu\tau$  processes. We have argued that the  $R_D, R_{D^{(*)}}$  anomaly needs further experimental scrutiny, while  $t \rightarrow ch$  and  $h \rightarrow \mu\tau$  search would plainly continue, whether  $R_D, R_{D^{(*)}}$  remain anomalous or not, just because the LHC experiments can readily do it. In fact, a weakened  $R_D, R_{D^{(*)}}$  problem would probably breathe life back into 2HDM-III considerations. On the other hand, unlike  $B \rightarrow D^{(*)}\tau\nu$  decay, the  $t \rightarrow ch$  and  $h \rightarrow \mu\tau$  decay vertices are dimension 4, hence essentially *fundamental*: they probe the existence of *extra Yukawa couplings* that the  $h(125)$  boson may sense. This latter point motivates us to move from “model” to theory, thus SM2: *SM, but with two Higgs doublets*.

Emphatically, there are no theorem that restricts the number of Higgs doublets to one. With one doublet firmly established, it seems highly probable that a second doublet exists.<sup>4</sup> This is in contrast with, e.g. leptoquarks, or singlet Higgs,<sup>5</sup> which we view as genuinely exotic. With an extra Higgs doublet, the natural question to ask is whether there are *extra Yukawa couplings*. The fear of FCNH caused Glashow and Weinberg to remove them by decree in 1977. But the experimental interest after Higgs boson discovery makes it clear that this is actually an experimental question. The question is a very potent one, as the CKM matrix and fermion masses are all rooted in Yukawa couplings. Since the CKM phase is insufficient for baryogenesis, might extra Yukawa couplings help?

It is truly remarkable that the SM possesses [43] all the necessary ingredients for baryogenesis, i.e. the Sakharov [44] conditions of (1) baryon number violation, (2)  $CP$  violation, and (3) departure from equilibrium (in the very hot early Universe). But then the agony is the insufficiency in the latter two conditions: CPV is way

---

<sup>4</sup>What about more doublets? Well, one extra at a time, unless there is some further, well motivated guiding principle for more.

<sup>5</sup>An extra scalar singlet could be conveniently added for model building, but it would be relatively arbitrary as it is not related to electroweak symmetry breaking. A scalar triplet would have issue with electroweak precision measurements.

too small, while the electroweak phase transition (EWPhT) seems only a crossover, rather than the needed first order transition. We shall see that a 2HDM with genuine extra Yukawa couplings offer hope on both counts.

### 10.3.1 Lagrangian for Yukawa Couplings in SM2

The Yukawa couplings for quarks in SM2 can be written in matrix notation as [30, 45],

$$\sum_{f=u,d} \bar{\mathbf{f}} \left[ \left( \frac{\mathbf{m}^f}{v} h^0 - \frac{\boldsymbol{\rho}^f}{\sqrt{2}} H^0 \right) \sin \gamma - \left( \frac{\boldsymbol{\rho}^f}{\sqrt{2}} h^0 + \frac{\mathbf{m}^f}{v} H^0 \right) \cos \gamma \right. \\ \left. + i \operatorname{sgn}(Q_f) \frac{\boldsymbol{\rho}^f}{\sqrt{2}} A^0 \right] R \mathbf{f} + \bar{\mathbf{u}} (\boldsymbol{\rho}^{u\dagger} \mathbf{V} L - \mathbf{V} \boldsymbol{\rho}^d R) \mathbf{d} H^+ + \text{h.c.}, \quad (10.13)$$

where  $L$ ,  $R$  are the usual left or right projections,  $\mathbf{m}^f$  is the diagonal mass matrix for  $f = u$ - or  $d$ -type quarks, whereas  $\boldsymbol{\rho}^f$  is the Yukawa matrix for the doublet that is not responsible for mass generation, hence should have off-diagonal components. The mixing angle  $\cos \gamma$  corresponds to  $\cos(\beta - \alpha)$  in 2HDM-II, i.e. the  $h^0$ - $H^0$  mixing angle, and  $\sin \gamma$  has opposite sign to usual  $\sin(\beta - \alpha)$ . Note that  $\tan \beta$  is unphysical when there is no  $Z_2$  to distinguish the two doublets, so it is better to use the notation [46] of  $\cos \gamma$  to avoid confusion and inconsistency. From (10.13), we easily recover (10.7) and (10.10) for  $t \rightarrow ch$  and  $h \rightarrow \mu\tau$  discussions (using analogous lepton couplings).

So, just what are the  $\boldsymbol{\rho}^u$  and  $\boldsymbol{\rho}^d$  (and likewise  $\boldsymbol{\rho}^\ell$ ) matrices? Since there are two Higgs doublets, one combination of the two Yukawa matrices gives the mass matrix,  $\mathbf{m}^f$ , which is diagonalized in usual way, and exhibit a clear mass hierarchy for  $f = u$ ,  $d$  and  $\ell$ . An orthogonal combination of the two Yukawa matrices gives rise to  $\boldsymbol{\rho}^f$ , after going through the same diagonalization transforms. While  $\boldsymbol{\rho}^f$  is in general not diagonal, it should reflect the structure of mass and CKM hierarchies. For example,  $d$ -type quarks are much lighter than corresponding  $u$ -type quarks, and there is a generational mass and CKM mixing angle hierarchy. Thus,  $\rho_{ij}^d$  is less significant in strength, while the largest elements are  $\rho_{tc}$  and  $\rho_{tt}$  [29] (where we have dropped the superscript  $u$ ), which, given  $\lambda_t = \sqrt{2}m_t/v \simeq 1$ , they can both be  $O(1)$ .<sup>6</sup> This is the excitement for  $t \rightarrow ch^0$  search, although the process is modulated by  $\cos \gamma$ , and could vanish even if  $\rho_{tc}$  is sizable. For  $\rho_{\mu\tau}$ , it should be the same order as  $\lambda_t$  or smaller, and modulated by  $\cos \gamma$  for  $\mu\tau h^0$  coupling. Thus, in general  $|\rho_{\mu\tau}| < O(\lambda_\tau)$  and should be considerably weaker than  $|\rho_{tc}| < O(\lambda_t) \sim 1$ . But the Higgs boson width is, of course, much smaller than the top width, hence both  $t \rightarrow ch^0$  and  $h^0 \rightarrow \mu\tau$  searches should continue.

<sup>6</sup>We have been cavalier in distinguishing  $\rho_{ct}$  and  $\rho_{tc}$ . To be sure,  $\rho_{ct}$  is constrained [29, 30] by  $B_q$  mixing and  $b \rightarrow s\gamma$  to be small, and can be realized naturally.

Note that, in  $\cos \gamma \rightarrow 0$  limit,  $h^0$  couplings become diagonal and would appear just like the SM Higgs boson, while  $H^0$  and  $A^0$  can have exotic, *new* Yukawa couplings. From the fact that we see no deviations so far [47] in  $h^0$  properties from SM Higgs, we are not far from the “alignment” limit. From hindsight, mass-mixing hierarchy plus alignment—two mechanisms at work together—actually works better than the Cheng-Sher ansatz in evading FCNH effects of  $h^0$  at low energies, but the NFC condition of Glashow and Weinberg is not needed. Nature seems to have prepared approximate alignment to further suppress low energy FCNH effect carried by  $h^0$ .

So why do we prefer to call this SM2, rather than just 2HDM-III? In part this is because 2HDM-II is too well known, and tends to guide ones thinking. Furthermore, 2HDM-III has picked up the baggage from the Cheng-Sher Ansatz, and people tend to forget that the FCNH effect of  $h(125)$  is in fact suppressed further by alignment. If we look back at how SM emerged, the mass-mixing hierarchy was not anticipated, but Nature does have her organization and control mechanism in regards flavor violation. This structure must be built into the two Yukawa matrices as we have already alluded to, such that the CKM matrix echoes the mass hierarchy. Thus, all  $\mathbf{m}^f$  exhibit mass hierarchy, and all  $\rho^f$  matrices have mass-mixing hierarchical suppression of off-diagonal elements, but need not be of the Cheng-Sher form.

In short, we just allow a second Higgs boson doublet, but place no further assumptions on it, except what we have already learned from SM so far. Hence, SM2, i.e. SM, but with two Higgs doublets. This is in strong contrast to the *ad hoc*  $Z_2$  symmetry assumption in 2HDM-II for sake of NFC.

### 10.3.2 Prognosis

Two developments offer strong support for us to take SM2 more seriously: approximate alignment, and electroweak baryogenesis (EWBG).

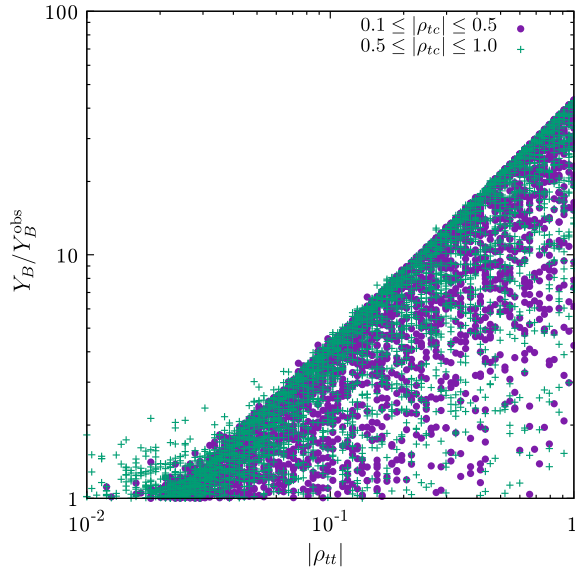
In 2HDM-II, the alignment phenomenon,  $\cos(\beta - \alpha) \rightarrow 0$ , gives the impression that it can only be realized via fine tuning. This is because  $\alpha$  depends on details of the Higgs potential, and there is no reason for  $\beta$  (defined by  $\tan \beta = v_1/v_2$  of the two doublets) and  $\alpha$  to differ by  $\pm\pi/2$ . What comes to mind, despite the wish to search for  $H^0, A^0, H^\pm$  bosons at the LHC, is to decouple [48] the second Higgs doublet  $\Phi'$ , by pushing its mass,  $m_{\Phi'}$ , to multi-TeV. This is unpleasant not just for LHC search, for if it is realized, extra Higgs boson effects may not be detectable in flavor physics.

A simple but not quite obvious phenomenon was uncovered in this context. It was shown [49] in SM2 that approximate alignment may correspond to Higgs quartic couplings  $\eta_i$  that are  $O(1)$  in strength,<sup>7</sup> without the need to push the exotic Higgs masses towards decoupling limit. This can actually work also in 2HDM-II, where it is the notation of  $\cos(\beta - \alpha)$  that gets in the way:  $\beta - \alpha$  is actually the angle between the Higgs basis (where only one Higgs doublet,  $\Phi$ , generates  $v$ ) and the

---

<sup>7</sup>More precisely, at least one [49] of the four parameters from the Higgs potential that enter  $m_{H^0}^2$ , including the inertial term (basically  $m_{\Phi'}^2/v^2$  mentioned in context of decoupling), has to be  $O(1)$ .

**Fig. 10.3** Impact of  $\rho_{tt}$  and  $\rho_{tc}$  on  $Y_B/Y_B^{\text{obs}}$ , where the phases  $\phi_{tt}$  and  $\phi_{tc}$  are scanned over 0 to  $2\pi$ , with other parameters randomly chosen. The purple points (green crosses) are for  $0.1 \leq |\rho_{tc}| \leq 0.5$  ( $0.5 \leq |\rho_{tc}| \leq 1.0$ )



neutral Higgs boson mass eigenbasis. In SM2, as we have mentioned, there is no  $Z_2$  symmetry to define, or distinguish between,  $\Phi_1$  and  $\Phi_2$ ,<sup>8</sup> it is therefore better to replace  $\cos(\beta - \alpha)$  by  $\cos \gamma$  [46], as we have stressed. Interestingly, given that absence of  $Z_2$  allows for extra Yukawa couplings such as  $\rho_{tt}$ , this  $O(\lambda_t)$  hence  $O(1)$  extra Yukawa coupling could further protect [46] the apparent alignment through loop corrections.

It is known that  $O(1)$  Higgs quartic couplings can provide first order electroweak phase transitions, one of the Sakharov conditions for baryogenesis that falls short in SM. Remarkably, it is found [50] that a finite  $\rho_{tt} \sim O(1)$  and generally complex because it is an extra Yukawa coupling, could efficiently drive electroweak baryogenesis (EWBG). The mechanism, proportional to  $\lambda_t \text{Im} \rho_{tt}$  [50], is in contrast with SM, where the mass and mixing hierarchies suppress drastically the effect of CPV, and falls far short of what is needed for baryogenesis. Discussing the details of EWBG is outside the scope of this book. Let us just illustrate the efficacy [50] of SM2 for EWBG by giving the plot (Fig. 10.3) for  $Y_B \equiv n_B/s$ , the ratio of baryon versus entropy density (baryon asymmetry of the Universe, BAU), normalized to the observed  $Y_B^{\text{obs}}$  [51].

Actually,  $\rho_{tc}$  can also generate  $Y_B$ . In Fig. 10.3, we separate into  $0.1 \leq |\rho_{tc}| \leq 0.5$  and  $0.5 \leq |\rho_{tc}| \leq 1.0$ , plotted as (purple) ellipses or (green) crosses. Given that there are no strong differences between the two,  $\rho_{tt}$  is the leading driver of  $Y_B$ , which can allow the range of up to a factor of 40 from  $Y_B^{\text{obs}}$ , hence rather robust. However, as  $|\rho_{tt}|$  approaches a few percent, its effect becomes diminished, but the (green) crosses

<sup>8</sup>Without  $Z_2$ ,  $\tan \beta$  is not physical, thus we use  $\eta_i$  instead of the usual  $\lambda_i$  notation for Higgs quartic couplings, writing the mass-giving doublet as  $\Phi$ , and  $\Phi'$  the exotic doublet that possesses FCNH couplings. The physical  $h^0$  and  $H^0$  are mixtures, by  $\cos \gamma$ , of the two  $CP$ -even neutral scalars from  $\Phi$  and  $\Phi'$ , where we assume a  $CP$  invariant Higgs potential.

populate  $Y_B/Y_B^{\text{obs}} \sim 2-3$  better than the (purple) ellipses. Thus,  $\rho_{tc}$  can provide a second mechanism for EWBG, but it requires  $O(1)$  value with near maximal phase. Compared with SM, *SM2 has two mechanisms for EWBG*, which should not be taken lightly.

In this vein, the measurements of  $b \rightarrow s\gamma$ ,  $\tau \rightarrow \mu\gamma$ ,  $R_{D^{(*)}}$  and  $B^+ \rightarrow \tau^+\nu_\tau$ ,  $\mu^+\nu_\nu$  decay rates make Belle II a unique probe of matter asymmetry of the Universe, analogous to  $\sin 2\phi_1/\beta$  measurement in the B factory era. We remark that, unlike 2HDM-II, the extra Yukawa couplings in the lepton sector can make the ratio  $\mathcal{B}(B^+ \rightarrow \mu^+\nu_\nu)/\mathcal{B}(B^+ \rightarrow \tau^+\nu_\tau)$  deviate [52] from the SM value, which can be a unique probe. This makes the recently observed  $2.4\sigma$  excess in  $\mathcal{B}(B^+ \rightarrow \mu^+\nu_\nu)$  by Belle [53] rather intriguing, which should be made a priority in early Belle II analysis. At the LHC, there are same sign top and triple-top signatures via associated production of  $tH^0$  and  $tA^0$  [54],

$$c + g \rightarrow tH^0, tA^0 \rightarrow tt\bar{c}, t\bar{t}c, t\bar{t}t, \quad (10.14)$$

analogous to  $tZ$  production of (10.4). The same-sign top signature could probe finite  $\rho_{tc}$  with  $300 \text{ fb}^{-1}$ , whereas triple-top can be an exquisite signature<sup>9</sup> at HL-LHC with  $3000 \text{ fb}^{-1}$ . But positively identifying  $H^0$ ,  $A^0 \rightarrow t\bar{c}, t\bar{t}$  as the source even if discovered is not so easy. In any case, the study is only at its infancy, but this illustrates further that the top quark has entered flavor physics, in particular as a probe of the Higgs sector.

## References

1. Albrecht, H., et al. [ARGUS Collaboration]: Phys. Lett. B **192**, 245 (1987)
2. Sirunyan, A.M., et al. [CMS Collaboration]: Phys. Rev. Lett. **120**, 231801 (2018)
3. Aaboud, M., et al. [ATLAS Collaboration]: Phys. Lett. B **784**, 173 (2018)
4. Tanabashi, M., et al. [Particle Data Group]: Phys. Rev. D **98**, 030001 (2018). <http://pdg.lbl.gov/>
5. Hou, W.-S.: Phys. Lett. B **296**, 179 (1992)
6. Chatrchyan, S., et al. [CMS Collaboration]: Phys. Rev. Lett. **112**, 171802 (2014)
7. Aaboud, M., et al. [ATLAS Collaboration]: JHEP **1807**, 176 (2018)
8. Azatov, A., Panico, G., Perez, G., Soreq, Y.: JHEP **1412**, 082 (2014)
9. Bardhan, D., Bhattacharyya, G., Ghosh, D., Patra, M., Raychaudhuri, S.: Phys. Rev. D **94**, 015026 (2016)
10. Aad, G., et al. [ATLAS Collaboration]: Eur. Phys. J. C **76**, 55 (2016)
11. Sirunyan, A.M., et al. [CMS Collaboration]: JHEP **1707**, 003 (2017)
12. Fuyuto, K., Hou, W.-S., Kohda, M.: Phys. Rev. D **93**, 054021 (2016)
13. Altmannshofer, W., Gori, S., Pospelov, M., Yavin, I.: Phys. Rev. D **89**, 095033 (2014)
14. Hou, W.-S., Kohda, M., Modak, T.: Phys. Rev. D **96**, 015037 (2017)
15. Glashow, S.L., Weinberg, S.: Phys. Rev. D **15**, 1958 (1977)
16. Fritzsche, H.: Phys. Lett. B **73**, 317 (1978)

---

<sup>9</sup>Note there are single top,  $t\bar{t}$  then  $t\bar{t}t\bar{t}$  signatures in SM at hadron colliders, with triple top practically absent.

17. Cheng, T.-P., Sher, M.: Phys. Rev. D **35**, 3484 (1987)
18. ATLAS collaboration: ATLAS-CONF-2013-081
19. Craig, N., Evans, J.A., Gray, R., Park, M., Somalwar, S., Thomas, S., Walker, M.: Phys. Rev. D **86**, 075002 (2012)
20. Aad, G., et al. [ATLAS Collaboration]: JHEP **1406**, 008 (2014)
21. Khachatryan, V., et al. [CMS Collaboration]: Phys. Rev. D **90**, 112013 (2014)
22. Aad, G., et al. [ATLAS Collaboration]: JHEP **1512**, 061 (2015)
23. Khachatryan, V., et al. [CMS Collaboration]: JHEP **1702**, 079 (2017)
24. Aaboud, M., et al. [ATLAS Collaboration]: JHEP **1710**, 129 (2017)
25. Aaboud, M., et al. [ATLAS Collaboration]: Phys. Rev. D **98**, 032002 (2018)
26. Kao, C., Cheng, H.-Y., Hou, W.-S., Sayre, J.: Phys. Lett. B **716**, 225 (2012)
27. Sirunyan, A.M., et al. [CMS Collaboration]: JHEP **1806**, 102 (2018)
28. ATLAS Collaboration: ATL-PHYS-PUB-2013-012
29. Chen, K.-F., Hou, W.-S., Kao, C., Kohda, M.: Phys. Lett. B **725**, 378 (2013)
30. Altunkaynak, B., Hou, W.-S., Kao, C., Kohda, M., McCoy, B.: Phys. Lett. B **751**, 135 (2015)
31. Chang, D., Hou, W.-S., Keung, W.-Y.: Phys. Rev. D **48**, 217 (1993)
32. Bjorken, J.D., Weinberg, S.: Phys. Rev. Lett. **38**, 622 (1977)
33. Barr, S.M., Zee, A.: Phys. Rev. Lett. **65**, 21 (1990)
34. Diaz-Cruz, J.L., Toscano, J.J.: Phys. Rev. D **62**, 116005 (2000)
35. Han, T., Marfatia, D.: Phys. Rev. Lett. **86**, 1442 (2001)
36. Crivellin, A., Greub, C., Kokulu, A.: Phys. Rev. D **86**, 054014 (2012)
37. Fajfer, S., Kamenik, J.F., Nišandžić, I., Zupan, J.: Phys. Rev. Lett. **109**, 161801 (2012)
38. Blankenburg, G., Ellis, J., Isidori, G.: Phys. Lett. B **712**, 386 (2012)
39. Harnik, R., Kopp, J., Zupan, J.: JHEP **1303**, 026 (2013)
40. Khachatryan, V., et al. [CMS Collaboration]: Phys. Lett. B **749**, 337 (2015)
41. Aad, G., et al. [ATLAS Collaboration]: JHEP **1511**, 211 (2015)
42. Sirunyan, A.M., et al. [CMS Collaboration]: JHEP **1806**, 001 (2018)
43. Kuzmin, V.A., Rubakov, V.A., Shaposhnikov, M.E.: Phys. Lett. B **155**, 36 (1985)
44. Sakharov, A.D.: Pisma Zh. Eksp. Teor. Fiz. **5**, 32 (1967) [JETP Lett. **5**, 24 (1967)]
45. Mahmoudi, F., Stål, O.: Phys. Rev. D **81**, 035016 (2010)
46. Hou, W.-S., Kikuchi, M.: Phys. Rev. D **96**, 015033 (2017)
47. Aad, G., et al. [ATLAS and CMS Collaborations]: JHEP **1608**, 045 (2016)
48. Gunion, J.F., Haber, H.E.: Phys. Rev. D **67**, 075019 (2003)
49. Hou, W.-S., Kikuchi, M.: EPL **123**, 11001 (2018)
50. Fuyuto, K., Hou, W.-S., Senaha, E.: Phys. Lett. B **776**, 402 (2018)
51. Ade, P.A.R., et al. [Planck Collaboration]: Astron. Astrophys. **571**, A16 (2014)
52. Chang, P., Chen, K.-F., Hou, W.-S.: Prog. Part. Nucl. Phys. **97**, 261 (2017)
53. Sibidanov, A., et al. [Belle Collaboration]: Phys. Rev. Lett. **121**, 031801 (2018)
54. Kohda, M., Modak, T., Hou, W.-S.: Phys. Lett. B **776**, 379 (2018)

# Chapter 11

## Conclusion



The 2008 Nobel Prize in Physics was given jointly to Nambu, for spontaneous symmetry breaking, and Kobayashi and Maskawa, for CP violation. Thus marked the transition from the B factory era to the LHC era, although the latter was delayed by a couple of years.

The 2013 Nobel Prize in Physics was given to Englert and Higgs, for the Higgs mechanism, and the prediction of the Higgs particle. Other than that, the truly striking thing from the LHC, from Run 1 through Run 2 so far, is the absence of any New Physics. Not only SUSY remains elusive, nothing else was uncovered. Instead, as covered in various preceding chapters, we have a handful of flavor anomalies, plus the long standing muon  $g - 2$  issue.

So, where do we stand?

It looks like the Long Shutdown 2 (LS2) period of LHC, extending by a year or two into Run 3, would see a bright and flavorful golden harvest. It would be the days of reckoning for the flavor anomalies, and the arrival of Belle II data would give us an independent crosscheck, if not new discoveries. As Run 2 has five times the data of Run 1, the High Energy frontier remains of interest. But the expected data increase of LHC Run 3 is only a factor of two from Run 2, hence the Run 3 plus LS3 period is a bit less interesting at the High Energy frontier. Given Belle II data accumulation, and other flavor pursuits such as kaons and muons would also bear fruit, we foresee a *decade* of plentitude in our quest for TeV scale physics via flavor.

### Whither Beyond?

To this author, from an experimental point of view, it is better to stick to the simplest (rather than elaborate) explanation of an effect that calls for New Physics. That has been our guiding principle. But the problem of electroweak symmetry breaking, and the problem of flavor, seem as far apart as ever. To be conservative on where New Physics may emerge on the flavor front, one has to look where the SM can be extended,<sup>1</sup> which can be in the following:

---

<sup>1</sup>The SUSY extension is not conservative from the flavor point of view. Not only it is a large extension—doubling number of all fields, hence introducing a very large number of parameters—

- Gauge sector

We have touched upon the  $Z'$  in Chap. 5, and sporadically in a few other places. In general,  $Z'$  with FCNC is quite arbitrary as a model. But the  $L_\mu - L_\tau$  model may be worthy of note, and has been employed for  $P'_5$  and  $R_{K^{(*)}}$  anomalies, as well as muon  $g - 2$ .

Another possibility is  $SU_R(2)$ , or restoration of parity at high energy. Though not touched upon specifically, probes of right-handed interactions were discussed in Chaps. 5 and 6, even the top quark as probe (Chap. 10). In general, new gauge interactions must be broken, with scale considerably higher than the weak scale. But very weakly coupled gauge bosons could be light, which may enter (Chap. 7) the Dark Sector.

- Higgs sector

We discussed charged Higgs boson effects in Chap. 4, using two Higgs Doublet Model II as example, such as the special constraint on  $m_{H^\pm}$  (and  $\tan\beta$ ) coming from  $b \rightarrow s\gamma$  and  $B \rightarrow \tau\nu$ . 2HDM-III (i.e. without a  $Z_2$  symmetry to eliminate FCNH couplings) was considered in context of  $R_{D^{(*)}}$  anomaly, but fell out of favor because of various constraints. If the  $R_{D^{(*)}}$  anomaly weakens in strength, this may be an interesting direction. Effects of exotic neutral scalar and pseudoscalars were covered in Chaps. 6–10, for example  $t \rightarrow ch$  and  $h \rightarrow \mu\tau$  where  $h(125)$  picks up exotic component via mixing. We have not explored CPV induced purely from enlarging the Higgs sector, as these could easily generate too large EDMs.

We will return to 2HDM-III, emphasized by us as “SM2”, before our Summary and Outlook.

- Fermion sector (or matter fields)

All matter fields, except the right-handed neutrino, carry some SM gauge charge(s), the extension of which should impact on observables of interest. We have used the sequential 4th quark generation as our prime example in Chaps. 2 and 3. This is in part because the extension from CKM3 to CKM4, bringing in new mixing angles as well as CPV phases, is bound to touch upon all experimental measurables of interest. But interest in this extension has come to a halt with finding null CPV in  $B_s$  mixing, and that the  $h(125)$  production cross section is SM-like, rather than enhanced by an order of magnitude. A Requiem is given in Appendix B.

Replacing the 4th generation, heavy vector-like quarks (VLQ) continue to be searched for at the LHC, which is in part motivated by alleviating the Higgs mass quadratic divergence due to top correction (top partners under “Little Higgs”), and thus an issue of EWSB, rather than flavor. VLQs have been used in model building, e.g. in conjunction with  $L_\mu - L_\tau$  symmetry towards flavor anomalies, but these tend to be much heavier than the ones currently searched for by ATLAS and CMS.

- Neutrino sector

Here we refer to neutrino mixing and the presence of right-handed neutrinos, where

---

but the extension is motivated from EWSB, or the protection thereof, not from flavor physics. In fact, flavor and CPV cause major problems for having TeV scale SUSY, since it runs easily into conflict with flavor physics measurements, and there is a question of naturalness.



the possibility of Majorana masses is an intriguing possibility, bringing in physics ideas with rich impact, such as the seesaw mechanism [1], and leptogenesis. We have seen clear evidence for neutrino mass since 1998 [2], which definitely goes beyond the original minimal SM. But we have barely touched upon this rapidly evolving field, which has a life of its own, separate from flavor physics. The closest link is our Chap. 9.

Neutrino mixing appears strikingly different from CKM mixing.

## In Praise of CKM

We have to express our great appreciation of the CKM structure.

The three generation structure of SM was predicted by Kobayashi and Maskawa, before the second quark generation was even complete! The textbook argument is that, even with two quark generations, one has enough phase freedom in the quark fields to remove CPV phases in the  $2 \times 2$  CKM matrix that governs the  $\bar{u}_i \gamma_\mu L d_j W^\mu$  weak coupling. Only by having three generations of quarks would the weak interactions break  $CP$  invariance, and the CPV phase turns out to be *unique*, which is another attractive feature. Inspecting Fig. 1.6 once again, one can only admire the success of the KM model that, after more than four decades of extensive experimental effort, not only the third generation fermions were discovered one after the other, three generation unitarity of (1.4) holds, with all data meeting consistently in the same parameter region. The picture has only improved in the past decade.

What no one really predicted is the mass-mixing hierarchy in the quark sector, which adds to the flavor enigma.

But our goal is to probe beyond SM, on flavor and the link to TeV scale physics. Although KM as the dominant source of CPV in the laboratory seems proven so far, it predicts that the  $b \rightarrow s$  unitarity triangle represented by (3.4) should have the same area as the  $b \rightarrow d$  unitarity triangle represented by (1.4), as shown pictorially in Fig. 3.4 (or Fig. A.2). The usual convention of taking  $V_{cs} V_{cb}^*$  real is implied (though not necessary), and the extremely small phase of  $V_{ts} V_{tb}^*$  (see also (A.6)) then gives the SM prediction that the analogous CPV phase in tagged  $B_s \rightarrow J/\psi \phi$  study would be much, much smaller than for  $B_d \rightarrow J/\psi K_S$ . This is now confirmed in (3.28), and only the LHCb experiment has the capability to probe further into the minuscule SM value of  $\sin 2\Phi_{B_s} \simeq -0.04$  given in (3.8), with the CMS experiment following behind as a distant crosscheck.

## Baryogenesis, SM2, and Extra Yukawas

Equation (3.28), however, was a big disappointment to one, and some. As sketched in Appendix B, there was great hope ca. 2010–2011 that  $\sin 2\Phi_{B_s}$  could be found to be large and negative. This was not just because of the correlation with sizable  $\Delta\mathcal{A}_{K\pi}$  in 4th generation extension of SM (Chap. 3), but because of the drastic jump in CPV strength (in the Jarlskog invariant), from (B.1) to (B.2), that seemed enough for generating baryon asymmetry of the Universe (BAU), or electroweak baryogenesis (EWBG):  $CP$  violation fo(u)r the Heaven and the Earth.

So, Nature seems to limit the generation number to 3. Then what? With the extra CPV phases, and great enhancement provided in (B.2) gone, are we left with baryogenesis from leptogenesis? Possibly, but that would be outside the realm of traditional flavor physics, and a triumph for neutrino flavor physics. There is the further down side that laboratory verification would be generally more difficult, if not impossible.

In this regard, we have advocated in the previous chapter the extension of Higgs doublets to two, but with the *conservative* approach of allowing for flavor changing neutral Higgs, or FCNH, couplings. That is, one should not impose the traditional  $Z_2$  symmetry to remove FCNH couplings, but keep the possibility of having *extra Yukawas*, hence extra CPV sources. On one hand, this is because imposing a  $Z_2$  symmetry is a rather strong, ad hoc assumption. On the other hand, as demonstrated by the *experimental* interest in searching for  $t \rightarrow ch$  and  $h \rightarrow \mu\tau$  processes after Higgs boson discovery, LHC experimentalists would not stop at the “instruction” of NFC for removing FCNH, as finding such decays would then lead to a shift in doctrine. Simply put, if we just discovered that the Higgs boson is lighter than the top quark, how can one not search?

If one would naturally take  $t \rightarrow ch$  and  $h \rightarrow \mu\tau$  seriously, “Because we can!”, why should we shun the possibility for similar couplings involving lower generations? It is true that we have a rather large increase in the number of physical extra Yukawa couplings, but given that flavor parameters dominate the number of parameters in SM, this is not particularly new. Furthermore, as we have advocated, the  $\lambda_t \text{Im} \rho_{tt}$  mechanism replaces the Jarlskog invariant handily, and one has a robust source of CPV for electroweak baryogenesis. With approximate alignment, or small  $h^0-H^0$  mixing, relatively easy to accommodate with  $O(1)$  Higgs quartic couplings, which are needed for first order electroweak phase transition, we have dubbed the two Higgs doublet model without further assumptions, other than what we already know in flavor sector, SM2. This is nothing but the SM, but with 2 Higgs doublets. The explicit flavored Yukawa couplings of the  $h^0, H^0, A^0, H^\pm$  Higgs bosons are given in (10.13), which we strongly suggest to be taken seriously in the coming experimental and theoretical studies.

## Summary and Outlook

In the decade since the advent of the LHC, SM has checked out gloriously, in particular in the discovery of the Higgs boson,  $h^0$ , the “last piece of the (particle) puzzle”. But No New Physics is found! LHC would go through LS2, then Run 3, and then LS3, before entering the decade-long HL-LHC running from 2026 onwards. Be it with Run 2, or the subsequent Run 3 data, search for New Physics would certainly continue. But chances for discovering New Physics such as SUSY, or new particles that couple with SM strength, seems increasingly diminished. To push further, and to probe new effects or New Particles that involve couplings below SM strength, these are the reasons why HL-LHC must run its course.

On the flavor front, let us recall a decade's progress since the B factory era:

- $\Delta\mathcal{S}$ : the once favorite “ $\Delta\mathcal{S}$  problem” ceased to be a problem even before LHC started, but remains a topic for Belle II;
- $\Delta\mathcal{A}_{K\pi}$ : while experimentally sound, it is now viewed as due to hadronic effect, with color-suppressed  $C$  amplitude enhanced to that of  $T$  in strength; hadronic effect in  $B$  decays are large;
- $A_{\text{FB}}(B \rightarrow K^*\ell^+\ell^-)$ : hint of discrepancy in lower  $q^2$  bins was not confirmed by LHCb;
- $\sin 2\Phi_{B_s}$ : the mild hint at Tevatron for *large and negative* values were put to rest by LHCb measurement of  $\phi_s \equiv 2\Phi_{B_s} \cong 0$ .

In fact,  $\phi_s \equiv 2\Phi_{B_s} \cong 0$  was one of the greatest FPCP measurements at the LHC, which practically eliminated the NP possibility of the “ $\Delta\mathcal{A}_{K\pi}$  problem”. The other great FPCP measurement at the LHC is the measurement of  $B_s \rightarrow \mu^+\mu^-$ . Finding it consistent with SM put an end to the saga at the Tevatron, the dream of an up to three orders of magnitude enhancement inspired by SUSY. Thus, there is also no indication for SUSY from flavor physics.

A third highlight of flavor physics at the LHC is the landmark observation of  $t\bar{t}h^0$  production: we have now directly measured the top Yukawa coupling,  $\lambda_t \simeq 1$ . This is the “mother of most FPCP loop effects” in SM. But since the observed cross section is SM-like, it did not seem to cause any sensation.

The increasing sensation has been with the “flavor anomalies”.

To BaBar's credit, years after PEP-II dumped its last beam, meticulous studies of  $B \rightarrow D^{(*)}\tau\nu$  (via  $\tau \rightarrow \mu\nu\nu$ ) over the  $B \rightarrow D^{(*)}\mu\nu$  ratio, BaBar unleashed the  $R_D, R_{D^*}$  anomaly just before the Higgs boson was discovered. Having eliminated  $A_{\text{FB}}$  from the B factories, before long, LHCb had its own  $P'_5$  anomaly, by 2013, in  $B \rightarrow K^*\mu^+\mu^-$  angular variables. And by taking the ratio of  $B \rightarrow K\mu^+\mu^-$  rate with that of  $B \rightarrow Ke^+e^-$ , by 2014 LHCb had the  $R_K$  anomaly, extending to  $R_{K^*}$  in 2017. Before the latter, the inventive LHCb was able to study the  $B \rightarrow D^{(*)}\tau\nu$  to  $B \rightarrow D^{(*)}\mu\nu$  ratio and concurring with BaBar's finding in 2015, and the  $R_{D^*}$  anomaly was elevated to a true sensation.

Given that No New Physics has been found in high  $p_T$  searches at the LHC, the CMS experiment took note of the flavor anomalies by 2018. In one study, viewing the possibility that a  $Z'$  caused the shift in Wilson coefficient,  $\Delta C_9 \sim -1$ , CMS zoomed in on  $Z \rightarrow \mu^+\mu^-Z'(\rightarrow \mu^+\mu^-)$  search, setting bounds on the  $L_\mu - L_\tau$  gauge boson. In another study, CMS took the LQ interpretation of  $R_{D^{(*)}}, R_{K^{(*)}}$  anomalies and searched for  $b$ - $\tau$  leptoquarks. These were briefly touched upon in the relevant subsections, and there would be more high  $p_T$  studies to come.

In previous chapters, we have favored  $Z'$  over LQ, arguing that the latter is more exotic. Inasmuch as they are our current best hope, here we would like to give some caution, or reminder, on flavor anomalies from the purely experimental perspective.

- LUV: Is  $R_{K^{(*)}}$  anomaly real?

These ratios should have the least theoretical uncertainty, but  $R_K|_{1.0}^{6.0}$ ,  $R_{K^*}|_{0.045}^{1.1}$ ,  $R_{K^*}|_{1.1}^{6.0}$ , are  $2.6\sigma$ ,  $2.2\sigma$ ,  $2.4\sigma$  below SM expectation, respectively, where the lower and upper ranges are in units of  $\text{GeV}^2$ . But  $R_{K^*}|_{0.045}^{1.1}$  covers the photon peak (the  $1.1 \text{ GeV}^2$  upper range, rather than  $1.0 \text{ GeV}^2$ , is to include the  $\phi$  resonance), where dimuon has a slightly higher threshold than dielectron, but otherwise it is expected to be SM-like, as it is photon dominant, and the photon coupling is universal.

Having all three measurements behaving the same way, when  $R_{K^*}|_{0.045}^{1.1}$  is expected to respect universality, it makes one wonder, according to Occam's principle, whether there is not a *simpler* common cause.

- Is  $P'_5$  anomaly real?

One should recall that, when  $P'_5$  anomaly was first announced in 2013 with  $1 \text{ fb}^{-1}$  data, the discrepancy was  $3.7\sigma$  in the  $q^2$  bin below  $J/\psi$ . But when updated to  $3 \text{ fb}^{-1}$  in 2015, where the statistics allowed splitting the bin in two, the discrepancy remained at  $3.4\sigma$ . Though nothing wrong in statistical sense, it is certainly not too good. With only CMS having comparable statistics, the result was found, in 2017, to be consistent with SM. There is thus cause for caution.

If  $P'_5$  from LHCb Run 2 update continues the sluggish trend, the likelihood of fluctuation among many variables, or the  $c\bar{c}$  threshold (hadronic) effect, would increase in likelihood.

- Is  $R_{D^{(*)}}$  anomaly real?

When LHCb announced their  $R_{D^*}$  value is in agreement with BaBar's, the theory community went wild. Though Belle was always consistent with both BaBar and SM, it was basically taken as "junior". It is then worthy of note that the two 2018 results, from LHCb and Belle, are both consistent with SM! Both utilize  $\tau \rightarrow 3$ -prong final state, and one wonders whether there is some common systematics in taking the  $R_{D^*}$  ratio in the muon final state (LHCb has not been able to touch  $R_D$  as yet).

One should keep in mind that this *tree level* effect is a very large one, unlike the weakly coupled  $Z'$  case for  $R_{K^{(*)}}$  and  $P'_5$ .

As we have said (see footnote 2 of Introduction), anomalies come and go, and *they mostly go*, which has been the case for all the discrepancies from the B factories in the 2000s. The current flavor anomalies have been more persistent, but they all bear the fingerprint, to some degree, of LHCb. LHCb is certainly a spectacularly successful experiment, but this point enhances our anticipation for Belle II to rejoin as confirmation/competition experiment, with perhaps CMS as well on  $P'_5$  and  $R_{K^{(*)}}$ .

But even if just one of these "anomalies" bear out with Run 2, or Belle II B physics data, we would have our Eureka moment. We certainly hope that, as Run 2 or Belle II data unfold, more indications for New Physics would be uncovered. And the list of possibilities is long.

With NA62 and KOTO finally making progress on  $K \rightarrow \pi\nu\nu$  (and  $K \rightarrow \pi X^0$ !), with Muon g-2 and MEG II experiments plowing the muon front, as well as COMET, Mu2e, and electric dipole moment experiments, we foresee a flavorful harvest in LHC

Long Shutdown 2 period and beyond, even towards HL-LHC. The outlook is bright in the flavor quest for New Physics.

Flavor physics and (beyond) the TeV scale: Never give up!

## References

1. Fukugita, M., Yanagida, T.: Phys. Lett. B **174**, 45 (1986)
2. Tanabashi, M., et al.: [Particle Data Group]. Phys. Rev. D **98**, 030001 (2018). <http://pdg.lbl.gov/>

# Appendix A

## A CP Violation Primer

### A.1 Generalities

CP violation is defined as a difference in probability between a particle process from the antiparticle process, e.g. between  $B \rightarrow f$  and  $\bar{B} \rightarrow \bar{f}$ . As is typical in quantum phenomena, it requires the presence of two interfering amplitudes. However, besides the familiar  $i$  from quantum mechanics, it needs *complex dynamics* as well.<sup>1</sup> That is, the interference involves the presence of two different kinds of phases. Let us elucidate how CPV occurs.

Consider the amplitude  $A = A_1 + A_2$  for the particle process, which is a sum of two terms, where amplitude  $A_j$  has both a CP invariant phase  $\delta_j$  (quantum mechanical  $i$ ) and a CPV phase  $\phi_j$  ( $i$  from CPV dynamics). Absorbing an overall phase by defining  $A_1 = a_1$  to be real, one has

$$\begin{aligned} A &= A_1 + A_2 = a_1 + a_2 e^{i\delta} e^{+i\phi}, \\ \bar{A} &= \bar{A}_1 + \bar{A}_2 = a_1 + a_2 e^{i\delta} e^{-i\phi}, \end{aligned} \tag{A.1}$$

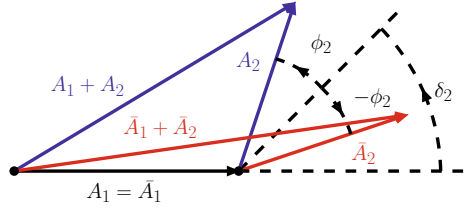
where  $a_2 \equiv |A_2|$ . The  $\delta$  and  $\phi$  are called the “strong” and “weak” phases, respectively. The strong phase  $\delta$  arise from (re)scattering or quantum time evolution, and does not distinguish between particle or antiparticle, hence the sign is unchanged between  $A$  and  $\bar{A}$ . However, the dynamical or weak phase  $\phi$  changes sign for the antiparticle process  $\bar{A}$ . This enrichment of quantum interference leads to a possible asymmetry between particle and antiparticle probabilities, for example, involving  $\bar{B}^0$  versus  $B^0$ . From (A.1), one finds

$$A_{CP} \equiv \frac{\Gamma_{\bar{B}^0 \rightarrow \bar{f}} - \Gamma_{B^0 \rightarrow f}}{\Gamma_{\bar{B}^0 \rightarrow \bar{f}} + \Gamma_{B^0 \rightarrow f}} = \frac{2a_1 a_2 \sin \delta \sin \phi}{a_1^2 + a_2^2 + 2a_1 a_2 \cos \delta \cos \phi}, \tag{A.2}$$

---

<sup>1</sup> Imagine  $e$  of electrodynamics is complex. This is not possible as it is a gauge coupling.

**Fig. A.1** Mechanism for CPV, the geometric picture for (A.2)



defined with respect to quarks (e.g.  $\bar{B}^0$  contains a  $b$  quark). As  $\mathcal{A}_{CP}$  vanishes with either  $\delta$  or  $\phi \rightarrow 0$ , CPV requires the presence of *both* CP conserving *and* CPV phases.

Equation (A.1) is illustrated in Fig. A.1, which shows geometrically how the  $\mathcal{A}_{CP}$  of (A.2) materializes. By a phase choice, we place  $A_1 = \bar{A}_1$  on the real axis. Then  $A_2$  and  $\bar{A}_2$ , which are of the same length  $|A_2| = |\bar{A}_2| = a_2$ , are as depicted, where  $A_2$  ( $\bar{A}_2$ ) is rotated by  $+\phi$  ( $-\phi$ ) from the common  $\delta$  phase angle. We see that, if  $\delta = 0$ , then  $A_1 + A_2$  and  $\bar{A}_1 + \bar{A}_2$  are at angle  $\phi$  above or below the real axis, and are of equal length. If, however,  $\phi = 0$ , then  $A_1 + A_2$  and  $\bar{A}_1 + \bar{A}_2$  coalesce into the same vector, hence are necessarily of equal length. Only when *both*  $\delta \neq 0$  *and*  $\phi \neq 0$  do we have  $|A_1 + A_2| \neq |\bar{A}_1 + \bar{A}_2|$ , as one can see from the asymmetry formula (A.2).

### CP Violation in Standard Model with 3 Generations

In the KM model with 3 generations, one needs the presence of all 3 generations in a process to make CPV occur [1]. In the standard phase convention [2] of keeping  $V_{us}$  and  $V_{cb}$  real, the unique CPV phase is placed in the 13 element  $V_{ub}$ , and hence the 31 element  $V_{td}$  as well by unitarity of  $V$ . We give the CKM matrix  $V$  in Wolfenstein form [2, 3],

$$V = \begin{pmatrix} V_{ud} & V_{us} & V_{ub} \\ V_{cd} & V_{cs} & V_{cb} \\ V_{td} & V_{ts} & V_{tb} \end{pmatrix} \simeq \begin{pmatrix} 1 - \lambda^2/2 & \lambda & A\lambda^3(\rho - i\eta) \\ -\lambda & 1 - \lambda^2/2 & A\lambda^2 \\ A\lambda^3(1 - \rho - i\eta) & -A\lambda^2 & 1 \end{pmatrix}, \quad (\text{A.3})$$

where,

$$\lambda \equiv V_{us} \simeq 0.22, \quad A\lambda^2 \equiv V_{cb} \simeq 0.04, \quad A\lambda^3\sqrt{\rho^2 + \eta^2} \equiv |V_{ub}| \sim 0.003. \quad (\text{A.4})$$

For those with any interest in flavor and CPV physics, it is useful to memorize (A.3), and the orders of magnitude in (A.4). The latest measured strength of the CPV phases  $\phi_3 \equiv \arg V_{ub}^*$  and  $\phi_1 \equiv \arg V_{td}$  (Belle notation for phases) can be found in [2].

The matrix  $V$  is unitary, i.e.

$$V^\dagger V = V V^\dagger = I. \quad (\text{A.5})$$

It can be readily checked that this relation holds for the Wolfenstein form of  $V$  in (A.3) to  $\lambda^3$  order. At this order,  $V_{ts}$  is real and negative, but it picks up a tiny

imaginary part at  $\lambda^4$  order (see below). Note that  $\sqrt{\rho^2 + \eta^2} \sim 1/3$ , compared with  $\lambda \cong 0.22 \sim 1/4.5$ . Thus, together with  $A \sim 0.8$ ,  $|V_{ub}|$  is actually closer to  $\lambda^4$  [4] rather than  $\lambda^3$  order, while  $|V_{td}|$  is of order  $\lambda^3$ .

Since we highlight CPV in  $b \rightarrow s$  and  $b\bar{s} \leftrightarrow s\bar{b}$  ( $B_s^0 - \bar{B}_s^0$  oscillations) transitions as frontiers for probing physics beyond SM, we extend (A.3) to  $\lambda^5$  order,

$$V \cong \begin{pmatrix} 1 - \frac{1}{2}\lambda^2 - \frac{1}{8}\lambda^4 & \lambda & A\lambda^3(\rho - i\eta) \\ -\lambda + A^2\lambda^5(\frac{1}{2} - \rho - i\eta) & 1 - \frac{1}{2}\lambda^2 - (\frac{1}{8} + \frac{1}{2}A^2)\lambda^4 & A\lambda^2 \\ A\lambda^3(1 - \bar{\rho} - i\bar{\eta}) & -A\lambda^2 + A\lambda^4(\frac{1}{2} - \rho - i\eta) & 1 - \frac{1}{2}A^2\lambda^4 \end{pmatrix}, \quad (\text{A.6})$$

where the definitions of (A.4) for the three upper-right off-diagonal elements, namely  $V_{us}$ ,  $V_{cb}$  and  $V_{ub}$ , remain the same, and [2]  $\bar{\rho}/\rho = \bar{\eta}/\eta = 1 - \frac{1}{2}\lambda^2$ . We see that  $V_{ts}^*V_{tb}$  picks up a CPV phase at  $\lambda^4$  order, while the real part is at  $\lambda^2$  order. This implies a rather small phase angle as compared with the phase in  $V_{td}^*V_{tb}$ , where the imaginary and real parts of the latter are not drastically different in strength.

It is useful to visualize the so-called unitarity triangles that arise from the unitarity relation, (A.5). Take the  $db$  element of  $VV^\dagger = I$  for example, one has

$$V_{ud}V_{ub}^* + V_{cd}V_{cb}^* + V_{td}V_{tb}^* = 0. \quad (\text{A.7})$$

The usual convention is to normalize by  $A\lambda^3$ , then  $V_{cd}V_{cb}^*/A\lambda^3 \cong -1$ , and  $V_{ud}V_{ub}^*/A\lambda^3 \cong \rho + i\eta$  (for our purpose, let us not distinguish between  $\bar{\rho} + i\bar{\eta}$  and  $\rho + i\eta$ ), and  $V_{td}V_{tb}^*/A\lambda^3$  follows by unitarity. Equation (A.7) is represented by the triangle  $-V_{cd}V_{cb}^* - O - V_{ud}V_{ub}^*$  in Fig. A.2.

For the  $sb$  element of  $VV^\dagger = I$ , one has

$$V_{us}V_{ub}^* + V_{cs}V_{cb}^* + V_{ts}V_{tb}^* = 0. \quad (\text{A.8})$$

If one represents this in the same plot as (A.7), one notes that  $V_{ud}V_{ub}^*/A\lambda^3 \cong \rho + i\eta$  is replaced by  $V_{us}V_{ub}^*/A\lambda^3 \cong \lambda(\rho + i\eta)$ , or the corresponding side has shrunk by  $\lambda \cong 0.22$  in length. At the same time,  $V_{cd}V_{cb}^*/A\lambda^3 \cong -1$  becomes  $V_{cs}V_{cb}^*/A\lambda^3 \cong +1/\lambda$ , which is now extended by  $1/\lambda$  times, and positive. It is represented by the long horizontal solid line extending to the right. Again,  $V_{ts}V_{tb}^*/A\lambda^3$  follows by unitarity, which is represented by the slightly slanted dotted line pointing left (back to the ‘‘origin’’). Thus, (A.8) is represented by the rather squashed and elongated triangle in Fig. A.2.

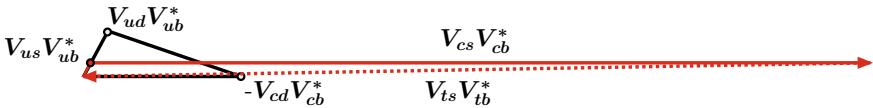


**Fig. A.2** Geometric representations of (A.7) and (A.8), the latter being the long, squashed triangle. It is common to take the lower left point as the origin



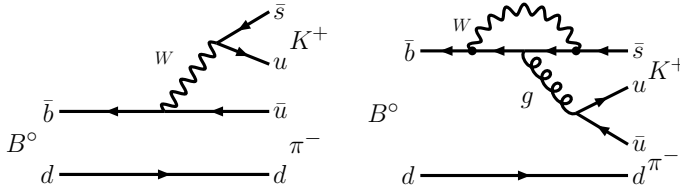


Fig. A.3 Tree and Penguin diagrams for  $B^0 \rightarrow K^+\pi^-$  decay

## A.2 Illustration: Direct $CP$ Violation

Direct CPV (DCPV), which was established in  $B^0 \rightarrow K^+\pi^-$  decay ca. 2004, gives the most intuitive illustration of the previous section. That is, we have  $f = K^+\pi^-$  in (A.2). Experimentally, the measurement of DCPV in  $B^0 \rightarrow K^+\pi^-$  decay is the most straightforward, being just a counting experiment. One simply counts the difference between the number of events in  $K^-\pi^+$  versus  $K^+\pi^-$  final states, with  $m_{K\pi}$  reconstructing to  $m_{B^0}$ , and with background under control. It is a matter of waiting for enough statistics. This is also a so-called self-tagged mode, since the charge of the  $K^\pm$  points back to the decaying particle being a  $B^0$  or a  $\bar{B}^0$ .

In Fig. A.3 we show the leading tree ( $T$ ) and penguin ( $P$ ) diagrams for  $B^0 \rightarrow K^+\pi^-$  decay. Reading off from (A.3), one can readily see that the tree  $b \rightarrow u\bar{u}$  diagram carries a weak phase  $\phi_3 = \arg V_{us}V_{ub}^*$ , while  $P$  is dominated by  $V_{cs}V_{cb}^* \cong -V_{ts}V_{tb}^*$ , which is practically real. If the  $T$  and  $P$  amplitudes develop a relative strong phase  $\delta$  (some absorptive part in the amplitudes), the interference between  $T$  and  $P$  would lead to *direct* (i.e., in decay amplitude itself) CPV. Indeed, this was observed in 2004 [5, 6], and  $\mathcal{A}_{B^0 \rightarrow K^+\pi^-} \equiv \mathcal{A}_{CP}(B^0 \rightarrow K^+\pi^-) \sim -10\%$  is not small, recalling that  $|\epsilon'|$  is at the  $10^{-6}$  level in the kaon system. This illustrates rather clearly (A.1) and (A.2), where, to good approximation,  $a_1 = |P|$  and  $a_2 = |T|$ . Unfortunately, the strong phase difference  $\delta$  is of hadronic nature, the computation of which is rather challenging, and theorists do not generally agree with each other.

The whimsical name of the “penguin” diagram is attributed to a bet by John Ellis in the 1970s. Let us not get deeper into the historical anecdote, but note that, if one complains that Fig. A.3b bears no resemblance to a “penguin”, then neither does a Feynman diagram bear any resemblance to Feynman (although unlike the “penguin”, Feynman did pen it)!

## A.3 Time-Dependent $CP$ Violation

The idea for mixing- or time-dependent  $CP$  violation (TCPV) study at B factories is quite beautiful. Rather than derive the TCPV formalism [7, 8], where we may get lost in the details, we give the formula and elucidate its content, thereby hopefully

get to appreciate part of its beauty. In this way we also prepare for the discussion of actual experimental studies in Chap. 2.

The TCPV asymmetry for  $B^0 \rightarrow f$  decay, where  $f$  is a  $CP$  eigenstate, is

$$\begin{aligned} A_{\text{CP}}(\Delta t) &\equiv \frac{\Gamma(\bar{B}^0(\Delta t) \rightarrow f) - \Gamma(B^0(\Delta t) \rightarrow f)}{\Gamma(\bar{B}^0(\Delta t) \rightarrow f) + \Gamma(B^0(\Delta t) \rightarrow f)} \\ &= -\xi_f (\mathcal{S}_f \sin \Delta m \Delta t + \mathcal{A}_f \cos \Delta m \Delta t). \end{aligned} \quad (\text{A.9})$$

The first part of (A.9) is defined quite analogous to (A.2), except that it is a little more delicate:  $B^0(\Delta t)$  denotes the state at time  $\Delta t$  that evolved from a  $B^0$  state at  $\Delta t = 0$ , and likewise for  $\bar{B}^0(\Delta t)$ . To avoid clutter, and to compare better with (A.2) in a more transparent way, we have used a looser notation for what are actually differential decay rates (when conducting the analysis). Let us understand the second half of (A.9), where  $\xi_f$  is the  $CP$  eigenvalue of  $f$ ,  $\Delta m \equiv \Delta m_{B_d}$ , and (BaBar uses  $\mathcal{C}_f \equiv -\mathcal{A}_f$ , i.e. picking up the initials for sine and cosine)

$$\mathcal{S}_f = \frac{2 \text{Im } \lambda_f}{|\lambda_f|^2 + 1}, \quad \mathcal{A}_f = \frac{|\lambda_f|^2 - 1}{|\lambda_f|^2 + 1}, \quad (\text{A.10})$$

are CPV coefficients, where  $\lambda_f$  is defined as

$$\lambda_f = \frac{q}{p} \frac{\langle f | S | \bar{B}^0 \rangle}{\langle f | S | B^0 \rangle}. \quad (\text{A.11})$$

We see that  $\lambda_f$  depends on both  $B^0$ - $\bar{B}^0$  mixing (see Sect. 1.3), i.e.  $B_{H,L} = p B^0 \mp q \bar{B}^0$  (where  $H, L$  stands for the nominally ‘‘heavy’’ and ‘‘light’’ states), and decay to final state  $f$ . This is why TCPV is also called CPV in mixing-decay interference. The lifetime difference between the two neutral  $B$  mesons have been ignored to yield the simpler form of (A.9). This is a very good approximation for the  $B_d^0$ - $\bar{B}_d^0$  system (but not so good for  $B_s^0$ - $\bar{B}_s^0$  system, as will be touched upon in Chap. 3), so  $q/p \cong e^{-2i\phi_1}$ , hence  $|q/p| \cong 1$ . Using this last point, one can easily check that  $\mathcal{A}_f$  is nothing but the DCPV asymmetry in  $B^0$  decay, hence this notation is more transparent than BaBar’s usage of  $\mathcal{C}_f$ .

For the golden  $J/\psi K_S$  mode, the decay amplitude is real in the standard phase convention of (A.3), since it is dominated by the (color-suppressed)  $b \rightarrow c\bar{c}s$  tree diagram, where  $V_{cs}^* V_{cb}$  carries practically no weak phase. Thus,

$$\mathcal{S}_{J/\psi K_S} \cong \sin 2\phi_1, \quad \mathcal{A}_{J/\psi K_S} \cong 0, \quad (\text{A.12})$$

to very good accuracy. This is explained in Chap. 2. Many other  $b \rightarrow (c\bar{c})_{\text{charmonium}}$  modes are also studied and, correcting for  $\xi_f$ , adds to the statistics.

Inspecting (A.2), (A.9), (A.10) and (A.12) altogether, one can now interpret (A.9) and gain some insight into the beauty and power of TCPV measurement, especially in the  $J/\psi K^0$  mode (both  $J/\psi K_S^0$  and  $J/\psi K_L^0$ ). As stated, the  $B^0 \rightarrow J/\psi K^0$  mode is

dominated by a single decay amplitude, the color-suppressed  $b \rightarrow c\bar{c}s$  tree diagram, with practically no weak phase in the decay amplitude. But there are two paths from an initial  $B^0$  (i.e.  $B^0$  at time  $\Delta t = 0$ ) to decay to the  $J/\psi K^0$  final state: a direct  $B^0 \rightarrow J/\psi K^0$  decay, or via  $B^0$  oscillating to  $\bar{B}^0$ , then  $\bar{B}^0 \rightarrow J/\psi K^0$  decay. This corresponds to  $A_1$  and  $A_2$  of (A.2). As there is no CPV phase in either  $B^0$  or  $\bar{B}^0$  decay to  $J/\psi K^0$ , one is measuring the CPV phase in the  $B^0$  to  $\bar{B}^0$  oscillation amplitude. Here, the  $CP$  conserving phase is just the quantum mechanical time evolution phase  $e^{i\Delta m\Delta t}$ , which is *measured* experimentally. Thus, we measure the CPV phase factors  $\mathcal{S}_f$  and  $\mathcal{A}_f$ , in the  $\sin \Delta m\Delta t$  and  $\cos \Delta m\Delta t$  oscillation coefficients, when measuring the  $t$ -dependent asymmetries as defined in the first part of (A.9). The  $\mathcal{S}_f$  and  $\mathcal{A}_f$  corresponds to  $\sin \phi$  in (A.2). With  $B^0$ - $\bar{B}^0$  mixing dominated by the top quark,  $\mathcal{S}_{J/\psi K^0}$  measures a pure weak phase, and there is no “hadronic” or other ambiguity.

We stress that, with  $\phi_1$  a fundamental, unique phase in the 3 generation CKM matrix  $V$ , its measurement is as fundamental as determining the electromagnetic coupling constant  $\alpha$ , the strong coupling constant  $\alpha_s$ , or the Weinberg angle  $\sin \theta_W$ . The same could be said about  $|V_{us}|$ ,  $|V_{cb}|$  and  $|V_{ub}|$  in the standard convention [2]. And all fundamental fermion masses.

#### A.4 Extraction of $\gamma/\phi_3$ : “DK Method”

Let us now briefly illustrate how a sophisticated approach to DCPV can in fact measure a fundamental CPV phase.

The CKM phase  $\phi_3$  (see Fig. 1.6) is the angle between  $V_{ud}V_{ub}^*$  and  $V_{cd}V_{cb}^*$ , which is the phase angle of  $V_{ub}^*$  in the standard phase convention. There are three different methods to extract  $\phi_3$  experimentally. All exploit the interference between  $B^- \rightarrow D^{(*)0}K^{(*)-}$  ( $b \rightarrow c\bar{u}s$ ) and  $B^- \rightarrow \bar{D}^{(*)0}K^{(*)-}$  ( $b \rightarrow u\bar{c}s$ , which carries the CPV phase) in some common final state by selecting specific  $D^{(*)0}$  and  $\bar{D}^{(*)0}$  decays, where the crucial parameter is the ratio  $r_B$ ,

$$r_B = \left| \frac{A(B^- \rightarrow \bar{D}^{(*)0}K^{(*)-})}{A(B^- \rightarrow D^{(*)0}K^{(*)-})} \right|, \quad (\text{A.13})$$

which ranges from 0.1 to 0.2.

The GLW method [9, 10] considers  $D$  decays to  $CP$  eigenstates, hence both the Cabibbo-suppressed and allowed decays go into the same final state, leading to interference. To enhance  $r_B$  and make the amplitudes of  $B$  and  $D$  mesons compatible for both decays, the ADS method [11] considers Cabibbo-allowed  $\bar{D}$  decay and doubly-Cabibbo-suppressed  $D$  decay. Extensive measurements of  $\phi_3$  are performed at the  $B$  factories, CDF and LHCb, which can be found in PDG and the HFAG/HFLAV web pages.

The most effective method, and most promising for high statistics, comes from the Dalitz plot [12] or GGHZ [13] method. For three-body decays such as  $D^0 \rightarrow K_S^0 \pi^+ \pi^-$  with large branching fractions, the interference can be studied across the Dalitz plot. Belle and BaBar have measured [2]  $\phi_3$  using this method with good accuracy, which are statistics limited. The beauty of the Dalitz analysis is that one can do a bin-by-bin fit for the variation of the strong phase across the Dalitz plot, and the eventual measurement of  $\phi_3$  would be *hadronic model independent*. With its large and ever increasing statistics, it seems that  $\gamma \equiv \phi_3$  measurement would be dominated by LHCb for the foreseeable future. As of summer 2018, the LHCb accuracy has reached  $5^\circ$ , and one can follow HFLAV for the world average.

There is no strong expectation for a sizable deviation from CKM unitarity.

# Appendix B

## Requiem to 4th Generation

The 4th Generation, 4G, has been pronounced dead more than once in the past, the most serious of which is neutrino counting,  $N_\nu$ , on the  $Z$ -pole, which turned up three. But there can be heavy neutral leptons. Another is the  $S-T$  electroweak precision observables, where the  $S$  measurement seemed damning. But it was then shown that a near degenerate  $t'-b'$ , correlated with heavy Higgs boson mass, could satisfy the  $S-T$  constraint.

The most recent has been the  $h(125)$  production cross section, and the fact that this relatively light boson is rather SM-Higgs-like. Adding  $t'$ ,  $b'$  to the top in the triangle loop, given that top is already near saturation, one has a factor of  $(1 + 1 + 1)^2 = 9$  enhancement in gluon-gluon fusion (ggF) production from SM, which is not observed. To most, this simple fact closes the story. R.I.P. was flagged at ICHEP 2012 in Melbourne.

But how did 4G get back on the map in the first place? As discussed in Chap. 2, first it was the hint, starting in 2004, of DCPV for  $B^+ \rightarrow K^+\pi^0$  being seemingly different in sign from  $B^0 \rightarrow K^+\pi^-$ . This resulted in the Belle  $\Delta\mathcal{A}_{K\pi}$  paper in 2008, suggesting the culprit is the electroweak penguin,  $P_{EW}$ . It was clear that 4G could provide  $m_{t'}$  enhancement, and CPV phase through  $V_{t's}^* V_{t'b}$ . And if true, the corollary is that CPV in  $B_s$  mixing,  $\sin 2\Phi_{B_s}$ , would be large and negative. The results coming out from Fermilab in 2008 hinted at this (Chap. 2), and a 4G meeting organized at CERN in summer 2008 gave the “*Four Statements about the Fourth Generation*” [14]. 4G became semi-in-vogue, with great anticipation by 2010. Note that  $S-T$  observables demanded near degeneracy of  $t'$ ,  $b'$ , hence common doublet mass  $m_Q$ .

Alas, when LHCb opened box in 2011, as announced at Lepton-Photon 2011 in Mumbai, the value was consistent with zero, rather than the wished-for.

But the faithful marched on, as 4G had a trump card: changing from 3G to 4G, the Jarlskog invariant jumped by  $10^{15}$  or more! To see this, the relevant source of CPV in 3G is the Jarlskog invariant [15],

$$J_3 = (m_t^2 - m_u^2)(m_t^2 - m_c^2)(m_c^2 - m_u^2) (m_b^2 - m_d^2)(m_b^2 - m_s^2)(m_s^2 - m_d^2) A, \tag{B.1}$$

where  $A$  is twice the area of any unitarity triangle. Besides small  $A$ , the combined suppression factor of  $m_s^2 m_c^2 m_b^4 / v^8$  makes  $J_3$  fall short by at least  $10^{-10}$  from the CPV strength needed for baryogenesis, let alone the requirement of first order electroweak phase transition. With 4G, treating first two generations as effectively degenerate and shifting 1–2–3 to 2–3–4, we have [16]

$$J_4 \simeq (m_t^2 - m_c^2)(m_t^2 - m_r^2)(m_t^2 - m_c^2) \\ (m_b^2 - m_s^2)(m_b^2 - m_b^2)(m_b^2 - m_s^2) A_4, \quad (\text{B.2})$$

where  $A_4$  is the area of some unitarity triangle by treating 1–2 as degenerate. One easily sees the huge jump in CPV strength,  $J_4/J_3 \gg 10^{10}$ , which seems sufficient for baryogenesis, although order of phase transition remains an issue. Compared with this heavenly factor (matter dominance of our Universe), the setback on earth, that the 4G in  $P_{EW}$  mechanism was nullified by  $\sin 2\Phi_{B_s} \simeq 0$ , is of minor concern. In fact, the 1–2–3 to 2–3–4 shift that lead from (B.1) to (B.2) was stimulated by the  $\Delta\mathcal{A}_{K\pi}$  difference, i.e. 4G through  $P_{EW}$ . But “removing the scaffolding” is not an objection.

By December 2011, the hint for a 125 GeV “Higgs” was apparent. But since a similar hint just above 140 GeV rose, and sank, the 125 GeV hint could go likewise, and the faithful pressed on. In the meantime, Tevatron bounds on 4G quarks had risen above  $tW$  threshold. So when LHC finally took data, early studies quickly [17, 18] pushed the bound on  $m_b$  to approach the unitarity bound, which meant that the 4G Yukawa coupling  $\lambda_Q = \sqrt{2}m_Q/v$  was becoming quite strong. What could this mean?

Investigating the unitarity bound, we found [19] first that, starting from the  $u_i d_j W$  left-handed vector coupling, one could derive the Goldstone  $G$  coupling from the longitudinal  $W$  ( $W_L$ ) coupling, which is exactly of the Yukawa form (reverse of Goldstone theorem), includes the CKM matrix, but without the need to invoke the Higgs boson, i.e. without ever invoking a Lagrangian. Hence, the Yukawa coupling was claimed *empirical*.

To understand the approach to unitarity bound, one then finds that  $Q\bar{Q} \rightarrow Q\bar{Q}$  scattering is actually dominated by Goldstone exchange. This gives a rather different impression from the usual view, that the issue with unitarity bound violation may not lie in the UV, but arises from interactions at longer distance. A “Gap Equation”, reminiscent of Nambu–Jona-Lasinio but different, was constructed [19] from the scattering problem, i.e. turning the  $Q\bar{Q} \rightarrow Q\bar{Q}$  scattering into a self-energy problem by closing a  $Q$  on a  $\bar{Q}$ .

As 2011 turned 2012, a nontrivial numerical solution to the gap equation was achieved. A nontrivial self-energy solution means *dynamical  $m_Q$  generation*, which in turn breaks the gauge symmetry and is exciting. Furthermore, mass generation was possible only for  $\lambda_Q > 4\pi$ , i.e. analogous to  $\pi\pi N$  interaction strength; but it cannot be the latter, since the  $\pi N$  system inspired NJL equation, whereas the gap equation is not NJL. The paper was written and submitted, just at the time when news came that the  $h(125)$  is claimed a discovery by both ATLAS and CMS. At ICHEP 2012

in Melbourne, 4G was viewed dead like all other dynamical electroweak symmetry breaking notions. It took a year and half to get the demonstration paper [20] published.

In Fall 2013, it became clear that the vector boson fusion (VBF) process, the direct check on  $VVh(125)$  coupling, was not yet firmly established, and cannot be with Run 1 data. This is not surprising, given the cross section is 1/12 that of ggF. With discussion and paper titles such as “Higgs couplings are dilaton-like”, or a “Higgs-like dilaton”, it seemed that the  $h(125)$  boson could in fact be a *dilaton*  $\mathcal{D}$ , with couplings to vector bosons and fermions suppressed by the dilaton scale. Despite all this, the inertia was such that one could not move forward, until the twin jolt of 2015.

One stimulus was the jest [21] “*The Higgs boson may be fictitious!*” from Phil Anderson, the discoverer of SSB and “Higgs mechanism” from solid state physics (photons become plasmons inside a superconductor), prior to Nambu, and Higgs and Brout and Englert. Asked by Nature Physics to comment on the experimental observation of a “Higgs particle” far below twice the mass gap ( $2\Delta$  in condensed matter language) in a sophisticated condensed matter system, he was challenging the nature of the  $h(125)$  boson as possibly *emergent*, i.e. whether it was in any Lagrangian. The second stimulus was the experimental claim of  $5\sigma$  measurement of VBF by combined analysis of ATLAS and CMS Run 1 data [22]. It is clear that combining two analyses, each above  $3\sigma$ , could become  $5\sigma$ . But was such combination called for when much more data is to come? There is the issue of bias, and that, given the *importance* of checking whether  $VVh$  coupling strength obeys the prediction of SM, it may be best to do so first within each experiment, and preferably in a single channel (eventually).

With these two motivations, a paper was written in 2016, arguing for  $h(125)$  possibly descending as a dilaton through the no-scale but ultrastrong gap equation. Not surprisingly, one could not get it published, and it remained frozen as 1606.03732v3 on the arXiv.

The work was reactivated [23] when one received a reply from Anderson himself, but three years after the query. The argument for ggF discovery in  $\gamma\gamma$  and  $ZZ^*$  final states was refined, and most issues could be dealt with, although the excess in  $h(125) \rightarrow b\bar{b}$  above the  $Z$  lump in  $VH$  ( $H$  being our  $h(125)$ ) production looked real. But in the end [23], the fact that  $t\bar{t}h$  production, observed by both CMS and ATLAS in 2018, were within 20% or so of SM expectation, made it hard not to accept  $h(125)$  as a particle very close to the Higgs boson of SM. To tune (via  $h$  as dilaton) in  $gg \rightarrow h \rightarrow \gamma\gamma, VV^*, f\bar{f}$  is one thing, but to tune<sup>2</sup>  $gg \rightarrow t\bar{t}h$  yet again to SM is hard to swallow ...

*Subtle is the Lord, but malicious He is not.*

---

<sup>2</sup> Nominally, with  $t\bar{t}h$  coupling suppressed, it is still possible to emit the  $h(125)$  off the gluon lines in  $gg \rightarrow t\bar{t}$  production by a greatly enhanced  $ggh$  coupling. But to mimic SM cross section would be fortuitous.

## References

1. Kobayashi, M., Maskawa, T.: *Progr. Theor. Phys.* **49**, 652 (1973)
2. Tanabashi, M., et al.: [Particle Data Group]. *Phys. Rev. D* **98**, 030001 (2018). <http://pdg.lbl.gov/>
3. Wolfenstein, L.: *Phys. Rev. Lett.* **51**, 1945 (1983)
4. Hou, W.-S., Wong, G.-G.: *Phys. Rev. D* **52**, 5269 (1995)
5. Aubert, B., et al.: [BaBar Collaboration]. *Phys. Rev. Lett.* **93**, 131801 (2004)
6. Chao, Y., Chang, P., et al.: (Belle Collaboration). *Phys. Rev. Lett.* **93**, 191802 (2004)
7. Carter, A.B., Sanda, A.I.: *Phys. Rev. Lett.* **45**, 952 (1980); *Phys. Rev. D* **23**, 1567 (1981)
8. Bigi, I.I.Y., Sanda, A.I.: *Nucl. Phys. B* **193**, 85 (1981)
9. Gronau, M., London, D.: *Phys. Lett. B* **253**, 483 (1991)
10. Gronau, M., Wyler, D.: *Phys. Lett. B* **265**, 172 (1991)
11. Atwood, D., Dunietz, I., Soni, A.: *Phys. Rev. Lett.* **78**, 3257 (1997)
12. Poluektov, A., et al.: [Belle Collaboration]. *Phys. Rev. Lett.* **70**, 072003 (2004)
13. Giri, A., Grossman, Y., Soffer, A., Zupan, J.: *Phys. Rev. D* **68**, 054018 (2003)
14. Holdom, B., Hou, W.-S., Hurth, T., Mangano, M.L., Sultansoy, S., Ünel, G.: *PMC Phys. A* **3**, 4 (2009)
15. Jarlskog, C.: *Z. Phys. C* **29**, 491 (1985)
16. Hou, W.-S.: *Chin. J. Phys.* **47**, 134 (2009). [[arXiv:0803.1234](https://arxiv.org/abs/0803.1234) [hep-ph]]
17. Chatrchyan, S., et al.: [CMS Collaboration]. *Phys. Lett. B* **701**, 204 (2011)
18. Chatrchyan, S., et al.: [CMS Collaboration]. *JHEP* **1205**, 123 (2012)
19. Hou, W.-S.: *Chin. J. Phys.* **50**, 375 (2012). [[arXiv:1201.6029](https://arxiv.org/abs/1201.6029) [hep-ph]]
20. Mimura, Y., Hou, W.-S., Kohyama, H.: *JHEP* **1311**, 048 (2013)
21. Anderson, P.W.: *Nat. Phys.* **11**, 93 (2015)
22. Aad, G., et al.: [ATLAS and CMS Collaborations]. *JHEP* **1608**, 045 (2016)
23. Hou, W.-S.: *Symmetry* **10**, 312 (2018). [[arXiv:1606.03732](https://arxiv.org/abs/1606.03732) [hep-ph]]



# Index

## Symbols

- $A_{\text{FB}}(B \rightarrow K^* \ell^+ \ell^-)$ , 89–92, 96  
 $A_{\text{SL}}$  “anomaly” of  $D\emptyset$ , 43  
 $B \rightarrow K^* \gamma$ , 60, 98, 107, 115, 116  
 $B \rightarrow K^* \gamma$  veto, 100, 101  
 $B \rightarrow D^{(*)} \tau \nu_\tau$ , 71, 73–75  
 $B \rightarrow K + \text{nothing}$ , 101–104  
 $B \rightarrow K^{(*)} \ell^+ \ell^-$ , 85, 88, 90–92, 96  
 $B \rightarrow K^{(*)} \nu \nu$ , 99–101, 103  
 $B^+ \rightarrow J/\psi K^+$ , 25, 28, 29, 108, 110  
 $B^+ \rightarrow K^+ \pi^0$ , 22, 23  
 $B^+ \rightarrow \pi^+ \ell^+ \ell^-$ , 88  
 $B^+ \rightarrow \tau^+ \nu_\tau$ , 66–71, 74, 77, 99–101, 108, 124, 147  
 $B^0 \rightarrow K^+ \pi^-$ , 18, 19, 22, 23  
 $B^0 \rightarrow K^{*0} J/\psi$ , 97  
 $B^0 \rightarrow K^{*0} \mu^+ \mu^-$ , 94  
 $B^0 \rightarrow \eta' K_S$ , 16, 17  
 $B^0 \rightarrow \mu^+ \mu^-$ , 112, 114, 115  
 $B^0 \rightarrow \phi K^{*}$ , 29  
 $B^0 \rightarrow \phi K_S$ , 15, 28, 115  
 $B^0 \rightarrow \tau^+ \tau^-$ , 114, 115  
 $B^0 \rightarrow K_S^0 \pi^0 \gamma$ , 107, 115–117  
 $B_c \rightarrow \tau \nu$ , 80  
 $B_c$  lifetime, 80  
 $B_d^0 - \bar{B}_d^0$  mixing, 5, 6, 11, 12, 23, 89, 135, 197, 198  
 $B_q \rightarrow \mu^+ \mu^-$ , 113, 114  
 $B_s \rightarrow J/\psi K^+ K^-$ , 54  
 $B_s \rightarrow J/\psi \pi^+ \pi^-$ , 54  
 $B_s \rightarrow \mu^+ \mu^-$ , 107–115, 189  
 $B_s \rightarrow \mu^+ \mu^-$  effective lifetime, 113  
 $B_s^0 \rightarrow J/\psi \phi$ , 42, 44, 50, 51, 53  
 $B_s^0 - \bar{B}_s^0$  mixing, 33–40, 42, 50, 53, 92, 135, 195  
 $D^*$  polarization, 81  
 $D^0 - \bar{D}^0$  mixing, 135–143  
 $D_s^+ \rightarrow \ell^+ \nu_\ell$ , 72, 73  
 $K \rightarrow \pi + \text{nothing}$ , 151  
 $K \rightarrow \pi X^0$ , 149–151  
 $K^+ \rightarrow \pi^+ \nu \bar{\nu}$ , 143–148, 150  
 $K^0 - \bar{K}^0$  mixing ( $\Delta m_K$ ), 7, 8, 135  
 $K_L \rightarrow \pi^0 \nu \bar{\nu}$ , 143–150  
 $P'_5$  Anomaly, 94–96, 98, 151, 171, 189, 190  
 $R_{D^{(*)}}$  Anomaly, 75–81, 162, 174, 186, 189, 190  
 $R_{J/\psi}$ , 80  
 $R_{K^{(*)}}$  Anomaly, 96, 98, 103, 162, 189, 190  
 $R_{A_c}$ , 80  
 $T$ -violation, 160  
 $Z_2$  symmetry, 172, 177, 188  
 $\Delta \Gamma_{B_s}$ , 38, 42, 44, 50, 52, 54  
 $\Delta m_{B_d}$ , 6, 7, 23  
 $\Delta m_{B_s}$ , 35, 38, 39, 49  
 $\Delta \mathcal{A}_{K\pi}$  problem, 11, 18, 21–25, 27–29, 33, 34, 46, 47, 49, 53, 55, 91, 92, 189, 201  
 $\Delta S$  problem, 11, 16–18, 25, 28, 33, 34, 46, 47, 189  
 $\Sigma^+ \rightarrow p \mu^+ \mu^-$ , 123, 125, 126  
 $\Upsilon(1S) \rightarrow \text{nothing}$ , 122, 127  
 $\Upsilon(1S) \rightarrow \gamma a_1^0$ , 125, 126  
 $\Upsilon(nS)$  probes, 121, 122, 125–127  
 $\Xi_b^0$  oscillations, 167  
 $\mu \rightarrow e$  conversion, 158  
 $\mu \rightarrow e$  transition, 159  
 $\mu \rightarrow e \gamma$ , 155–157, 174  
 $\nu_{\mu} - \nu_\tau$  mixing, 156, 161–163, 174  
 $\pi^+ \pi^-$  tag, 122, 126, 127  
 $\pi^0 \rightarrow \nu \bar{\nu}$ , 150, 151  
 $\cos 2\Phi_{B_s}$ , 38, 42, 52  
 $\sin 2\Phi_{B_s}$ , 33, 34, 37, 38, 42–45, 47, 49, 50, 52–55, 186, 187, 189, 201

$\sin 2\beta/\phi_1$ , 4, 5, 7, 15, 33, 34, 37, 50, 194, 197, 198  
 $\tan \beta$ , 60, 64, 67, 68, 71, 76, 107, 108, 114, 126, 163, 179  
 $\tau$  lifetime, 162  
 $\tau$  polarization, 81  
 $\tau \rightarrow \bar{p}\pi^0$ , 166  
 $\tau \rightarrow \ell M^0$ , 164  
 $\tau \rightarrow \ell\ell\ell'$ , 162–165  
 $\tau \rightarrow \ell\gamma$ , 156, 157, 161–164  
 $\tau \rightarrow \mu$  transition, 11, 156, 161  
 $\tau \rightarrow \mu\gamma$ , 175, 176  
 $\tau \rightarrow \mu\mu\mu$ , 164  
 $\tau^\pm \rightarrow \Delta\pi^\pm$ , 166, 167  
 $\epsilon'/\epsilon$ , 144, 152, 196  
 $\epsilon_K$ , 144  
 $b \leftrightarrow s$  transitions, 42, 53  
 $b \rightarrow s\bar{s}s$ , 17  
 $b \rightarrow c\tau\nu_\tau$  ( $B \rightarrow \tau\nu_\tau + X$ ), 67  
 $b \rightarrow d$  triangle, 36, 37  
 $b \rightarrow s$  triangle, 37  
 $b \rightarrow s\bar{q}q$ , 11, 14, 16, 17, 28, 47  
 $b \rightarrow s\ell^+\ell^-$ , 85–88, 90, 92  
 $b \rightarrow s\gamma$  ( $B \rightarrow X_s\gamma$ ), 59–62, 64–67, 71, 87, 115  
 $b \rightarrow s\nu\bar{\nu}$ , 86–88, 99  
 $b \rightarrow sg$ , 67  
 $c\bar{c}$  threshold, 95, 96  
 $e^+e^- \rightarrow \gamma A'$ , 129, 130  
 $e^+e^-$  collider, 4, 8, 12, 128  
 $h \rightarrow \mu\tau$ , 174–177, 179  
 $h^0$ – $H^0$  mixing angle  $\cos \gamma$ , 174–179, 181, 188  
 $q^2$  bins, 100, 101, 104  
 $t \rightarrow cZ$ , 170  
 $t \rightarrow cZ' \rightarrow c\mu^+\mu^-$ , 171  
 $t \rightarrow ch$ , 173, 179, 188  
 $tZ'$  associated production, 171  
 $t\bar{t}h$  production, 56, 169, 170, 189, 203  
 $x_D$ , 135, 137, 140, 141  
 $y_D$ , 135, 137, 140, 141  
 $y_{CP}$ , 138  
 $\mathcal{A}_{J/\psi K^+}$ , 25–27  
 $\mathcal{A}_{J/\psi K^0}$ , 13  
 $\mathcal{A}_{K^+\pi^-}$ , 19–22, 24, 29  
 $\mathcal{A}_{K^+\pi^0}$ , 20, 21, 24, 29  
 $\mathcal{A}_{K^0\pi^+}$ , 29  
 $\mathcal{A}_{K^0\pi^0}$ , 29  
 $\mathcal{A}_{CP}(b \rightarrow s\gamma)$ , 96  
 $\mathcal{S}_f, \mathcal{A}_f$ , 15, 16, 197, 198  
 $\mathcal{S}_{J/\psi K^0}$ , 13  
 $\mathcal{S}_{\phi K_S}$ , 15, 16  
 $\mathcal{S}_{c\bar{c}s}$ , 16

$\mathcal{S}_{f_0(980)K_S}$ , 16  
 $\mathcal{S}_{s\bar{q}q}$ , 16  
 “ $A_{FB}$  problem”, 92, 93, 189  
 “ $\Delta A_{CP}$  problem”, 142  
 “GN bound”, 146, 147, 150, 151  
 “anomaly”, 2, 3, 6  
 2HDM-II, 65, 68, 76, 77, 80, 81, 108, 125, 126, 161, 172, 173, 186  
 2HDM-III, 165, 172, 174, 175, 177, 178, 186

## A

Abelian flavor symmetry, 118  
 ACME experiment, 161  
 ALEPH experiment, 67, 68  
 Alignment, 173, 174, 176–178, 180  
 Amplitude scan method, 39, 41  
 AMS, 128  
 Angular analysis, 52, 55, 94–96  
 Approximate alignment, 180, 188  
 ARGUS experiment, 5, 11, 169  
 Asymmetric beam energies, 12, 14, 107, 116, 117  
 Asymmetry sum rule, 29  
 ATLAS experiment, 3, 44, 55, 56, 171–174, 203  
 Axial-vector current, 68  
 Axion-Like Particle (ALP), 104, 133, 152

## B

BaBar experiment, 4, 5, 12–14, 16, 19, 20, 22, 61, 63, 71, 74–76, 78, 88, 92, 100, 103, 116, 117, 123, 128–130, 133, 137, 139, 167  
 Bag parameter, 7, 35  
 Barr-Zee mechanism, 174  
 Baryogenesis, 155, 178, 202  
 Baryon Asymmetry of the Universe (BAU), 11, 155, 181, 187  
 Baryon Number Violation (BNV), 166, 167  
 Beam-constrained mass  $M_{bc}$ , 18, 19  
 Belle detector, 13, 14, 19  
 Belle experiment, 4, 12–14, 16, 18, 20–22, 28, 61, 62, 70, 71, 73, 78, 79, 82, 88, 92, 100, 103, 122, 129, 137, 138, 162, 163, 166  
 Belle II experiment, 3, 18, 29, 79, 81, 96, 98, 104, 116, 117, 124, 127, 129, 133, 143, 164, 165, 182, 185, 190  
 BESIII experiment, 129, 143  
 Beyond the Standard Model (BSM), 1, 3, 18, 28, 34, 37, 74, 91, 92, 113, 141, 142, 144, 155, 156, 195

- B factory, 3, 7–9, 11, 12, 14, 16, 18, 20, 26, 39, 61, 62, 69, 71, 74, 89, 91, 92, 100, 122, 135, 138–140, 155, 163, 164, 166, 167, 185
- B–L conservation (violation), 166
- Box diagram, 6, 24, 35, 38, 46, 48, 49, 85, 86, 89, 99, 136, 137, 143
- BSM Higgs boson, 99, 100, 102, 103, 107, 108, 110, 121, 123, 125, 126, 186
- BTeV experiment, 109
- C**
- Cabibbo-allowed, 73, 143
- Cabibbo-Favored (CF), 137, 138, 170
- Cabibbo-Suppressed (CS), 137
- Calibration mode, 25, 28
- CDF experiment, 20, 33, 34, 36, 38, 40, 43, 50–55, 92, 109, 110, 114, 139, 142
- Charged Higgs boson  $H^\pm$ , 59, 60, 64–69, 71, 72, 74, 75, 81, 108, 186
- Charmless  $b \rightarrow s$  transition, 11
- Cheng-Sher Ansatz, 175–177, 180
- Chiral gauge theory, 6
- Circular Electron-Positron Collider (CEPC), 1
- CKM, 8, 9, 24, 25, 28, 36, 46, 47, 71, 72, 90, 96, 194, 198
- CKMfitter, 8, 36
- CKM matrix, 5, 7, 11, 136, 144, 169, 174, 178, 180, 187
- CLEO experiment, 20, 59–61, 68, 108, 126, 167
- CMS experiment, 44, 55, 56, 96, 99, 110–112, 114, 167, 170–176, 203
- Color-suppressed  $b \rightarrow c\bar{c}s$ , 25
- Color-suppressed tree (C), 23, 25, 28, 55, 197, 198
- COMET experiment, 158, 190
- Complex dynamics, 193
- Contact interaction, 158
- CP invariant phase, 23
- CP Violation (CPV), 2, 5, 7, 11, 13, 28, 29, 52, 142, 146, 193
- CPV phase, 23, 24, 38, 49, 160, 161, 169
- Current conservation, 64, 86, 87, 107
- D**
- $D\bar{0}$  experiment, 26–28, 34, 38, 39, 42, 50–55
- Dalitz analysis, 137, 139, 140, 143, 199
- Dalitz plot, 29
- Dark boson, 133
- Dark Higgs ( $h'$ ), 128
- Dark Matter (DM), 99–103, 121, 124, 126, 128, 133
- Dark photon ( $A'$ ), 128–131, 133, 152
- Dark sector, 121, 128, 129
- Dark-like object, 150, 151
- Decay at rest, 144, 147, 156
- Decay constant, 7, 35, 68, 71, 73, 108
- Decay in flight, 147
- Dimuon charge asymmetry  $A_{SL}$ , 42
- Direct CPV (DCPV), 11, 18–20, 22, 23, 25, 28, 29, 96, 196, 197
- Displaced-vertex signature, 132
- DK method, 198
- DORIS, 8
- Doubly Cabibbo-Suppressed (DCS), 137, 138
- E**
- E391a experiment, 145–147, 150
- E787/E949 experiments, 144, 145, 147, 150
- Electric Dipole Moment (EDM), 160, 161, 174, 177
- Electromagnetic calorimetry, 60, 61, 69, 71, 130, 148, 157
- Electroweak baryogenesis (EWBG), 180–182, 187, 188
- Electroweak penguin ( $P_{EW}$ ), 23–25, 46–49, 55, 85, 88, 89, 91, 92, 143, 144, 150, 169, 201
- Electroweak phase transition (EWPhT), 178
- Electroweak precision tests (EWPT), 46
- Electroweak symmetry breaking (EWSB), 1, 3, 56, 87, 89, 169, 185
- Energy difference  $\Delta E$ , 18, 19
- Energy frontier, 3
- Entanglement, 12
- Exotic Higgs-strahlung, 128, 133
- Extra Dimensions, 159
- Extra U(1), 129
- Extra Yukawa couplings, 181
- F**
- Fermilab, 158
- Fermi motion, 61
- Final state interaction, 52
- Final state rescattering, 138, 139, 141
- Flavor Changing Neutral Current (FCNC), 15, 108, 135
- Flavor Changing Neutral Higgs (FCNH), 80, 165, 170, 172–176, 178, 180, 188
- Flavor changing  $Z'$ , 25, 28, 95, 96, 98, 151, 185

Flavor physics, 2, 3, 8, 9, 45, 89, 96, 117, 133, 161, 169, 170, 180, 182, 185, 187, 189  
 Flavor tagging, 14, 20, 39, 44, 45, 50–52, 55, 163  
 Form factors, 94, 95  
 Forward-backward asymmetry ( $A_{FB}$ ), 85, 89–92, 96  
 Forward Detector, 123, 124  
 Four-fermion operators, 80, 91, 96, 166  
 Fourth generation (4G), 4, 24, 25, 27, 46–49, 53, 55, 56, 89, 91–93, 114, 141, 142, 150, 186, 201  
 FPCP conference, 36, 40, 75, 78  
 Full reconstruction (tag), 63, 69, 71, 74, 75, 81, 82, 100, 122, 124

**G**

Gauged  $L_\mu - L_\tau$ , 96, 98, 104, 132, 151, 185, 186, 189  
 GIM mechanism, 7, 47–49, 60, 113, 143, 162, 170, 172  
 Grand Unified Theory (GUT), 156, 157, 161  
 Grossman–Nir bound, 146, 150, 151

**H**

Hadronic effect (uncertainty), 16–18, 23, 25, 28, 29, 55, 60, 96, 137, 142, 159, 189  
 Heavy Flavor Averaging Group (HFAG), 16, 20–22, 54, 62, 63, 88, 110, 141, 162, 163  
 Heavy Flavor Averaging Group (HFLAV), 78, 136, 141  
 Heavy neutral Higgs bosons  $H^0$ ,  $A^0$ , 174, 177, 180  
 Helicity suppression, 68, 69, 108  
 Hermiticity, 101, 123, 124, 149  
 Higgs affinity, 6, 46–48, 68, 86, 102, 137, 143  
 Higgs boson, 1, 102, 125, 173, 180, 201  
 Higgs portal, 102, 103  
 Higgs quartic couplings, 180  
 High Luminosity LHC (HL-LHC), 171, 173, 182, 188  
 HyperCP events, 102, 123, 125–127

**I**

ICHEP conference, 4, 19, 66, 79, 92, 111  
 Inami–Lim functions, 48, 143  
 Inclusive  $A' \rightarrow \mu^+ \mu^-$ , 131, 133  
 Initial State Radiation (ISR), 129

INTEGRAL, 128  
 Interaction Region (IR), 14  
 International Linear Collider (ILC), 1, 125  
 Invisible  $\Upsilon(1S)$  decay, 133  
 Invisibly decaying  $A'$ , 129–131, 133  
 IP (beam) profile, 116, 117, 138

**J**

Jarlskog invariant, 187, 188, 201  
 J-PARC, 147, 148, 158

**K**

KEKB, 3, 12–14, 123, 124  
 Kinematic exclusion, 147, 148, 150, 151  
 Kinetic mixing ( $\epsilon$ ), 128, 129  
 KK excitations, 159  
 Kobayashi–Maskawa (KM), 5, 7, 187, 194  
 KOTO experiment, 147–151, 190  
 K-short ( $K_S$ ) vertexing, 116, 117, 138

**L**

Large Hadron Collider (LHC), 1, 3, 5, 33, 37, 44, 45, 49, 66, 71, 89, 91, 92, 96, 102, 103, 107, 108, 110, 112, 117, 121, 124, 125, 127, 148, 164, 169, 170, 185  
 Large  $N_C$ , 23  
 Lattice QCD, 7, 72, 73, 152, 159  
 LEP, 34, 67  
 Leptogenesis, 155, 163, 186, 187  
 Lepton charge asymmetry  $A_{SL}$ , 42  
 Lepton Flavor Violation (LFV), 155, 157, 162–165  
 Lepton number conservation, 156  
 Lepton Universality Violation (LUV), 97, 98, 162  
 Lepton-Photon Symposium, 55, 93  
 Leptoquark (LQ), 80, 81, 178, 189  
 LHCb detector, 44  
 LHCb experiment, 3, 18, 20, 28, 29, 33, 44, 45, 54, 55, 78, 79, 88, 92–98, 102, 109–112, 114, 131, 142, 143, 164, 165, 167, 190  
 Light muonic force, 133  
 Light  $Z'$ , 132  
 Little Higgs, 186  
 Long  $B$  lifetime, 8  
 Long Distance (LD), 137, 141  
 Long-lived  $A'$ , 131, 132

Loops, 2, 6, 8, 11, 15, 25, 47, 60, 64, 85, 86, 89, 90, 99, 102, 107, 108, 114, 121, 128, 156, 161, 169  
 Luminosity frontier, 3  
 Luminosity leveling, 113

**M**

Mass-mixing hierarchy, 180  
 Mediator/portal, 128  
 MEG (II) experiment, 156, 157, 190  
 Minimal Flavor Violation (MFV), 91, 114  
 Minimum Ionizing Particle (MIP), 123, 124  
 Mixing-decay interference, 197  
 Mixing-dependent CPV, 8, 23, 115, 140  
 Moriond conference, 78, 97  
 Mu2e experiment, 158, 190  
 Muon  $g - 2$ , 129, 130, 132, 151, 159, 163  
 Muon  $g-2$  experiment, 159, 190  
 Muonic-coupled  $Z'$ , 132  
 Muonic dark force, 132, 151

**N**

NA62 experiment, 147, 148, 150, 151, 190  
 Natural Flavor Conservation (NFC), 172, 177  
 N(2)EDM experiment, 160, 161  
 Neural Network (NN), 51, 53, 110  
 Neutrino counting, 46  
 Neutrino mixing (oscillation), 155, 156, 186, 187  
 New Physics (NP), 2, 3, 5, 9, 11, 15–17, 20–22, 24, 25, 29, 33, 39, 44, 45, 49, 55, 60–62, 64, 65, 67, 68, 72, 73, 82, 90–92, 96, 97, 107, 115, 118, 121, 127, 137, 141–147, 150–152, 160, 161, 172, 185, 188  
 Next-to-Next-to-Leading Order (NNLO), 60, 62–66, 116  
 NJL equation, 202  
 Nondecoupling, 6, 8, 24, 46–49, 53, 64, 86, 89, 90, 169, 170

**O**

Occam's principle, 190  
 Off-resonance data, 60  
 Opposite Side Tagging (OST), 39, 40, 51  
 Oscillation probability, 39

**P**

PAMELA, 128

Partial reconstruction, 60  
 Particle identification (PID), 14, 19, 20, 40, 44, 45, 55, 78, 147  
 PEP-II, 12–14, 122, 123  
 Perturbative QCD factorization (PQCD), 20, 24, 47

Phil Anderson, 203  
 Photon detection inefficiency, 150, 151  
 Photon energy cut, 61, 62, 66  
 Photon helicity, 116  
 Photonic penguin, 85–87, 89, 90, 108  
 Polarization in  $B \rightarrow VV$ , 29  
 Positron excess, 128, 133  
 Proton decay, 166  
 Proton size problem, 133  
 Pseudoscalar density, 68  
 PSI, 12, 156, 160

**Q**

QCD Factorization (QCDF), 20, 24  
 Quantum coherence, 12, 13, 143  
 Quark mixing matrix, 8

**R**

Radiative return (ISR), 122  
 Rare  $B$  reconstruction, 18  
 RBC+UKQCD collaboration, 152  
 Right-handed neutrinos, 165  
 Right-handed (RH) interactions, 107, 115–117, 186  
 Right-handed  $tcZ'$  coupling, 171  
 R-parity violating SUSY, 108

**S**

Sakharov conditions, 11, 178  
 Same Side Tagging (SST), 39, 40, 51, 138  
 Same-sign top, 182  
 Self-tagging, 18, 196  
 Semileptonic  $B_s^0$  decay, 39  
 Semileptonic tag, 71, 100, 101  
 Shape function, 61  
 Short Distance (SD), 137, 143, 144  
 Silicon vertex detector, 14, 38, 40, 44, 45, 78, 80, 109, 114, 116, 117, 131  
 Single Event Sensitivity (SES), 148–150  
 Single photon trigger, 129, 130, 133  
 Singlet Higgs boson, 102, 103, 125, 178  
 Six-quark operators, 167  
 Slepton mixing, 156, 157, 163  
 SM2, 172, 174, 178–180, 188  
 Soft Collinear Effective Theory (SCET), 24

Spontaneous symmetry breaking, 6, 87, 169, 203

Squark mixing, 35, 118

Standard Model (SM), 1, 5, 15, 35, 38, 55, 71, 76, 79, 92, 96, 99, 111, 113, 141, 143, 169

Standard phase convention, 5

Strong penguin amplitude ( $P$ ), 15, 17, 20, 22, 24, 25, 47, 85, 196

Strong phase, 20, 22–25, 27, 28, 52, 53, 138–140, 143, 193, 196

Super B factory, 3, 17, 63, 66, 71, 74, 89, 91, 96, 100, 101, 103, 107, 117, 124, 127, 143, 164

SuperKEKB, 3

Super proton-proton Collider (SppC), 1

Supersymmetry (SUSY), 3, 15, 24, 25, 35, 46, 53, 60, 64–68, 108–110, 114, 117, 121, 125, 126, 156, 157, 159, 160, 162, 163, 185

**T**

Tagged  $B_s^0 \rightarrow J/\psi\phi$ , 52

Tau/charm factory, 155, 163

Tevatron, 3, 5, 20, 26, 33, 34, 36, 38, 44, 45, 49, 55, 108, 110, 135, 138

Time-dependent CPV (TCPV), 11–15, 22, 23, 25, 42, 50–53, 107, 115–117, 138, 139, 143, 197, 198

Top Changing Neutral Couplings (TCNC), 170

Tree amplitude ( $T$ ), 20, 22, 85, 196

Triple product correlations, 29, 82

Triple-top, 182

Two Higgs doublets (2HDM), 64, 67, 172, 177

Two-sided bound, 39, 100, 104, 110

Two track vertex trigger, 39, 40, 42

**U**

Ultracold neutrons (UCN), 160

Unique CPV phase, 5, 187

Unitarity bound violation, 202

Unitarity triangle, 8, 9, 37, 136, 187, 195, 196

Untagged  $B_s^0 \rightarrow J/\psi\phi$ , 43

UTfit, 36, 53

**V**

Vacuum expectation value (v.e.v.), 1, 7, 61, 64, 86, 89, 98, 102, 107, 169, 177

Vector portal, 103

Vector-Like Quarks (VLQ), 56, 98, 99, 151, 186

**W**

Weakly Interacting Massive Particle (WIMP), 102, 103

Weak phase, 20, 24, 46, 47, 91, 92, 96, 193, 196, 198

Width difference, 137

Width mixing, 37, 38, 42, 43, 52, 135, 138–140

Wilczek process, 126

Wilson coefficients, 47, 49, 90–92, 94–96, 116

Wolfenstein parametrization, 36, 194, 195

**Y**

Yukawa coupling, 3, 6, 7, 46–48, 56, 68, 86, 98, 108, 165, 169, 172, 174, 176, 178–180, 188, 189, 202

Yukawa matrices  $\rho^f$ , 179, 180

**Z**

$Z'$  model, 53

Z penguin, 24, 85–87, 89, 90, 99, 144